Metabolic engineering of yeast for xylose utilization via the Weimberg pathway and for xylitol production

Dissertation
zur Erlangung des Doktorgrades
der Naturwissenschaften

vorgelegt beim Fachbereich Biowissenschaften
der Johann Wolfgang Goethe-Universität
in Frankfurt am Main

von
Priti Regmi
aus Kathmandu (Nepal)

Frankfurt am Main, 2023
(D 30)

vom Fachbereich Biowissenschaften

der Johann Wolfgang Goethe-Universität, Frankfurt am Main

als Dissertation angenommen

Dekan: Prof. Dr. Sven Klimpel

1. Gutachter: Prof. Dr. Eckhard Boles
2. Gutachterin: Prof. Dr. Claudia Büchel

Datum der Disputation:

Contents

1 Summary

Xylose, an abundant sugar fraction of lignocellulosic biomass, is a five-carbon skeleton molecule. Since decades, utilization of this sugar has gained much attention and has been in particular focus as a substrate for production of biofuels like ethanol by microbial hosts, including *Saccharomyces cerevisiae*. In this yeast, xylose is naturally not used as a carbon source, but its utilization could be achieved by metabolic engineering either via the oxidoreductive route or through the isomerase pathway. Both pathways share xylulose as a common intermediate that must be phosphorylated before entering the endogenous metabolism via the non-oxidative pentose phosphate pathway (noxPPP). Besides this, in some bacteria a non-phosphorylating oxidative pathway for xylose degradation exists, known as Weimberg pathway, where a molecule of xylose is converted by a series of enzymes - xylose dehydrogenase (XylB), xylonate dehydratase (XylD), 3-keto-2-deoxy-xylonate dehydratase (XylX) and α-ketoglutarate semialdehyde dehydrogenase (KsaD) - to form α-ketoglutarate (AKG). Besides having several useful properties as a product, AKG could also be used for cell growth as an intermediate of the tricarboxylic acid (TCA) cycle. One target of the present study is to establish a functional Weimberg pathway in *S. cerevisiae*. Previous studies have shown that this task is not trivial, for instance due to the toxicity of xylonate (the first metabolite of the pathway) and the involvement of an iron-sulfur cluster dependent enzyme, the D-xylonate dehydratase. The assembly of iron-sulfur clusters on a heterologous protein in yeast is known to be challenging.

To establish the Weimberg pathway in yeast, the genes *xylB*, *xylD*, and *xylX* were obtained from *Caulobacter cresentus* and *ksaD* was from *Corynebacterium glutamicum*. In a variant, the dehydratase *xylD* was replaced with *orf41* from *Arthrobacter nicotinovorans*, which is believed to be independent of iron-sulfur clusters. Growth of yeast cells on xylose as a sole carbon source was expected as an indicator of a functional Weimberg pathway. However, the heterologous expression of the codon optimized genes was not sufficient to reach this goal. Due to the complexity of the interactions of the heterologous pathway with the endogenous cellular processes, it was assumed that potential limitations could be overcome by adaptive laboratory evolution, using xylose as a sole source of carbon. Increasing selection pressure was applied on a strain with Weimberg pathway genes integrated into the genome over several generations. As a variant of the evolutionary engineering approach, mutator strains were generated. For this, *RAD27* and *MSH2* genes were deleted, which are involved in nucleotide excision and mismatch repair mechanisms, respectively. Some of the resulting strains PRY24, PRY25, PRY27 and PRY28 were able grow in xylose as a sole carbon source after evolutionary engineering. As a control, a non-

mutator strain PRY19 was also included. Strikingly, only the mutator strains were able to consume xylose as a sole carbon source, which shows the feasibility of the approach.

In addition to the mutator strain strategy, a further approach employed in the present study was the simultaneous expression of the Weimberg pathway in the cytosol and mitochondria. This was based on the reasoning that the iron-sulfur cluster biogenesis on XylD may be improved in the organelle and that the AKG is an intermediate of the TCA cycle. In the strain AHY02, all enzymes of the pathway were tagged with mitochondrial targeting signals in addition to a full cytosolically localized pathway. The localization of the mitochondrial variants was confirmed by fluorescence microscopy. Together with AHY02, CEN.PK2-1C wild type strain was also included as a control for evolution. When a selection pressure on xylose was applied, both strains - AHY02 and CEN.PK2-1C - were able to grow in the course of evolution. Deletion of the xylulokinase (*XKS1*) gene was found to be detrimental for both evolved strains in xylose-containing media. This suggests that the evolution of the endogenous oxidoreductive and noxPPP genes is responsible for growth of the evolved cells. For the evolved strain AHY02, it could also be possible that the Weimberg pathway genes supported to growth in addition to the oxidoreductive route. To elucidate the underlying molecular mechanisms, genome sequencing and reverse engineering approaches would be necessary in future.

In addition to screening for growth on xylose as a sole carbon source, a less stringent screening system was created to examine even a minor flux of xylose towards AKG. For this, all genes necessary for conversion of isocitrate to AKG where deleted, yielding a glutamate auxotrophic strain. In this system, the cells can grow on other carbon sources, whereas xylose is only provided as a source of AKG for the synthesis of glutamate. The strains PRY59 and PRY60 with the complete Weimberg pathway including xylonate dehydratases XylD and Orf41, respectively, were made glutamate-auxotrophic via deletion of *IDH2*, *IDP1*, *IDP2* and *IDP3.* Expectedly, they were able to grow only with glutamate supplementation. However, when PRY59 and PRY60 were grown on glucose or maltose supplemented with 10 g/L or 40 g/L xylose, growth could not be observed. This suggests that xylose is not being converted to AKG, at least not in a sufficient amount to be used as a glutamate source. Thus, the establishment of the Weimberg pathway in *S. cerevisiae* is a challenging task, possibly due to multiple known and unknown limitations.

The second part of this thesis is aiming at converting xylose to a commercially valuable compound xylitol. As a sweetener, xylitol is a commonly used ingredient, especially in candies, beverages and dental care products. Since there is no requirement of insulin for its metabolism, xylitol is also suitable for diabetic patients. Production of xylitol is currently

performed via chemical process, which have different disadvantages like high pressure and high temperature requirement.

To create a more environmentally friendly alternative, *S. cerevisiae* was employed as a microbial host for xylitol production. Conversion of xylose to xylitol occurs naturally in *S. cerevisiae* through the action of the xylose reductase (XR). The first step for xylitol production is the uptake of xylose via transporters followed by the XR-catalyzed conversion to xylitol in the cytoplasm. The biotransformation ends up with the secretion of xylitol through a transporter. In the present thesis, different hexose transporters were tested for the uptake of xylose, as well as for uptake and efflux of xylitol. The transporter variant Gal2$_{6SA/N376Y/M435I}$, which is known from previous studies to be superior for xylose transport, also showed the best properties for xylitol uptake. Since Gal2 acts as a facilitator, it was assumed that it could also mediate the efflux of xylitol. To disentangle the uptake of xylose and the efflux of xylitol, a test system was devised, in which the disaccharide xylobiose is taken up by the heterologously expressed CDT-2 transporter from *Neurospora crassa*. Xylobiose is subsequently cleaved into xylosyl-moieties by β-xylosidases (likewise from *N. crassa*) and reduced to xylitol by the XR intracellularly. Using this test system, it could be shown that xylitol efflux is facilitated by a different transporter, while Gal2$_{6SA/N376Y/M435I}$ had even a negative influence on this process. This points out the complexity of the import-export dynamics in yeast and shows that a bidirectional xylose transporter is likely unidirectional when xylitol is used as a substrate.

The XR-catalyzed conversion of xylose to xylitol requires redox cofactors. Most XRs found in nature, including those in *S. cerevisiae*, are dependent on NADPH. In order to find a suitable xylose reductase candidate, different reductases - *S. cerevisiae GRE3*, *Pichia stipitis XYL1*, *Candida parapsilosis XYL1* and *Aspergillus niger* XyrB - were compared. The highest yield of xylitol was obtained with *Pichia stipitis XYL1*. Except *Candida parapsilosis XYL1* (NADH dependent), which did not improve the xylitol production over the empty vector control, all other xylose reductases are reported to be NADPH dependent. Cytosolic NADPH supply route in *S. cerevisiae* is limited and mainly attributed to the oxidative pentose phosphate pathway (oxPPP). In this work, investigations were performed on various metabolic control mechanisms with a goal to increase the cytosolic NADPH pool, which could be beneficial for not only production of xylitol but also might be useful for other NADPH-dependent reactions.

To increase the entrance of glucose-6-phosphate into the oxidative pentose phosphate pathway, the phosphoglucose isomerase gene (*PGI1*) was downregulated by promoter replacements. The introduction of weaker promoters did improve the yields of xylitol per

consumed glucose, but at the same time decreased the volumetric production due to a negative effect on the cellular fitness. As a complementary strategy, the overexpression of the endogenous glucose-6-phosphate dehydrogenase gene *ZWF1* strongly improved the production of xylitol under all conditions. The additional overexpression of plasmid-encoded *ZWF1*, together with genes encoding the 6-phosphogluconolactonase (*SOL3*) and 6-phosphogluconate dehydrogenase (*GND1*) did not lead to further improvements, suggesting that the downstream enzymes of the oxPPP are not limiting the production of xylitol. As a rather pleiotropic strategy to modulate the activity of the PPP and thereby the supply of NADPH, as reported in previous work, the deletion of the *PHO13* gene was attempted. However, this modification did not show beneficial effects in the context of this study.

As an additional strategy targeting the central carbon metabolism, a heterologous NADP$^+$-dependent glyceraldehyde-3-phosphate dehydrogenase gene (*GPD1* from *Kluyveromyces lactis*) was introduced. This led to higher xylitol yields per consumed glucose, but it was clearly inferior to the overexpression of *ZWF1* in terms of the volumetric production. When, in addition to the expression of *GPD1*, the endogenous glyceraldehyde-3-phosphate dehydrogenase gene *TDH3* was knocked out to increase the availability of substrate for Gpd1, it resulted in a negative growth phenotype and thus lower overall product yields

In previous work, the deletion of the acetaldehyde dehydrogenase gene *ALD6* was reported to be beneficial for xylose catabolism via the oxidoreductive pathway and for the NADPH-dependent reduction of D-galacturonic acid, although the Ald6 enzyme produces NADPH. These observations are supported by this work, where a higher xylitol titer was observed in a *Δald6* strain. The presented data suggest that this may be, at least partly, explained by a compensatory mechanism, as the Zwf1 activity was increased in the *Δald6* strain background.

Finally, a strategy to increase the pool of NADPH by NADH phosphorylation was tested. For this, the normally mitochondrial NADH kinase Pos5 was expressed without the mitochondrial targeting sequence in addition to the native variant. This led to a slightly increased xylitol yield per consumed glucose, however, only during the fermentative phase of the diauxic growth, in which the supply of NADH is high. This is consistent with the higher preference of Pos5 for NADH compared to NAD$^+$.

In summary, the overexpression of the glucose-6-phosphate dehydrogenase gene *ZWF1*, followed by the deletion of the acetaldehyde dehydrogenase gene *ALD6*, proved to be the

most promising strategies to volumetrically improve the production of xylitol in *S. cerevisiae.* When combined, these strategies did not show an additive effect. Furthermore, the downregulation of the phosphoglucose isomerase, introduction of an $NADP^+$-dependent glyceraldehyde-3-phosphate dehydrogenase and cytosolic expression of an NADH kinase showed a potential to improve the supply of NADPH, especially under conditions of constant glucose supply, such as fed-batch or simultaneous saccharification and fermentation regimes. These observations are likely relevant for optimization of further NADPH-dependent production routes.

2 Introduction

2.1 Biomass as a resource for sustainable production of chemicals

As the world continues to face the challenge of dwindling fossil resources, climate change, and a growing population, there is an increasing need to develop sustainable strategies that enable the efficient use of natural resources on our planet. The continuous increase in energy consumption and CO_2 emissions is a global concern, and the need for sustainable and affordable energy sources is becoming increasingly urgent. According to Wang et al. 2021, global energy consumption is expected to rise by 23 % by 2040, equivalent to an increase of 516 EJ. This trend is accompanied by a significant carbon footprint, with 33 Gt of CO_2 emissions recorded in 2019 (Monir et al. 2021). The IEA predicts that the carbon footprint will remain constant at 33 Gt in 2040, making it essential to develop and produce energy resources in order to achieve the goal of net zero CO_2 emissions by 2050.

The overall biomass constituent of the biosphere is estimated to be approximately 550 gigatons of carbon (Gt C) and is distributed among all the kingdoms of life. This includes archaea (7 Gt C), viruses (0.2 Gt C), bacteria (70 Gt C), protists (4 Gt C), fungi (12 Gt C), animals (2 Gt C), and primarily terrestrial plants (450 Gt C) (Bar-On et al. 2018). In this context, use of lignocellulosic biomass certainly represents one of the most sustainable solutions to address the global energy crisis and climate change. Utilization of lignocelluloses has the potential to reduce greenhouse gas emissions, mitigate climate change, and create economic opportunities in rural areas. In addition, it can help to ensure food security by promoting the production of sustainable food crops and reducing competition between food and fuel production. The utilization of lignocelluloses for high value compounds represents a critical and promising avenue for addressing some of the most pressing challenges facing our planet today, and is an area of research that continues to attract attention and investment (Langeveld et al. 2010).

Lignocellulosic biomass (plant biomass waste) is a sustainable resource that consists of different types of polysaccharides and phenolic compounds like cellulose, hemicelluloses, pectin, and lignin along with a small percentage of proteins and minerals (Guerriero et al. 2016). Cellulose is a linear polysaccharide that consists of multiple units of anhydroglucose held together by β-1,4-glycosidic linkage and form giant straight-chain molecule (Walker and Wilson 1991). It provides around 30 % of the dry weight of plant wood residues (Chen 2014a). Hemicellulose is the structural backbone of the plant cell

wall that is composed of a branched polymer of different sugars (i.e., hexose and pentose form). It is the second most abundant polysaccharide in the plant cell wall. On the basis of the sugar residues present in the structural polymer as the backbone, hemicelluloses are classified likely into xylan, galacto(gluco)mannans, and xyloglucans. Hemicelluloses are comprised of different hexoses (e.g. D-mannose, D-galactose), pentoses (D-xylose, L-arabinose) and sugar acids (D-galacturonic acid, D-glucuronic acid). Depending on the type of biomass xylose can make up 5 - 35 % of the total dry weigh and is thus often the second most abundant monosaccharide besides D-glucose (Gírio et al. 2010). The present thesis aims at xylose (D-xylose) utilization via heterologous expression of Weimberg pathway or for the overproduction of xylitol which is an industrially attractive compound

2.2 *Saccharomyces cerevisiae* as a cell factory

The study of *S. cerevisiae* metabolism can be traced back to the XVII century (1680), when the Dutch naturalist Anton van Leeuwenhoek began examining its morphology. However, it was not until 1785 that the French scientist Charles Cagniard de la Tour discovered that fermentation was not a purely chemical process but was instead driven by microorganisms. The discovery of the microbial nature of fermentation opened up a new era in the study of *S. cerevisiae* metabolism, laying the foundation for further research in the field. Since the original DNA sequence of the reference *S. cerevisiae* strain was released in 1996 (Goffeau et al. 1996) and the Saccharomyces Genome Database became available (Cherry et al. 2012; Dwight et al. 2004), the genotype-phenotype relation of *S. cerevisiae* has been characterized in more detail. In recent years, *Saccharomyces cerevisiae* has emerged as a versatile cell factory for the production of both chemicals and pharmaceutical compounds, owing to its GRAS (Generally Regarded as Safe) status and the availability of advanced molecular biology techniques and robust fermentation technologies. The industrial biotech market is highly interested in *S. cerevisiae* due to its potential to become a workhorse for the production of sustainable chemicals. *S. cerevisiae* has several advantages that makes it a suitable host for the production of chemical compounds. For instance, it can tolerate relatively low pH, allowing the recovery of the acidic products in their protonated form, which reduces downstream costs. Additionally, it has a very high glycolytic flux, and appropriate engineering strategies can enable high productivities. Several studies have also shown that it is possible to expand the substrate range of *S. cerevisiae* for the utilization of naturally abundant pentose sugars like xylose and arabinose, which can be directly coupled to the production of chemicals, opening new possibilities for the development of sustainable processes (Ha et al. 2011; Lynd et al.

1999). Numerous works aim to engineer *S. cerevisiae* as a cell factory for the production of different classes of compounds, including organic acids, such as succinic and lactic acid, biofuels, such as bioethanol and farnesene, recombinant therapeutic proteins such as insulin and pharmaceuticals such as the antimalarial precursor artemisinic acid through the engineering of the isoprenoid pathway (Raab et al. 2010; Porro et al. 1995; Ro et al. 2006; Kjeldsen 2000).

In the pursuit of producing bioethanol from lignocellulosic biomass, significant research efforts have been directed towards engineering *Saccharomyces cerevisiae* to consume xylose. However, recent studies have focused on non-ethanol target molecules, exploring the potential of using xylose metabolism for the production of a variety of value-added chemicals, including advanced biofuels, fine chemicals, and pharmaceuticals. The present thesis aims at two different products from xylose – α-ketoglutarate (AKG) and xylitol - using *Saccharomyces cerevisiae* as a host organism.

2.2.1 Carbohydrate metabolism in *S. cerevisiae*

Carbohydrates are of vital importance for all forms of life from microorganisms to humans. Circulation of carbon molecules occurs in a fashion where synthesis of carbohydrates is majorly done by photosynthetic forms of life including plants. On the other hand, degradation of complex carbohydrates is carried out in nature mainly by microbial communities. Thus, metabolism of carbohydrate is widespread, among which glycolysis is a simplest carbohydrate breaking pathway which occurs in all forms of life where glucose is converted to pyruvate via different intermediates. In yeast, pyruvate derived from glycolysis is either used for the production of ethanol (fermentation) or it enters the tricarboxylic acid (TCA) cycle, which is localized in mitochondria, via formation of acetyl CoA by pyruvate dehydrogenase.

In *S. cerevisiae*, the catabolic pathways such as glycolysis, pentose-phosphate pathway, and TCA cycle, are responsible for breaking down nutrients and generating energy in the form of ATP and reducing power as cofactors NADPH, NADH and $FADH_2$. The glyoxylate cycle, which is linked to the TCA cycle, plays an anaplerotic role by replenishing intermediate metabolites to sustain TCA cycle operation and allowing growth on C2 and C3 compounds. The reduced carriers generated through the TCA cycle are then oxidized via the electron transport chain, located on the inner mitochondrial membrane, generating
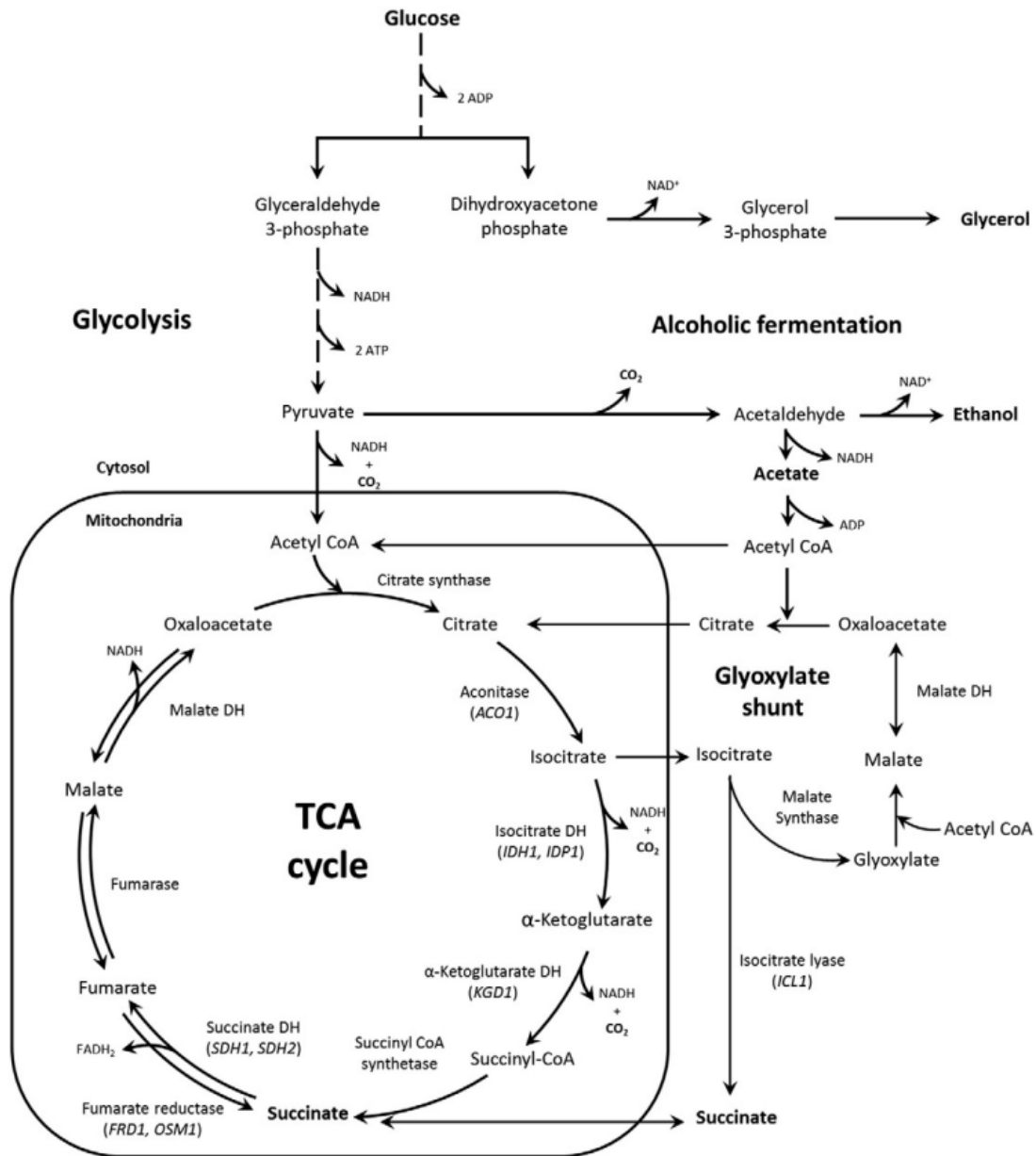
Figure 2.1 Metabolic pathway model for sugar consumption and energy production in *S. cerevisiae*: Glycolysis, tricarboxylic acid cycle and glyoxylate shunt are shown. The figure was taken from Rezaei et al. 2015.

a proton gradient used by the ATPase to synthesize ATP through oxidative phosphorylation. Gluconeogenesis is one of the main anabolic pathways used by *S. cerevisiae* to generate hexose phosphates during growth on C2 and C3 substrates (Figure 2.1).

2.3 Xylose utilization in *S. cerevisiae*

2.3.1 Hexose transporters and their variants for xylose uptake

S. cerevisiae is a single-celled organism belonging to the eukaryotic group, which has a remarkable ability to thrive in various environments such as sugary fruits and fermented beverages. Due to the changing sugar concentrations in its natural environments, yeast metabolism faces a challenge, and a complex regulatory system is necessary to maintain cellular equilibrium. Hexose transporters are crucial to this system as they aid in the uptake of sugars into the cell. *S. cerevisiae* uses transporters from the major facilitator superfamily (MFS) to facilitate the uptake of monosaccharides, as noted by (Boles and Hollenberg 1997) and (Wieczorke et al. 1999). This family of transporters is widespread across various species (Pao et al. 1998). In yeast, the Hxt family of transporters is not only diverse in terms of the kinetic properties, but is also differentially regulated at the transcriptional level, as highlighted by Özcan and Johnston 1999. These transporters facilitate efficient uptake of hexose but have a lower affinity for xylose, which contributes to diauxic growth (Sedlak and Ho 2004).

The Hxt family of hexose transporters in *S. cerevisiae* is a complex and tightly regulated group of proteins, consisting of Hxt1 to Hxt17, Gal2, and glucose sensors Snf3 and Rgt2 (Kruckeberg 1996; Boles and Hollenberg 1997; Özcan and Johnston 1999). In a null strain EBY.VW4000 lacking all known hexose transporters, glucose consumption and transport activity are completely abolished (Wieczorke et al. 1999). The transporters Hxt1 to Hxt4 plus Hxt6 and Hxt7 are most important for the uptake of glucose (Diderich et al. 2001; Özcan and Johnston 1999; Reifenberger et al. 1997; Reifenberger et al. 1995; Diderich et al. 1999; Boles and Hollenberg 1997). In addition, Hxt5, Hxt8 to -11, Hxt13 to -17, Gal2, and the maltose transporters Agt1, Mph2 and Mph3 are all able to transport glucose and, when ectopically produced, individually support growth in a strain lacking all other transporters (Wieczorke et al. 1999).

Glucose and xylose can be transported by the members of the Hxt family, but their affinity for xylose is much lower compared to glucose (Kotyk 1967; Kötter and Ciriacy 1993). Hence, both sugars are consumed simultaneously only under glucose-limited conditions (Meinander and Hahn-Hägerdal 1997). Hxt1, Hxt2, Hxt4 and Hxt7 have been described to uptake xylose but with very low affinity with K_m values of 880, 260, 170, and 130 mM respectively (Saloheimo et al. 2007). In a different study, Farwick et al. 2014 reports a similar K_m values of 200 and 225 mM for Hxt7 and Gal2 respectively with xylose as a substrate.

All the Hxts described are in case of glucose and xylose, and a limited study were focused for the transport of xylitol. Study from Jordan and colleagues found that Hxt11 and Hxt15 facilitate the uptake of xylitol. Authors kinetically characterized Hxt11, Hxt13, Hxt15, Hxt16, Hxt17 and found out only Hxt11 and Hxt15 were able to transport xylitol, with a higher value of V_{max} observed for Hxt15 (5.9 nmol min^{1} mg^{-1}) when compared to Hxt11 (2.6 nmol min^{1} mg^{-1}). Furthermore, a facilitative mechanism of transport of xylitol by Hxt11 and Hxt15 was shown (Jordan et al. 2016).

2.3.1.1 Relevance of *GAL2* and its variants in the context of xylose transport

In *Saccharomyces cerevisiae*, glucose exerts strict repression even in the presence of inducers, requiring the engineering of strains to utilize non-physiological substrates by constitutively expressing the *GAL2* ORF (Farwick et al. 2014; Becker and Boles 2003). Horak and Wolf 1997 investigated the lifespan and fate of the Gal2 in *Saccharomyces cerevisiae*. They observed that Gal2 has a relatively short lifespan and undergoes endocytosis-mediated degradation in the vacuole. Glucose is a sugar which represses Gal2 transcription as well as triggers catabolite degradation, leading to Gal2 protein ubiquitination, endocytosis, and degradation in the vacuole (Horak and Wolf 1997). Tamayo Rojas et al. 2021 found that introducing six serine to lysine in Gal2 (Gal2$_{6SA}$) prevented ubiquitination and stabilized the membrane-bound Gal2 protein, resulting in an extended lifespan at the membrane which represents a potential strategy for overcoming the glucose-induced degradation of Gal2 and improving its utilization of non-physiological substrates.

The Gal2 transporter is composed of 12 transmembrane (TM) helices, like the related Hxt proteins. The residue N376 located in the TM helix 8 was found to be pivotal for the recognition of hexoses. Substitution of asparagine by different amino acids, including valine, tyrosine and phenylalanine, enabled the transport of xylose, which was no longer competitively inhibited by glucose (Farwick et al. 2014). However, this property came with a reduced xylose transport capacity. Based on this, Rojas and colleagues found that Gal2 mutation N376Y, when combined with M435I, led to a significant increase of the xylose transport velocity in pure xylose or glucose-xylose mixtures (Rojas et al. 2021).

The M435I mutation in Gal2 transporter is another important mutation worth discussing in the context of its impact on transporter function. Nishizawa et al. 1995 reported the region spanning from M435 to Glu535 is critical for substrate recognition in Gal2, including the galactose recognition sequence. Rojas et al. 2021 conducted a structure model-based analysis and suggested that the replacement of methionine at position 435 with isoleucine

may have resulted in a positive localization effect on transmembrane domain 10, which may explain the observed behavior of the N376Y/M435I mutants. Authors reported that the M435I mutation, obtained through error-prone PCR, significantly altered transport characteristics when combined with the N376Y mutation. The resulting strain exhibited the highest growth on xylose alone or glucose-xylose mixtures and was considered a superior variant for improved growth on xylose. While the M435I mutation alone was found to impair transport of both glucose and xylose, the combined effect with N376Y resulted in a more favorable phenotype. Similarly, random mutagenesis study done by Reznicek et al. 2015 found clones with higher affinity to xylose associated with the M435T mutation, obtained from error-prone mutagenesis. Study from Tamayo Rojas et al. 2021 furthermore showed that the combination of the stabilized N-terminal tail (6SA) with the Gal2 mutations N376Y and M435I gives a further improved xylose uptake. GFP fluorescence images confirmed that the mutation 6SA stabilizes Gal2$_{N376Y/M435I}$ thus making it to a fully glucose-insensitive xylose transporter. When superior characteristics such as membrane stabilization, insensitivity to competitive inhibition and a higher pentose transport rate were combined in one construct (Gal2 $_{6SA/N376Y/M435I}$) the uptake of xylose was improved compared to all known xylose transporter variants (Rojas et al. 2021).

Gal2 has also been reported to transport xylitol (Tani et al. 2016). However, it remains unclear how the mutations described above affect the transport of xylitol. The present thesis describes the function of different hexose transporters, including Gal2 variants, in the context of xylitol transport.

2.3.2   Metabolism of xylose in *S. cerevisiae*

S. cerevisiae contains necessary robust transporters and metabolic pathways for consumption of glucose. However, the abundant sugar from lignocellulosic biomass, xylose, is not utilized naturally by *S. cerevisiae*. Although the transport of xylose can be accomplished by some hexose transporters, the main bottleneck lies in the metabolism of this yeast. Different pathways for assimilation of xylose exist in nature, such as the oxidoreductive pathway, the xylose isomerase pathway, the xylulose-1-P/ribulose-1-P pathway, the Dahms pathway and the Weimberg pathway (Figure 2.2).

The oxidoreductive pathway is most commonly found in fungi. Xylose is firstly converted to xylitol by a xylose reductase (XR). Xylitol is then oxidized by xylitol dehydrogenases (XDH) to form xylulose. Thereafter, conversion of xylulose to xylulose 5-P is mediated by a xylulokinase (XKS1), the only known kinase responsible for the production of xylulose-5-P. The enzymes of the non-oxidative pentose phosphate pathway (noxPPP) - D-

ribulose-5-phosphate epimerase (RPE), D-ribulose-5-phosphate keto isomerase (RKI), transketolase (TKL) and transaldolase (TAL) - catalyze in five more steps the conversion of xylulose-5-P to fructose-6-P and glyceraldehyde-3-P, which can then be directly integrated into the glycolytic reactions. Although *S. cerevisiae* naturally harbors all the gene candidates, there are several bottlenecks, due to which *S. cerevisiae* cannot consume xylose as a sole carbon source.

There are several aldose reductases in *S. cerevisiae*, which can convert xylose to xylitol, among which Gre3 is reported as the main XR. This step requires the cofactor NADPH (Träff et al. 2001; Träff et al. 2002). Conversion of xylitol to xylulose requires activity of XDH. Xyl2 is the main XDH in yeast responsible for the reaction using NAD^+ as a cofactor, but several unspecific dehydrogenases exist as well (Toivari et al. 2004). Hence, conversion of xylose to xylulose requires two reactions, where two different enzymes have preference for different cofactors, thereby creating a cofactor imbalance.

To resolve this, xylose can be isomerized directly to xylulose with the heterologous expression of a xylose isomerase (XI). The XI pathway converts xylose into xylulose, and thereby the redox imbalance is overcome. This is typically used by prokaryotes, namely by *E. coli*, *Bacillus sp.*, and *Lactobacillus sp.* (Lokman et al. 1991; Lawlis et al. 1984; Rygus et al. 1991). Besides this, xylose isomerase is also found in some fungi such as *Piromyces sp.* and *Orpinomyces sp.* (Silva et al. 2021; Madhavan et al. 2009). XI aids in improved xylose utilization, which was shown to relieve the cofactor imbalance problem (Jeffries 1985). The redox imbalance is not the only hurdle for xylose consumption by yeast, as the conversion of xylulose-5-P to reach glycolytic intermediates faces limited expression of a number of genes. There have been numerous studies, in which these bottlenecks were overcome and *S. cerevisiae* was enabled to consume xylose as a carbon source. For instance, strains were fully able to grow in xylose as a sole carbon source when a xylose isomerase, *XKS1* and noxPPP genes *TAL1, TKL1, RPE1, RKI1* were overexpressed (Farwick et al. 2014; Kuyper et al. 2005).

Two different pathways for xylose degradation are reported, which do not involve PPP. Xylose once converted to xylulose is furthermore converted to X1P or R1P, the later formation requires a two-step reaction. X1P and R1P are then cleaved by a X1P aldolase (XPA) or R1P aldolase (RPA), respectively, to form glycolaldehyde and dihydroxyacetone phosphate (DHAP). The pathway has already been tested in *E. coli* (Cam et al. 2016). Some engineering work, like the deletion of the endogenous xylulose-5-kinase, was able
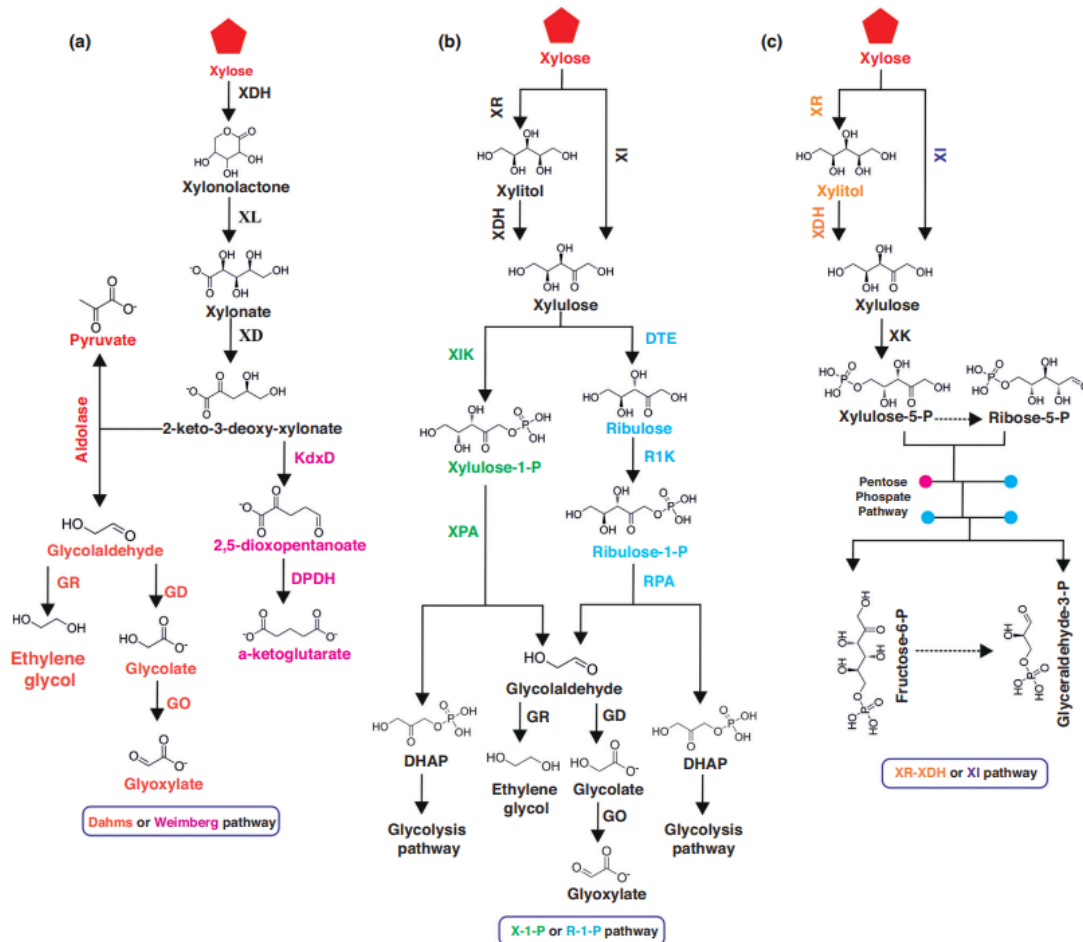
Figure 2.2: Xylose metabolic pathways in different microorganisms. **A)** Dahms pathway and Weimberg pathway, in which xylose is converted by XDH, XL, XD to form 2-keto-3-deoxyxylonate which finally forms either ethylene glycol and glyoxylate (Dahms pathway) or α-ketoglutarate (Weimberg pathway). **B**) Xylulose-1-P and ribulose-1-P pathways. Xylulose formed from the oxidoreductive route or isomerase pathway is converted to either X1P or R1P. Thereafter, in the X1P pathway, X1P is converted by XPA to DHAP and glycolaldehyde, whereas in the R1P pathway, R1P is converted by RPA to DHAP and glycolaldehyde. **C)** The oxidoreductive route or xylose isomerase pathway that leads conversion of xylose to fructose-6-P and glyceraldehyde-3-P. Enzymes are shown beside the arrows. XR, xylose reductase; XDH , xylitol dehydrogenase; XI, xylose isomerase; XK, Xylulokinase; XDH , xylose dehydrogenase; XL, xylonolactonase; XD, xylonate dehydratase; KdxD, 2-keto-3-deoxy-D-xylonate dehydratase; DPDH, 2,5-dioxopentanoate dehydrogenase; GD, glycolaldehyde dehydrogenase; GR, glycolaldehyde reductase; GO, glycolate oxidase. X1K, xylulose-1-kinase; XPA, xylulose-1-phosphate aldolase; DTE, D-tagatose epimerase; R1K, ribulose-1-kinase; RPA, ribulose-1-phosphate aldolase; PEP, phosphoenolpyruvate; DHAP, dihydroxyacetone phosphate. The figure was taken from Li et al. 2019.

to uplift the production of ethylene glycol (EG) up to 90% of its theoretical yield (Alkim et al. 2015). Production of ethanol and EG has also been reported with *S. cerevisiae* as a host organism (Chomvong et al. 2016). An engineered R1P route, where xylulose is epimerized to ribulose, which is then phosphorylated and cleaved to give glycoaldehyde and DHAP, was reported only in *E. coli* (Pereira et al. 2016).

2.3.3 Production of xylitol in *S. cerevisiae*

The discovery of xylitol can be traced back to 1891, when German and French chemists independently discovered this naturally occurring sugar alcohol. Xylitol was later recognized as a potent sweetener that did not increase blood sugar levels (Islam and Indrajit 2012), leading to its incorporation into diabetic diets in several countries. In the 1970s, the dental benefits of xylitol were revealed through the "Turku Sugar Studies" (Scheinin et al. 1975). Since then, various xylitol-substituted products have been introduced globally, capitalizing on its numerous health and nutritional benefits. Over 35 countries have approved the use of xylitol in a variety of products including food, pharmaceuticals, and oral health products such as chewing gums, toothpaste, syrups, and confectionery items (Barathikannan and Agastian 2016). The widespread adoption of xylitol-based products underscores the potential of this sweetener in promoting human health and well-being.

Using xylitol as a sweetness enhancer in food preparation improves certain properties of food such as taste, color, longevity, and texture (Gasmi Benahmed et al. 2020). Xylitol is extensively used in the manufacturing of chewing gums, chocolate, hard candies, wafer fillings, pastilles, pectin jellies, ice cream fillings, and other sweets. Additionally, xylitol provides flexibility, a pleasing and cooling effect to the confectioneries. In the manufacturing of xylitol-based chewing gums, the cooling effect is promoted by the endothermic property (34.8 cal/g) of xylitol. Since it does not undergo the Maillard reaction, xylitol will not char on heating, and because of this property, it gives a unique taste and color to the food items. It is also used to sweeten the flour used in making bread, rusks, and cakes, and as a sanding material in the preparation of sweets and confectioneries, making it highly recognized as a food preservative.

Xylitol is found in small amounts in various fruits and vegetables, as well as in the fibers of hardwood trees and corn cobs. However, due to the low quantity of xylitol present in natural sources, its extraction from these sources is inefficient. Currently, the chemical method of xylitol production is commercially used to meet the demand for xylitol. In this method, xylose extracted from lignocellulosic biomass undergoes catalytic hydrogenation to produce xylitol (Chen et al. 2010). Biotechnological methods for the production of xylitol from lignocellulosic biomass can be employed to reduce the high production costs (Mathew et al. 2018) making it an energy efficient process with a higher purity.

2.3.3.1 Xylose reductase: An enzyme forming xylitol from xylose

Xylose reductase (XR) is a member of the aldo-keto reductase (AKR) superfamily (Ellis

2002). While most members of this superfamily depend on NADPH, a few, including XR (AKR2B5), 3-hydroxysteroid dehydrogenase (AKR1C9), and 3-dehydroecdysone 3b-reductase (AKR2E1), can utilize both NADH and NADPH (Ellis 2002). Most AKRs are monomeric, but XRs function as non-cooperative, tightly associated dimers with a subunit molecular mass of 33 to 40 kDa (Rizzi et al. 1988; Yokoyama et al. 1995). While the specific function of many AKRs is not well-defined, they are believed to act as general detoxification catalysts by reducing reactive carbonyl-containing compounds (Grimshaw 1992). It has also been proposed that they function in osmotic regulation by controlling levels of intracellular polyols (Bedford et al. 1987).

Various XR genes have been expressed in different hosts (Anderlund et al. 2001; Dahn et al. 1996; Walfridsson et al. 1997). Currently, the primary structures of yeast XRs, which have a clear physiological role in the conversion of xylose, are well-known (Lee 1998). Yeast aldose reductases (ALRs) can be divided into two groups based on whether they have strict specificity for NADPH or show dual coenzyme specificity. XRs from xylose-fermenting *Candida parapsilosis* (Lee et al. 2012), *Candida shehatae* (Ho et al. 1990), and *Candida tenuis* (Neuhauser et al. 1997) have dual coenzyme specificity, which sets them apart from most ALRs that strictly require NADPH. However, the reported dual-coenzyme-specific XRs are still mainly NADPH-dependent, particularly in a coenzyme mixture that simulates physiological conditions.

For instance, *Saccharomyces cerevisiae* Gre3 (ScGre3) and *Pichia stipitis* Xyl1 (PsXyl1) are reported to have $K_{cat/Km}$ values of 1.06 mM^{-1} sec^{-1} (Jeong et al. 2002), and 35.92 mM^{-1} s^{-1} (Verduyn et al. 1985), respectively. In contrast, the *Aspergillus niger* XyrB (AnXyrB) was found to have a notably high $K_{cat/Km}$ value of approximately 178 mM^{-1} s^{-1} (Terebieniec et al. 2021). Interestingly, Lee et al. 2003 described a unique characteristic of NADH-dependent xylose reductase in *C. parapsilosis* (CpXyl1). This enzyme showed a $K_{cat/Km}$ value of 1.46 mM^{-1} s^{-1} for xylose and an unusual coenzyme specificity, with a greater catalytic efficiency with NADH ($K_{cat/Km}$ = 1.39×10^4 mM^{-1}s^{-1}) than with NADPH ($K_{cat/Km}$ = 1.27×10^2 mM^{-1}s^{-1}), which distinguishes it from all other characterized aldose reductases. Anaerobic xylose fermentation by *S. cerevisiae* was first demonstrated by heterologous expression of PsXyl1, together with the xylitol dehydrogenase PsXyl2 (Kötter and Ciriacy 1993). Both genes were also used in many subsequent studies, in which the strains were further optimized for ethanol production and xylitol was regarded as an undesired byproduct (Walfridsson et al. 1997). In the present thesis, different codon optimized reductases ScGre3, PsXyl1, AnXyrB, CpXyl1 will be thoroughly characterized for their xylitol production.

2.3.4   Cellular NADPH sources in the context of xylose utilization

The utilization of cofactor couples $NADP^+$/NADPH and NAD^+/NADH in most biochemical pathway represents a fundamental distinction. In general, catabolic reactions are associated with NAD^+/NADH, while anabolic reactions are linked to $NADP^+$/NADPH. Specifically, NAD^+/NADH serves as the cofactor couple used by the respiratory chain, as well as in the oxidation of glucose to ethanol or lactate via glycolysis. Conversely, $NADP^+$/NADPH serves as the main cofactor couple in biosynthesis. However, the pentose catabolism pathway in fungi deviates from this norm, as both cofactor couples are required for catabolic reactions as the catabolism of xylose necessitates the utilization of both NADPH and NAD^+ cofactor couples.

2.3.4.1   The pentose phosphate pathway

The phosphorylated glucose molecule glucose-6-phosphate (G-6-P), is channeled either to storage carbohydrates via glucose-1-phosphate, to glycolysis or to the PPP. G-6-P is the starting molecule of the oxidative pentose phosphate pathway, where it is oxidized to 6-phospho-gluconolactone by G-6-P dehydrogenase (G-6-PDH) with the concomitant reduction of $NADP^+$ to NADPH. G-6-PDH is encoded by *ZWF1*. Subsequently, the 6-phospho-gluconolactone is converted to 6-phosphogluconate by 6-phosphogluconolactonase (encoded by the paralogs *SOL3* and *SOL4*). This reaction (hydrolysis of the lactone ring) can occur spontaneously, but at a slow rate. Thereafter, 6-phosphogluconolactone is oxidized to ribulose-5-phosphate and CO_2 by 6-phosphogluconate dehydrogenase (encoded by the paralogs *GND1* and *GND2*) with $NADP^+$ as electron acceptor. Thus, in this so-called oxidative pentose phosphate pathway, two NADPH molecules and one CO_2 molecule are formed when glucose-6-phosphate is sequentially oxidized to ribulose-5-phosphate. This pathway plays a metabolic role in providing ribose-5-P and erythrose-4-phosphate, which is a precursor for aromatic amino acid biosynthesis. Moreover, the reaction catalyzed by G-6-PDH generates a significant amount of NADPH, making it a crucial enzyme in cellular metabolism. G-6-PDH is present in all organisms and cell types where it has been searched, and it is considered a housekeeping gene due to its central role in metabolism.

The non-oxidative phase of the pentose phosphate pathway involves a series of reactions that are catalyzed by the enzymes ribulose-5-phosphate isomerase or ribulose-5-phosphate epimerase, transaldolase, and transketolase. These reactions begin with the conversion of ribulose-5-phosphate into two molecules of fructose-6-phosphate and one molecule of glyceraldehyde-3-phosphate. Unlike the oxidative phase, no NADPH or ATP

is generated in this phase.

The regulation of PPP genes is complex and involves multiple transcription factors. Yap1 has been shown to regulate the expression of *ZWF1* and *TAL1* genes during oxidative stress (Lee et al. 1999). Another transcription factor, Stb5, has also been identified as a regulator of PPP genes and other genes coding for NADPH-dependent enzymes (Larochelle et al. 2006). Stb5 is required for growth in the presence of oxidative stress and binds to the promoter regions of PPP genes such as *ZWF1*, *SOL3, GND1*, and *TKL1*, as well as to promoters of *ALD6* and *IDP2,* where most of them are involved in NADPH synthesis (Grabowska and Chelstowska 2003; Minard et al. 1998). In addition to regulating PPP genes, Stb5 also has a role in directing glucose metabolism. It represses the *PGI1* gene, which codes for phosphoglucose isomerase (Pgi1), an enzyme that converts glucose-6-phosphate to fructose-6-phosphate in glycolysis. By repressing *PGI1* expression, Stb5 can direct glucose-6-phosphate to PPP or to storage carbohydrates instead of glycolysis. The regulation of Stb5 appears to be different from that of Yap1, suggesting a complex regulatory network that controls the expression of PPP genes and directs glucose metabolism in response to stress (Larochelle et al. 2006).

The major source of cytosolic NADPH production in *S. cerevisiae* grown on glucose has been attributed to glucose-6-phosphate dehydrogenase (Zwf1) and 6-phosphogluconate dehydrogenase (Gnd1) in the pentose phosphate pathway (PPP), with the cytosolic aldehyde dehydrogenase (Ald6) as a secondary source and isocitrate dehydrogenase (Idp2) as a third source (Grabowska and Chelstowska 2003; Minard and McAlister-Henn 2005).

Another often described genetic manipulation for improvising the xylose metabolism and upregulation of different PPP genes is the disruption of *PHO13*. Pho13 is also well known to be involved in the resistance to toxic compounds like furfural (Fujitomi et al. 2012). There have been several studies, where a functionally disrupted *PHO13*, either via mutation or direct deletion, is conferring a better growth in xylose (Ni et al. 2007; Kim et al. 2013; Fujitomi et al. 2012; van Vleet et al. 2008; Li et al. 2014; Lee et al. 2014). In 2015, Kim and colleagues found out that the deletion of *PHO13* was able to upregulate nine genes when grown in glucose and xylose (Kim et al. 2015). Among them, *SOL3* and *GND1* belong to oxidative PPP, *TAL1* is a transaldolase and is a part of non-oxidative PPP, and *GOR1* and *YEF1* are involved in NADPH regeneration pathway. Additionally, a putative gluconokinase YDR248C, a transposable element YHR182C-A, and the uncharacterized gene YLR152C were found to be overexpressed due to the deletion of *PHO13*. The direct elevation in the expression of PPP genes *SOL3, GND1*, *TAL1* strongly suggests that the

PHO13 disruption is linked to pentose metabolism by modulating the PPP activity (Kim et al. 2015). Moreover, Collard and colleagues showed that Pho13 acts as a phosphatase of several sugar phosphates, which may lead to a metabolic imbalance during the pentose metabolism (Collard et al. 2016). Thus, the beneficial effects of the *PHO13* deletion may be explained both at the transcriptional and at the enzyme activity level.

2.3.4.2 NAD(H) kinases

Located in chromosome XVI, *POS5* (YPL188W) of *S. cerevisiae* encodes an ATP dependent NAD^+ (NADH) kinase, which exclusively functions in mitochondria. In the cytosolic part of the cell, $NADP^+$ is converted to NADPH by the several reactions mentioned in above chapter 2.6.3.1, whereas in the mitochondria, NADH serves as the substrate for NADPH generation through the NADH kinase activity of Pos5, which is a protein required for the response to oxidative stress (Outten and Culotta 2003). The activity of mitochondrial $NADP^+$ phosphatase (Bernofsky and Utter 1968) allows the recycling of $NADP^+$ to NAD^+ and its further use in the TCA cycle.

In *S. cerevisiae*, NADPH biosynthesis depends on three NADH kinases and various $NADP^+$ dependent dehydrogenases (Shi et al. 2011). In *S. cerevisiae*, NADH cannot directly be converted to NADPH, or vice versa, due to the lack of transhydrogenase activity (Bruinenberg 1986). Moreover, the compartmentalization of $NADPH/NADP^+$ and $NADH/NAD^+$ is also important since it is believed that the mitochondrial membrane is impermeable to these cofactors (Outten and Culotta 2003; van Roermund et al. 1995). Thus, cofactor is segmented in different compartment thereby making a need of shuttle system to balance NADH/NADPH in mainly cytosol and mitochondria. The cytosolic phosphorylation could be performed via NAD^+ kinases like Utr1 and Yef1 whereas mitochondria require the activity of Pos5 (Kawai et al. 2001; Shi et al. 2005). The evidence of the NADP(H) shuttle system in *S. cerevisiae* was suggested based on the viability of the mutant strain lacking the cytosolic NAD^+ kinases (Δ*utr1*Δ*yef1*) and the lethality of the triple mutant (Δ*utr1*Δ*yef1*Δ*pos5*), which implies that cytosolic $NADP^+$ can be supplied by Pos5 from the mitochondrial $NADP^+$ pool (Bieganowski et al. 2006; Shi et al. 2005). To increase the cytosolic NADPH pool, biotechnologists have overexpressed a cytosolic version of Pos5. For instance, a study from Zhao and his team shows that the expression of *POS5* in the cytosol is even more effective than the overexpression of *ZWF1* to increase the NADPH availability in the cell for carotenoid synthesis (Zhao et al. 2015).

2.3.4.3 Aldehyde dehydrogenases

Aldehyde dehydrogenases (ALDH) play a crucial role in yeast metabolism of

acetaldehyde, particularly during growth in ethanol. Yeast contains five isoforms of aldehyde dehydrogenase, namely Ald2, Ald3, Ald4, Ald5, and Ald6 (Navarro-Aviño et al. 1999). Among these, Ald2 and Ald3 primarily catalyze the oxidation of 3-aminopropanal to β-alanine for CoA generation in the cytosol (White et al. 2003). On the other hand, Ald4, Ald5, and Ald6 are responsible for acetaldehyde metabolism, which is generated during ethanol metabolism and is vital for yeast survival when ethanol serves as the carbon source. Among these three enzymes, Ald4 and Ald5 predominantly use NAD^+ as a cofactor and are localized in the mitochondria, while Ald6 exclusively utilizes $NADP^+$ and is localized in the cytosol. Notably, the pentose phosphate pathway, a major source of NADPH, is less active when ethanol is the carbon source. In this case, Ald6 functions as the principal pathway for NADPH production and is considered a cytosolic source of NADPH (Zhang et al. 2018; Grabowska and Chelstowska 2003).

2.3.4.4 Glyceraldehyde-3-phosphate dehydrogenases

Three different genes, *TDH1, TDH2*, and *TDH3*, encode glyceraldehyde-3-phosphate dehydrogenase (GAPDH) in *Saccharomyces cerevisiae*; *TDH3* is the predominant isoform (McAlister and Holland 1985). Despite its traditional role as a housekeeping protein, Tdh3 was identified as a moonlighting protein (Gancedo et al. 2016) due to its involvement in telomere-mediated transcriptional silencing (Ringel et al. 2013), suggesting the gene's tight regulation. Study from Linck et al. 2014 discovered that the individual deletion of all three isozymes negatively affects growth in glucose as a carbon source to different extents. These findings underscore the importance of tight regulation of GAPDH expression to maintain proper glycolytic function in yeast.

While all three *S. cerevisiae* GAPDH isoforms are NAD^+ dependent and produce NADH during catalysis, there are other microorganisms where GAPDH can use $NADP^+$ as a cofactor, producing NADPH instead. For example, the GAPDH enzyme (Gdp1) from *Kluveromyces lactis* (EC 1.2.1.13) has been reported to be $NADP^+$ dependent (Verho et al. 2002; Verho et al. 2003). Similarly, the gapN enzyme from *Streptococcus* sp. is $NADP^+$ dependent, producing NADPH (Bro et al. 2006). Hence, the heterologous expression of GAPDH genes encoding $NADP^+$-dependent enzymes in *S. cerevisiae* could potentially increase the cellular concentration of NADPH. This, in turn, could be useful for increasing product yields that are dependent on NADPH.

2.4 Oxidative non-phosphorylating pathways of xylose metabolism

In contrast to PPP and non-PPP routes described above, two oxidative non-phosphorylating pathways were discovered in some bacteria. In these pathways, xylose is first oxidized by a xylose dehydrogenase (XDH) yielding D-xylonolactone, which is subsequently hydrolyzed by a D-xylonolactonase (XL) to D-xylonate. In case of the Weimberg pathway, two molecules of water are eliminated successively by a D-xylonate dehydratase (XD) and a 2-keto-3-deoxy-D-xylonate dehydratase (KdxD) yielding α-ketoglutarate semialdehyde, which is finally oxidized to α-ketoglutarate by the α-ketoglutarate semialdehyde dehydrogenase (KgsaDH). In the case of Dahms pathway, 2-keto-3-deoxy-D-xylonate is cleaved to pyruvate und glycolaldehyde by a 2-keto-3-deoxy-D-xylonate aldolase (KdxA) (Stephens et al. 2007; Johnsen et al. 2009; Weimberg 1961). Dahms pathway (Dahms 1974) can be considered as a variation of the Weimberg pathway, where an aldolase catalyzes the reaction of 2-keto-3-deoxy-xylonate to pyruvate and glycolaldehyde, which both are then able to enter the central carbon metabolism (Figure 2.2).

Compared to the oxidoreductive and the isomerase pathway, the Weimberg pathway is an interesting alternative as it can be a more carbon-efficient way for utilization of xylose and to produce molecules derived from α-ketoglutarate. In the process of converting xylose to α-ketoglutarate via noxPPP/glycolysis/TCA enzymes, carbon is lost in form of CO_2. On the contrary, the same conversion via the Weimberg pathway shows no carbon loss. Furthermore, by using intermediates of the Weimberg pathway as precursors to produce target molecules, growth-decoupled production can be achieved more easily. This concept was already partially realized to produce 1,4 -butanediol with *E. coli* (Liu and Lu 2015). This pathway opens a metabolic route for the conversion of xylose into α-ketoglutarate without carbon loss and, thus, is particularly interesting to produce TCA-cycle derived organic acids.

Weimberg in 1961 discovered the Weimberg pathway in *Pseudomonas putida*. Later *Caulobacter cresentus*, a freshwater bacterium was explored with efficient enzymes that convert xylose to AKG via Weimberg pathway. Genes XylB, XylD, KsaD, XylX when expressed in *S. cerevisiae* were shown in a glucose xylose mixture to produce AKG via xylose (Borgström et al. 2019). Gene XylB encodes xylose dehydrogenase which converts xylose to xylonate which is known for being toxic to yeast. Conversion of xylonate to 2-keto-3-deoxy xylonate is one of the main bottlenecks of Weimberg pathway due to the

inefficient activity of XylD as the bacterial origin dehydratase requires [4Fe-4S] for their activity (Yukawa et al. 2021). Iron sulfur cluster biogenesis is a complex process and requires several cellular networks for the synthesis, detailed explained in chapter 2.5. 2-keto-3-deoxyxylonate by action of XylX, forms alphaketoglutarate semialdehyde which subsequently is converted to alphaketoglutarate by KsaD. Borgström and colleagues reported that genomically integrated XylB, XylD, KsaD, XylX genes in a *FRA2* deleted strain background enabled *S. cerevisiae* to actively expresses the Weimberg pathway as shown by detecting all pathway intermediates by mass spectroscopy when the cells were grown in glucose-xylose mixtures (Borgström et al. 2019).

2.4.1   α-Ketoglutarate

Since this thesis aims at the utilization of xylose via the Weimberg pathway, the applications and metabolism of its final product, α-ketoglutarate (AKG), is discussed in the following sections in more detail.

2.4.1.1 Application of AKG

AKG plays a crucial role at the intersection between carbon and nitrogen metabolic pathways. As a key intermediate of the tricarboxylic acid (TCA) cycle, one of the fundamental biochemical pathways in carbon metabolism, AKG production is of high interest. Additionally, AKG is a major carbon skeleton for nitrogen assimilation reactions. Within yeast, AKG participates in numerous enzymatic reactions, particularly in the conversion of ornithine and AKG to L-glutamic acid and L-glutamic γ-semialdehyde, which is facilitated by the mitochondrial enzyme ornithine aminotransferase. If AKG can be derived from xylose, yeast can be able to grow in xylose as a sole sugar and finally several other industrially valuable molecules such as succinate, glutamate, 1, 4 - butanediol, and ornithine could be further produced from it.

AKG acts as a starting molecule for synthesis of several amino acids. There are several additional reported roles of AKG in *Saccharomyces cerevisiae*; for instance, cells grown in a medium supplemented with AKG showed enhanced level of constituents like total protein, glycogen and trehalose. Additionally, those cells showed higher reproductive ability in aged cultures (Burdyliuk and Bayliak 2017). It has been reported that wild type yeast cells grown on AKG were more resistant to hydrogen peroxide, menadione, and transition metal ions (Fe^{2+} and Cu^{2+}). A publication has reported AKG to be effective against freeze-thaw and carbohydrate induced stress in *Saccharomyces cerevisiae* in terms of viability and fermentative capacity (Bayliak et al. 2017).

2.4.1.2 Metabolism of AKG in *S. cerevisiae*

The precursor molecule for AKG is isocitrate which is found in various compartments such as the cytosol, mitochondria, and peroxisomes. In *Saccharomyces cerevisiae*, four isocitrate dehydrogenases are present that facilitate the oxidative decarboxylation of isocitrate to AKG. Among the isozymes, three are NADP$^+$ specific homodimers that share 70% protein sequence identity. The mitochondrial matrix contains the Idp1 protein encoded by gene *IDP1*, which is a constitutively expressed protein (Haselbeck and McAlister-Henn 1991). Conversely, Idp2, encoded by *IDP2*, is a cytosolic protein (Loftus et al. 1994) that is highly repressed by glucose and is primarily expressed under aerobic conditions, implying its role as an oxidative metabolism enzyme (Bojunga and Entian 1999; Haurie et al. 2001). Idp2 is also a significant source for cytosolic NADPH, as the reaction utilizes NADP$^+$ for its activity (Minard and McAlister-Henn 2001). Idp3, encoded by *IDP3*, is located in peroxisomes and is only expressed when yeast cells are grown on fatty acid carbon sources, which induce this organelle and associated functions. (Henke et al. 1998; van Roermund et al. 1998).

Yeast IDH, the fourth isozyme, is an octamer consisting of four Idh1 and four Idh2 subunits. (Cupp and McAlister-Henn 1992, 1991; Cupp and McAlister-Henn 1993). These subunits are encoded by the *IDH1* and *IDH2* genes, respectively, and share 42% sequence identity. IDH is a mitochondrial enzyme that participates in the TCA cycle. McCammon and McAlister-Henn 2003 conducted a study, which found that the loss of mitochondrial NADP$^+$ dependent Idp1 and cytosolic Idp2 is detrimental in stabilizing mitochondrial DNA in an IDH dysfunctional yeast. Additionally, a high petite frequency was observed with the disruption of *IDP1*. Authors demonstrated that the deletion of *IDH2*, *IDP1*, and *IDP2* caused yeast to be auxotrophic for glutamate. Whereas the deletion of *IDP1* in an *idh2*-deleted strain severely affected glutamate synthesis, the strain was unable to grow at all in media without glutamate supplementation when all three genes *IDH2*, *IDP1*, and *IDP2* were deleted.

2.5 Iron-Sulfur cluster biogenesis in *S. cerevisiae* with respect to the functionality of heterologous enzymes

Fe/S clusters are primordial protein cofactors ubiquitously found in all organisms (Beinert et al. 1997). In eukaryotes, Fe/S proteins participate in many key processes of life and are found in mitochondria, cytosol, and nucleus. In mitochondria, they are involved in, e.g., the TCA cycle (aconitase), the electron transfer of the respiratory chain (complexes I, II, and III), and in lipoate (lipoate synthase), biotin (biotin synthase), and heme (ferrochelatase)

biosynthesis. In the eukaryotic cytosol, Fe/S proteins function in amino acid biosynthesis, tRNA modification (e.g., radical SAM protein Tyw1), post-transcriptional regulation of the iron metabolism (vertebrate iron regulatory protein 1; IRP1), or ribosomal protein translation (the ABC protein Rli1; human–ABCE1). Important nuclear Fe/S proteins participate in DNA replication (various DNA polymerases and primases) and DNA repair, chromosome segregation or telomere length regulation (various ATP-dependent DNA helicases) (Lill and Mühlenhoff 2008; Gari et al. 2012; Netz et al. 2011; Paul and Lill 2015; Stehling and Lill 2013; Stehling et al. 2012).

The biogenesis of all cellular Fe/S proteins is initiated by the ISC assembly machinery in mitochondria. In *S. cerevisiae*, the process begins with the cysteine desulfurase complex Nfs1–Isd11 that donates the sulfur required for assembling of [2Fe–2S] cluster on the
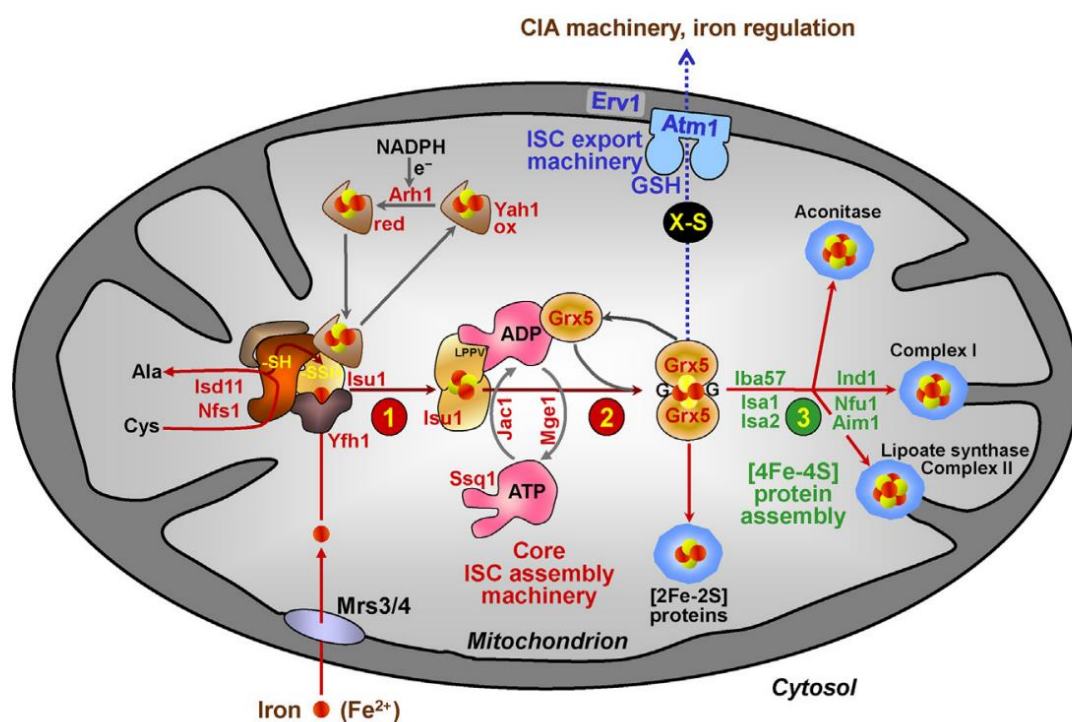
Figure 2.3: Model of mitochondrial Fe/S protein biogenesis on eukaryotes. Iron sulfur cluster protein maturation occurs in three steps. Step1 involves assembly of a [2Fe–2S] cluster on the scaffold protein Isu1. Second step involves a transfer of [2Fe–2S] to a dimer of mitochondiral glutaredoxin Grx5. In third and final step, all mitochondrial [4Fe–4S] proteins are assembled facilitated by components as Iba57–Isa1–Isa2, Nfu1, Aim1, Ind1, assisted by step1 and 2 again for genetation of a sulfur and X-S molecule which requires export to cytosol via ABC transporter (Atm1) and sulfhydryl oxidase Erv1. The figure was taken from Lill et al. 2015.

scaffold protein Isu1 (Mühlenhoff et al. 2003; Wiedemann et al. 2006). Generation of the [2Fe–2S] cluster on Isu1 further requires reduction by an electron transfer chain from NAD(P)H via ferredoxin reductase Arh1 to a [2Fe–2S] ferredoxin Yah1 (Sheftel et al. 2010;

Shi et al. 2012; Lange et al. 2000). The de novo generation of the [2Fe–2S] cluster on the scaffold Isu1 has recently been already reconstituted *in vitro* with purified components by (Webert et al. 2014). In the second step, [2Fe–2S] cluster is released by Hsp70 chaperone (Dutkiewicz et al. 2006; Mühlenhoff et al. 2003) and transferred to the monothiol glutaredoxin Grx5 (Bandyopadhyay et al. 2008; Rouhier et al. 2007; Uzarska et al. 2013). In its holoform, Grx5 exists as a homodimer and bridges the [2Fe–2S] cluster. The final step of mitochondrial Fe/S protein biogenesis involves the participation of six different ISC proteins, including Isa1, Isa2, Iba57, Nfu1, Aim1, and Ind1 (Bych et al., 2008; Sheftel et al., 2009) (Figure 2.3). Holo-Grx5 may transfer its [2Fe–2S] cluster to the Isa proteins through direct interaction (Banci et al., 2014). However, the exact mechanism of this reaction is currently unknown (Brancaccio et al., 2014). Three additional ISC factors have target specificity and may assist in the insertion of [4Fe–4S] clusters into dedicated apoproteins (Figure. 2.4). For example, Nfu1 and BolA3 seem to preferentially mature lipoate synthase and respiratory complexes I and II, while Ind1 appears to be specific for Fe/S cluster insertion into complex I (Bych et al. 2008; Cameron et al. 2011; Navarro-Sastre et al. 2011; Roret et al. 2014).

Cytoplasmic iron sulfur cluster assembly (CIA)machinery is responsible for Fe/S protein assembly in the cytosol and nucleus, and consists of several proteins that use the still unknown compound X-S and cytosolic glutaredoxins (Paul and Lill 2015; Mühlenhoff et al. 2010). The export of X-S is supported by the ABC transporter Atm1 at the mitochondrial inner membrane (Lill 2009; Lill et al. 2012; Sharma et al. 2010).
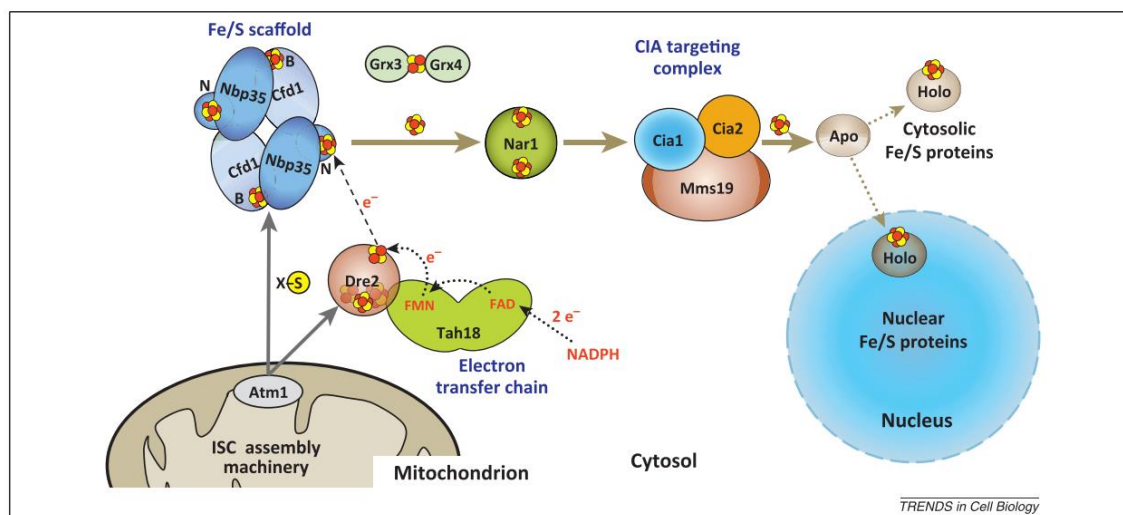
Figure 2.4: Maturation of cytosolic and nuclear Fe/S proteins in cytosol and nucleus of yeast. First, bridging [4Fe–4S] clusters (B) are assembled on the Cfd1–Nbp35 heterotetrameric scaffold complex with the aid of sulfur generated from X-S. Nbp35 with action of Tah18 and Dre2 generates N-terminal Fe/S cluster (N) of Nbp35. In second step, by action of the Fe/S protein Nar1 and the CIA targeting complex Cia1–Cia2–Mms19, the bridging Fe/S clusters are released from Cfd1–Nbp35 and transferred to apoproteins (Apo). Biogenesis further requires, at an unknown step, the

cytosolic multidomain monothiol glutaredoxins Grx3–Grx4, which bind a glutathione-coordinated, bridging [2Fe–2S] cluster. The thick arrows mark the flow of the Fe/S clusters. Abbreviations: CIA, cytosolic iron–sulfur protein assembly; ISC, iron–sulfur cluster. The figure was taken from Netz et al. 2014.

In yeast, the CIA machinery is comprised of eight known proteins and operates in two steps (Figure 2.4). In the first step, the Fe/S cluster is synthesized on the hetero-tetramer of the P-loop NTPases Cfd1–Nbp35 (Hausmann et al. 2005; Netz et al. 2007; Roy et al. 2003). This reaction requires the core components of the mitochondrial ISC assembly machinery, including Nfs1–Isd11 as a sulfur donor. An electron transfer chain consisting of NADPH, the diflavin reductase Tah18, and the Fe/S protein Dre2 is also necessary for stable insertion of the Fe/S clusters into Nbp35, although the exact molecular function of this chain is still unknown (Zhang et al. 2008; Netz et al. 2010). Grx3–Grx4 monothiol glutaredoxins are also required for cluster synthesis on Dre2. In the second step, the Fe/S cluster is transferred from the Cfd1–Nbp35 scaffold to target apoproteins, and this reaction requires the CIA proteins Nar1, Cia1, and possibly Cia2 (Balk et al. 2004; Balk et al. 2005; Weerapana et al. 2010). While the molecular mechanisms of CIA protein functions are still poorly defined, this system is conserved in virtually all eukaryotes.

Iron sulfur cluster biogenesis is a complex mechanism that is not fully understood, making it difficult to predict a precise way to increase the iron sulfur cluster availability in the cytosol. However, there are some reported approaches in the literature that aids in increasing the activity of [4Fe-4S] cluster dependent proteins in the cytosol. According to (Kumánovics et al. 2008), Fra1 and Fra2 are proteins located in the cytosol that play a role in interpreting the Fe/S cluster signal. If they are absent, the iron regulon is activated. These proteins are thought to be involved in a complex that interprets the signal originating from the mitochondrial Fe/S synthesis. Fra2 belongs to a protein family with an unknown function that is named after one of its members in *E. coli*, BolA. There is some evidence to suggest that BolA-like proteins work in conjunction with monothiol glutaredoxins, but this is not yet fully understood. Fra2 plays a role in negatively regulating transcription from the iron regulon, and when it is deleted in yeast, there is an increase in Fe-S cluster biosynthesis and increased activity of enzymes dependent on it. Deletion of *FRA2* in yeast also upregulates the Fe-S metabolism, which enhances xylonate dehydratase (XylD) activity as shown by a study where deletion of *FRA2* led to a seven-fold increase in the production of ethylene glycol, product formation that is dependent on [4Fe-4S] cluster for their activity (Salusjärvi et al. 2017).

2.6   Evolutionary engineering

The most frequently employed approach for increasing the production of chemicals, among others, include either overexpressing genes from native or heterologous biosynthetic pathways or downregulating genes from competitive branches. However, in some cases, direct manipulating on gene expression levels – the "rational" metabolic engineering - may not be sufficient to achieve the desired outcome. Identifying the rate-limiting steps in biosynthetic pathways can be a time-consuming process, particularly when it is already difficult to predict the genes involved. In such cases, genome engineering provides a solution by introducing random mutations into the genome, rather than relying on rational manipulation. This approach, combined with proper selection pressure, enables the identification of desired clones and the responsible genetic elements more easily.

Evolutionary engineering is a powerful tool that enables researchers to identify genetic variants that enhance metabolic characteristics, such as increased product yield, tolerance to toxic compounds, and improved growth rates, among others. Many successful attempts have been made to develop strains with superior phenotypes using this approach. In the case of xylose consumption, several studies have demonstrated the feasibility of enhancing characteristics for xylose fermentation through evolutionary engineering. An improved xylose utilizing *S. cerevisiae* was developed by Zha and the coworkers via evolutionary engineering approach resulting in more than two times higher ethanol yield (Zha et al. 2014). Papapetridis and colleagues genetically engineered a strain for forced co-consumption of glucose and xylose. After evolutionary engineering and genome sequencing, they discovered genetic targets to improve the simultaneous fermentation of both sugars (Papapetridis et al. 2018). Selective pressure can be focused on a specific enzyme or cellular process by genetic engineering of strain prior to evolution. For instance, deletion of genes encoding glucose-phosphorylating enzymes in pentose-fermenting *S. cerevisiae* strains enabled *in vivo* evolution of hexose-transporter variants that efficiently transported xylose and L-arabinose, two key sugars in lignocellulosic hydrolysates, in the presence of glucose (Farwick et al. 2014).

Introduction of mutations into genomes through techniques such as deletions, duplications or changes in amino acid residues can be a powerful tool in the development of superior strains with various biotechnological applications. The success of evolutionary engineering strategies often relies on the incorporation of mutations, combined with traditional evolutionary protocols, advanced strain engineering and selection techniques to generate

desired traits.

2.6.1 Yeast mutators

The accurate transmission of genetic material through mitotic clonal cell expansion or sexual reproduction with low mutation rates and rare chromosomal structural variations is well-documented in the scientific literature (Nishant et al. 2010; Lynch et al. 2008). To maintain this precision, numerous genes and pathways are involved in preventing mutagenesis during DNA replication, repair, recombination, and chromosome segregation. These genes are critical in regulating the mutation rate, as their defects can increase the frequency of mutations, the so-called mutator phenotype.

Accuracy and fidelity of DNA replication is essential for maintaining genome stability. DNA replication must be precisely regulated to ensure that the genome is replicated only once per cell cycle. Disruption of this process can lead to deregulated DNA replication, resulting in over-replication of certain genomic regions and subsequent genomic instability (Siddiqui et al. 2013; Blow and Dutta 2005; Arias and Walter 2007). Despite the remarkable precision of DNA replication, errors may occur during the process which can lead to DNA damage and subsequent genomic rearrangements (van Nguyen et al. 2001; Green et al. 2010; Alexander et al. 2015; Green and Li 2005). These errors need to be processed by proofreading enzymes that detect and remove mismatched nucleotides. Below, two proteins involved in DNA repair, whose genes were deleted to create mutator strains, are described in more detail.

2.6.1.1 Rad27 – a nuclease involved in excision repair mechanisms

Eukaryotic chromosomal replication is a complex process that involves the synthesis of both the leading and lagging strands. Unlike the continuous synthesis of the leading strand, the lagging strand is synthesized discontinuously through the formation of multiple Okazaki fragments. These fragments consist of a short RNA primer that is extended by polymerase δ to the next downstream fragment after a polymerase switch. To maintain continuity of the lagging strand, the RNA primer must be removed, a process that has been shown to require the simultaneous action of a DNA polymerase, RNase H1, Rad27, and DNA ligase I. In vitro reconstitution experiments have demonstrated that correct processing of Okazaki fragments occurs through this mechanism (Turchi and Bambara 1993; Waga and Stillman 1994; Waga et al. 1994).

Eukaryotic cells possess sophisticated DNA repair mechanisms to maintain genome integrity. Excision repair is one such mechanism that removes DNA lesions, classified into

two classes - base excision repair (BER) and nucleotide excision repair (NER). BER removes single base lesions caused by DNA damage such as oxidative damage or uracil residues. NER, on the other hand, repairs larger lesions like those caused by exposure to UV radiation or chemicals. These repair mechanisms prevent mutations and are crucial for genome stability (Wood 1997; van Houten 1990; Braithwaite et al. 1998).

Rad2 nuclease family is involved in nucleotide excision repair (NER) in yeast. Rad2 protein, a member of this family, plays a crucial role in NER by its nuclease activity (Habraken et al. 1993; Wang et al. 1993). Rad27 is another member of the Rad2 nuclease family, possessing both 5′→3′ exonuclease and flap endonuclease activities (Harrington and Lieber 1994; Zhu et al. 1997). Inactivation of *RAD27* results in a temperature sensitive phenotype, mutator phenotype, chromosome instability, and sensitivity to methylmethane sulfonate (MMS) (Reagan et al. 1995; Johnson et al. 1995; Sommers et al. 1995).

Deletion of the *RAD27* gene in yeast results in a range of phenotypes, including elevated rates of spontaneous mutagenesis characterized by duplications between separated short direct repeats (Tishkoff et al. 1997), elevated spontaneous recombination rates (Vallen and Cross 1995), increased micro and minisatellite instability (Kokoska et al. 1998; Richard et al. 1999; White et al. 1999), destabilization of telomeric repeats (Parenteau & Wellinger, 1999) (Parenteau and Wellinger 1999)., a 4-fold reduction in non-homologous end joining (Wu et al., 1999), and a deficiency in base excision repair (Johnson et al., 1998; Wu & Wang, 1999). The accumulation of single-stranded DNA fragments during replication in Δ*rad27* mutants strongly suggests the biological consequences of disturbances of these processes (Parenteau and Wellinger 1999; Merrill and Holm 1998).

2.6.1.2 Msh2 – a component of the mismatch repair system

The mismatch repair (MMR) pathway plays a critical role in maintaining the integrity of the genome by repairing errors in DNA replication and repair. In addition to correcting mismatches, MMR also repairs insertion-deletion loops that result from strand slippage at repetitive sequences. In budding yeast, the key components of MMR include Msh2, Msh3, Msh6, Pms1, and Mlh1. Msh2-Msh6 (MutSα heterodimer) complex recognizes mismatches, whereas the Msh2-Msh3 (MutSβ heterodimer) complex recognizes insertion-deletion loops. Upon recognition of the lesion, Msh2-Msh6 and Msh2-Msh3 recruit Pms1-Mlh1 (MutLα), a heterodimeric complex that functions as a DNA endonuclease, to the daughter strand. Recognition of mispairing also activates multiple downstream factors (for example, Exo1, PCNA, RFC, RPA, and DNA pol δ) for repair by lesion excision and strand resynthesis. Pms1-Mlh1 cleaves the DNA strand, allowing removal of the erroneous

nucleotides, which are subsequently replaced with the correct ones (Figure 2.5) (Prolla et al. 1994; Lee et al. 2007). However, the detailed molecular mechanisms by which MMR factors function in the cellular environment still remain to be fully elucidated (Boiteux and Jinks-Robertson 2013). Msh2 role on increasing the mutation rate is already examined by Boyce and Idnurm 2019 where deletion of *MSH2* confers higher mutation rates. In *S. cerevisiae*, mutational rate was 200 times increased with the deletion of *MSH2* shown from results of Lang et al. 2013.
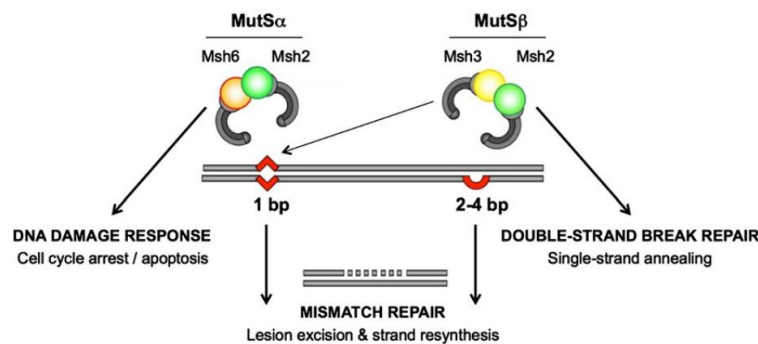
Figure 2.5: Role of Msh2 in recognition of unmatched nucleotides or multiple nucleotide errors. The figure was taken from Tosti et al. 2014.

2.7   Aim of this thesis

The aim of present study is to explore potential ways to utilize xylose, which is a significant component of lignocellulose, for the production of valuable compounds and chemicals. Two different approaches are being pursued for xylose conversion. The first approach involves the heterologous expression of the Weimberg pathway in *S. cerevisiae*, which is an oxidative xylose degradation pathway that converts xylose to AKG using various genes. This shall enable the growth of *S. cerevisiae* on xylose as a sugar source, and provides possibilities for the production of various other compounds and chemicals derived from the TCA cycle using xylose as a substrate. In this study, all pathway genes from *Caulobacter crescentus, Corynebacterium glutamicum*, and *Arthrobacter nicotinovorans* will be codon-optimized and expressed as genomically integrated copies to make optimized and stable expression. The expression of Weimberg pathway genes will be tested in different compartments - cytosol and mitochondria - as mitochondrial localization might be beneficial for the pathway's functionality. It may be challenging to achieve growth on xylose via the Weimberg pathway, despite the expression of all pathway genes, and therefore optimized gene expression or the identification of crucial growth-supporting factors may be necessary. In such cases, evolutionary engineering will be employed as a strategy to

achieve the desired characteristics. The evolutionary engineering approach is the most effective method to achieve the desired results, especially when the pathway is complex and limited by many known and unknown factors. To determine the activity of the Weimberg pathway, a screening strain is required to detect the flux of xylose to AKG. Specifically, the screening strain will be made auxotrophic for glutamate by deleting genes that convert isocitrate to AKG, allowing for the direct assessment of the Weimberg pathway's activity in *S. cerevisiae*.

The second part of the present PhD thesis focuses on producing xylitol from xylose. Xylitol is a valuable compound due to being a low calorie sweetener. While yeast naturally harbors the gene xylose reductase for the production of xylitol, the current large-scale methods for xylitol production are based on purely chemical processes and involve high temperature and pressure, and require a purification step. Thus, *S. cerevisiae* can be an attractive host for xylitol production, being well-known for producing various chemicals and compounds. Present study aims to maximize the yield of xylitol using *S. cerevisiae* by using several approaches. Specifically, the study will investigate the transport characteristics of hexose transporters and their variants towards xylose and xylitol, including their import and export. Additionally, xylose reductases derived from different organisms will be compared with respect to their ability to catalyze the conversion of xylose to xylitol in yeast. Since the reductase requires NADPH as a cofactor, present thesis employs different strategies to find the best genetic manipulation that boosts the cytosolic pool of NADPH. In total, genetic engineering and screening approaches will be used to study the transport of xylitol across the yeast plasma membrane, as well as to optimize the conversion of xylose to xylitol in the cytosol of yeast.

3 Materials and Methods

This section elaborates all the different methods and techniques used throughout the study. Furthermore, current chapter lists different chemicals, reagents, enzymes etc. that were purchased from various suppliers. Molecular biology techniques used throughout the study as well as the details of the plasmids and yeast strains used are also given. If experiments were done following the manual of kits, catalogue reference is mentioned.

3.1 List of bacterial strains used for the study

E. coli strain DH10B is used for construction of all plasmids. Table 3.1 describes the detailed genotype of each plasmid used.

Table 3.1. Plasmid backbones used:

Nomenclature	Description	References
p423*HXT7*	2µ-plasmid, *HIS3*-marker, expression of genes under the control of the truncated constitutive *HXT7*-promoter and the *CYC1*-terminator with optional 6 His affinity tag, *E. coli* Ampicillin-marker and pBR322- origin	(Becker and Boles 2003)
p424*HXT7*	2µ-plasmid, *TRP1*-marker, expression of gene under control of the truncated constitutive *HXT7*-promoter and the *CYC1*-terminator with optional 6His affinity tag, *E. coli* Ampicillin-marker and pBR322- origin	(Becker and Boles 2003)
p425*HXT7*	2µ-plasmid, *LEU2*-marker, expression of genes under control of the truncated constitutive *HXT7*-promoter and the *CYC1*-terminator with optional 6His affinity tag, *E. coli* Ampicillin-marker and pBR322- origin	(Becker and Boles 2003)
p426*HXT7*	2µ-plasmid, *URA3*-marker, expression of genes under control of the truncated constitutive *HXT7*-promoter and the *CYC1*-terminator with optional 6His affinity tag, *E. coli* Ampicillin-marker and pBR322- origin	(Becker and Boles 2003)
p423*MET25*	2µ-plasmid, *HIS3*-marker, expression of genes under the control of the truncated constitutive *MET25*-promoter and the *CYC1*-terminator with optional 6 His affinity tag, *E. coli* Ampicillin-marker and pBR322- origin	(Mumberg et al. 1994)
p424*MET25*	2µ-plasmid, *TRP1*-marker, expression of genes under the control of the truncated constitutive *MET25*-promoter and the *CYC1*-terminator with optional 6 His affinity tag, *E. coli* Ampicillin-marker and pBR322- origin	(Mumberg et al. 1994)
p426*MET25*	2µ-plasmid, *URA3*-marker, expression of genes under the control of the truncated constitutive *MET25*-promoter and the *CYC1*-terminator with	(Mumberg et al. 1994)

	optional 6 His affinity tag, *E. coli* Ampicillin resistance marker and pBR322- origin.	
pRS62K	2µ-plasmid, *kanMX4*-marker (G418), expression of genes under control of the truncated constitutive *HXT7*-promoter and the *CYC1*-terminator with optional 6His affinity tag, *E. coli* Ampicillin resistance marker and pBR322-origin.	Prof. Boles group, Frankfurt
pRS62N	2µ-plasmid, *natNT2*-marker (ClonNAT), expression of genes under control of the truncated constitutive *HXT7*-promoter and the *CYC1*-terminator with optional 6His-affinitytag, *E. coli* Ampicillin resistance marker and pBR322-origin	Prof. Boles group, Frankfurt
pUG6K	Plasmid as a template for PCR-amplification of a loxP-flanked deletion cassette with *kanMX4*-marker (G418) the under control of the *A. gossypii TEF*-promoter and -terminator, *E. coli* Ampicillin resistance marker and pBR322-origin	(Güldener et al. 1996)
pYTK001	Golden Gate entry plasmid containing: CamR*,* ColE1, Esp3I *GFP*-drop out-cassette.	(Lee et al. 2015).
pYTK095	Golden Gate assembly vector for subcloning containing: AmpR, ColE1, Esp3I-restriction sites.	(Lee et al. 2015).
SiHV008	[ConLS'-gfp dropout-ConRE'-*KanMX*-2µ-KanR-ColE1] recipient parent plasmid for transient expression	Prof. Boles Group, Frankfurt
FGD97	CEN6/ARS4-plasmid, *ura3*-marker, expression of genes under the control of the truncated constitutive (*MET25*-promoter-*ADH3* gene- linker- GFP envy) and the *CYC1*-terminator, *E. coli* Ampicillin resistance marker.	Prof. Boles Group, Frankfurt
LBGV071	GFP based CRISPR vector backbone CloNAT as a marker	Prof. Boles Group, Frankfurt
SiHV138	GFP based CRISPR vector backbone G418 as a marker *[pROX3-CAS9-tcyc1, pSNP52-GFP-tSUP4, KanMX, 2µ, AmpR,ColE1]*	Prof. Boles Group, Frankfurt
pRCCK	CRISPR vector backbone with G418 as a marker *[pROX3-CAS9-tcyc1, pSNP52-GFP-tSUP4, KanMX, 2µ, AmpR,ColE1]*	(Generoso et al. 2016)
pRCCN	CRISPR vector backbone with CloNAT as a marker *[pROX3-CAS9-tcyc1, pSNP52-guideRNA-tSUP4, CloNAT, 2µ, AmpR, ColE1]*	(Generoso et al. 2016)
GDV079	[ConLS'-gfp-dropout-ConRE'-*LEU2* 3'Hom-KanR-ColE1-*LEU2*-5'Hom]. *LEU2* integration plasmid, without KanMX dominant marker	Prof. Boles Group, Frankfurt
ALFV001	[ConLS'-gfp-dropout-ConRE'-*URA3*'Hom-KanR-ColE1-*URA3*-5'Hom] *URA3* integration plasmid, without *KanMX* dominant marker	Prof. Boles Group, Frankfurt

Table 3.2. Plasmid used in this study:

Nomenclature	Background	References
FWV157	pRCCK-*ZWF1*	Prof. Boles Group, Frankfurt
AHB15	ALFV001- LS-pHHF1-acp1-XylB-tENO1-R1, L1-pTDH3-aco-XylD-*tSSA1*-R2, L2-pHHF2-cox4-KsaD-tADH1-R3, L3-pTEF2-lpd1-XylX-tENO2-RE	Adriana Happel Bachelors Thesis 2021
PRV41	GDV079- LS-R1-L1-XylD-R2-L2-KsaD-R3-L3-XylX-RE	This study
PRV43	LS-linker-R1-L1-Orf41-XylX-Ksa*D*-RE	This study
PRV36	GDV079-LS-pTEF1- XylX-tGPM1- RE	This study
PRB1	p426*MET25-xylB*	This study
PRB2	p425 *HXT7- xylD*	This study
PRB3	p425*HXT7-orf41*	This study
PRB4	pRCCN-*GRE3*	This study
PRB5	p423 *HXT7-ksaD*	This study
PRB12	GDV097-ACP1 *xylB*	This study
PRB13	GDV097-Aco *xylD*	This study
PRB15	GDV097-Lpd1 *xylX*	This study
PRB18	FGD97-CoxIV*ksaD*	This study
PRB20	pRCCN-*RAD27*	This study
PRB21	pRCCN-*MSH2*	This study
PRB24	p426*HXT7 -HXT1*	This study
PRB25	p426*HXT7 -HXT2*	This study
PRB26	p426*HXT7 HXT3*	This study
PRB27	p426*HXT7- HXT4*	This study
PRB28	p426*HXT7- HXT5*	This study
PRB29	p426*HXT7- HXT7*	This study
PRB30	p426*HXT7- HXT10*	This study
PRB31	p426*HXT7- HXT14*	This study
PRB32	p426*HXT7- GAL2* WT	This study
PRB33	p426*HXT7- GAL2*$_{6SA}$	This study
PRB34	p426*HXT7- GAL2*$_{N376Y/M435I}$	This study
PRB38	p425- *HXT11*	This study
PRB39	p426- *HXT15*	This study
PRB40	p425-Sc *XYL2*	This study
PRB41	p423-*HXT5*	This study
PRB42	p426- *GAL2*$_{6SA/N376Y/M435I}$	This study
PRB43	SiHV138-*IDH2*	This study
PRB44	p425-Cp *XYL1*	This study
PRB45	p425-Ps *XYL1*	This study
PRB46	p425-*GRE3*	This study
PRB47	p426-*HXT11*	This study
PRB48	pRCCK-*IDP2*	This study
PRB49	pRCCK-*pPGI1*	This study
PRB50	pRCCK-*pZWF1*	This study
PRB51	p425-An *XYRB*	This study
PRB52	p425-codpt*GRE3*	This study
PRB53	LBGV071-*XKS1*	This study
PRB55	SiHV138-*xylD*	This study
PRB56	SiHV138-*IDP3*	This study
PRB59	p426-*GDP1* (*Kluveromyces lactis*)	This study
PRB60	p423-NcCDT2	This study
PRB62	SiHV138- *IDP1*	This study
PRB63	SiHV138-*TRP1*	This study

PRB64	p424Met25 GH43-2	This study
PRB65	p423 *GAL2*	This study
PRB66	p423-*ZWF1* (*ZWF1* sequence of PRY48)	This study
PRB67	SiHV138 -XylX	This study
PRB68	p423-*ZWF1* (*ZWF1* sequence of PRY63)	This study
PRB71	p425- *HXT7*	This study
PRB72	SiHV138-*ksaD*	This study
PRB77	PRB64, *pHXT7*-GH43-7-*tSSA1*	This study

3.2 List of yeast strains

This chapter collectively includes the information about the yeast strain employed in present study with their genetic description. In general, strain background used were CEN.PK2-1C background which is auxotrophic for uracil, leucine, histidine, and tryptophan. Most of the gene manipulation were done via CRISPR/Cas9. For some strains creation, dominant marker based strain construction was done.

Table 3.3: List of yeast strains

Nomenclature	Gene description	References
CEN.PK2-1C	*leu2-3,112 ura3-52 trp1-289 his3Δ1 MAL2-8c SUC2*	EUROSCARF, Frankfurt
EBY.VW4000	CEN.PK2-1C *Δhxt1-17 gal2Δ::loxP stl1Δ::loxP agt1Δ::loxP mph2Δ::loxP mph3Δ::loxP*	(Wieczorke et al. 1999).
AFY10	EBY.VW4000 *glk1Δ::loxP hxk1Δ::loxP hxk2Δ::loxP ylr446wΔ::loxP [pyk2Δ::PGK1p-opt.XKS1-PGK1t TPI1p-TAL1-TAL1t TDH3p-TKL1-TKL1t PFK1p-RPE1-RPE1t FBAp-RKI1-RKI1t kanMX]*	(Farwick et al. 2014)
PRYS1	CEN.PK2-1C, Δ*gre3:: pMET25-xylB-tcyc1*	This study
PRYS4	CEN.PK2-1C, Δ*fra2*	This study
PRYS5	Δ*gre3::pMET25-xylB-tcyc1*; Δfra2	This study
PRY12	PRYS1, Δ*ura3::pPGK1-ksaD-tEFM1*	This study
PRY14	PRY5, Δ*leu2::xylD, xylX, ksaD*	This study
PRY15	PRY13, Δ*leu2:: xylB, xylD, ksaD, xylX*	This study
PRY17	PRY12, Δ*fra2:: xylD*	This study
PRY18	PRY12, Δ*fra2::orf41*	This study
PRY19	PRY17, Δ*leu2:: xylX*	This study
PRY20	PRY18, Δ*leu2:: xylX*	This study
PRY24	PRY19, Δ*rad27*	This study
PRY25	PRY19, Δ*msh2*	This study
PRY27	PRY20, Δ*rad27*	This study
PRY28	PRY20, Δ*msh2*	This study
PRY36	EBY.VW4000, Δ*trp1*	This study
PRY37	PRY19 Δ*idh2*	This study
PRY38	PRY20 Δ*idh2*	This study
PRY39	CEN.PK2-1C, Δ*gre3*	This study
PRY40	PRY37, Δ*idp2*	This study
PRY41	PRY38, Δ*idp2*	This study

PRY46	PRY39, Δ*pho13*::KanMX	This study
PRY47	PRY48, Δ*pho13*::KanMX	This study
PRY48	PRY39, *pZWF1::pHXT7* *(ZWF1 sequence with loss of glutamate residue at position59)*	This study
PRY49	PRY48, *pPGI1::pCOX9*	This study
PRY50	PRY48, *pPGI1::pRNR2*	This study
PRY51	PRY48, *pPGI1::pREV1*	This study
PRY52	PRY48, Δ*xks1*	This study
PRY53	PRY39, Δ*leu2*::POS5, CloNAT	This study
PRY54	PRY48, Δ*leu2*::POS5 , CloNAT	This study
PRY55	PRY39, Δ*ald6*	This study
PRY56	PRY48, Δ*ald6*	This study
PRY57	PRY40, Δ*idp3*	This study
PRY58	PRY41, Δ*idp3*	This study
PRY59	PRY57, Δ*idp1*	This study
PRY60	PRY58, Δ*idp1*	This study
PRY63	PRY39, *pZWF1::pHXT7* has (*ZWF1* from CEN.PK2-1C)	This study
PRY76	PRY36, *pZWF1::pHXT7*	This study

3.3   Oligonucleotides and synthetic genes

DNA oligomers used throughout the study are mentioned in the Table 3.4. DNA was ordered from Biomers. A stock solution of 100 µM was prepared using water and the volume given by the company. For oligos shorter than 60 base pair, the catridge method of purification was done, and for oligos larger than 60 bp, the HPLC method of purification was done. All synthetic codon-optimized genes from were ordered from Twist Bioscience. For all synthetic genes, codon optimization was done using tool jcat (www.jcat.de, Grote et al. 2005). For GH43-7 codon optimization was done with AK Boles algorithm calculator.

Table 3.4. Oligonucleotides used in this study:

Nomenclature	Sequence (5'- 3')	Purpose
PRP003-MET25ovGRE3-fw	TTCTTGCTCCGTTAAAGTGAACTTTTTTTCGATTTCTAGGCGGATGCAAGGGTTCGAATC	To get PCR product of *pMET25- xylB -tCYC1*
PRP004-CYC1ovGRE3-rev	GTAATATAAATCGTAAAGGAAAATTGGAAATTTTTTAAAGGGGCGAATTGGGTACCGG	To get PCR product of *pMET25- xylB - tCYC1*
PRP007-MET25-rev	CATTTGCCAACCACCACAG	Binds to *pMET25*
PRP_009_GRE3.2_Fw	TGGTTGTAGAATCAAGCCCGGTTTTAGAGCTAGAAATAGCAAGTTAAAATAAGG	To create PRB1
PRP_0010_GRE3.2_Rv	CCGGGCTTGATTCTACAACCAGATCATTTATCTTTCACTGCGGAG	
PRP_0013_ XYLB	AGTATGGATTTTACTGGCTGGA	Binds to terminator of *GRE3*
PRP014_Fw	GCTGCCAAATTGCCGAGGCATAATCACTAAGAAGTTTT	Binds to *tRPL3* with *xylD* overhangs

37

	GTTAGAAAATAAATCATTTT TTAATTG	
PRP_015Rv	GCGTAATACGACTCACTAT AGGGCGAATTGATTGTAGC AAAGATTGTAAGGAAATAG C	Binds to *tRPL3* with *xylD* overhangs for cloning it to p425H7
PRP016_RPL3ORF41ovFw	TCTGAATTCTTGCAAACTT CTGGTATCTAAGAAGTTTT GTTAGAAAATAAATCATTTT TTAATTG	Binds to *orf41* with *tRPL3* overhangs
PRP_017_HXT7Fw	TCTCCTTTCGAAACTTAATA ATAAAACAATATCATCCTTT CGTAGGAACAATTTCGGGC	Binds to *pHXT7* with *MDM34* overhangs (to integrate at *FRA2*)
PRP_018_tRPL3_Rv	TATTGGAATAAGTTTTTCG GTGTTATATATACATATA TATTGTAGCAAAGATTGTA AGGAAATAGC	Binds to *tRPL3* with *NIF3* overhangs (to integrate at *FRA2*)
PRP_019_Orf41Fw	ACAAAAAGTTTTTTTAATTT TAATCAAAAAATGAC	Binds to *orf41* and *pHXT7* in p425 Orf41
PRP_020_Orf41Rv	AAAAAATGATTTATTTTCTA ACAAAACTTCTTAGATAC	Binds to *orf41* and *tRPL3* in p425 Orf41
PRP_021_XylD1Fw	ACAAAAAGTTTTTTTAATTT TAATCAAAAAATGTC	Binds p425XylD connecting both *pHXT7* and *xylD*
PRP_022_XylD1Rv	AATGTCGTAAGCAGCTCTC C	Bind to *xylD* internally
PRP_023_XylD2Fw	TGCTGATGATTGGAGAGCT G	Bind to *xylD* internally
PRP_024_XylD2Rv	AAAAAATGATTTATTTTCTA ACAAAACTTCTTAG	Binds to *xylD* internally
PRP_029_KsaD1_Fw	TTATCTACTTTTTACAACAA ATATAAAACAATGATC	They binds in *pPGK1* and *ksaD* region
PRP_030_KsaD1_Rv	GAAAACTGGGTTAGTAGCA GAC	Internal primer for *ksaD*
PRP_031_KsaD2_Fw	GCTGAAATGTCTGCTACTA ACC	Internal primer for *ksaD*
PRP_032_KsaD2_Rv	AGAATTTTATACTTAGGCTA CAGATCAAAG	They binds in *tEFM*1 region
PRP_033_XylXGG_Fw	TTCAAGCTTACGTCTCG	Binds to *xylX* with GG overhang
PRP_034_XylXGG_Rv	ACCGTTATCTCGTCTCAGG TCGGTCTCAGGATTTATAA CAAACCTCTACCAGC	
PRP_036_MTSGFP_Fw_Xyl Dov	GCTGCCAAATTGCCGAGG CATAATCACTAAGCGGCCG CTGGTGCTGGTTCTAAAGG CGAGGAATTGTTTAC	Binds to GFP with overhangs to *xylD*
PRP_038XyLD_Rv_GFPov	TAAACAATTCCTCGCCTTA GGGTTGTCGCCTAGGCCC GGGTTAGTGATTATGCCTC GGC	Binds to *xylD* with overhangs to linker and GFP
PRP_040_XylD_Fw_ovAcoMt s	GTCTGCTAGATCTGCTATC AAGAGACCAATCGTTAGAG GTTTGATGTCAAACAGAAC TCCGAG	Binds to *xylD* with ACOMTS overhangs
PRP_042_EFM1_Rv_GG	GCTGTGAGACCAGTACTGA AATTCATGACACAAATAAC G	Binds to *tEFM1* with GG overhangs.
PRP_045_XylB_Rv_ gg Part 3	CGTCTCAGGTCGGTCTCA GGATTTATCTCCAGCCTGC ATC	To get GG part3 of *xylB*

PRP_048_KsaD_Fw_ gg part 3	CGTCTCGTCGGTCTCATAT GATCACTGCTACTGC	To get GG part3 of *ksaD*
PRP_049_KsaD_Rv_gg part 3	CGTCTCAGGTCGGTCTCA GGATTTATCTGTCGATTTC TCTTGG	
PRP_050_pMET25Rv_XylDo v	GACCTAAACCTTCTCGGAG TTCTGTTTGACATCAAACC TCTAACGATTGGTCTCTTG ATAGCAGATCTAGCAGACA ACATGAGTATGGATGGGG GTAATAG	Binds to *pMET25* with AcoMTS and *xylD* overhangs
PRP_051_GFPFw_XylDlinker diffov	GCTGCCAAATTGCCGAGG CATAATCACTAACCCGGGC CTAGGCGACAACCCTTCTA AAGGCGAGGAATTGTTTAC	Binds to GFP with linker and *xylD* overhangs
PRP_052_XylDRv_GFPLinke rov	GGAACTACACCTGTAAACA ATTCCTCGCCTTTAGAAGG GTTGTCGCCTAGGCCCGG GTTAGTGATTATGCCTCGG C	Binds to *xylD* with linker + GFP overhangs
PRP_058_Orf41_gg Rv	CGTCTCAGGTCGGTCTCA GGATTTAGATACCAGAAGT TTGCAAG	To get GG part3 of *orf41*
PRP_066_XylDFw_Aco_Ov	AATCAAAAAATGTTGTCTG CTAGATCTGCTATCAAGAG ACCAATCGTTAGAGGTTTG ATGTCAAACAGAACTCCGA G	Binds to *xylD* with overhangs to MTS Aco
PRP_068_XylB_Rv_GFPov	CTACACCTGTAAACAATTC CTCGCCTTTAGAACCAGCA CCAGCGGCCGCTTATCTC CAGCCTGCATC	Binds to *xylB* with GFP overhangs.
PRP_069_Met25_Rv_AcoOv	CAAACCTCTAACGATTGGT CTCTTGATAGCAGATCTAG CAGACAACATGAGTATGGA TGGGGGTAATAG	Binds to *pMET25* with overhangs to MTSAco
PRP_070_GFPRv_linker_ov	GCGGCCGCTGGTGCTGGT TCTAAAGGCGAGGAATTG	Binds to GFP with overhangs to linker
PRP_071_XylXFw_mitaACO mtsov	ATGTTGTCTGCTAGATCTG CTATCAAGAGACCAATCGT TAGAGGTTTGATGGGCGTA TCTGAATTCCTAC	Binds to *xylX* with overhangs to MTS Aco
PRP_072_XylX_rv_mit_linker ov	CTCGCCTTTAGAACCAGCA CCAGCGGCCGCTTATAACA AACCTCTACCAGC	Bind to *xylX* with overhangs to linker
PRP_074_KsaD_Rv_linkerun d mtGFP0v	CTCGCCTTTAGAACCAGCA CCAGCGGCCGCTTATCTGT CGATTTCTCTTGG	Binds to *ksaD* with overhangs to linker and GFP
PRP_075_XylB Fw_MTSACP1ov	ACCTTCTGCGTACCGCACT ATAATGGGCCGTTCCGTTA TGTCCAACACCATACTCGC ACAAAGATTTTATATGTCAT CAGCCATTTATCC	Binds to *xylB* with MTSACP1 overhangs
PRP_077_Met25Rv_MTSAC P1ov	AACGGCCCATTATAGTGCG GTACGCAGAAGGTGCCAC GCGGGAAGAAATGCGGCA AACGGATCTAAACATGAGT ATGGATGGGGGTAATAG	Binds to *pMET25* with MTS*ACP1* overhangs

PRP_078_mtGFP_Fw_newlinkerov	CCCGGGCCTAGGCGACAACCCTTCTAAAGGCGAGGAATTG	Binds to GFP with overhangs to linker.
PRP_079_KsaDFw_mitMtCoX4ov	AGATTTTTCAAGCCAGCCACAAGAACTTTGTGTAGCTCTAGATATCTGCTTATGATCACTGCTACTGC	Binds to *ksaD* with MTS *COX4* overhangs
PRP_081_Met25_Rv_mtCOX4ov	CAAAGTTCTTGTGGCTGGCTTGAAAAATCTTATAGATTGACGTAGTGAAAGCATGAGTATGGATGGGGGTAATAGAATTG	Binds to *pMET25* with overhangs to MTS *COX4*.
PRP_082_Met25_Rv_MTS_LPD1ov	GAAAAGGCACGCTTATTATTTAGGAGTGATCTGATTCTTAACATGAGTATGGATGGGGGTAATAG	Binds to *pMET25* with MTS *LPD1* overhangs
PRP_083_XylX_Fw_Mts_LPD1_ov	ATCACTCCTAAATAATAAGCGTGCCTTTTCGTCCACAGTCAGGACATTGATGGGCGTATCTGAATTC	Binds to *xylX* with *LPD1* MTS overhangs
PRP_084	CCTTTAGAAGGGTTGTCGCCTAGGCCCGGGTTATAACAAACCTCTACCAGC	Binds to *xylX* gene with overhang to a linker
PRP_089_Rv	AACGGCCCATTATAGTGCGGTACGCAGAAGGTGCCACGCGGGAAGAAATGCGGCAAACGGATCTAAACATGAGTATGGATGG	Binds to *pMET25* with MTS *ACP1* overhangs
PRP_090_COX4_MTS_Fw_Met25_ov	GATACAATTCTATTACCCCCATCCATACTCATGCTTTCACTACGTCAATC	Binds to MTS *COX4* with overhangs to *pMET25*
PRP_091_COX4MTS_Rv_KsaD_ov	ACAACCGTGCAAAGCAGTAGCAGTGATCATAAGCAGATATCTAGAGCTACAC	Binds to MTS *COX4* with overhangs to *ksaD*
PRP_092_ACP1_Fw_Met25ov	GATACAATTCTATTACCCCCATCCATACTCATGTTTAGATCCGTTTGCC	Binds to MTS *ACP1* with overhangs to *pMET25*
PRP_093_ACP1MTS_Rv_XylB_ov	CTTTAACGAGGGATAAATGGCTGATGACATATAAAATCTTTGTGCGAGTATGG	Binds to MTS *ACP1* with overhangs to *xylB*
PRP_094_MTSLPD1_Fw_Met25_ov	TACAATTCTATTACCCCCATCCATACTCATGTTAAGAATCAGATCACTCC	Binds to MTS *LPD1* with overhangs to *pMET25*
PRP_095_MTSLPD1_Rv_XylX_ov	ATCTTCAGGTAGGAATTCAGATACGCCCATCAATGTCCTGACTGTGG	Binds to MTS *LPD1* with overhangs to XylX
PRP_096_MTS_ACo_Fw_Met25_ov	ACAATTCTATTACCCCCATCCATACTCATGTTGTCTGCTAGATCTG	Binds to MTS *ACO* with overhangs to *pMET25*
PRP_097_AcoMTS_Rv_XylD_Ov	AAACCTTCTCGGAGTTCTGTTTGACATCAAACCTCTAACGATTGG	Binds to MTS *ACO* with overhangs to *xylD*
PRP_099_XylD_Fw	ATGTCAAACAGAACTCCG	Binds to *xylD* internally
PRP_100_XylD _Rv	TTAGTGATTATGCCTCGG	Binds to *xylD* internally
PRP_101_Orf41_Fw	ATGACTTCTTTGATCTTGCC	Binds to *orf41* internally
PRP_102_ Orf41_Rv	TTAGATACCAGAAGTTTGCAAG	Binds to *orf41* internally

PRP_103_HXT7_Fw_Fra2ov	TCTCCTTTCGAAACTTAATA ATAAAACAATATCATCCTTT CGTAGGAACAATTTCGGG	Binds to *pHXT7* with overhangs to *FRA2*
PRP_104_RPL3_Rv_Fra2ov	TATTGGAATAAGTTTTTCG GTGTTATATATACATATA TATTGTAGCAAAGATTGTA AGGAAATAG	Binds to *tRPL3* with overhangs to *FRA2*
PRP_105_AcoMTS_Rv_ Orf41	CAGAAGATGGCAAGATCAA AGAAGTCATCAAACCTCTA ACGATTGG	Binds to MTS Aco with overhangs to *orf41*
PRP_108_ Orf41_Fw_Aco_ov	GCTATCAAGAGACCAATCG TTAGAGGTTTGATGACTTC TTTGATCTTGCC	Binds to *orf41* with overhangs to MTS Aco
PRP_109_ORF41Rv_GFP_o v	CTCGCCTTTAGAACCAGCA CCAGCGGCCGCTTAGATA CCAGAAGTTTGCAAG	Binds to *orf41* with overhangs to Linker and GFP
PRP_115_KsaD_Rv	AAACAATTCCTCGCCTTTA GAACCAGCACCAGCGGCC GCTTATCTGTCGATTTCTC TTGG	Binds to *ksaD* with linker and GFP overhangs
PRP_116_XylX_Rv_linkOv	AAACAATTCCTCGCCTTTA GAACCAGCACCAGCGGCC GCTTATAACAAACCTCTAC CAGC	Binds to *xylX* with linker overhangs.
PRP_119_XylX_Fw	ATGGGCGTATCTGAATTCC	Binds to *xylX* gene internally
PRP_120_XylX_Rv	TTATAACAAACCTCTACCA GCAAG	Binds to *xylX* gene internally
PRP_138_Fw_pRCCK_msh2 _gRNA	ACGAACTGGTCCGCTCCG TTGTTTTAGAGCTAGAAAT AGCAAGTTAAAATAAGG	To generate PRB21
PRP_139_Rv_msh2_gRNA	CAACGGAGCGGACCAGTT CGTGATCATTTATCTTTCAC TGCGGAG	
PRP_145_ msh2_fw	ATTCTCTGATGTATCAGAG GAG	Binds internally to *MSH2* gene
PRP_146_ msh2_Fw	AGCGGAGTACTCGAAAAG	Binds in promoter region of *MSH2*
PRP_147_ msh2_Rv	TAGAGCCTTATTGCCTTTA GG	Binds to terminator region of *MSH2*
PRP_148_ msh2_Fw_donordna	TTATCTGCTGACCTAACAT CAAAATCCTCAGATTAAAA GTTTAATATTACAACGACAT CTTAAGTGAGAATCGATAG ATA	Donor DNA for the deletion of *MSH2*
PRP_149_ msh2_Rv_donor Dna	TATCTATCGATTCTCACTTA AGATGTCGTTGTAATATTA AACTTTTAATCTGAGGATTT TGATGTTAGGTCAGCAGAT AA	
PRP_151_Lpd1_Fw_gg_part 3	CGTCTCGTCGGTCTCATAT GTTAAGAATCAGATCACTC C	Binds to *xylX* with *LPD1* part 3 overhangs
PRP_152_AcoFw_gg part 3	CGTCTCGTCGGTCTCATAT GTTGTCTGCTAGATCTGC	Binds to MTS *ACP1* with part3GG overhangs
PRP_153_ACP1_Fw_part3_ gg	CGTCTCGTCGGTCTCATAT GTTTAGATCCGTTTGCC	
PRP_154_rad27_Fw_Donor dna	CATTGGAAAGAAATAGGAA ACGGACACCGGAAGAAAA AATGGGGGTTCTTTTTCCA	Donor DNA for *RAD27* deletion (PRP154+PRP176)

	CTTTCTTCTTTTGGTCCTTC ACCT	
PRP_155_rad27_Fw	AGATCTAAACAAAATGCTG TCAC	Binds to promoter region of *RAD27*
PRP_156_ rad27_Rv	TGAAGGACCAAAAGAAGAA AG	Binds to terminator region of *RAD27*
PRP_157_Fw_ Rad27_gRNA	CTGTAAGACAGCAAGACG GTGTTTTAGAGCTAGAAAT AGCAAGTTAAAATAAGG	To generate PRB20
PRP_158_Rv_ Rad27_gRNA	ACCGTCTTGCTGTCTTACA GGATCATTTATCTTTCACT GCGGAG	
PRP_160_Fw_pGK1_ura3_o v	GTGAGTTTAGTATACATGC ATTTACTTATAATACAGTTT TTTGTTTGCAAAAGAACA AAACTG	Binds to *pPGI* overhang at *URA3* region
PRP_161_tEFM1_ov_ura3_R v	ACTGCACAGAACAAAAACC TGCAGGAAACGAAGATAAA TCTACTGAAATTCATGACA CAAATAACG	Binds to *tEFM1* overhang to *URA3* region
PRP_162_Leu2_Fw_ovpTEF 1	TAAAGTTTATGTACAAATAT CATAAAAAAAGAGAATCTT TCCTTGCCAACAGGGAG	Binds to *pTEF1* with overhangs to *LEU2* locus
PRP_163_tGPM1_ov Leu2	AGCAATATATATATATATAT TTCAAGGATATACCATTCT ATATTGCTATAACATGTCAT GTCACC	Binds to *tGPM1* with overhangs to *LEU2* locus
PRP_170_Gre3del_donordna _Fw	TTGTTCATATCGTCGTTGA GTATGGATTTTACTGGCTG GACTTTAAAAAATTTCCAAT TTTCCTTTACGATTTATATT AC	Donor DNA to delete *GRE3*
PRP_171_ Gre3_Donor_Dna_Rv	GTAATATAAATCGTAAAGG AAAATTGGAAATTTTTTAAA GTCCAGCCAGTAAAATCCA TACTCAACGACGATATGAA CAA	
PRP_176_Rad27_DonorDNA _Rev	AGGTGAAGGACCAAAAGA AGAAAGTGGAAAAAGAACC CCCATTTTTTCTTCCGGTG TCCGTTTCCTATTTCTTTCC AATG	Donor DNA for *RAD27* deletion.
PRP_178_ Gre3_Fw	TTCTTGGTGAGTGAATCAT TTCAG	Binds to outer region of *GRE3* gene
PRP_179_ Gre3_Rv	AGGCTCTAGAAACTGTATG AGTATATC	
PRP_191_pRCCK_IDH2_Fw	CTTAGAGGTCTCAGATCCC CTTCTACCGGCAAATACAG TTTTGAGACCGACGTCCTG	To generate PRB43
PRP_192_pRCCK_IDH2_Rv	CAGGACGTCGGTCTCAAAA CTGTATTTGCCGGTAGAAG GGGATCTGAGACCTCTAAG	
PRP_193_IDH2_donor Dna _Fw	ACAGATCGGGAACGAACA ACAATTATAATATTTTTTAA TAAAGTCCTATTCTTTTCCC TCTCAGGTTTTTTCACGCC TTG	Donor DNA for deleting *IDH2*
PRP_194_IDH2_donor dna Rv	CAAGGCGTGAAAAAACCTG AGAGGGAAAAGAATAGGA	

	CTTTATTAAAAAATATTATA ATTGTTGTTCGTTCCCGAT CTGT	
PRP_197_IDP1_donor dna_Fw	CAATTGTGAGACAACAGAC GCACAAGGAAGATCGCCC AGCTCGAATTTACGTAGCC CAATCTACCACTTTTTTTTT TCAT	Donor DNA to delete *IDP1*
PRP_198_IDP1_donor dna_Rv	ATGAAAAAAAAAGTGGTA GATTGGGCTACGTAAATTC GAGCTGGGCGATCTTCCTT GTGCGTCTGTTGTCTCACA ATTG	
PRP_199_pRCCK_IDP2_Fw	ATCCGCTTATGTTACTACC GGTTTTAGAGCTAGAAATA GCAAGTTAAAATAAGG	To get PRB48
PRP_200_pRCCK_IDP2_Rv	CGGTAGTAACATAAGCGGA TGATCATTTATCTTTCACTG CGGAG	
PRP_201_IDP2_donordna_F w	GGAGGTAAGAAGGTAACG TACGTATATATATAAAATCG TAACTTACTCAATGACAGA TTGATTTATTTATATTATAT ATT	Donor DNA To delete *IDP2*
PRP_202_IDP2_donordna_R v	AATATATAATATAAATAAAT CAATCTGTCATTGAGTAAG TTACGATTTTATATATATAC GTACGTTACCTTCTTACCT CC	
PRP_203_IDH2_Fw	ACCAAACACAAACAACGAC	Binds to promoter region of *IDH2*
PRP_204_IDH2_Rv	TTATTAAAAAATATTATAAT TGTTGTTCGTTCC	Binds to promoter region of *IDH2*
PRP_205_IDP1_Fw	AGGACGATGTCCATGATG	Binds to promoter of *IDP1*
PRP_206_IDP1_Rv	TAAATTCGAGCTGGGCG	Binds together promoter and terminator of *IDP1*
PRP_207_IDP2_Fw	ATGGAAGTCGTCAATAGC	Binds to the promoter of *IDP2*
PRP_208_IDP2_Rv	AGTAAGTTACGATTTTATAT ATATACGTACG	Binds to the terminator of *IDP2*
PRP_217_GRE3_Fw_HXT7o v	AAACACAAAAACAAAAAGT TTTTTTAATTTTAATCAAAA AATGTCTTCACTGGTTACT C	Binds to not codon optimized sequence of *GRE3* with overhangs to *pHXT7*
PRP_218_GRE3_Rv-tcyc1ov	GGAGGGCGTGAATGTAAG CGTGACATAACTAATTACA TGATCAGGCAAAAGTGGG G	Binds to not codon optimized sequence of *GRE3* with overhangs to *tCYC1*
PRP_221_CpXYL1- Codopt_Fw_pHXT7_ov	AACACAAAAACAAAAAGTT TTTTTAATTTTAATCAAAAA ATGTCTACTGCTACTGCTT C	Binds to Cp *XYL1* with overhang to *pHXT7*
PRP_222_CpXYL1_Codopt_ Rv_tcyc1ov	GGAGGGCGTGAATGTAAG CGTGACATAACTAATTACA TGATTAAACGAAAACTGGG ATGTTAG	Binds to Cp *XYL1* with overhang to *tCYC1*
PRP_223_Ps_XYL1_codopt_ Fw_pHXT7ov	AAACACAAAAACAAAAAGT TTTTTTAATTTTAATCAAAA AATGCCATCTATCAAGTTG AAC	To create PRB45

PRP_224_Ps-XYL1-Codopt_Rv-tcyc1_Ov	GGAGGGCGTGAATGTAAGCGTGACATAACTAATTACATGATTAAACGAAGATTGGGATCTTG	
PRP_228_IDP2_Rv	TCAGTGAAAACAGAAGATCATATG	Binds to terminator of *IDP2*
PRP_229_AnXyrB_Fw_pHXT7ov	AAACACAAAAACAAAAAGTTTTTTTAATTTTAATCAAAAAATGTCTAACTTGGAACACACTAAG	Binds to An *XYRB* with overhangs to *pHXT7*
PRP_230_AnXyrB_Rv_tcyc1ov	GGAGGGCGTGAATGTAAGCGTGACATAACTAATTACATGATTATTCGTCGTCACCGAAG	Binds to An *XYRB* with overhangs to *tCYC1*
PRP_231_pHHF2_Fw_ura3ov	GTGAGTTTAGTATACATGCATTTACTTATAATACAGTTTTTGTGGAGTGTTTGCTTGG	Binds to *pHHF2* with overhangs to *URA3* region
PRP_232_tADH1_Rv_pTDH3ov	TCTTTGAAATGGCAGTATTGATAATGATAAACTCGAACTGGAAATGGGGAGCGATTTGC	Binds to *tADH1* with overhangs to *pTDH3*
PRP_233_pTDH3_Fw_tENO1ov	CGGCATGCCGAGCAAATGCCTGCAAATCGCTCCCCATTTCCAGTTCGAGTTTATCATTATCAATACTG	Binds to *pTDH3* with overhangs to *tADH1*
PRP_234_tENO1_Rv_ura3ov	CTGCACAGAACAAAAACCTGCAGGAAACGAAGATAAATCATACATGGGTGACCAAAAGAG	Binds to *tENO1* with overhangs to *URA3* locus
PRP_237_pREV1 _pPGI1	TGTCACCGTCAGAAAAATATGTCAATGAGGCAAGAACCGGGTGTTGTTATCCGATACAACCG	Binds to *pREV1* with overhangs to *pPGI1* region
PRP_238_pREV1ov_pPGI1	CAGTGGCCAGTTTGAAGTTAGTGAATGAGTTATTGGACATCGCTGGATATGCCTAGAAATG	Binds to *pREV1* with overhangs to *PGI1* gene
PRP_239_pRNR2_Fw_pPGI1ov	TGTCACCGTCAGAAAAATATGTCAATGAGGCAAGAACCGGAGTCGAACAAGAAGCAGG	Binds to *pRNR2* with overhangs to *pPGI1* region
PRP_240_pRNR2_Rv_ov_pPGI1	CAGTGGCCAGTTTGAAGTTAGTGAATGAGTTATTGGACATGGTAATTGGACAAATAAATACGTG	Binds to *pRNR2* with overhangs to *PGI1* gene
PRP_241_pREV1_Rv	TGAGAAAATCTGTCAACTCGTTAC	Binds to promoter region of *pREV1*
PRP_242_pRNR2_Rv	TGGATTCTTTGGTAGATAGCCAATC	Binds to promoter *pRNR2*
PRP_243_Gre3codpt_Fw_pHXT7ov	AAACACAAAAACAAAAAGTTTTTTTAATTTTAATCAAAAAATGTCTTCTTTGGTTACTTTGAAC	Binds to *GRE3* with overhangs to *pHXT7*
PRP_244_Gre3codopt_Rv-tcyc1ov	GGAGGGCGTGAATGTAAGCGTGACATAACTAATTACATGATTAAGCGAAAGTTGGGAACTTAC	Binds to *GRE3* with overhangs to *tCYC1*

PRP_245_LBGV071-Xks1_Crispr_Fw	CTTAGAGGTCTCAGATCATCTAGAGCCTCTAACCACAGTTTTGAGACCGACGTCCTG	To create PRB67
PRP_246_LBGV071_Xks1_CRISPR_Rv	CAGGACGTCGGTCTCAAAACTGTGGTTAGAGGCTCTAGATGATCTGAGACCTCTAAG	
PRP_247_ XKS1_Donor DNA_fw	CTCTCGAGAAAAACAAAAGGAGGATGAGATTAGTACTTTAAATATGTTTGAATAATTTATCATGCCCTGACAAGTACACA	Donor DNA for the deletion of *XKS1* gene
PRP_248_XKS1_Donor DNA_Rv	TGTGTACTTGTCAGGGCATGATAAATTATTCAAACATATTTAAAGTACTAATCTCATCCTCCTTTTGTTTTTCTCGAGAG	
PRP_249_IDP3_donordna_Fw	AAACACAAGCAACACTTTAGAGATAGTTGTCCAAGTTAAAACCAATCCGCCATTCATTTGAAAAGACAAGTCTGGCCTAG	Donor DNA for the deletion of *IDP3*
PRP_250_IDP3_DonorDna_Rv	CTAGGCCAGACTTGTCTTTTCAAATGAATGGCGGATTGGTTTTAACTTGGACAACTATCTCTAAAGTGTTGCTTGTGTTT	
PRP_251_pIDP3_Fw	ACATGACAAATCCAGAAGTATCG	Binds to promoter region of *IDP3*
PRP_252_tIDP3_Rv	TTGCATTATGCGATGATTGTAGG	Binds to terminator region of *IDP3*
PRP_255_pCOX9_Fw	ATGAGTCCCTCTTTATATGGGC	Binds to *pCOX9* internally.
PRP_256_XKS1_Rv	TCCGAACGGGGAACAAAATG	Binds internally to *XKS1*
PRP_257_IDP3.2_CRISPR_guide_Fw	CTTAGAGGTCTCAGATCGATATTGCCATATTTAGATGGTTTTGAGACCGACGTCCTG	To generate PRB56 (worked)
PRP_258_IDP3.2_CRISPR_guide_Rv	CAGGACGTCGGTCTCAAAACCATCTAAATATGGCAATATCGATCTGAGACCTCTAAG	
PRP_259_XylD _CRISPR_guide_Fw	CTTAGAGGTCTCAGATCATAGCTGCTAGAAAACAAGAGTTTTGAGACCGACGTCCTG	To generate PRB55
PRP_260_XylD_CRISPR_guide_Rv	CAGGACGTCGGTCTCAAAACTCTTGTTTTCTAGCAGCTATGATCTGAGACCTCTAAG	
PRP_261_IDP3_Fw	AGCATGCTTAATGCCGAATC	Binds to promoter region of *IDP3*
PRP_262_IDP3_Rv	TTCTTTCATTCTTGCCTCATCG	Binds internally to *IDP3*
PRP_263_XylDdel_donorDNA_fw	AACACAAAAACAAAAAGTTTTTTTAATTTTAATCAAAAAGAAGTTTTGTTAGAAAATAAATCATTTTTTAATTGAGCATT	Donor DNA to delete *xylD*
PRP_264_XylDdel_DonorDNA_Rv	AATGCTCAATTAAAAAATGATTTATTTTCTAACAAAACTTCTTTTTGATTAAAATTAAA	

	AAAACTTTTTGTTTTTGTGTT	
PRP_275_CRISPR_Pho13_Fw	CTTAGAGGTCTCAGATCAACAGCTGACGCATAACCAGGTTTTGAGACCGACGTCCTG	To generate PRB54
PRP_276_CRIPSR_Pho13_Rv	CAGGACGTCGGTCTCAAAACCTGGTTATGCGTCAGCTGTTGATCTGAGACCTCTAAG	
PRP_279_pUG6K_Pho13ov_Fw	TATCAAGCTCGAGCCAAATCACAAAAAAAGCCTTATAGCTTGCCCTGACAAAGAATATACAACTCGGGAAATTCGTACGCTGCAGGTCGAC	For deleting *PHO13* via kanMX cassette.
PRP_280_pUG6K_Pho13ov_Rv	AAAACAACAAACCTGAATATTTTTCCTTTTCAAAAAGTAATTCTACCCCTAGATTTTGCATTGCTCCTGCATAGGCCACTAGTGGATCTG	
PRP_284_NcCDT2_pHXT7ov_Fw	AAACACAAAAACAAAAAGTTTTTTTAATTTTAATCAAAAAATGGGCATCTTCAACAAGAAG	To generate PRB60 and PRB61
PRP_285_NcCDT2_tcyc1_Rv	GGAGGGCGTGAATGTAAGCGTGACATAACTAATTACATGATCAAGCAACAGACTTGCC	
PRP_286_NcCDT2_Fw	TTTGGCACCAACTACATCAAC	Internal primer to bind in NcCDT2
PRP_287_NcCDT2_Rv	AACTCAAACTGGACGGTG	
PRP_288_pRNR2-Fw	AATACAACGAGTCGAACAAG	Binds to the promoter *pRNR2*
PRP_289_POS5_Rv	TTATGCTCCTTAAAATCAAACGG	Binds internally to *POS5*
PRP_290_POS5_Fw	AAGTTCCTCCGGTTTTAGC	Binds internally to *POS5*
PRP_295_SiHV138_XylX_Fw	CTTAGAGGTCTCAGATCATTCAGGATAGGGATACCCCGTTTTGAGACCGACGTCCTG	To create PRB67
PRP_296_SiHV138_XylX_Rv	CAGGACGTCGGTCTCAAAACGGGGTATCCCTATCCTGAATGATCTGAGACCTCTAAG	
PRP_297_XylX del_donordna_Fw	TAAAGTTTATGTACAAATATCATAAAAAAAGAGAATCTTTTAGAATGGTATATCCTTGAAATATATATATATATTGCT	Donor DNA to delete *xylX*
PRP_298_XylXdel_Donordna_Rv	AGCAATATATATATATATTTCAAGGATATACCATTCTAAAAGATTCTCTTTTTTTATGATATTTGTACATAAACTTTA	
PRP_299_IDP1_Fw	AAAAGTAATCAATCGAGGCC	Binds to outer region of gene *IDP1*
PRP_300_IDP1_Rv	TGATAAAGGGACCGTGAATG	
PRP_301_IDP1_Fw	ATCTGTCGAATCTCGTGACG	Binds internally to *IDP1*
PRP_302_IDP1_Rv	TGTCTTTGAACCGACCGTC	Binds internally to *IDP1*

PRP_303_CRISPR_TRP1_Fw_GG	CTTAGAGGTCTCAGATCAACTGCATGGAGATGAGTCGGTTTTGAGACCGACGTCCTG	To create PRB63
PRP_304_CRISPR_TRP1_Rv_GG	CAGGACGTCGGTCTCAAAACCGACTCATCTCCATGCAGTTGATCTGAGACCTCTAAG	
PRP_305_Donor DNA_TRP1del_Fw	GTGAGTATACGTGATTAAGCACACAAAGGCAGCTTGGAGTGTTATTACTGAGTAGTATTTATTTAAGTATTGTTTGTGCA	Donor DNA for the deletion of *TRP1* gene
PRP_306_Donor DNA_TRP1del_Rv	TGCACAAACAATACTTAAATAAATACTACTCAGTAATAACACTCCAAGCTGCCTTTGTGTGCTTAATCACGTATACTCAC	
PRP_307_TRP1_Fw	ATCTGGTGAATCCTTTGAAGG	Binds to the outer region of *TRP1* gene
PRP_308_TRP1_Rv	TCCTGATTCCGCTAATAGG	
PRP_309_CRSPR_Fw_SiHV138	CTTAGAGGTCTCAGATCGCTACGGACACACTGATCCCGTTTTGAGACCGACGTCCTG	To generate PRB62
PRP_310_CRISPR-Rv_SiHV138	CAGGACGTCGGTCTCAAAACGGGATCAGTGTGTCCGTAGCGATCTGAGACCTCTAAG	
PRP_313_ZWF1_Rv_tcyc1ov	AATGTAAGCGTGACATAACTAATTACATGACTAATTATCCTTCGTATCTTCTGGCTTAG	Binds to *ZWF1* with overhangs to *tCYC1*
PRP_314_TRP1_Fw	TCCATTGGTGAAAGTTTGC	Binds to the internal region of *TRP1* gene
PRP_315_TRP1_Rv	TACACCATTTGTCTCCACAC	
PRP_316_pHXT7_Leu2ov_Fw	TAAAGTTTATGTACAAATATCATAAAAAAAGAGAATCTTTCTCGTAGGAACAATTTCGG	Binds to *pHXT7* overhang to terminator of *LEU2*
PRP_317_ALD6_ovtSSA1_Rv	AAAGAAAAAAATTGATCTATCGATTTCAATTCAATTCAATTTACAACTTAATTCTGACAGCTTTTAC	Binds to *ALD6* with overhangs to *tPGK1*
PRP_318_tSSA1_ALD6ov_Fw	TGCATACACTGAAGTAAAAGCTGTCAGAATTAAGTTGTAAATTGAATTGAATTGAAATCGATAG	Binds to *tPGK1* with overhang to *ALD6*
PRP_319_tSSA1_Leu2ov_Rv	AGCAATATATATATATATATTTCAAGGATATACCATTCTAACATAGAAATATCGAATGG	Binds to *tPGK1* with overhang to *pLEU2*
PRP_320_pHXT7_Rv_Pho13_ov	TATTGGTTATCTTTATTGGTACACCTTGTTGAGCAGTCATTTTTTGATTAAAATTAAAAAAACTTTTTGTTTTTG	Binds to *pHXT7* overhang to *PHO13*
PRP_321_Pho13_Rv	TTATTGGTTAAGGTGTAGATGTC	Binds to *PHO13* internally
PRP_322_Pho13_Rv_tSSA1ov	AAAGAAAAAAATTGATCTATCGATTTCAATTCAATTCAAT	Binds to *PHO13* overhang to *tPGK1*

	CTATAACTCATTATTGGTTA AGGTG	
PRP_323_tSSA1_Pho13ov_Fw	ACTTGGTGACATCTACACC TTAACCAATAATGAGTTATA GATTGAATTGAATTGAAAT CGATAG	Binds to *tPGK1* overhang to *PHO13*
PRP_324_GH43-2_Fw	ATGGCTCCATTGATCACTC AC	Internal primer for gene GH43-2
PRP_325_GH43-2_Rv	TCACTTACCAGCTGGTTGC	Internal primer for gene GH43-2
PRP_326_GH43-2_pMET25_ov_Fw	GTCGTCAGATACATAGATA CAATTCTATTACCCCCATC CATACATGGCTCCATTGAT CACTCAC	To create PRB64
PRP_327_GH43-2_tcyc1_ov_Rv	GAGGGCGTGAATGTAAGC GTGACATAACTAATTACAT GATCACTTACCAGCTGGTT GC	
PRP_328_AHY02_XylXdeleti on_donordna_Fw	GTTCTGTATGGGCACAGAC AACCTAAACGAGATCTATC CTAACTCGAGGCTGAGCA GTTACAGAGATGTTACGAA CC	Donor DNA to delete *xylX* in AHY02
PRP_329_AHY02_XylXdeleti on_donor dna_Rv	GGTTCGTAACATCTCTGTA ACTGCTCAGCCTCGAGTTA GGATAGATCTCGTTTAGGT TGTCTGTGCCCATACAGAA C	
PRP_330_CRISPRGG_GDH 1del_Fw	CTTAGAGGTCTCAGATCAC AACCCTTGGAGTCAGATAG TTTTGAGACCGACGTCCTG	To create PRB73
PRP_331_GGCRISPR_GDH 1del_Rv	CAGGACGTCGGTCTCAAAA CTATCTGACTCCAAGGGTT GTGATCTGAGACCTCTAAG	
PRP_332_GDH1_Fw	ACATCCACTCAGGTCATTA TTCTC	Binds to promoter of *GDH1*
PRP_333_GDH1_Rv	TGTCTGTTGATGCTTTACA AAACTAC	Binds to terminator of *GDH1*
PRP_334_GDH1_Fw	TCTTTTCGAACAACACCCA G	Binds to *GDH1* internally
PRP_335_GDH1_Rv	AAGACCTTACCGTCCTTAG TG	Binds to *GDH1* internally
PRP_336_CRISPRKsaDdel_ Fw	CTTAGAGGTCTCAGATCTA GCTGGGTATGGACCACCG GTTTTGAGACCGACGTCCT G	To create PRB72
PRP_337_CRISPRKsaDdel_ Rv	CAGGACGTCGGTCTCAAAA CCGGTGGTCCATACCCAG CTAGATCTGAGACCTCTAA G	
PRP_338_donordna_KsaD del_Fw	GTGAGTTTAGTATACATGC ATTTACTTATAATACAGTTT TGATTTATCTTCGTTTCCTG CAGGTTTTTGTTCTGTGCA GT	Donor DNA for deletion of *ksaD*
PRP_339_KsaDdel_donordn a_Rv	ACTGCACAGAACAAAAACC TGCAGGAAACGAAGATAAA TCAAAACTGTATTATAAGTA	

	AATGCATGTATACTAAACT CAC	
PRP_340_pUG6N_XylX del_Fw	TAAAGTTTATGTACAAATAT CATAAAAAAAGAGAATCTT TTTCGTACGCTGCAGGTCG AC	primer to amplify pUG6N for integrating G418 in *xylX*
PRP_341_pUG6N_XylXdel_ Rv	AGCAATATATATATATATAT TTCAAGGATATACCATTCT AGCATAGGCCACTAGTGG ATCTG	
PRP_342_GDH1del_donor dna_fw	TATTCTAATATAACAGTTAG GAGACCAAAAGAAAAAGA AATAGTCTAAAAGAAAGAA AAGAGGAAAGTTCATAAAA AGT	To introduce donor DNA for the deletion of *GDH1*
PRP_343_GDH1del_donordn a_Rv	ACTTTTTATGAACTTTCCTC TTTTCTTTCTTTTAGACTAT TTCTTTTTCTTTTTGGTCTC CTAACTGTTATATTAGAATA	
PRP_344_PsXYL1_R276H_F w	AAAGTCTAACACTGTTCCA CACTTGTTGGAAAACAAGG ACGTTAAC	To introduce RH mutation in Ps *XYL1*. i.e, to make PRB75
PRP_345_PsXYL1_R276H_ Rv	GTTAACGTCCTTGTTTTCC AACAAGTGTGGAACAGTGT TAGACTTT	
PRP_346_PsXYL1_KR/ND mut_Fw	ATCGCTATCATCCCAAGAT CTGACACTGTTCCAAGATT G	To introduce KR/ND mutation in Ps *XYL1*. i.e, to make PRB74
PRP_347_PsXYL1_KR/ND mut_Rv	CAATCTTGGAACAGTGTCA GATCTTGGGATGATAGCGA T	
PRP_348_AHY02_KsaDdel_ donordna_Fw	CAAAAACAACAATCAATAC AATAAAATAAGATCTATCCT AACTCGAGGCGAATTTCTT ATGATTTATGATTTTTATTA TT	Donor DNA for the deletion of *ksaD* in AHY02
PRP_349_AHY02_KsaDdel_ donordna_Rv	AATAATAAAAATCATAAATC ATAAGAAATTCGCCTCGAG TTAGGATAGATCTTATTTTA TTGTATTGATTGTTGTTTTT G	
PRP_350_TPNOX_pMET25o vFw	GTCAGATACATAGATACAA TTCTATTACCCCCATCCAT ACATGAAGGTTACTGTTGT TGG	To create PRB76
PRP_351_TPNOX_tcyc1ov_ Rv	GGAGGGCGTGAATGTAAG CGTGACATAACTAATTACA TGACTAAGCGTTAACAGAT TGAGC	
PRP_352_GH43- 7_pHXT7ov_Fw	AAACACAAAAACAAAAAGT TTTTTTAATTTTAATCAAAA AATGCCATTGGTCAAGAAC C	All these primers used to create PRB77 (i.e, to introduce *pHXT7-* GH43-7- *tSSA1* into PRB64)
PRP_353_GH43- 7_tSSA1ov_Rv	AAAGACATTTTCGTTATTAT CAATTGCCGCACCAATTGG CTTATTCGTTGTCTCTAAC GTAAGC	
PRP_354_GH43-7_fw	AGAAAAGCACGTTTTGACC TC	

PRP_355_pHXT7_tcyc1ov_Fw	GCTCGAAGGCTTTAATTTGCGGCCGGTACCCAATTCGCCCCGTAGGAACAATTTCGGG	
PRP_356_pHXT7_tGH43-7_ov_Rv_	CCTGGCAAGATTGGGTTCTTGACCAATGGCATTTTTTGATTAAAATTAAAAAAACTTTTTGTTTTTG	
PRP_357_tSSA1_Rv	AAAACGACGGCCAGTGAGCGCGCGTAATACGACTCACTATAATAAAATTAAAGTAGCAGTACTTCAACC	
PRP_358_tSSA1_GH43-7ov_Fw	TAAGAACCAACAAGATGCTTACGTTAGAGACAACGAATAAGCCAATTGGTGCGGC	
PRP_359_p424_tSSA1_ov_Fw	GCTAACACTAATGGTTGAAGTACTGCTACTTTAATTTTATTATAGTGAGTCGTATTACGCGCGC	
PRP_360_tcyc1_pHXT7ov_Rv	ACCTCAGAAGAACACGCAGGGGCCCGAAATTGTTCCTACGGGGCGAATTGGGTACC	
PRP_361_GH43-7_Fw	GAACCAACAAGATGCTTACGTTAGAGACAACGAATAA	Internal primer to bind on GH43-7
PRP_362_GH43-7_Rv	TTATTCGTTGTCTCTAACGTAAGCATCTTGTTGGTTC	Internal primer to bind on GH43-7

3.4 Chemicals, enzymes and kits

Reagents, enzymes, and kits used and their respective company are listed in table 3.17. If not stated differently, all other chemicals were bought from Roth. Table 3.18 lists all the devices details with the respective supplier company.

Table 3.17: List of chemicals, enzymes and kits used throughout the study

Product	Producer
Bacterial trypton	Difco
Bacteriological peptone	Oxoid
Carbenicillin	Roth
Chloramphenicol	Roth
ClonNAT (Nourseothricin)	Werner BioAgents
DNA loading dye	NEB, Fermentas
dNTPs	NEB
DreamTaq, incl. buffer	NEB
G418-sulfate, Geneticin	Calbiochem
Geneticin (G418)	Merck
Glass beads (0.45 mm)	Roth
Glucose-6-phosphate	Roth
Kanamycin sulfate	Roth
Maltose	Difco

MgCl$_2$	Roth
β-Nicotinamide-adenine-dinucleotide phosphate disodium hydrate (NADP$^+$)	Roche
β-Nicotinamide-adenine-dinucleotide phosphate disodium hydrate (NADP$^+$)	Roche
PEG-4000	Roth
PEG-8000	Roth
Phusion DNA polymerase, incl. buffer	NEB
Q5 DNA polymerase, incl. buffer	NEB
Restriction enzymes, incl. buffer	NEB
Roti-Quant	Roth
Sheared salmon sperm DNA	Ambion
Synthetic oligonucleotides	biomers, microsynth
T4 DNA ligase	NEB
T7 DNA ligase	NEB
Taq DNA ligase	NEB
Tris-HCl	Roth
Yeast extract	Difco
Yeast nitrogen base (YNB) w/o amino acids and w/o ammonium sulfate	Difco
Xylobiose	TCI chemicals
Kits:	
GeneJET Plasmid Miniprep kit	Thermo Scientific
NucleoSpin Gel and PCR clean up	Macherey-Nagel
Pierce™ Rapid Gold BCA Protein Assay Kit	Thermo Scientific

Table 3.18. Devices used in study:

Device	**Producer**
Agarose gel-electrophoresis chambers	Neolab
Cell electroporator, Gene Pulser	Bio-Rad
Cell growth quantifier	Aquila Biolabs
Fluorescence spectrophotometer, *CLARIOstar Plus*	BMG LABTECH
Incubator	Multitron Standard, Infors HT
Nanodrop 1000 spectrophotometer	Thermo Fisher Scientific
PCR Cycler, labcylcler triple block	SensoQuest
PCR Cycler, Piko thermal cycler	Finnzymes
pH-meter 765 Calimatic	Knick
Pipette, 0.1-2.5 µL	starlab
Pipette, 0.5-10 µL	starlab
Pipette, 10-100 µL	starlab
Pipette, 100-1000 µL	starlab
Shaker	Infors HT
Spectrophotometer Ultrospec 2100 pro	Amersham Bioscience
Thermomixer comfort	eppendorf
Vibrax VXR basic	IKA

Rotating wheel	Stuart SB1, Woodely equipment Company

HPLC system	
BioLC	**Producer/ Model no.**
Pump system	LPG-3400SD, Thermo Scientific
Autosampler	WPS-3000SL, Thermo Scientific
Column oven	TCC-100, Thermo Scientific
Degasser	SRD3400, Thermo Scientific
RI-detector	RI-101, Thermo Scientific
Wave length detector	VWD-3400RS, Thermo Scientific
Ultimate3000:	
Autosampler	WPS-3000SL, Thermo Scientific
Column oven	TCC-3000SD, Thermo Scientific
Pump system	ISO-3100SD, Thermo Scientific
Degasser	SRD3200, Thermo Scientific
RI-detector	RI-101, Thermo Scientific
Columns	
HPLC column, ICSep 801 FA, HPLC-column 250x4.0mm	Concise Separations

3.5 Microorganism culture

3.5.1 Cultivation of *Saccharomyces cerevisiae*

The culture of *Saccharomyces cerevisiae* was done in a specified medium according to the need of the experiment. Liquid cultures were shaken in an orbital shaker at 180 rpm at 30 °C. Solid media were incubated at 30 °C.

3.5.2 Culture media

Generally, YP medium was used for the culture of yeast cells. Sterile sugar solutions were always added after the autoclaving. To prepare plates, 20 g/L agar or agarose was used prior to autoclaving.

Table 3.5 Composition of YP medium:

Bacto peptone	20 g/ L
Bacto yeast extract	10 g/ L
Carbon source	20 g/ L

3.5.2.1 Synthetic complete medium for *Saccharomyces cerevisiae* cultivations

Synthetic complete medium known as SC was used for culture experiments that involved selection of auxotrophic markers. Stock solutions of amino acid mix were prepared as 20X stock except uracil (ura), leucine (leu), histidine (his) and tryptophan (trp) as these are the often employed auxotrophic markers. Solid media were prepared with 20 g/L of agar or agarose according to the requirement of the experiment and added to the media prior to autoclaving but after the pH adjustment.

Table 3.6 SC Media composition

Yeast nitrogen base w/o amino acids and ammonium sulfate	1.7 g/L
Ammonium sulfate	5 g/L
20X Amino acid mix	50 mL/L
Carbon source	10-20 g/L

pH was maintained at 6.3 by addition of KOH except mentioned in the text.

Relevant carbon source was added only after autoclaving.

Table 3.7 Preparation of 20 X amino acid mix

Compound	mg/L in H_2O	Concentration in the 20X mix [mM]	Concentration In the medium [mM]
Adenine	224	1.66	0.083
Arginine	768	4.41	0.221
Methionine	768	5.15	0.258
Tyrosine	288	1.59	0.080
Isoleucine	1152	8.78	0.439
Lysine	1152	7.88	0.394
Phenylalanine	960	5.81	0.291
Valine	1152	9.83	0.492
Threonine	1152	9.67	0.484

The mix were autoclaved and store at 4 °C.

Table 3.8 Supplement amino acid stock solutions:

Substance	mg/L in H$_2$O	Concentration in the SL [mM]	ml SL per liter of medium	Final conc. in the medium [mM]	Storage condition
Uracil	1.2	10.71	16	0.171	RT
Histidine	2.4	15.47	8	0.124	4 °C
Tryptophan	2.4	11.57	8	0.093	4 °C
Leucine	3.6	27.44	16	0.439	4 °C

3.5.3   Antibiotic supplements

Certain cultivations required special additives of antibiotics. Antibiotics like Carbenicillin, Chloramphenicol, Kanamycin were used for *E. coli*, whereas G418, CloNAT were employed for yeast. Stock solutions of respective antibiotics were prepared, sterile filtered and added to the medium after autoclaving when the media temperature reached maximally 65 °C. The following list provides information about the concentrations and preparations.

Table 3.9: Medium additives for growth and selection of bacterial and yeast strains.

Medium supplement	Stock solution	Final concentration
Carbenicillin	100 mg/mL in ddH$_2$O	100 µg /mL
Chloramphenicol	34 mg/mL in 70% (v/v) ethanol	34 µg /mL
ClonNAT (Nourseothricin)	100 mg/mL	100 µg /mL
Geneticin (G418)	200 mg/mL	200 µg /mL
Hygromycin B	200 mg/mL	200 µg /mL
Kanamycin sulfate	50 mg/mL in ddH$_2$O	50 µg /mL

3.6   Microorganisms culture techniques

3.6.1   Sterilization techniques

For all the heat-sensitive chemicals and reagents, a sterile filter was used with a pore diameter of 0.2 µm. Substances resistant to higher temperatures were sterilized using an autoclave running for 20-45 min at a temperature of 120 °C and pressure of 1 bar.

3.6.2 Cultivation and storage of microorganisms

3.6.2.1 Cultivation on solid medium

Bacterial and yeast strains were either streaked on agar plates from their glycerol stock or regenerated from single colonies from earlier plate. The media preparation and supplementation procedure was followed as listed in chapter 3.5.2. Bacterial strains (*E. coli* DH10B) were cultivated at 37 °C for 1 day while the appearance of colonies of yeast required 2-7 days depending on the strain employed. If needed, solid cultures of them were stored at 4 °C for up to 4 weeks.

3.6.2.2 Liquid culture of microorganisms

To cultivate *E. coli*, the inoculum derived either from glycerol stock or fresh culture, was inoculated in 5 ml LB medium in 10 ml glass tubes with appropriate antibiotic added and thereafter shaken at 37 °C 180 rpm min^{-1} in an orbital shaker overnight. Yeast strains were cultivated in YP or SC media with the required carbon source and antibiotics. The revival of cells from cryopreserved stock for yeasts was done followed by single colony isolation and thereafter processed with liquid cultivation of yeast. If yeast cells need to be cultured for DNA isolation, cultures were done in a 10 ml glass tube with 5 ml media inside. For the fermentation and growth experimental works, yeast was generally pre -cultured in a 100 ml flask with 30 ml media inside. The main culture was done in a 300 ml flask with 50 ml media inside, except mentioned specifically. In case of yeast competent cell preparation, culture was done in 100 ml flask with 50 ml media inside. Media compositions and tables of supplements are listed in chapter 3.5.

3.6.2.3 Drop test

For the drop test, preculture was done by scrapping several colonies from the transformation plate. They were grown in SC drop-out liquid media until OD_{600nm} reached 1-3. After this culture was centrifuged at 3000x g for 2 min, the pellet was washed with sterile water and centrifuged again. The washing step was repeated once. Then, the cell pellet was mixed with water, and OD_{600nm} was measured. The OD_{600nm} was adjusted to 1; from this, dilution was performed to 10^{-1}, 10^{-2}, and 10^{-3}. Agarose-containing plates were generally prepared a week before and stored at 4 °C. Before starting the drop test, agarose plates were dried out in a laminar hood for 2-3 hours. Afterward, 4 µl of samples were dropped on to plates and let dry for 15 minutes. Later, for yeast, the plates were incubated at 30 °C. Images for drop test were processed using Vision Capt Viber Lourmat (from Peqlab.com).

3.6.2.4 Measurement of cell density

In order to track the growth of microorganisms, absorbance is measured with OD_{600nm} value measured in a spectrophotometer using a light of wavelength λ=600 nm. Dilution of the samples was made if necessary.

3.6.2.5 Long term storage of microorganisms

If the genetically modified bacterial or yeast strain needs to be stored for longer, cryopreservation techniques were followed. For this, 500 µL of well-grown culture was thoroughly mixed with 50 % (v/v) sterile glycerol in cryo tubes, mixed well, and thereafter stored at -80 °C.

3.7 Molecular biological techniques

3.7.1 Polymerase chain reaction for DNA- amplification

One of the most frequently used molecular techniques is PCR. Amplification of DNA was done by PCR using oligomers of suitable annealing temperature. For cloning purposes, primarily the DNA polymerases Q5 High- Fidelity DNA Polymerase (Chapter 3.7.1.1) and Phusion High-Fidelity DNA Polymerase (Chapter 3.7.1.2) from New England Biolabs were chosen since they have a proofreading activity. Most of the PCRs in the present study were done with Q5 polymerase. For DNA amplification, other than cloning, which only aims to approximate the band size, the DNA-polymerase DreamTaq DNA Polymerase (Chapter 3.7.1.3) from Thermo Fisher Scientific was used.

3.7.1.1 Q5 high-fidelity DNA polymerase PCR procedure

The Q5 high-fidelity DNA polymerase was used for DNA amplifications involved in cloning and DNA sequencing. After the PCR run, the PCR reaction was mixed with the Loading Dye, Purple (6X) from New England Biolabs and analyzed via agarose gel electrophoresis in a 1 % agarose gel.

Table 3.10: Reaction mix for Q5 DNA polymerase.

Component	Stock solution	Concentration in mix	Volume used
Q5 Reaction buffer	5X	1X	10 µL
dNTPs	10 mM	200 µM	1 µL
Primer mix	10 µM each	0.5 µM each	2.5 µL
Q5 DNA polymerase	2000 U mL^{-1}	1 U	0.3 µL
Template		10-20 ng	

Volume was added up to 50 µL with ddH$_2$O.

Table 3.11: PCR conditions for standard PCR protocol using Q DNA polymerase.

Step	Temperature	Duration	Function
1	98 °C	30 s	Denaturation of DNA
2	98 °C Tm 72 °C	10 s 20 s 30 s per kb	Denaturation of DNA Primer annealing DNA extension
3	72 °C	5 min	Final extension

Preheated lid of the thermocycler to 96 °C, step 2 was repeated 30 times and stored at 10 °C.

The online tool NEB Tm Calculator of New England Biolabs was used to calculate the annealing temperature (T$_m$) of the primer pair used. In general, primers were designed to melt at 60 °C to accumulate a highly versatile set of primers which can be individually combined throughout this study.

3.7.1.2 Phusion high- fidelity DNA polymerase PCR procedure

The Phusion high-fidelity DNA polymerase was used for DNA amplifications involved in cloning and DNA sequencing, whenever PCR with Q5 reaction failed for any reasons. After the run, the PCR reaction was mixed with the Gel Loading Dye, Purple (6X) from New England Biolabs and analyzed via agarose gel electrophoresis in a 1 % (w/v) agarose gel.

Table 3.12 Reaction mix for Phusion DNA polymerase

Component	Stock solution	Concentration in mix	Volume used
Phusion HF buffer	5X	1X	10 µL
dNTPs	10 mM	200 µM	1 µL
Primer mix	10 µM each	0.5 µM each	2.5 µL
Phusion DNA polymerase	2000 U/ mL	1 U	0.3 µL
Template		10-20 ng	

volume was added up to 50 µL with ddH$_2$O

Table 3.13 PCR conditions for standard PCR protocol using Phusion DNA polymerase.

Step	Temperature	Duration	Function
1	98 °C	30 s	Denaturation of DNA
2	98 °C Tm 72 °C	10 s 20 s 30 s per kb	Denaturation of DNA Primer annealing DNA extension
3	72 °C	5 min	Final extension

The online tool NEB Tm Calculator of New England Biolabs was used to calculate the annealing Temperature (T_m) of the primer pair used. In general, primers were designed to melt at 60 °C to accumulate a highly versatile set of primers that can be individually combined throughout this study.

3.7.1.3 DreamTaq DNA polymerase PCR procedure

The DreamTaq DNA polymerase was used for diagnostic purposes where the amplicon can be less accurate with the nucleotide sequences. The buffer used for the Dream Taq was 10X DreamTaq Green Buffer which already contains loading dye for later analysis via agarose gel electrophoresis in a 1 % agarose gel.

Table 3.14: Reaction mix for Dream Taq DNA polymerase.

Component	Stock solution	Concentration in mix	Volume used
Q5 Reaction buffer	5X	1X	10 µL
dNTPs	10 mM	200 µM	1 µL
Primer mix	10 µM each	0.5 µM each	2.5 µL
Q5 DNA polymerase	2000 U/ mL	1 U	0.3 µL
Template		10-20 ng	

volume was added up to 20 µL with ddH$_2$O.

Table 3.15: PCR conditions for standard PCR protocol using Dream Taq DNA polymerase.

Step	Temperature	Duration	Function
1	98 °C	30 s	Denaturation of DNA
2	98 °C T_m-5 °C 72 °C	10 s 20 s 30 s per kb	Denaturation of DNA Primer annealing DNA extension
3	72 °C	5 min	Final extension

Preheated lid of the thermocycler to 96 °C, step 2 was repeated 35 times and stored at 10 °C.

The online tool T_m Calculator of Thermo Fisher Scientific was used to calculate the annealing temperature of the primer pair used.

3.7.2 Agarose gel electrophoresis for DNA analysis

Gel electrophoresis is a commonly used technique to separate DNA fragments by applying an electric field to move them through an agarose gel. As DNA has a negative charge, applying a voltage causes the negatively charged fragments to migrate towards the positively charged electrode. The voltage and duration of separation are adjusted based on the size of the DNA fragments being separated, with a 135 mV voltage for 30 minutes typically used for isolating DNA fragments ranging from 500 bp to 5000 bp. In this study, the DNA samples were mixed with New England Biolabs' Gel Loading Dye, Purple (6X), and placed onto a 1 % (w/v) agarose gel in 1X TAE buffer. The size of the DNA fragments was estimated using Thermo Fisher Scientific's Gene Ruler 1kb Plus DNA Ladder, which was applied next to the DNA samples in the gel and placed according to the required specifications.

Table 3.16: 1x TAE-buffer

TRIS	40 mM
EDTA	1 mM

pH was adjusted to 8 with acetic acid

3.8 Molecular biological techniques

3.8.1 Plasmid assembly

The successful expression of heterologous genes in the host organism, *S. cerevisiae*, is reliant on the construction of plasmids derived from other organisms. Plasmid construction involves either the creation of an *E. coli* intermediate plasmid or an *E. coli*-yeast shuttle vector depending on the experimental requirements. Golden Gate part plasmids are typically constructed using *E. coli* origin of replication, while yeast expression plasmids requires either 2µ or CEN.ARS origin of replication. Similarly, the *E. coli*-yeast shuttle vectors comprise *E. coli* ori and either 2µ or CEN.ARS plasmids. Mainly, three techniques were adopted in constructing the plasmids: Homologous Recombination cloning, Gibson Isothermal assembly, and Golden Gate cloning.

3.8.2 Golden Gate assembly

Golden Gate cloning is a rapid and efficient method for combining various plasmid parts in a tube. The method involves the use of Type II restriction enzymes, digestion, and ligation to obtain different variants of cassettes in a short period. One of the benefits of this method is its ability to screen cassettes via GFP-based fluorescence. In this study, the instructions outlined in the literature Lee et al. 2015 for Golden Gate assembly were followed, but used Esp3I instead of BsmBI due to its better temperature optima ranging from 37 °C to 55 °C. BsaI-HFv2 was another enzyme used in the cloning process, with both enzymes and buffers obtained from New England Biolabs. The standard protocol for Golden Gate cloning is outlined in Tables 3.17 and 3.18, unless otherwise specified.

Table 3.17: Golden Gate assembly mix.

Component	Stock Solution	Concentration in Mix	Volume used
T4 ligase buffer	10X	1X	1 µL
Type IIS endonuc. (BsaI/Esp3I)	10 000- 20 000 U/mL	5-10 U	0.5 µL
T7 DNA ligase	3 000 000 U/ mL	1 500 U	0.5 µL
DNA (each piece)	variable	50 ng	

volume was added up to 5 µL with ddH$_2$O

Table 3.18: Conditions of Golden Gate assembly.

Repeats	Temperature	Duration	Function
1x	37 °C	10 min	Initial digestion
25x/15x	37 °C 16 °C	1.5 min 3 min	Digestion Annealing and ligation
1x	37 °C	5 min	Digestion
1x	50 °C	5 min	Digestion and ligase inactivation
1x	80 °C	10 min	Inactivation

preheated lid of the thermocycler to 96 °C, stored at 10 °C

The assembly step was repeated 15 times for reactions up to 5 parts, while reactions of 6 and more parts were repeated 25 times.

In case the parts to be assembled contained internal recognition sites of BsaI or Esp3I, the assembly was performed using the modified Golden Gate protocol. This protocol reduces the digestion temperature to 34 °C, and the final digestion step is skipped.

3.8.3   Gibson isothermal assembly

Gibson assembly is an enzymatic method for assembling DNA molecules *in vitro*, as described by Gibson et al. 2009. The method involves digestion of DNA with an exonuclease, annealing of single-stranded DNA, closure of gaps between strands by DNA polymerase, and ligation by DNA ligase. To assemble plasmids, a 50 ng backbone DNA was mixed with up to five other DNA fragments at a molar ratio of up to 1:3. This DNA mixture was added to a 2X Gibson isothermal assembly master mix (5 µl) and ddH$_2$O to make a total volume of 10 µl. The reaction mix was incubated at 50 °C for 1 hr and transformed with about 3 µl into the *E. coli* strain DH10B. After selection on appropriate plates, the correct assembly was verified by restriction digest and sequencing.

Table 3.19: The solution of the Gibson mix recipe is mentioned below:

PEG-8000	25 %
Tris-HCl, pH 7.5	500 mM
MgCl2	50 mM
DTT	50 mM
dNTP	1 mM
NAD	5 mM

Stored at -20 °C

Table 3.20: 2X Gibson isothermal assembly master mix.

Isothermal reaction buffer	1 X
T5 exonuclease	10 U/ µL
Taq DNA ligase	40 U/ µL
Phusion DNA polymerase	2 U/ µL

store 5 µL aliquots at -20 °C

3.8.4   Yeast homologous recombination cloning

Using host *Saccharomyces cerevisiae* for plasmid cloning with *E.coli-* yeast shuttle vector is a high-efficiency cloning method. This is a useful tool where synthetic enzymes are not required, and yeast employs its own machinery for cloning the respective gene when selection pressure is applied. For this, about 30-40 bp homologous overhangs were transformed into yeast using transformation protocol (described in chapter 3.8.10). Following the transformation, cells were plated in specified media and incubated for about 3-4 days at 30 °C. Once cells grew, colonies were scrapped from the plate, and DNA isolation was done. 1 µl of yeast DNA was then transformed to electro competent *E. coli* for segregation of plasmid. Thereafter, *E. coli* was grown in specified antibiotic-containing media. The culture was then used for the preparation of individual plasmid, and verifications of plasmids were done via restriction digestion and then sequencing.

3.8.5   Preparation and transformation of electro-competent *Escherichia coli* cells

For the preparation of electrocompetent *E. coli* cells, 5 mL preculture of LB-medium was inoculated with a single colony of *E. coli* DH10B from a plate. The preculture was incubated at 37 °C and 180 rpm^{-1}. From the preculture, a 30 °C prewarmed 1 L baffled shake flask containing 400 mL LB medium was inoculated and incubated at 30 °C until an OD_{600nm} of 0.6-0.7 was reached. After this, the culture was transferred to precooled 50 mL tubes, and the culture was cooled in ice for 30 min. The cells were centrifuged at 4000x g and 4 °C for 15 min. To wash the cells, the cells were resuspended in 25 mL ice-cold ddH_2O and pooled into 50 mL suspensions, which were centrifuged at 4000x g and 4 °C for 15 min. This washing step was repeated until the culture could be condensed in one 50 mL tube. Washing of cell pellet was done in 4 mL 10 % (w/v) ice-cold sterile glycerol and centrifuged at 4000x g and 4 °C for 15 min. The cells were resuspended in 4 mL 10 % (w/v) ice-cold sterile glycerol aliquoted to 50 µL each and frozen at -80 °C directly.

For the transformation of *E. coli*, 1 μl of DNA or 20 ng of DNA was put on the surface of frozen electrocompetent cells, and the solution was let to unfreeze. Thereafter, the cell DNA mixture was mixed and transferred to a sterile electroporation cuvette, and an electric pulse of 2.5 kV was applied to the gene Pulser from BioRad (settings: electrical resistance 200 Ω, capacity 25 μF). These electroporated cells were then incubated at 37 °C for 1 hr to recover the electrical stress and to express the genetic marker. Thereafter culture was centrifuged at max speed at room temperature for 30 sec. Culture supernatant was all removed except 30 μl. This remaining culture was mixed and then spread plated in LB with appropriate antibiotics.

3.8.6   Preparation of plasmid DNA from *Escherichia coli* cells

The GeneJET Plasmid Miniprep Kit from Thermo Scientific was used to isolate plasmid DNA from *E. coli* cells. The procedure was performed according to the protocol supplied with the kit.

3.8.7   Preparation of genomic DNA from *Saccharomyces cerevisiae* cells

Genomic DNA isolation of yeast cells was done by harvesting the cell pellet from overnight culture or scrapping colony directly from the plate. For harvesting the cells, a centrifugation was done at 3000x g for 2 min. Cells were then washed with sterile water and then resuspended with 400 μl buffer 1. It was mixed well by vortexing, and further lysis was done by 400 μl Buffer 2. After mixing, about three full PCR tubes, glass beads (∅ 0.25 - 0.5 mm), and 8 minutes of shaking on a VXR basic Vibrax (IKA) at max speed at room temperature, the supernatant was obtained by centrifuging the mix at a max speed of 4 °C. Thus, obtained supernatant was carefully removed by pipette and transferred to a fresh tube. In this, 325 μl of cold YP-buffer 3 was added, and the sample was vortexed and then incubated on ice for 10 minutes to precipitate proteins and other contaminants. The sample was centrifuged (10 - 15 min, 4 °C, 16000x g), 700 μl of the supernatant was transferred to a fresh Eppendorf tube, and 700 μl isopropanol was added. After mixing vigorously, the sample was incubated for 10 minutes at RT to allow precipitation of the DNA, which was then pelleted by centrifugation (≥ 30 min, RT, 16000x g). The DNA pellet was washed twice with 500 μl of cold (-20 °C) 70 % (v/v) ethanol, with centrifugation steps of 5 minutes at RT and max speed, then dried at RT for 10 minutes and dissolved in 15 – 30 μl sterile ddH$_2$O depending on the size of the DNA pellet. Thus obtained DNA was stored at -20 °C until further use.

Table 3.21: Composition of buffer 1.

EDTA (Titriplex III)	10 mM
Tris-HCl, pH 8	25 mM
RNase A*	100 µg/ mL

autoclaved and stored at 4 °C

*added after autoclaving

Table 3.22: Composition of buffer 2.

NaOH	0.2 M
SDS	1 % (w/v)

stored at room temperature

Table 3.23: Composition of buffer 3.

Potassium acetate	3 M

pH adjusted to 5.5 and stored at 4 °C

3.8.8   Quick preparation of genomic DNA from *S. cerevisiae* cells for PCR-based applications

Freshly grown yeast cells were taken from solid media with the help of a sterile wooden tip and mixed well in 100 µL of the extraction solution consisting of 200 mM lithium acetate and 1 % SDS (w/v). In the case of liquid culture, available 100 µL yeast culture (OD$_{600nm}$ ≥ 0.4) was mixed with 100 µL of the extraction solution. It is strictly recommended not to use high cell biomass. The extraction mix was thoroughly mixed and incubated for more than 10 min at 70 °C. For precipitating the DNA, 300 µL 96 % (v/v) ethanol was added, thoroughly mixed, and centrifuged at 15000x g for 3 min. The supernatant was removed, and 500 µL 70% (v/v) ethanol was added. The mixture was centrifuged at 15000x g for 3 min, and the supernatant was discarded. The sediment was suspended in 100 µL ddH$_2$O and centrifuged at 15000x g for 1 min to transfer the DNA-containing supernatant into a new reaction tube. After this, the tube was allowed to dry by heating it at 70 °C for 10 min or until the ethanol evaporated completely. For general use, 1 µL was used for a 25 µL PCR. This protocol was developed by Lõoke et al. 2011.

3.8.9 DNA sequencing

To obtain high-quality sequencing results, purified DNA was used for both plasmid DNA and PCR products. DNA purification was conducted using the NucleoSpin Gel and PCR clean-up kit from Macherey-Nagel. After DNA purification, DNA concentration was measured, and samples were sent for sequencing. For PCR products, the amount of DNA sent for sequencing was determined based on the size of the amplicon, with a recommended amount of 18 ng/100 bp in a total volume of 15 µL mixed with 2 µM primers. For plasmid DNA, 500-800 ng of DNA was sent in a total volume of 15 µL mixed with 2 µM primers. Sequencing reactions were outsourced to Microsynth Seqlab, which uses the Sanger chain-termination method.

3.8.10 Yeast cell transformation

Yeast transformation was carried out with the heat shock method. A single colony was inoculated in 50 ml YP medium in a 100 ml shaking flask. If the strain is slow growing, the preculture duration is extended until they develop an OD_{600nm} of 1-3. Once the appropriate OD_{600nm} was reached, the cells were sedimented at 3000x g for 2 min and washed in 25 ml of sterile water. The mix was then centrifuged at 3000x g for 2 min. The supernatant was discarded, and the cell pellet was dissolved in 500 µl sterile water and transferred to a 2 ml tube. The centrifugation was repeated at 3000x g for 2 min, and the supernatant was discarded. The pellet was then mixed with water to make aliquots of 50 µl total volume in fresh ep tube, making 5 OD_{600nm} equivalents of cells in each. The aliquot was centrifuged at 3000x g for 30 sec, and the supernatant was discarded. For the transformation, 240 µL 50 % (w/v) PEG 4000, 36 µL 1M lithium acetate, 10 µL ssDNA (salmon sperm), and 500-1000 ng DNA in 54 µL ddH$_2$O were added to the cells and mixed thoroughly with a pipette. After this, a one-hour heat shock was performed at 42 °C. Transformation employing only auxotrophic markers was directly spread on the plate. In the case of dominant markers, recovery of 3 hrs was made in the YP media with the required carbon source. In the multi-plasmid transformation involving auxotrophic and dominant markers, regeneration was done in SC selective media omitting amino acids according to the requirements. Afterward, cells were harvested by centrifugation at 3000x g for 30 sec, the supernatant was removed, and mixed well with 30 µl water, and plated in desired media. The plate was incubated at 30 °C for 3-4 days.

3.8.11 Mitochondrial expression of genes

Mitochondrial expression of the genes in yeast was performed by tagging mitochondrial

targeting sequence (MTS) into the N terminus of the protein sequence. The actual localization of protein was confirmed through the GFP tag at the C terminus of protein and verification of the fluorescence in mitochondria. For this, mitotracker (MitoTracker™ Red CMXRos M7512) - a dye that stains mitochondria was used, and the alignment of GFP fluorescence with the red fluorescence of mitotracker was operated.

3.8.11.1 Preparation of Mitotracker

The solution of the mitotracker was prepared using DMSO as a solvent. A stock solution of 4X mitotracker was prepared by mixing 50 µg of mitotracker with 94.07 µl of DMSO to give a final concentration of 1 mM. To stain the mitochondria, a working solution of mitotracker was used 250 nM. A solution containing a mitotracker was always handled in the dark as the substance was light-sensitive. 20 g/L of galactose (G) was used as a sugar source for the growth of yeast cells.

3.8.11.2 Preparation of samples for confocal microscopy

Yeast cells were precultured in low fluorescence Yeast nitrogen base with ammonium sulfate containing 20 g/L galactose. Cells were grown at 30 °C, 180 rpm overnight. Precultures were then centrifuged 3000x g for 2 min followed by inoculation of cell pellet to 5 ml of the same growth media used before. Cells were left to grow at 30 °C, 180 rpm for 3 hrs. After this, the mitotracker was added to a final concentration of 250 nM and incubated at 30 °C, 180 rpm for 20 min. This was followed by washing cells in sterile dd H_2O and resuspending in SCG (with 2 % galactose) after the second wash in water. If necessary, sample dilution was done to make a better distance between the cells under the microscopic observation. The 5 µl of samples were then transferred to the microscopic slide and observed under confocal microscopy.

3.8.12   Enzyme activity assays

The activity of certain yeast enzymes was measured using a method based on the principle of reagents absorbing specific wavelengths of light. This method relies on the fact that the increase or decrease of light absorption occurs at a specific wavelength that reflects the activity of a protein. Typically, microbial reactions involving cofactors NADH and NADPH absorb light at a wavelength of 340 nm. For reactions involving visible chromogenic differences in reactants or products, the wavelength was chosen to suit the absorbance of the compound. The choice of synthetic substrate and cofactor was dependent on the in-vivo metabolic route for the activity measurement.

3.8.12.1 Preparation of cell extracts

Inoculated from a suitable preculture, a 50 mL yeast culture was grown in 300 ml flask to an OD_{600nm} of 1-2. Standard growth condition for yeast was employed i.e, 30 °C at 180 rpm. Equal OD_{600nm} units of cells (100-150) were harvested at 3000x g for 2 min at room temperature for different samples in comparision. After that, cells were washed with 25 ml of sterile water and sedimented. If needed, the cells were stored at -80 °C for up to one week. In approximately the same volume of the sedimented cells, assay buffer and glass beads were added. Disruption of the cells was performed in the Vibrax VXR basic for 10 min at 4 °C and maximum speed. The disrupted cells were centrifuged for 5 min at 4 °C and 13000x g, and the supernatant was transferred to a fresh tube. This cell extract was stored on ice continuously. Using BSA as a standard, the protein concentration was estimated by BCA assay. Concentration of cell extract values obtained from BCA assay were normalized to those obtained from UV spectrophotometer 2100 at a wavelength of 280 nm to get a more accurate value of protein concentration. Protocol for BCA assay kit was referred to product manual (Thermo Scientific, Pierce™ Rapid Gold BCA Protein Assay Kit). A cOmplete™ EDTA-free protease inhibitor Cocktail from Merck was always added to the assay buffer to prevent proteolysis during the course of experiment. Specific activity was calculated in unit of µmol/min mg.

3.8.12.2 Enzymatic activity test of the Glucose-6-P dehydrogenase

Zwf1 - dependent reaction utilizes $NADP^+$ as a cofactor to convert Glucose -6 P to 6PGL. Thus, using substrate Glucose 6-P, and cofactor $NADP^+$, cell extract can be examined for the production of NADPH *in vitro*. The enzyme assay to measure Zwf1 activity was performed in imidazole buffer (Table 3.24) and measured at 340 nm. 0.25 mM glucose-6-phosphate, 500 µM $NADP^+$, and 10 µl protein extract were used in a total volume of 200 µl.

Table 3.24: Imidazole buffer 1X:

Imidazole	50 mM
MgCl2	10 mM
KCl	100 mM
EDTA	0.1 mM

pH was adjusted to 7.

3.9   High performance liquid chromatography

To monitor the metabolic products of the *S. cerevisiae* strains cultured, samples were taken and analyzed via HPLC. The samples were prepared by centrifugation of 1 ml culture in 1.5 ml Ep tube, at max speed for 15 minutes, from which 450 µl supernatant was taken and mixed with 50 % sulfosalicylic acid in an HPLC vial. A volume of 10 µl was required for HPLC injection. NucleoGel Sugar 810 FA from Concise Separations was a column equipped for the HPLC analysis. Xylonate was measured in BioLC on a UV at wavelength of 210 nm. For measurement of xylose in a mixture of xylose and xylonate, net amount of xylose was obtained by subtracting the UV_{210nm} measured xylonate from RI peak of xylose. This step is essential for the correct estimation of xylose because the RI peak of xylose and xylonate overlapped completely. Beside this, all other sugar and metabolites were measured in Ultimate HPLC. A standard curve was obtained using concentrations of 50 g/L, 20 g/L, 10 g/L, 1 g/L, 0.1 g/L, 0.01 g/L, and 0.001 g/L. Separation of constituents were executed with a column temperature of 30 °C and a flow rate of 0.4 mL/min of 0.5 mM H_2SO_4. The Chromeleon software from Thermo Scientific was used to operate the HPLC system and perform the analysis.

3.10   Evolutionary engineering of strains

Evolutionary Engineering of strains was done in a 300 ml flask with a 50 ml volume. The media used were SC selective media maintained at pH 5.5 with potassium phosphate buffer. For AKG based evolution experiment, the media used were SC with 1 % maltose at a pH of 6.3. Xylose /galactose, and glutamate/maltose were added, as mentioned in the result section. Batch cultures were from time to time transferred to fresh media by washing two times with 25 ml sterile water. Initial OD_{600nm} was generally maintained at 0.2 - 0.4. Glycerol stock was stored from culture to culture by centrifuging the cells and taking a dense amount of cells to maintain viability at -80 °C. The cells were mixed with 500 µl of 50 % glycerol and mixed well, thereafter stored at -80 °C. Possible contaminations were checked with microscopic analysis or genomic verification of some strain specific yeast genes.

3.10.1   Isolation of pure clones from evolutionary engineering samples

Pure clones from evolutionary samples were obtained by isolating a single colony using solid culture media. For this, evolutionary samples were streaked out in YPD agar containing plates. From this, three different colonies were taken, and each was restreaked

out two subsequent times in same agar media to ensure the clones to be genetically pure ones. The one which grows the best on xylose was chosen as a starting clone to examine reverse engineering of the evolved strain. This specific clone was also cryopreserved at -80 °C with preparation of glycerol stock.

3.11 Xylitol export test

For the preculture, yeast transformants were allowed to grow in SC media without uracil, leucine, histidine, tryptophan, and methionine for about 20 hours until they reached the exponential phase (OD_{600nm} of 0.7-1.5). Methionine was omitted from the media to rule out any repression effect on *pMET25* regulated expression of GH43-2. 10 g/L of maltose was employed as a carbon source. A 100 ml flask was employed with 25 ml media inside for the preculture. Cells were harvested by centrifugation at 3000x g for 2 min, washed once with sterile water, and centrifuged again. The obtained pellet was then dissolved in about 5ml of the same media used for pre-culture. From this, inoculation was done to 1 ml total volume of SC-ura-leu-his-trp-met supplemented with 10 g/L maltose, and 10 g/L xylobiose. Xylobiose was purchased from TCI chemicals (CAS RN: 6860-47-5, X0067). All fermentation was carried out in a 2 ml tube with 1 ml of total volume in triplicates. The culture was then shaken in a rotating wheel (Stuart SB1 Tube Rotator, Woodely equipment Company), rotating at 35 rpm, to maintain the equal distribution of cells in the media. The culture was measured with OD_{600nm} and HPLC samples were taken from time to time. Due to the small volume of culture experiment, HPLC samples were prepared by taking 100 µl from the culture, centrifuged at maximal speed for 15 minutes, and 45 µl supernatant was mixed with 5 µl sulfosalicylic acid (50 % w/v). Samples are then processed for the HPLC quantification of xylose, xylitol, and xylobiose.

4 Results

The primary goal of this thesis is to investigate the metabolic and biochemical pathways in *Saccharomyces cerevisiae* with the aim of enabling the yeast to utilize xylose, a pentose sugar, for either growth or the production of xylitol, a commercially valuable compound.

The initial aim of the thesis was to modify *S. cerevisiae's* metabolism to enable it to metabolize xylose through the Weimberg pathway, leading to α-ketoglutarate (AKG) production. However, since the engineered strains were incapable of using xylose as a carbon source, evolutionary engineering was employed, which involved limiting sugar or amino acid environments. Multiple rounds of evolution led to the development of clones that could grow solely on xylose. But, finally, the functional expression of Weimberg pathway could not be verified, and it remained unclear if the growth of the evolved clones were solely due to the activity of Weimberg pathway.

The second part of the PhD thesis aims to optimize the conversion of D-xylose sugar to the commercially valuable compound xylitol. Here, the effectiveness of various glucose/xylose transporters was tested for xylitol transport, assessing both influx and efflux aspects of the transporters, as well as their inhibition effect by other common sugars. Additionally, several heterologous reductases were tested for their catalytic activity in *S. cerevisiae*, examining the influence of cofactor availability on the reaction and exploring ways to maximize intracellular NADPH through modification of gene expression.

4.1 Expression of Weimberg pathway genes in *Saccharomyces cerevisiae*

To create the working strain for the oxidative Weimberg pathway, three different heterologous genes -*xylB*, *xylD*, and *xylX*- were taken from the freshwater bacterium *Caulobacter crescentus*. Gene *ksaD* was employed from *Corynebacterium glutamicum*, and *orf41* was obtained from *Arthrobacter nicotinovorans*. All the genes were obtained as a synthetic codon-optimized DNA to ensure its high expression in *S. cerevisiae*. The first gene, *xylB* was expressed via a 2μ plasmid or genomically integrated into the *GRE3* locus. Activity of the codon optimized *xylB* in *S. cerevisiae* in all engineered strains expressing *xylB* was confirmed by the production of xylonate, when measured with HPLC (result not shown). A 2μ plasmid based expression would make a high rate of conversion of xylose to xylonate, which is a first intermediate of Weimberg pathway. Similarly, genomic integration of *xylB* contributes to a stable expression of the gene. Due to xylonate being a toxic molecule for yeast, to maintain optimal level of xylonate production these two different

modes of expression were tested. All other genes of the pathway were expressed via a high copy number plasmid. Thus, transformed strains, as shown in Figure 4.1, were examined for their ability to grow in xylose as a carbon source. As seen in Figure 4.1, expression of the heterologous genes does not lead to the growth of strains in xylose as a sole carbon source. Cell viability was verified by adding glucose to the non-growing cells at 200 hours.
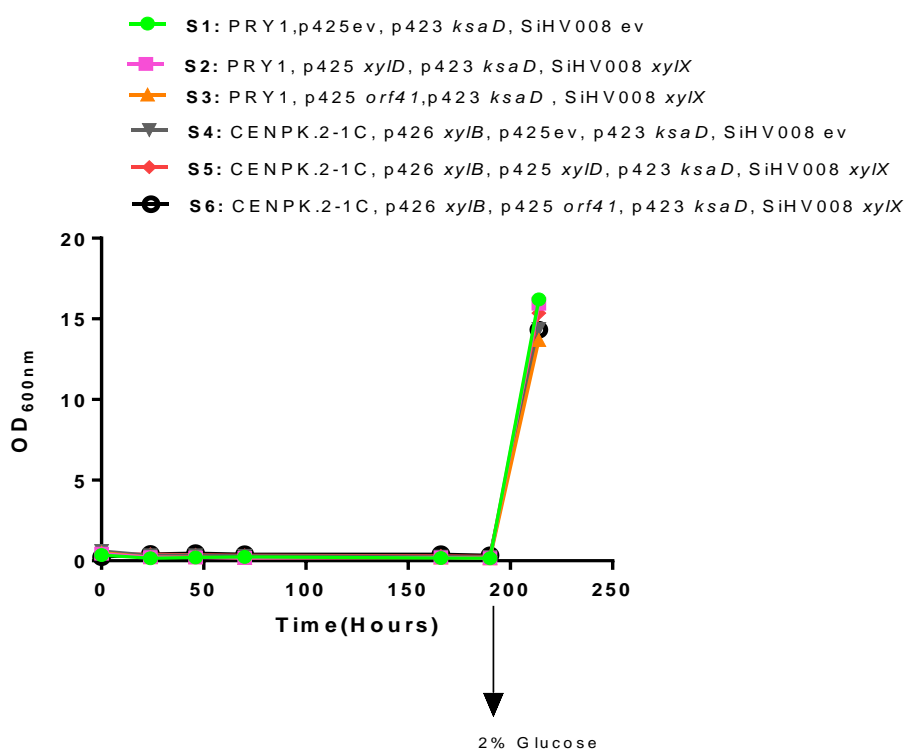

Figure 4.1: Transgenic strains expressing Weimberg pathway genes grown in SC selective media with 2 % xylose as a sugar source until 200 hours. Culture was spiked with 2 % glucose at 200 hours. Transformants S1, S2, and S3 are on strain background PRY1 (CEN.PK2-1C, *Δgre3*) whereas, S4, S5, S6 are strain background CEN.PK2-1c wild type. All plasmids used are 2µ based.

Some possible limitations of Weimberg pathway reported are:

1. Toxic effect of first intermediate product xylonate.

2. Limited activity of XylD due to inadequate supply of [4Fe-4S] cluster in the cytosol.

3. Lack of detailed knowledge of the expression of the other genes of the pathway.

4. The compartmentation of xylose generated AKG and its transport across the mitochondrial membrane to reach the TCA cycle.

5. Other unknown phenomena at the transcriptional or translational level.

To overcome the aforementioned challenges and address the cellular limitations to achieve optimal pathway functionality, an approach of evolutionary engineering was employed, as a collective and non-specific approach. The method involved applying selection pressure in xylose to direct the cell population towards evolution. In order to facilitate the evolution towards AKG production from xylose, three modifications were made to the strains before applying evolutionary pressure. Firstly, to increase the possibility of introducing mutations in the genome, mutator strains were created by deleting some crucial genes for DNA replication (*RAD27*) or mismatch repair system (*MSH2*) (Loeillet et al. 2020). As a second approach, a strain was created with concomitant expression of pathway genes in cytoplasm and mitochondria. As a final strategy for detecting the AKG molecule produced, a glutamate auxotrophic strain was made by deleting genes responsible for converting isocitrate to AKG in different localizations of the cell. Thus generated AKG detection strains were applied for the selection pressure to grow in xylose as an AKG source.

4.1.1   Yeast mutator strains – Evolutionary engineering

Deletion of *RAD27* and *MSH2* is reported to make yeast vulnerable to mutation due to the defect in replication and DNA repair machinery (Loeillet et al. 2020). Mutator strains PRY24, PRY25, PRY27, and PRY28 were constructed on the strain backgrounds PRY19 and PRY20 via deletion of *RAD27* or *MSH2*, as listed in table 3.3. Testing of the Msh2 mutagenic effect was done in the strain PRY25 and PRY28 by observing the frequency of the reversion of a premature stop codon in the trp 1-289 allele, which results in a truncated non-functional protein. When the strains were plated on media lacking tryptophan, the *Δmsh2* strains reverted about seven times more frequently compared to the parental strain (Figure 4.2). Higher number of colonies is observed for *Δmsh2* strain (Figure 4.2 D) compared to the wild type *MSH2* (Figure 4.2 C) when allowed to grow in SC media lacking tryptophan. Similarly, when two different CEN.PK2-1C background strains with *MSH2* deletion named - PRY25 and PRY28 were allowed to grow in the SC media without tryptophan, thereafter the colonies investigated via Sangers sequencing method revealed a different nucleotide incorporated to switch the premature stop codon to a functional codon for strain PRY25 and PRY28. As seen in Figure 4.3 A, B a reversion from stop codon TAG to TGG in PRY25 and TAG to TAT in PRY28 is observed. This finding strongly suggests a high occurrence of mutation in the genome due to deletion of *MSH2* in the strain tested. In contrast to *MSH2,* the mutagenic effect of another mutator gene employed in present study - *RAD27* was not examined in detail, and the deletion of *RAD27* for evolution of strains was solely based on literature evidence where authors found a high

number of mutant occurrence with the deletion of this gene (Loeillet et al. 2020).

The constructed *RAD27* or *MSH2* mutator strains PRY24, PRY25, PRY27, and PRY28 were subjected to evolutionary engineering in a 300 ml aerobic shake flask with SC media pH 5.5, supplementing xylose and galactose at different concentrations as shown in Figure 4.4.
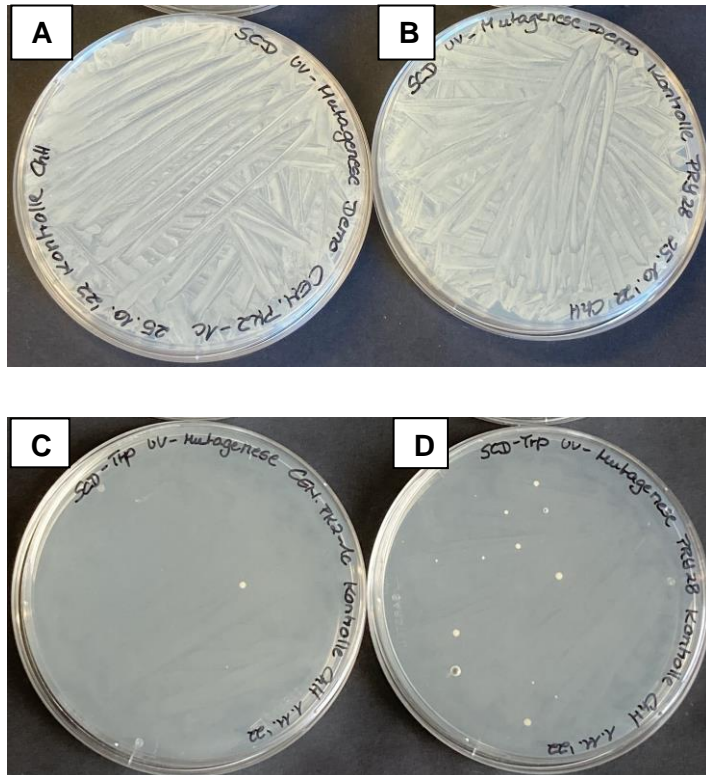

Figure 4.2: Role of *MSH2* in reverting *TRP1* stop codon. Number of the colonies growing able to grow in media without tryptophan supplementation. **A** (CEN.PK2-1C) and **B** (PRY28) in SCD media. **C** (CEN.PK2-1C) and **D** (PRY28) in SCD media without Tryptophan.
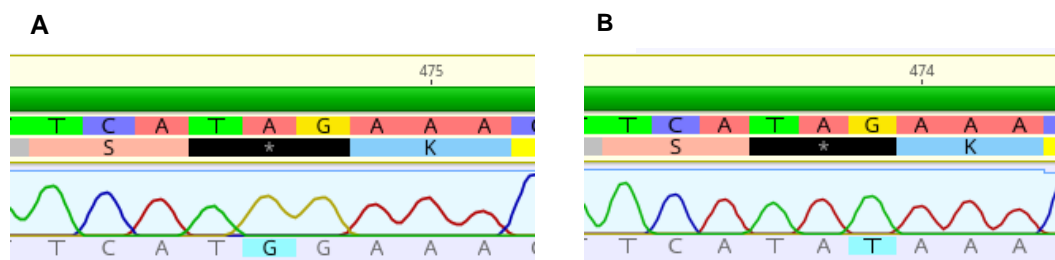

Figure 4.3: Stop codon TAG reverted on strains PRY25 and PRY28 able to grow in SCD without tryptophan media verified by sequencing. A single nucleotide change resulting conversion of stop codon TAG to TGG in PRY25 **(A)** and TAT in PRY28 **(B)**.

The cultures to varying intervals of time were transferred to fresh media followed by washing with sterile water. Figure 4.4 shows the result from evolutionary engineering

where clones can grow in xylose as a sole carbon source only after 203 days of evolution. Evolution was done in two different batches, E1 and E2. In E1, the evolution experiment was initiated with 0.05 % galactose-containing media, whereas E2 is a duplicate test executed on the same strains but without any galactose in the media, thus xylose employed as a sole carbon source from the beginning time point (day 0). Galactose was used as a supporting carbon source due to its ability to activate mitochondrial reactions, as the organelle activity is essential for the functionality of the pathway. Due to all the strains expressing XylB via multicopy expression plasmid with *URA3* as an auxotrophic marker, evolution experiment was initiated in SC- ura as a primary media background. Throughout the evolution, cell pellet washing and transfer to fresh media were done at days 77, 130, 203, 227, 248, 250, 252, 255, 271, 277, 282, 288, and 308. Media were tested with different sugar amounts thereby. Until day 77, growth didn't significantly differ among the strains tested. On day 77, cell pellets were washed, and E1 was transferred to xylose only, where again, cells did not grow unless galactose was added at day 121. Similarly, for E2 on this day, cultures were spiked with 0.04 % galactose, which led to a sharp rise in OD_{600nm}. This confirms the viability of cells from E2 and explains the stressed state of cells that remained viable until 77 days of sugar deprivation. When the second washing was done at day 130, media transferred to galactose and xylose, and cells grew maximally to an OD_{600nm} of 1. The third washing step was carried out at day 203, after which cell pellets were transferred to 2 % xylose-containing media. Clones PRY24, PRY27, and PRY28 showed a strikingly high growth at this time point for the E1 batch of evolution. For the E2 batch of evolution, PRY28 showed a growth increase in xylose sugar. At this stage, both sets of evolution E1 and E2 generated strains capable of growth in xylose to an OD_{600nm} of ~3. A confirmation of pentose sugar-attributed growth of evolved strain was done at day 255, where the growth test examined in media without xylose did not lead to growth, as seen in Figure 4.4 A and 4.4 B. Devoid of xylose for three days did not lead to an increase in OD_{600nm}, and strains were back to a growth state only after adding xylose at day 258. It has to be noted that from day 255 onwards, media used for growth was SC complete media to get rid of plasmid burden from media selection pressure. This would also ensure the selection of evolved lines in xylose medium to generate further pure population of cells and to rule out any possible accessory effect from *URA3* containing plasmid. Xylose concentration were differently used throughout the evolution experiment.

In contrast, non-mutator strain PRY19 in both E1 and E2 could not grow in xylose sugar until day 318. This result suggests a possible mutagenic event could have similarly occurred in mutator strains for both *Δrad27* and *Δmsh2* based strains as evolution occurs at day 203 for all the evolved lines in two different sets of evolution experiments E1 and
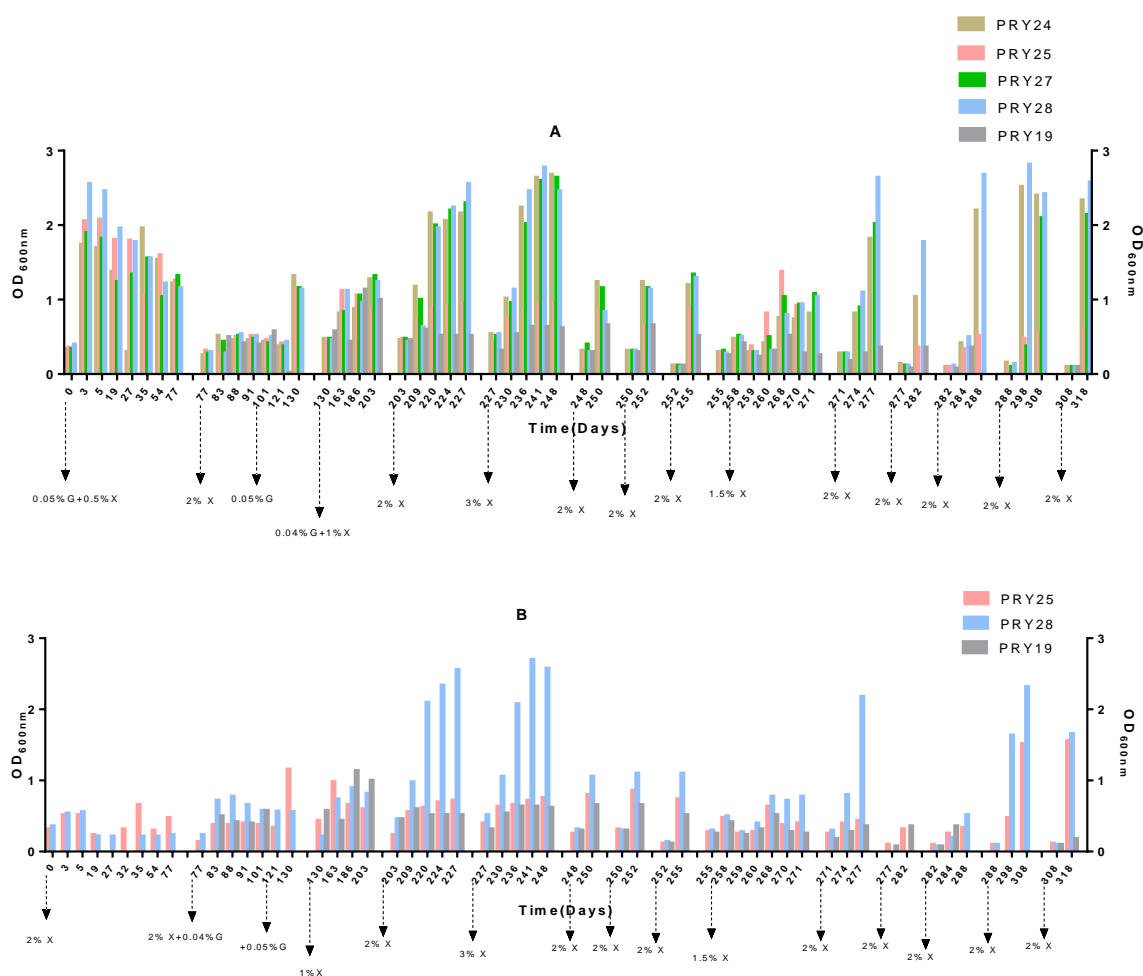
E2.

Figure 4.4: Evolutionary Engineering of mutator PRY24, PRY25, PRY27, PRY28 and non-mutator PRY19 strains in two different evolutionary batches E1 **(A)** and E2 **(B)**. Media used for evolution is SC media without uracil until day 255. From day 255, after washing transferred to synthetic complete media. Different sugar amounts used as mentioned in graph. Blank space in between columns represents washing step before reinoculation to fresh media. 'X' means xylose and 'G' means galactose.

After observing xylose growing evolution lines, single pure colonies were isolated from those cultures by streaking them out on YPD Agar. These clones were re-analyzed for the ability to grow in xylose, from which the best-growing colony was furthermore processed (result not shown). To test if the growth can be attributed to the Weimberg pathway or the endogeneous oxidoreductive pathway, the native oxidoreductive pathway was disrupted via deletion of *XKS1* gene that encodes for xylulokinase responsible for converting xylulose to xylulose-5-P. CRISPR/Cas9 mediated deletion of gene *XKS1* was performed in all evolved strains of PRY24, PRY25, PRY27, and PRY28. Among all, *XKS1* was successfully deleted for only evolved strain PRY25. For evolved strains PRY24, PRY27, and PRY28, no colony could be recovered from the plate after the transformation. For

evolved PRY25, the comparative test of different colonies (deleted and undeleted *XKS1*) from the transformation plate in xylose as a sole sugar is shown in Figure 4.5. Despite the positive PCR confirmation of *XKS1* deleted and undeleted colonies, all of them were not able to grow in xylose as a carbon source which could be presumably due to the CRISPR/Cas9 detrimental effect on the evolved phenotype. As seen in Figure 4.5, the *XKS1* non- deleted clones (green) from the plate are also unable to grow in xylose with no difference from CEN.PK2-1C used as a control strain for *XKS1* deletion. The loss of evolved phenotype with CRISPR/Cas9 based transformation could be due to the loss of some temporary adaptive changes in the strains which might have been responsible for xylose based growth. Besides disruption of the native pathway, when the evolved strains were applied for deletion of Weimberg pathway genes, no colony could be revived after the transformation for all the evolved strains PRY24, PRY25, PRY27, and PRY28. Disruption of the Weimberg pathway was attempted with guide RNAs targeting *xylX*, *ksaD*, or *xylD* separately, and all of them went unsuccessful, and no colony could be retrieved from the plate after the CRISPR-mediated transformation.
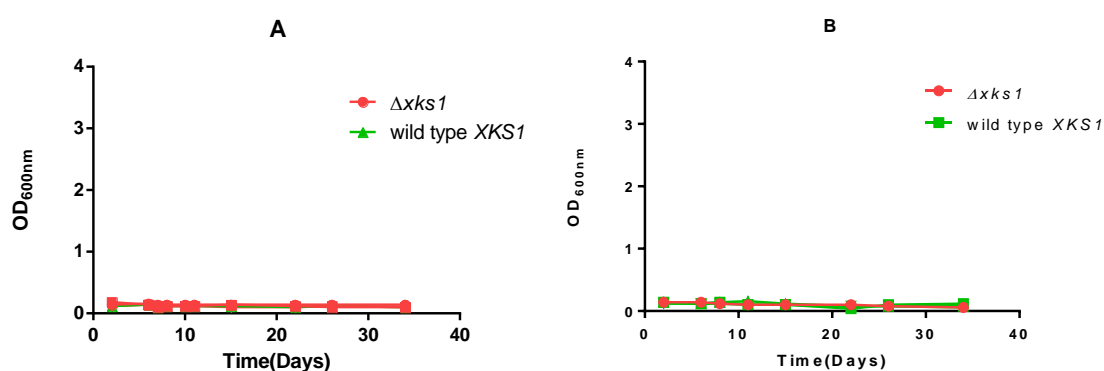

Figure 4.5: Deletion effect of *XKS1* in **(A)** CEN.PK2-1C wild type, and **(B)** evolved PRY28 strain for growth in SC media with 2 % xylose. Green colour refers to *XKS1* containing and red colour refers to *XKS1* deleted strain.

4.1.2   Cytosolic- Mitochondrial expression of Weimberg pathway

Mitochondria are a central organelle for functionality of Weimberg pathway in yeast. Cytoplasmic expression of this pathway relies on cofactor [4Fe-4S] cluster whose biogenesis occurs in mitochondria. Beside this, cytosolic- mitochondrial circulation of AKG is essential for xylose-based growth. Due to lack of understanding of all the intermediate substrate transport mechanisms and their possibly influencing interaction across mitochondrial membrane, present study put forward strain design through assembling the whole pathway in cytoplasm and mitochondria simultaneously. For this, cytosolically expressing strain PRY14 was further modified by integrating all Weimberg pathway genes

encoding N- terminal mitochondrial targeting signals and C- terminal GFP resulting in strain AHY02. To do so, all the individual genes were tagged with different MTS sequences at their N terminal end: *xylB* with Acp1, *xylD* with Aco1, *ksaD* with Cox4, *xylX* with Lpd1. Similarly, GFP envy was tagged at the C -terminal end of each gene. For the expression test, plasmid FGD97 was taken. Following assembly of plasmid, they were verified for localization of protein in mitochondria through confocal microscopy. They were investigated with alignment of the fluorescence mapping of the GFP and mitotracker (a dye that fluoresces mitochondria). The cells were then examined via confocal microscopy. As shown in Figure 4.6 an overlay of green and red fluorescence signals confirms the localization of these proteins in mitochondria.
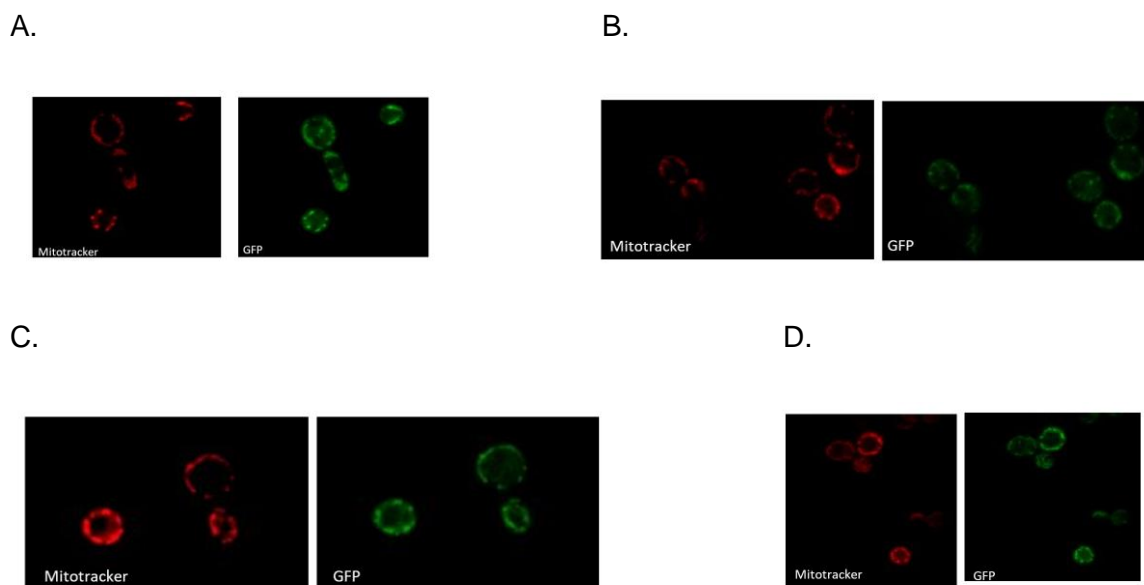

Figure 4.6: Mitochondrial localization of individual genes of the pathway visualized with confocal microscopy. Red fluorescence represents mitotracker, green fluorescence is GFP signal from yeast. Overlap of red mitotracker and green GFP signal confirms the localization of genes to mitochondria. Acp1-*xylB* **(A)**, Aco1-*xylD* **(B)**, Cox4-*ksaD* **(C)**, Lpd1-*xylX* **(D)**

After the confirmation of localization, sets of genes were expressed in the two different compartments mitochondria and cytoplasm. This was done via integration of cytosolically expressing genes into the *LEU2* locus, while mitochondrial expression was carried out by N- terminal tagging of each protein with respective MTS. A multicassette integration vector AHB15 was created having mitochondrial targeting signal for all Weimberg pathway proteins XylB, XylD, KsaD, XylX. They were then integrated into *URA3* locus of strain PRY14 which already contained the respective cytosolical Weimberg pathway proteins, resulting in strain AHY02. (Adriana Happel, Bachelor thesis 2021).

4.1.2.1 Evolutionary engineering of strain AHY02

Engineered strain AHY02 was not able to grow in xylose as a sole carbon source (Adriana Happel, Bachelor thesis, 2021). Therefore, the pressure was applied to strains by growing them in sugar (galactose) limiting condition, while xylose was supplied abundantly throughout the evolutionary process. The experiment was conducted for 295 days (Figure 4.7). Together with, as a control, the CEN.PK2-1C wild-type strain was introduced after six weeks of the start of the experiment. Evolution experiments were conducted in synthetic complete media at pH 5.5, with 0.1 % galactose and 1 % xylose. Washing and reinoculation were done on days 40, 44, 102, 178, 223, 225, 227, 230, 248, 254, 259, 265, and 285. Different amounts of sugar were applied in certain time intervals depending on growth and viability. For strain AHY02, there was a sharp rise in growth observed at day 184, when the cell pellet from day 178 was washed and inoculated to new xylose-containing media, albeit OD_{600nm} was below 1. Following this observation, cells were transferred furthermore to xylose-containing media to further proliferate the evolved cells and let them dominate the whole population. The same procedure was again followed on day 202, the washing step. At day 211, there is a spike in OD_{600nm} almost to 3 for strain AHY02. Presumably, the time given turned out the evolved cells to overgrow the whole flask. Later, a test was done when cells were grown in media without xylose; at day 230, cells only grew if xylose was supplied at day 236. A maximum OD_{600nm} of about 3 was observed for both AHY02 and CEN.PK2-1C wild-type strains at day 285. After day 295, the experiment was discontinued, and the examination of evolved phenotypes was more focused on. Apparently, the evolutionary experiment turned a xylose non-consumer strain into a xylose metabolizing strain for both yeast strain backgrounds (AHY02 and CEN.PK2-1C).
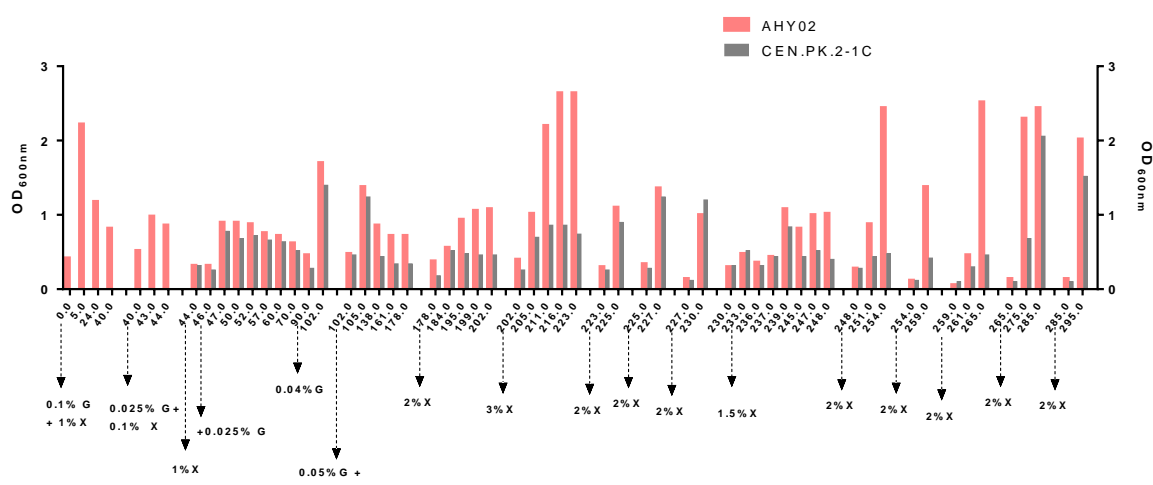
Figure 4.7: Evolutionary engineering experiment of AHY02 and CEN.PK2-1C with synthetic complete media containing different amounts of sugar as indicated in graph. Blank space in between columns represents washing step before reinoculation to fresh media. 'X' symbolizes xylose and 'G' symbolizes galactose.

4.1.2.2 Further characterization of xylose evolved strains AHY02 and CEN.PK2-1C

After the successful xylose growth of evolved candidates, as seen in Figure. 4.7, two different possibilities were assumed as described in chapter 4.1.1. Firstly, Weimberg pathway might have been activated during the evolution process. Secondly, special genetic events might have emerged that triggered the oxidoreductive branch and thus made xylose ultimately enter glycolysis. To know the exact pathway responsible for the growth, they were subjected to disruption of the oxidoreductive pathway or Weimberg pathway separately. To discontinue the oxidoreductive branch of evolved strains, *XKS1* (xylulokinase gene), the only gene responsible for converting xylulose to xylulose-5-P in *S. cerevisiae* was targeted. The CRISPR/Cas9-based deletion was successful for both AHY02, and CEN.PK2-1C evolved strain. On the other hand, to examine the possible role of the Weimberg pathway in AHY02 evolved clones, deletion of *xylX* or *ksaD* via CRISPR/Cas9 strategy and replacement of the Weimberg pathway cassette by *KanMX* resistant marker separately. For the disruption of gene, colonies were selected in media containing glucose as a carbon source. Unfortunately, no colony could be observed in all of the deletion strategies employed for the disruption of Weimberg pathway in evolved AHY02 due to unknown reasons.

For evolved variants, it is seen that (Figure, 4.8) all the *XKS1* deleted clones (red ones) could not grow in xylose; however, the ones that escaped CRISPR and retained *XKS1* (green ones) grow well. It can be assumed that the xylose-based growth in evolved strain is due to the activity of the oxidoreductive branch. The same colonies were re-checked for their consistency of xylose growth behavior after several weeks of storage and revival in YPD-containing media, test results show both the evolved strains AHY02 and CEN.PK2-1C are stable with the xylose growing phenotype, and the difference of *XKS1* deletion is still found to be reproducible (results not shown here). This suggests that evolutionary engineering could have generated stable genetic changes via some genome engineering that occurred during evolutionary engineering.

A difference in the growth patterns of evolved strains AHY02 and CEN.PK2-1C was seen when grown on xylitol compared to xylose. The aim of using xylitol as a carbon source is to gain more insight on the role of *XKS1* on xylitol consumption in evolved strains capable to utilize xylose as a carbon source. In this way, the role of oxidoreductive route in the evolved strain is furthermore clarified as this route of xylose consumption involves xylitol

as a first intermediate. Evolved strain CEN.PK2-1C showed higher growth with xylitol compared to evolved AHY02 (Figure 4.8 B and D), suggesting that later strain may not prefer xylitol as a carbon source. Further investigation on the role of *XKS1* in xylitol and xylose growth clearly shows in Figure 4.8 that a deletion of *XKS1* completely abolishes growth on xylose (Figure 4.8 A and C). For xylitol as a carbon source, the deletion of *XKS1* is observed lethal for the evolved strain CEN.PK2-1C (Figure 4.8 D), whereas the evolved AHY02 strain grows very poorly in xylitol as a carbon source even when *XKS1* is present (Figure 4.8 B). Taken together, these findings provides important insights into possible role of oxidoreductive route on xylose utilization for the evolved strains. Growth result on xylose and xylitol separately reflects the genetic and metabolic differences between evolved strains CEN.PK2-1C and AHY02 and their preferences for different carbon sources which furthermore suggests that different evolutionary pathways may lead to distinct patterns of carbon utilization.
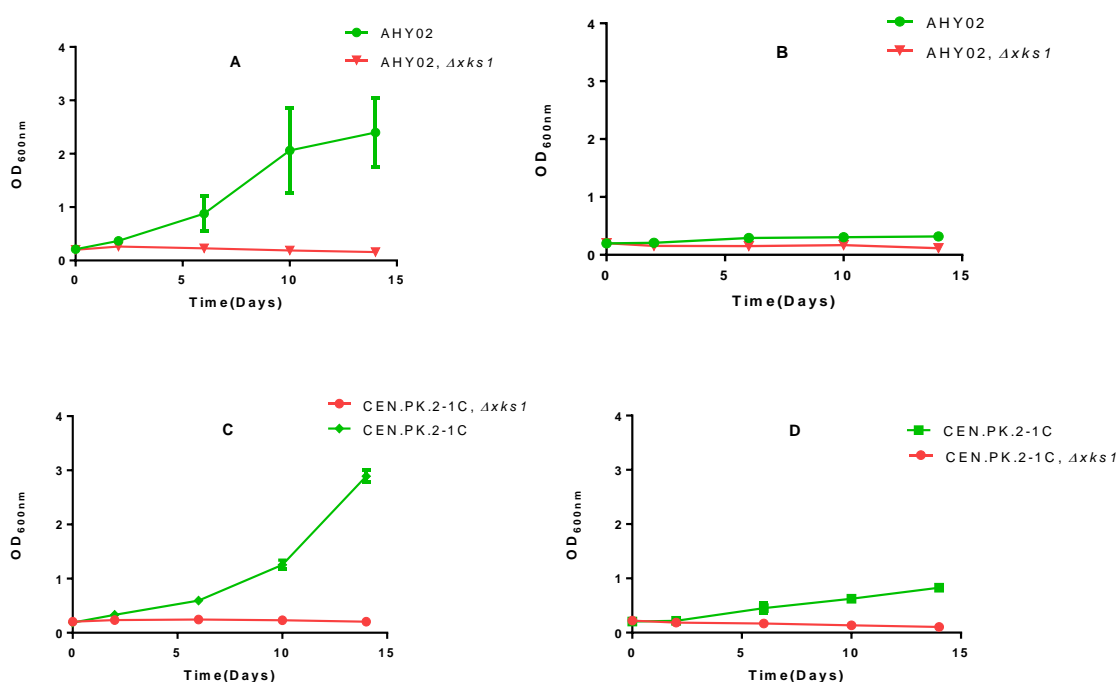
Figure 4.8: Effect of *XKS1* deletion on growth of evolved strains CEN.PK2-1C and AHY02. Media used is synthetic complete media. **(A)** and **(B)** represent evolved strain AHY02 in 2 % xylose or 2 % xylitol resp. **(C)** and **(D)** represents evolved strain CEN.PK2-1C in 2 % xylose or 2 % xylitol respectively, green lines are undeleted *XKS1* and red are *XKS1* deleted strains. Done in triplicates. Mean values and standard deviation of triplicate measurements are shown. The error bars may be smaller than the symbols.

4.1.3 Establishing a screening platform for evaluating the efficiency of the Weimberg pathway

To establish a screening platform for identifying the optimal xylose flux towards AKG, strain was modified in a way that it could not grow without external supplementation of glutamate. Glutamate can be enzymatically interconverted with AKG by glutamate dehydrogenases. Strains PRY19 and PRY20, which contain a complete set of the Weimberg pathway genes integrated into the genome at distinct loci and capable of producing AKG from isocitrate, were subjected to CRISPR/Cas9-mediated gene disruption, yielding the strains PRY59 and PRY60 (strategy detailed shown in Figure 4.9). To create auxotrophic strain PRY59 and PRY60, genes *IDH2*, *IDP1*, *IDP2*, and *IDP3*, which encode proteins involved in the conversion of isocitrate to AKG, were deleted. The deletion of the genes resulted in the inability of the strain to grow without supplementary glutamate, as evidenced by the essential role of glutamate addition in growth, as depicted in Figure 4.10 (A, B), where basal media employed was SC media with 2 % glucose as a carbon source. Despite being auxotrophic for AKG, the strains were still unable to grow upon the addition of xylose when concentration were varied to either 1 % or 4 % (Figure 4.10 A, B). This suggests a lack of conversion of xylose to AKG even with the expression of the Weimberg pathway. A longer time given for the optimal expression of the pathway until 28 days did not lead to growth of the strains PRY59 and PRY60 in xylose and maltose mixtures (Figure 4.12). Maltose was chosen instead of glucose as a carbon source to overcome the inhibition effect on xylose uptake. Presence of glucose, especially at a higher concentration, decreases the affinity of the native hexose transporters for xylose.

The results of this experiment indicates that the supplementation of glutamate was successful in rescuing the growth of the AKG-deficient strain, whereas the addition of up to 20 g/L AKG did not support growth as seen in Figure 4.10 (C, D). A slight improvement in growth was observed when the pH of the media was lowered to 5, however, this difference was not statistically significant (Figure 4.11). Despite supplementation with high concentrations of AKG, the strain was unable to grow, which implies that the uptake of AKG is not sufficiently enough. The slight increase in growth observed at a lower pH of 5 may indicate that the strain is sensitive to changes in the media environment and suggests that possibly a lower pH could be favorable condition for the passive uptake of protonated form of AKG.
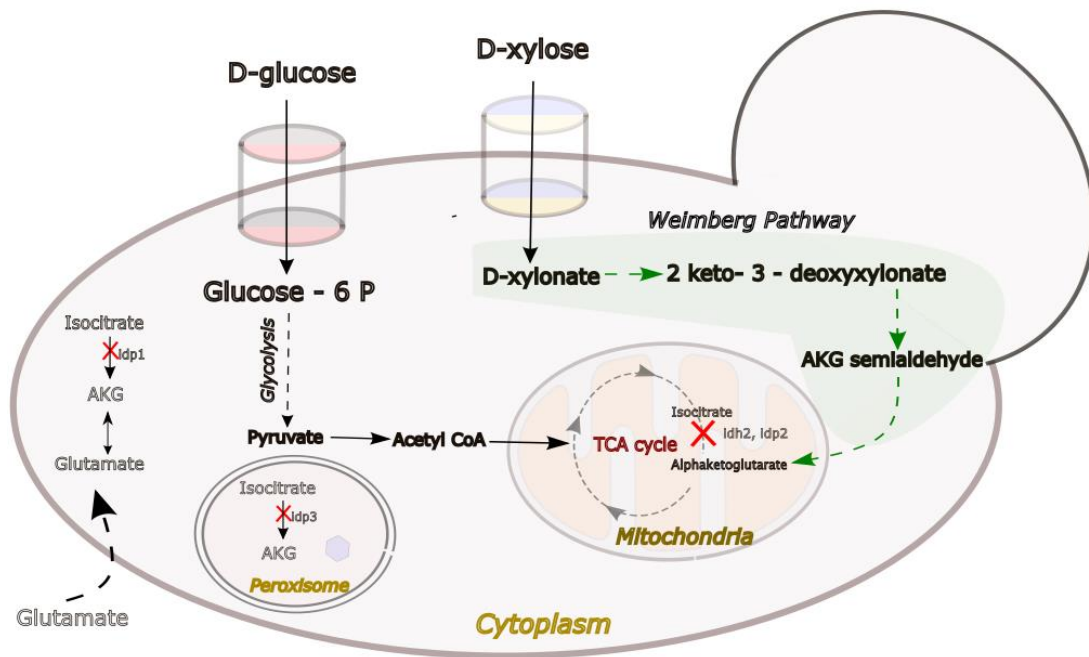
Figure 4.9*: Schematic representation of the screening system to detect activity of Weimberg pathway. Deletion of genes - *IDH2, IDP1, IDP2, IDP3*, done to make strain auxotrophic for glutamate (PRY59 and PRY60). In this strategy, all the Weimberg pathway genes were integrated into the genome. The pathway is expected to convert xylose to AKG and hence to complement the glutamate auxotrophy of the strain.
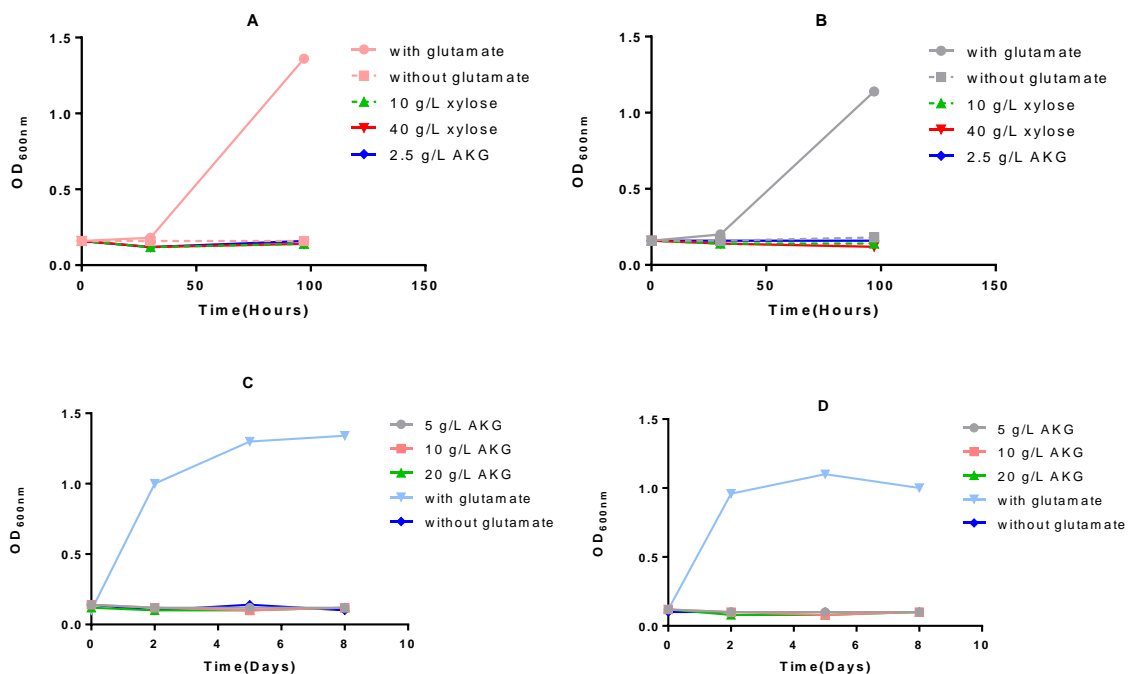
Figure 4.10: (A and **B)** -Dependency of strains PRY59 **(A)** and PRY60 **(B)** on glutamate, xylose or AKG for growth in SCD. **(C** and **D)**- Evaluation of PRY59 and PRY60 strains PRY59 **(C)** and PRY60 **(D)** with varying amounts of α-ketoglutarate (AKG) up to 20 g/L for growth. Media used for growth is Synthetic complete media at pH 6.3 with various sugar and additives as mentioned. Concentration of glutamate used was 20 mg/L.
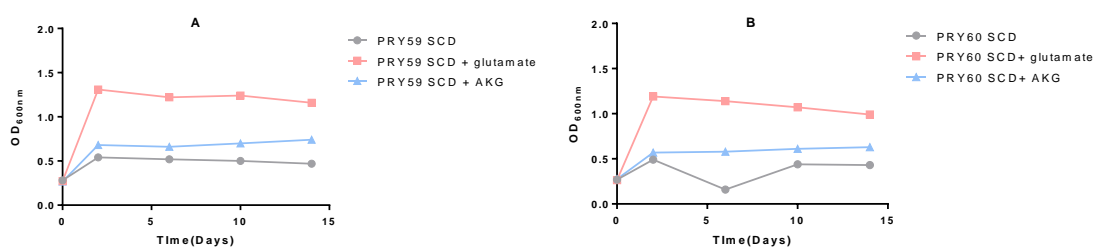
Figure 4.11: The growth of strains **(A)** PRY59 and **(B)** PRY60 on α-ketoglutarate (AKG) tested in SC medium at pH 5 containing 2 % glucose with addition of glutamate or AKG. Concentration of glutamate used was 20 mg/L and AKG was 2.5 g/L.
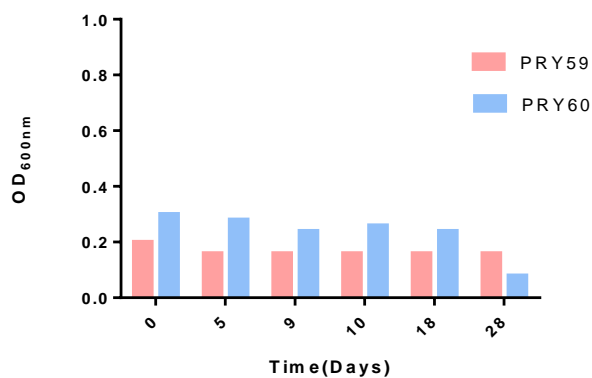
Figure 4.12: Prolonged growth of strains PRY59 (red) and PRY60 (blue) in SC media with pH 6.3 containing 10 g/L Maltose and 40 g/L xylose for a time duration of 28 days.

Based on the results presented in Chapter 4.1 of this thesis, it appears that implementing the Weimberg pathway in *S. cerevisiae* poses a significant challenge. Despite the implementation of various strain modification techniques and evolutionary engineering, this study did not observe the desired conversion process of xylose to AKG via the Weimberg pathway in *S. cerevisiae* highlighting the need for further research.

4.2 Xylitol Production

As a second strategy to utilize pentose sugar xylose, this work aims at its conversion to a commercially valuable compound xylitol. For this, a number of hexose transporters were tested for their ability to transport xylitol with an in-depth examination on xylitol import and export across the plasma membrane. Together with, several heterologous xylose reductases were tested in *S. cerevisiae* for the xylitol production. Due to the dependency of the reaction on NADPH, a coenzyme that provides reducing power, various ways to maximize yield of xylitol through different NADPH related genetic targets were examined.

4.2.1 Screening of putative transporters for the transport of Xylitol

In the bioconversion process, the transport of substrates across the membrane is crucial. This study focuses on examining the production of xylitol and any potential limitations in its transport. For this, strain AFY10 was tested with various native and engineered glucose/xylose transporters, as well as xylitol dehydrogenase, to assess its ability to use xylitol as a carbon source. Strain AFY10 is hxt^0 strain with several modification in the genome that allows for xylose metabolism (Farwick et al. 2014). This strain when additionally expressed with xylitol dehydrogenase (*XYL2*) is able to grow in xylitol as a sole carbon source (Jordan et al. 2016). In this study, the uptake efficiency of xylitol was evaluated using hexose transporters Hxt1, Hxt2, Hxt3, Hxt4, Hxt5, Hxt7, Hxt11, Hxt14, Hxt15 and Gal2. Additionally, mutant variants of Gal2 - $Gal2_{6SA}$, $Gal2_{N376Y/M435I}$, $Gal2_{6SA/N376Y/M435I}$ were tested for the uptake efficiency of xylitol. Among all, Hxt11 and Hxt15 are already known to be able to transport xylitol, whereas Hxt7 was shown unable to transport xylitol (Jordan et al. 2016). Similarly Gal2 and the mutant variants are reported to act as xylose transporting hexose transporter. Specifically, variant $Gal2_{6SA}$ is a membrane stabilized Gal2 due to the removal of ubiquitination signal (Tamayo Rojas et al. 2021), $Gal2_{N376Y/M435I}$ is described as a glucose insensitive xylose transporter (Rojas et al. 2021). Similarly, $Gal2_{6SA/N376Y/M435I}$ comprises combined mutation of $Gal2_{6SA}$ and $Gal2_{N376Y/M435I}$, and is shown to confer a higher xylose transport efficiency (Farwick et al. 2014; Rojas et al. 2021). Except Hxt7, Hxt11 and Hxt15, this work, for the first time, investigates the capacity of the above mentioned hexose transporter and their variants for their xylitol transport capacity. The ability of the AFY10 strain to grow in SC media with xylitol as a carbon source was determined through a drop test (Figure 4.13), that serves as a measure of the transporter's efficiency.

As depicted in Figure 4.13, among Hxt1, Hxt2, Hxt3, Hxt4, Hxt5, Hxt7, Hxt11, Hxt14, and

Hxt15 tested, Hxt15 was found to be the best importer of xylitol, followed by Hxt11. When Hxt15 is compared with Gal2 and its variants, it is observed that Hxt15 was comparable to the wild-type Gal2 and its mutated variant $Gal2_{6SA}$. However, the introduction of N376Y/ M435I amino acid modifications in the *GAL2* wild-type sequence had a stronger positive effect, leading to higher growth than any other hexose transporter or Gal2 variants tested. Additionally, the combination of the 6SA and N376Y/ M435I effects via plasmid expression resulted in growth similar to that of $Gal2_{N376Y/M435I}$ alone. These results indicate that $Gal2_{N376Y/M435I}$ and $Gal2_{6SA/N376Y/M435I}$ is the best importer of xylitol. This also confirms that the different amino acid sequence mutations in Gal2, which have already been proven to improve xylose transport, also lead to better xylitol import.
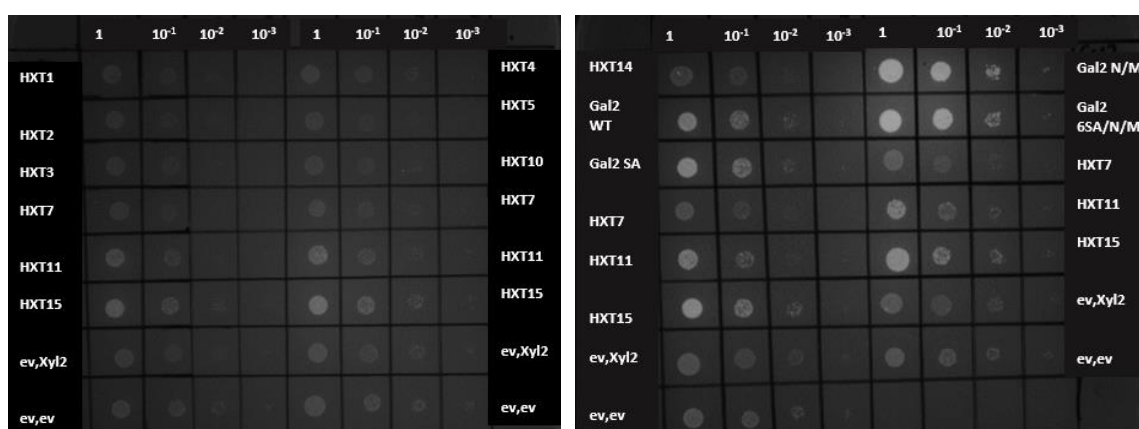

Figure 4.13: Strain AFY10 transformed with 2μ plasmids expressing indicated hexose transporters (p426 background) in combination with 2μ plasmids expressing *XYL2* (p425 background) from *S. cerevisiae.* The transformants were pre-grown in liquid selective SC medium with ethanol as a permissive carbon source and drop test performed in media SC-U-L with 2 % xylitol as a carbon source. Cells were grown at 30 °C for 6 days. Gal2 N/M refers to mutant $Gal2_{N376Y/M435I}$ and Gal2 6SA/N/M refers to $Gal2_{6SA/N376Y/M435I}$. (Hxt7, Hxt11, Hxt15, and ev are used as different controls and are repeatedly dropped on each side of the plate to allow a better visual comparision with other samples dropped in the same column).

To further analyze the transport efficiency of *GAL2* and its variants, a drop test of strain AFY10 transformed with different transporters and xylitol dehydrogenase (Sc*XYL2*) was performed at different xylitol concentrations. The best transporters, Hxt11, Hxt15, wild-type Gal2, $Gal2_{6SA}$, $Gal2_{N376Y/M435I}$, and $Gal2_{6SA/N376Y/M435I}$ (from Figure 4.13), were tested with xylitol concentrations of 2 %, 1 %, and 0.5 %. The results of the drop test in Figure 4.14 reveals a more apparent difference between the wild-type Gal2 and $Gal2_{6SA}$ when the xylitol concentration is kept at 1 %. These results indicate that the wild-type Gal2 shows no growth at 1 % xylitol, in contrast to $Gal2_{6SA}$, which still shows some growth, suggesting that $Gal2_{6SA}$ is a better importer when compared to the wild-type Gal2. Similarly, a significant difference was observed in the xylitol transport efficiency between the two best variants, $Gal2_{N376Y/M435I}$ and $Gal2_{6SA/N376Y/M435I}$, when cells were grown in a minimal amount

of xylitol (0.5 %). As shown in Figure 4.14, when the xylitol concentration was reduced from 1 % to 0.5 %, some growth was observed for Gal2$_{6SA/N376Y/M435I}$, while Gal2$_{N376Y/M435I}$ did not support growth at all. This further classifies Gal2$_{6SA/N376Y/M435I}$ as the best importer of xylitol among all the transporters employed in this study.
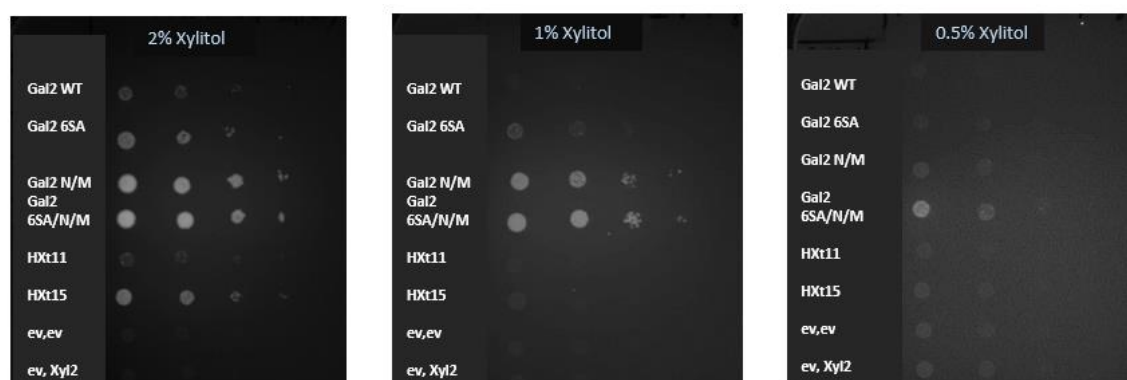

Figure 4.14: Strain AFY10 transformed with 2µ plasmids expressing indicated hexose transporters (p426 background) in combination with 2µ plasmids expressing *XYL2* (p425 background) from *S. cerevisiae*. The transformants were pre-grown in liquid selective SC medium with ethanol as a permissive carbon source and drop test performed in media SC-U-L with 2 %, 1 % and 0.5 % xylitol as a carbon source. Cells were grown at 30 °C for 11 days. Gal2 N/M refers to mutant Gal2$_{N376Y/M435I}$ and Gal2 6SA/N/M refers to Gal2$_{6SA/N376Y/M435I}$.

Furthermore, test was done to examine the effect of presence of other sugars like glucose or xylose on transport of xylitol. A drop test result indicates that the presence of glucose or xylose has an effect on the transport of xylitol by different transporters. Figure 4.15 shows that the presence of glucose strongly inhibits the transport of xylitol for Hxt11, and Gal2 wild type, and to a lesser extent for Gal2$_{6SA}$ and Hxt15. However, no glucose inhibition was observed for Gal2$_{N376Y/M435I}$ and Gal2$_{6SA/N376Y/M435I}$ variants. Similarly, the presence of xylose also showed some inhibition for Hxt11, Hxt15, Gal2 wild type, and Gal2$_{6SA}$, but not for Gal2$_{N376Y/M435I}$ and Gal2$_{6SA/N376Y/M435I}$ variants. The comparison of Hxt11 and Hxt15 suggests that Hxt11 is less sensitive to inhibition by xylose than Hxt15, while Hxt15 shows less inhibition by glucose. No growth was observed when cells were dropped on media with only xylose, which is due to the lack of a xylose isomerase activity in the strain AFY10. This control confirms that the growth on xylose/xylitol mixtures is due solely to the utilization of xylitol. Altogether, this study shows the Gal2$_{N376Y/M435I}$ and Gal2$_{6SA/N376Y/M435I}$ variants are the best importers of xylitol in the presence of glucose or xylose.
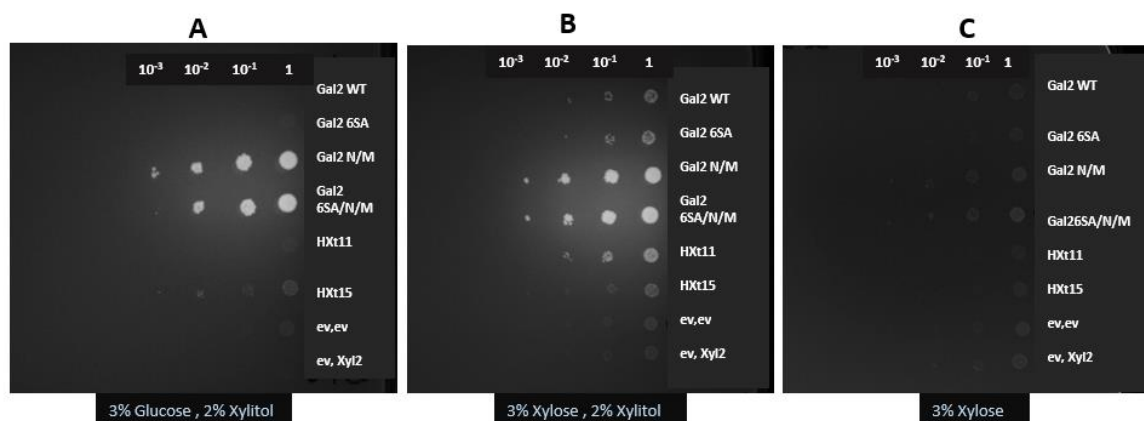
Figure 4.15: Strain AFY10 transformed with 2μ plasmids expressing indicated hexose transporters (p426 background) in combination with 2μ plasmids expressing *XYL2* (p425 background) from *S. cerevisiae.* The transformants were pre-grown in liquid selective SC medium with ethanol as a permissive carbon source and drop test performed in media SC-U-L with 2 %, 1 % and 0.5 % xylitol as a carbon source. Cells were grown at 30 °C for 11 days. Gal2 N/M refers to mutant $Gal2_{N376Y/M435I}$ and Gal2 6SA/N/M refers to $Gal2_{6SA/N376Y/M435I}$. **(A)** 3 % glucose and 2 % xylitol, **(B)** 3 % xylose and 2 % xylitol, and **(C)** 3 % xylose.

4.2.2 Testing of *GAL2* and its variants for the best production of xylitol

The study was continued to examine the potential of $Gal2_{6SA/N376Y/M435I}$ as a xylitol producer using xylose as a substrate. The *GAL2* variants, along with *HXT5* and *GRE3*, were transformed into hexose-transporter deficient (hxt^0) strain EBY.VW4000 and allowed to grow in SC media with glucose and xylose as the sugar source. Gal2 is known to transport xylose and the different mutations in Gal2 were shown to improve the xylose transport (Rojas et al. 2021). Similarly, *HXT5* is employed to maintain the consumption of glucose at a slow rate as this is a moderate affinity glucose transporter (Diderich et al. 2001). Additional expression of *GRE3* was done to increase the rate of conversion of xylose to xylitol. The results of the fermentation (Figure 4.16) show differences in glucose/xylose consumption and xylitol production among Gal2 wild type, $Gal2_{6SA}$, $Gal2_{N376Y/M435I}$, $Gal2_{6SA/N376Y/M435I}$, and four different controls. The highest glucose consumption was observed in the absence of the Gal2 transporter, as seen in C2 and C3 which depleted all glucose before 48 hours (Figure 4.16 A). Among these two strains, C2 produced a higher amount of xylitol, which was expected due to the presence of the Gre3 expressing plasmid responsible for converting xylose to xylitol. The mutation of six serine residues to alanine in *GAL2* (*GAL2_{6SA}*) to prevent ubiquitination had a positive effect on increasing the titer of xylitol as compared to the wild type. Similarly, $Gal2_{N376Y/M435I}$ had a higher yield of xylitol compared to the wild type or $Gal2_{6SA}$. Strikingly, the combined effect of 6SA and N376Y/M435I in *GAL2* resulted in a substantially higher yield of xylitol at all time points, with a titer of 6.18 g/L at 148 hours (Figure 4.16 B). Thus, the comparison of *GAL2* and its

mutated variants showed that Gal2$_{6SA/N376Y/M435I}$ enabled the highest xylitol titers and *GAL2* wild type the lowest. The mutants Gal2$_{6SA}$ and Gal2$_{N376Y/M435I}$ served as better candidates than the wild type, and the strains C1 and C4, which had no glucose transporter (Hxt5), expectedly did not grow at all.

Sample	Plasmid vectors used		
	p426	p425	p423
Gal2 WT	Gal2 WT	*GRE3*	*HXT5*
Gal2 6SA	Gal2 6SA	*GRE3*	*HXT5*
Gal2 N/M	Gal2 N/M	*GRE3*	*HXT5*
Gal2 6SA/N/M	Gal2 6SA/N/M	*GRE3*	*HXT5*
C1	ev	ev	ev
C2	ev	*GRE3*	*HXT5*
C3	ev	ev	*HXT5*
C4	ev	*GRE3*	ev
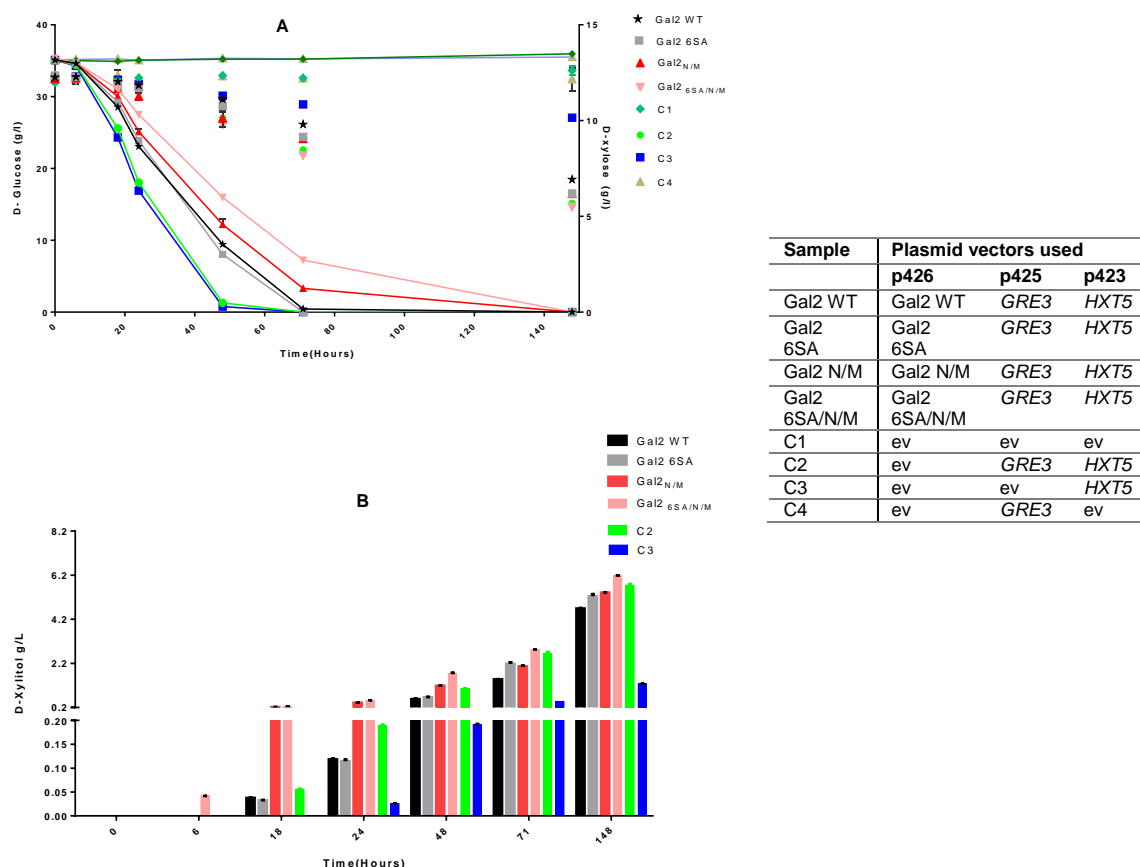
Figure 4.16: Fermentation of *hxt⁰* strain EBY.VW4000 expressing different Gal2 variants. The Gal2 constructs (wildtype-WT or the indicated mutants), Hxt5 and Gre3 were expressed from 2µ plasmid. The transformants were pre-grown in selective SC medium with 1 % maltose as a permissive carbon source. Fermentation was done in SC media containing 3 % glucose and 2 % xylose. **(A)** Glucose and xylose consumption at different time points. The consumption of glucose (solid lines, plotted on left Y axis) and xylose (symbols only, plotted on right Y axis). **(B)** Titer of xylitol obtained at different time points for each of the construct tested. Mean values and standard deviation of triplicate measurements are shown. The error bars may be smaller than the symbols. Gal2 N/M refers to mutant Gal2$_{N376Y/M435I}$ and Gal2 6SA/N/M refers to Gal2$_{6SA/N376Y/M435I}$.

4.2.2.1 Effect of plasmid based *GAL2$_{6SA/N376Y/M435I}$* expression in CEN.PK2-1C background

In this section, Gal2$_{6SA/N376Y/M435I}$ was examined for sugar transport and xylitol production in a commonly used laboratory strain background CEN.PK2-1C. For this, strain PRY39 (CEN.PK2-1C, *Δgre3*) was transformed with mutant variant transporter (Gal2$_{6SA/N376Y/M435I}$)

and xylose reductase from *Pichia stipitis* (PsXyl1). To clearly observe the effect of transporter, control was used which consisted of empty vector (ev) instead of mutant Gal2 (Gal2$_{6SA/N376Y/M435I}$). The results showed that the expression of Gal2$_{6SA/N376Y/M435I}$ increased xylose consumption and xylitol production with a difference of 20 % to the empty vector control (Figure 4.17), thereby demonstrating its beneficial effect on xylitol production even in a strain background, which contains all native hexose transporter genes. In EBY.VW4000 used in section 4.2.2 (Figure 4.16), xylose and glucose transport was solely dependent on one or two different transporters that the strain was transformed with. For glucose consumption, the transporter Gal2$_{6SA/N376Y/M435I}$ had a negative effect as it slowed down glucose transport, as shown in Figure 4.17 A, which is consistent with the observations of the previous chapter.
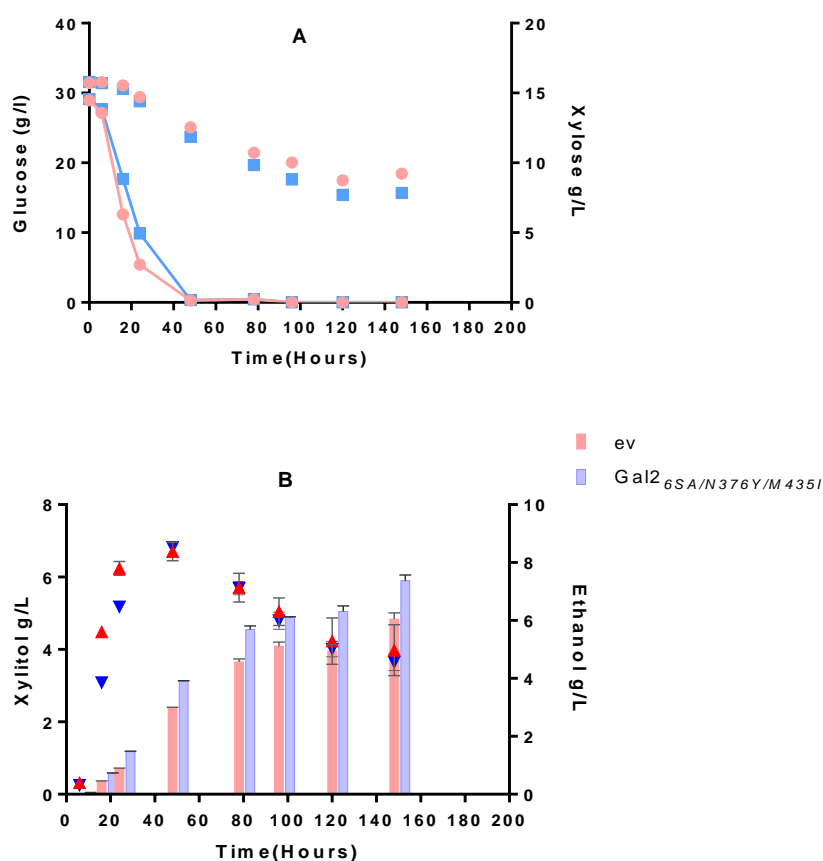
Figure 4.17: Effect of Gal2$_{6SA/N376Y/M435I}$ on xylitol production in strain PRY39 (CEN.PK2-1C, *Δgre3*). Gal2$_{6SA/N376Y/M435I}$ and PsXyl1 (codon optimized xylose reductase from *Pichia stipitis*) expressed via 2μ plasmid in strain PRY39. The transformants were pre-grown in selective SC medium with 2 % glucose as a permissive carbon source. Fermentation was done in SC media containing 3 % glucose and 2 % xylose. **(A)** Glucose and xylose consumption at different time points. The consumption of glucose (solid lines, plotted on left Y axis) and xylose (symbols only, plotted on right Y axis). **(B)** Titer of xylitol (plotted as bars), and amount of ethanol (symbols only) measured at different time points for each of the construct tested. Mean values and standard deviation of triplicate measurements are shown. The error bars may be smaller than the symbols.

4.2.3   Xylitol Efflux test of best xylitol importers

In the 4.2.2 chapter, it was shown that the presence of $Gal2_{6SA/N376Y/M435I}$ increases the yield of xylitol production for both EBY.VW4000 and CEN.PK2-1C strain background. Whereas it is known from the literature that $Gal2_{6SA/N376Y/M435I}$ has beneficial properties for xylose uptake, its superiority as the best xylitol importer was established in chapter 4.2.1. Since Gal2 has a facilitative transport mechanism, it is conceivable that it also might act in a bidirectional manner, supporting xylitol export. Therefore, it remained unclear if its beneficial effect as observed in previous chapters is due solely to an improvement of xylose uptake or a combined effect with xylitol efflux. To clarify the impact of xylose import and xylitol export, an experimental test system was designed (see Figure 4.18), where xylose is taken up in the form of xylobiose (a xylose disaccharide) by the specific transporter CDT-2 from *Neurospora crassa* and subsequently further processed to xylitol by a set of heterologously expressed enzymes (Li et al. 2015). Xylobiose is intracellularly cleaved by the β-xylosidase GH43-2 from *N. crassa* to xylose monomers that are subsequently reduced to xylitol by a xylose reductase (here PsXyl1). In parallel, PsXyl1 can use xylobiose as a substrate to produce xylosyl-xylitol which is, in turn, cleaved by a specialized β-xylosidase (GH43-7 from *N. crassa*) to xylose and xylitol. The heterologous genes encoding PsXyl1, CDT2, GH43-2 and GH43-7, as well as different Gal2 variants, were introduced on plasmids into the strain named PRY76. Strain PRY76 is a hxt^0 strain (EBY.VW4000) that additionally contains *TRP1* deletion and *ZWF1* overexpression. *TRP1* gene was deleted to ensure the optimal expression of p424 background plasmid that consists *TRP1* as an auxotrophic marker. Overexpression of *ZWF1* was done to upregulate oxidative PPP (Pentose Phosphate pathway) thereby to elevate cytosolic pool of NADPH required for conversion of xylose to xylitol (for details refer to chapter 4.2.6.1, Figure 4.22). The resulting transformants were incubated at a high cell density in media containing xylobiose and maltose (as a carbon source for the hxt^0 strain) and the production of xylitol was then measured in culture supernatants.

Figure 4.18: Xylobiose import dependency on *CDT-2*. The figure compares the results of (D) - with CDT-2 and (F) - without CDT-2. Strain PRY76 (EBY.VW4000, *Δtrp1*, *pZWF1::pHXT7*) transformed with either CDT2 or empty vector control in addition to GAL2$_{6SA/N376Y/M435I}$, GH43-2 + GH43-7, PsXyl1. All genes were expressed via 2μ plasmid. The transformants were pre-grown in selective SC medium with 1 % maltose as a permissive carbon source. Fermentation done in SC selective media without methionine to allow a higher expression of GH43-2 which is regulated by *pMET25*. Sugar amounts used were 1 % maltose and 1 % xylobiose.

	A	C	D	F
p426H7 e.v.	+			
p426 H7 *GAL2*		+		
p426 H7*GAL2_{6SA/N376Y/M435I}*			+	+
p423 H7 CDT-2	+	+	+	
p423 H7 e.v				+
p424 M25GH43-2 + pH7GH43-7	+	+	+	+
p425 H7Ps*XYL1*	+	+	+	+
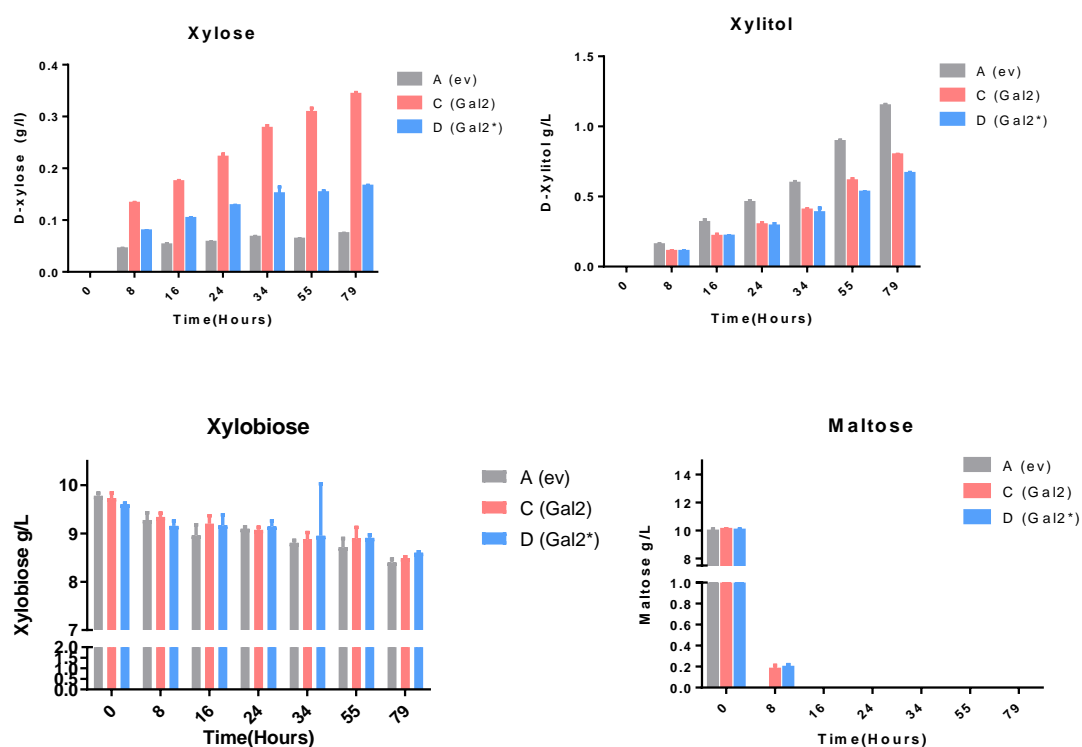
Figure 4.19: Xylitol efflux through different Gal2 variants. The figure compares the results of (A) – empty vector (ev); (C) - Gal2 WT (Gal2); and (D) - GAL2_{6SA/N376Y/M435I} (Gal2*) on efflux of xylitol. Strain PRY76 (EBY.VW4000, *Δtrp1*, *pZWF1::pHXT7*) transformed with either empty vector (A), Gal2 WT (C) *or* GAL2_{6SA/N376Y/M435I} (D). Additionally, all the constructs A, C and D contains CDT2, GH43-2 + GH43-7, and PsXyl1. All genes were expressed via 2μ plasmid. The transformants were pre-grown in selective SC medium with 1 % maltose as a permissive carbon source. Fermentation done in SC selective media without methionine to allow a higher expression of GH43-2 which is regulated by *pMET25*. Sugar amounts used were 1 % maltose and 1 % xylobiose. Amount of xylose, xylitol, xylobiose and maltose measured by HPLC are shown in the graph. Mean values and standard deviation of triplicate measurements are shown. The error bars may be smaller than the symbols.

First, it was confirmed that CDT-2 is necessary for xylobiose uptake (Figure 4.18). The plasmid combination "F", containing the empty vector control instead of CDT-2, showed only a minimal consumption of xylobiose and production of xylose, which did not change significantly over time. Xylitol was produced up to 1 g/L only in the presence of CDT-2

(plasmid combination "D"), which strongly suggests that the xylose in the culture supernatant "F" originated from extracellular xylobiose hydrolysis, e.g. due to partial cell lysis or by some secreted enzyme with xylobiose hydrolysis activity. If there was some degree of unspecific xylobiose uptake without CDT-2, the intracellular conversion to xylitol would have occurred in this control as well. The conversion of xylose to xylitol cannot occur extracellularly due to a lack of NADPH regeneration. Taken together, these observations show that Gal2$_{6SA/N376Y/M435I}$ cannot act as a xylobiose transporter and hence the disentanglement of substrate import and product export is possible with the experimental design proposed. When the Gal2 variants and the empty vector control are compared (Figure 4.19), it can be seen that the consumption of xylobiose and maltose is slightly delayed by the expression of Gal2, which is analogous to the delayed glucose uptake as observed in Figures 4.16 and 4.17. The efflux of xylose is increased with both Gal2 variants; interestingly, the efflux rate is higher for the wildtype protein, although the mutant shows superior properties for xylose uptake (Rojas et al. 2021 ; see also previous chapters). Thus, it is likely that the increased net uptake rate of the mutant is, at least partly, due to a reduction of the efflux rate during the facilitated diffusion process. On the other hand, the efflux of xylitol is obviously facilitated by one (or multiple) other transporter(s), as the empty vector control shows the highest rate, whereas the expression of Gal2 has an unexpectedly negative influence on extracellular xylitol titers. This can be explained by the competition of Gal2 with the xylitol exporter(s) regarding the limited capacity of the secretory pathway and the available space in the plasma membrane.

Taken together, this set of experiments strongly suggests that the increased production of xylitol upon expression of the mutant Gal2 as shown in previous sections can be attributed to an improvement of the xylose uptake and not to an increased rate of xylitol efflux.

4.2.4 Screening of the best heterologous xylose reductase for the increased titer of xylitol

In this section, the yield of xylitol through the enzymatic reduction of xylose by different reductases is compared. Four different reductases, derived from *Pichia stipitis* (PsXyl1), *Candida parapsilosis* (CpXyl1), *Aspergillus niger* (AnXyrB), and *Saccharomyces cerevisiae* (ScGre3), were chosen from literature and expressed together with transporter Gal2$_{6SA/N376Y/M435I}$ into the CEN.PK2-1C Δ*gre3* (PRY39) strain. All the reductase genes tested were codon optimized. Deletion of *GRE3* was done to minimize the basal amount of xylitol produced by the strain as *GRE3* is reported as the main reductase in *S. cerevisiae* responsible for xylitol production.
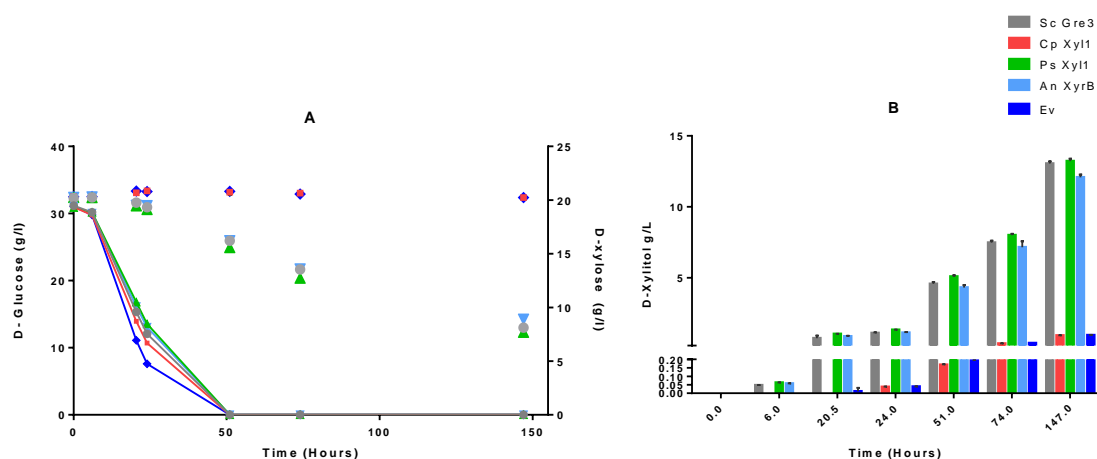
Figure 4.20- Comparative study of different xylose reductases in *S. cerevisiae* for the yield of xylitol. Strain PRY39 (CEN.PK2-1C, *Δgre3*) transformed with GAL2$_{6SA/N376Y/M435I}$ and different indicated reductases via 2μ plasmid. The transformants were pre-grown in selective SC medium with 2 % glucose as a permissive carbon source. Fermentation done in SC selective media with 3 % glucose and 2 % xylose. **(A)** Glucose and xylose consumption at different time points. The consumption of glucose (solid lines, plotted on left Y axis) and xylose (symbols only, plotted on right Y axis). **(B)** Titer of xylitol (plotted as bars), measured at different time points for each of the construct tested. Mean values and standard deviation of triplicate measurements are shown. The error bars may be smaller than the symbols.

Figure 4.21- Effect of codon optimization of *GRE3* for the titer of xylitol. Strain PRY39 (CEN.PK2-1C, *Δgre3*) transformed with GAL2$_{6SA/N376Y/M435I}$ and different indicated reductases (wild type *GRE3*, codon optimized *GRE3* and ev) via 2μ plasmid. The transformants were pre-grown in selective SC medium with 2 % glucose as a permissive carbon source. Fermentation done in SC selective media with 3 % glucose and 2 % xylose. **(A)** Glucose and xylose consumption at different time points. The consumption of glucose (solid lines, plotted on left Y axis) and xylose (symbols only, plotted on right Y axis). **(B)** Titer of xylitol (plotted as bars), measured at different time points for each of the construct tested. Mean values and standard deviation of triplicate measurements are shown. The error bars may be smaller than the symbols.

The yield of xylitol was measured at 148 hours and was found to be highest for PsXyl1 at 13.22 g/L, followed by ScGre3 at 13 g/L, and AnXyrB at 12 g/L (Figure 4.20 B). The difference between the reductases was not very significant as PsXyl1 performance was

only about 2 % and 10 % higher compared to ScGre3 and AnXyrB respectively. In a different set of fermentation, codon optimization of *GRE3* led to a slight improvement in performance but still lower than the PsXyl1, with a titer of 4.62 g/L for codon optimized *GRE3*, 4.29 g/L for wildtype *GRE3*, and 4.79 g/L for PsXyl1 (Figure 4.21 B). Thus, only a difference of 8 % rise was seen through codon optimization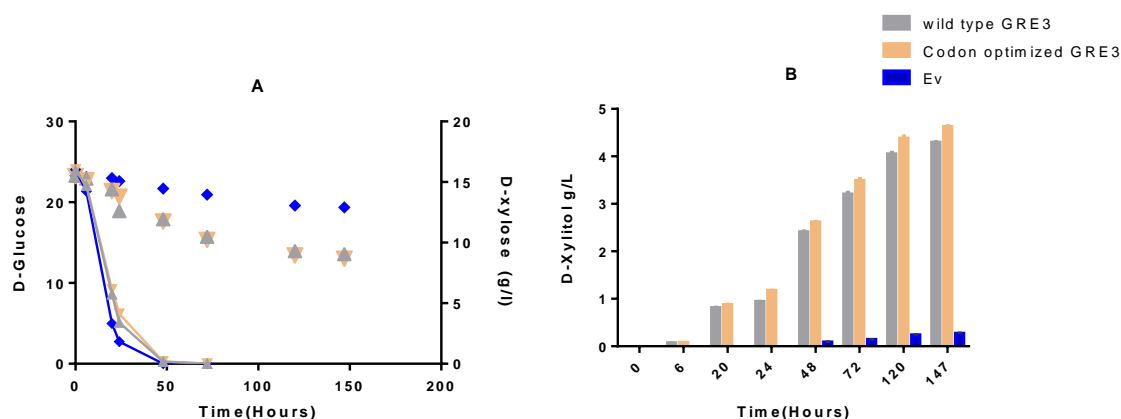 of *GRE3*. The codon optimized *GRE3* yielded 4 % xylitol lower than PsXyl1. In contrast to all reductases tested, the xylitol yield for *Candida parapsilosis* Xyl1 was observed to be almost the same as the empty vector control with a titer of 0.93 g/L and 0.95 g/L at 148 hours respectively (Figure 4.20 B), indicating that there may be a bottleneck with other factors affecting the activity of *Candida parapsilosis* Xyl1 in *S. cerevisiae*. Except CpXyl1 (NADH dependent), all other reductases used in the study were described to be NADPH dependent. To gain more insight on the reaction and its dependence on NADPH, several cellular sources of NADPH were modulated for optimal supply in the cytoplasm. This will be further described in the upcoming chapter. All the upcoming experiments are conducted with *XYL1* from *Pichia stipitis* as a xylose reductase due to its best capacity observed here.

4.2.5 Metabolic engineering of *S. cerevisiae* for the increased availability of reducing equivalents (NADPH) in cytosol

In the following chapters, focus was made on metabolic engineering of *Saccharomyces cerevisiae* in order to increase the availability of reducing equivalents, specifically NADPH, in the cytoplasm. NADPH is an important cofactor that is required for the enzymatic reduction of xylose to xylitol. Therefore, optimizing the cellular sources of NADPH can have a significant impact on the overall yield of xylitol. To achieve this goal, various cellular sources of NADPH were examined and the expression of these sources was modulated in order to achieve optimal NADPH supply in the cytoplasm. The aim of this work is to overcome the limitations posed by the cofactor availability on the overall xylitol production process. For this, individual testing of genes of oxidative pentose phosphate pathway were done. Experiments were then focused towards the manipulation of *ALD6*, *PHO13*, *POS5* genes on titer of xylitol. Following chapter describes the outcome of genetic engineering of different targets and their subsequent role in uplifting xylitol titer.

4.2.6 Oxidative pentose phosphate pathway

4.2.6.1 *ZWF1* overexpression

Metabolic engineering of *Saccharomyces cerevisiae* was performed to increase the availability of reducing equivalents (NADPH) in the cytoplasm. The first step was to overexpress the glucose-6-phosphate dehydrogenase (G-6-P) gene (*ZWF1*), which

encodes an essential enzyme involved in the oxidative pentose phosphate pathway. This gene conversion was achieved by replacing the *pZWF1* with a stronger promoter *pHXT7* in the genome to achieve a higher expression level of *ZWF1,* as done by Wernig et al. 2021. The resulting strain was named as "PRY48". When fermented in glucose and xylose, it was found to have doubled the amount of xylitol compared to the parental strain PRY39 (Figure 4.22). At 148 hours, strain PRY48 produced a maximum titer of ~11 g/L of xylitol, which is more than two times higher than the xylitol produced by PRY39 (~5 g/L). The overexpression of *ZWF1* was found to increase the yield of xylitol both in the glucose phase and ethanol phase of growth. The difference in xylitol titer between the two strains was even more pronounced during the ethanol phase of growth (from 60 hours). Interestingly, the amount of xylitol produced during ethanol phase of growth directly correlates with amount of ethanol consumed as PRY48 consumes ethanol higher than PRY39 strain after 48 hours of growth. In addition to the higher titer of xylitol, the results also showed that the consumption of the substrates glucose (or ethanol derived from glucose) and xylose was higher for PRY48 compared to PRY39, as seen in Figure 4.22.
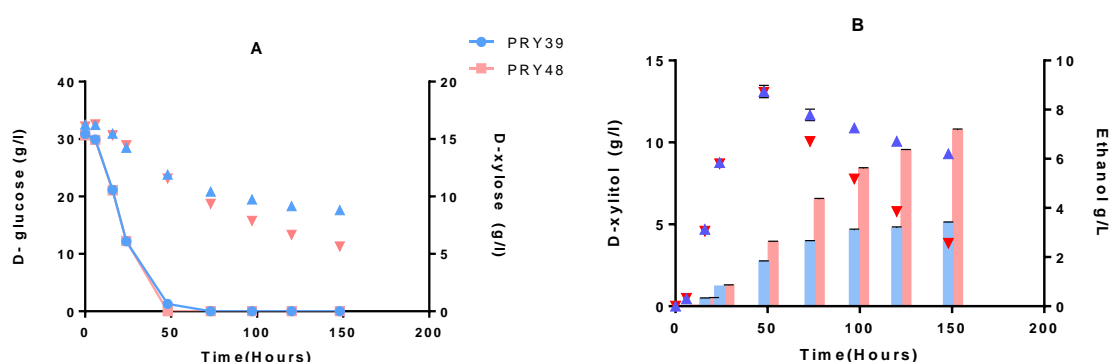
Figure 4.22: Influence of *ZWF1* overexpression in the titer of xylitol. Strains PRY39 (CEN.PK2-1C, *Δgre3*) and PRY48 (PRY39, *pZWF1::pHXT7*) transformed with GAL2$_{6SA/N376Y/M435I}$ and PsXyl1 via 2μ plasmid. The transformants were pre-grown in selective SC medium with 2 % glucose as a permissive carbon source. Fermentation done in SC selective media with 3 % glucose and 2 % xylose. **(A)** Glucose and xylose consumption at different time points. The consumption of glucose (solid lines, plotted on left Y axis) and xylose (symbols only, plotted on right Y axis). **(B)** Titer of xylitol (bars, plotted on left Y axis), and amount of ethanol (symbols only, plotted on right Y axis) measured at different time points for each of the construct tested. Mean values and standard deviation of triplicate measurements are shown. The error bars may be smaller than the symbols.

It has to be noted that Zwf1 protein sequence is polymorphic (see ZWF1/YNL241C sequence, SGD). The variant used in PRY48 has a deletion of a glutamate residue at position 59 compared to the reference strains S288C and CEN.PK. To determine if the loss of glutamate residue at position 59 has some role in the activity of the enzyme, the *ZWF1* variant containing Glu59 was cloned from the CEN.PK strain and overexpressed in the same background and in the same manner as in the strain PRY48. The resulting strain

was named PRY63. When measured in crude extracts from both strains, the specific activity of Zwf1 was found to be 50 % higher in PRY48, as shown in Figure 4.23. PRY48 and PRY63 specific activities were 0.90 and 0.60 µmol/min mg, respectively. Thus, all work done with *ZWF1* overexpression is performed with the sequence not containing the Glu59 codon (PRY48) instead of CEN.PK2-1C sequence (PRY63).
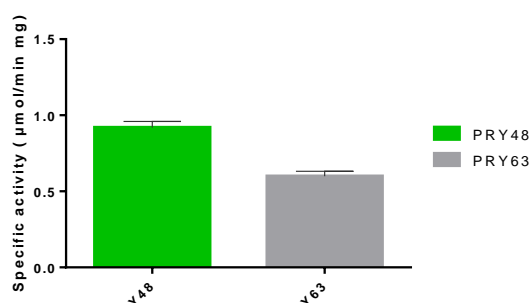
Figure 4.23: Glucose-6-P dehydrogenase activities in the strain PRY48 and PRY63. The activities of the glucose-6-P dehydrogenase/Zwf1 was measured in protein extracts from the indicated strains. Strains PRY48 and PRY63 were transformed with GAL2$_{6SA/N376Y/M435I}$ and PsXyl1 via 2µ plasmid. Cells were pre-grown in SC selective media with 2 % glucose as a permissive carbon source, and sample taken after 24 hours of fermentation. The activities are calculated as units per milligram of total protein. Values and error bars represent mean and standard deviation of three biological replicates for each genotype.

4.2.6.2 Simultaneous overexpression of Zwf1, Sol3 and Gnd1

After the observation of Zwf1 based positive effect for higher xylitol yield in above chapter (4.2.6.1), the importance of other genes of oxidative pentose phosphate pathway needed to be tested. For this, a plasmid based multicassette overexpression was done (FWV169) with *Z*wf1, *S*ol3, and Gnd1 in a plasmid with G418 as a dominant marker (Wernig et al. 2021).
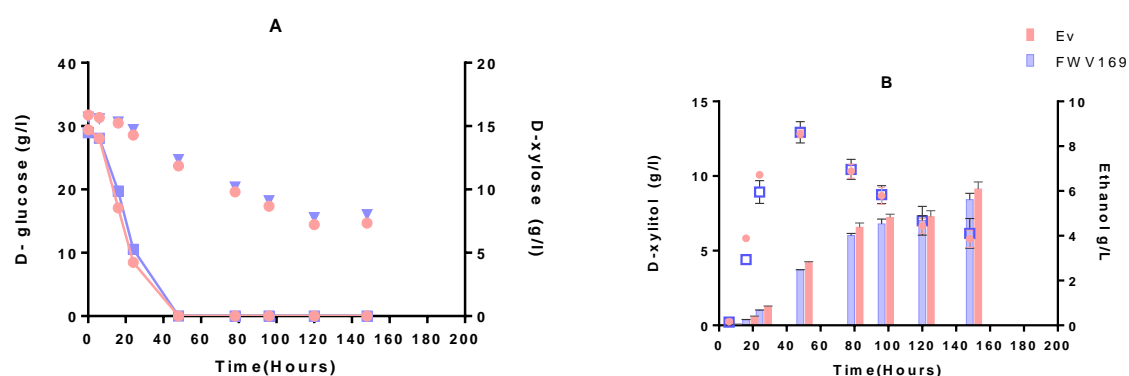
Figure 4.24: Strains PRY48 (PRY39, *pZWF1::pHXT7*) transformed with GAL2$_{6SA/N376Y/M435I}$, PsXyl1 and FWV169. FWV169 is a 2µ plasmid expressing *ZWF1, SOL3* and *GND1*. The transformants were pre-grown in selective SC medium with 2 % glucose as a permissive carbon source. Fermentation done in SC selective media with 3 % glucose and 2 % xylose. **(A)** Glucose and xylose

consumption at different time points. The consumption of glucose (solid lines, plotted on left Y axis) and xylose (symbols only, plotted on right Y axis). **(B)** Titer of xylitol (plotted as bars), measured at different time points for each of the construct tested. Mean values and standard deviation of triplicate measurements are shown. The error bars may be smaller than the symbols.

The fermentation result shows the combined higher expression of Zwf1, Sol3 and Gnd1 in a PRY48 strain did not further lead to higher titer of xylitol. The xylitol yield observed was similar to the empty vector control used for the experiment (Figure 4.24 B). This finding suggests either the Zwf1 overexpression in the strain background PRY48 was sufficient for intracellular xylitol production or the productivity might have been negatively affected with combined overexpression of oxidative pentose phosphate pathway genes.

4.2.6.3 *PGI1* downregulation

The objective of Pgi1 expression modulation strategy is to redirect the flux of glucose-6-P towards the oxidative pentose phosphate pathway. This is achieved by lowering the expression of the *PGI1* gene, which converts glucose-6-P to fructose-6-P in glycolysis. To do so, the promoter of *PGI1* was replaced with three different less strength promoters: *pCOX9*, *pRNR2*, and *pREV1* (Lee et al. 2015; Keren et al. 2013).
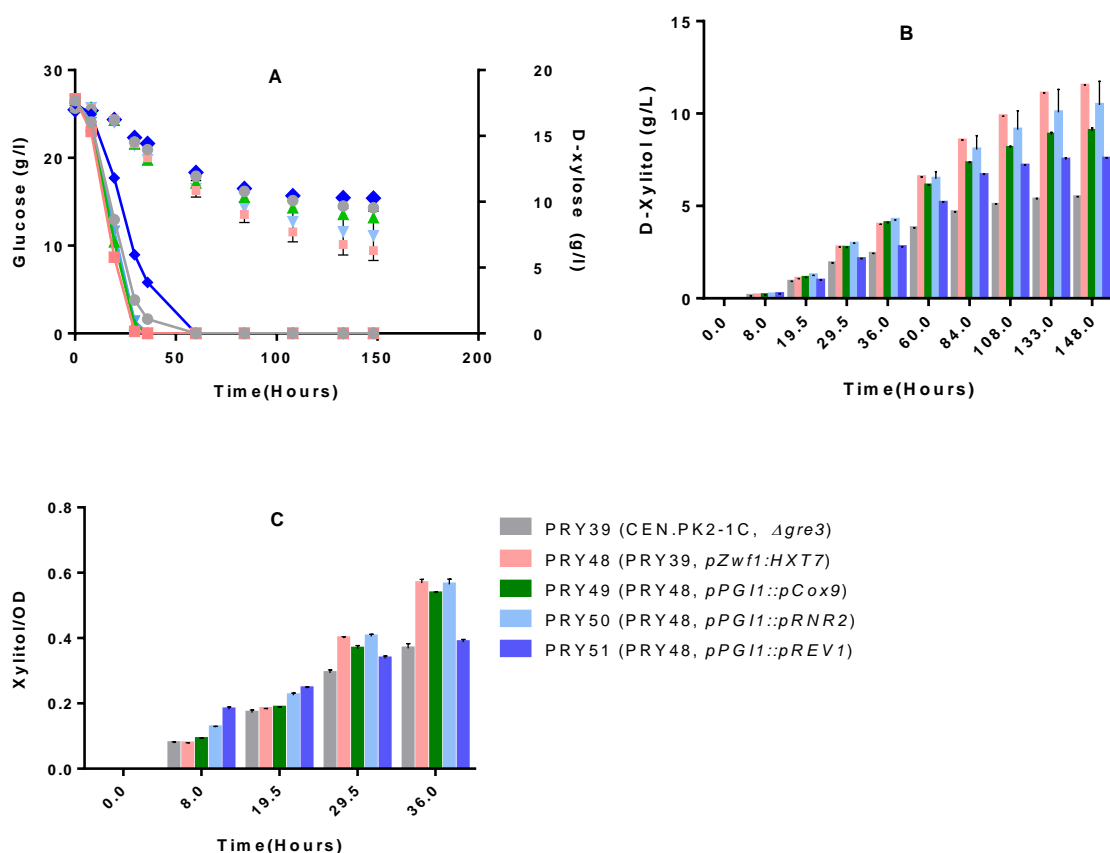
Figure 4.25: Engineered Strains PRY39 (CEN.PK2-1c, Δgre3), PRY48 (PRY39, *pZWF1::pHXT7*), PRY49(PRY48,*pPGI1::pCOX9*), PRY50(PRY48, *pPGI1::pRNR2*), PRY51 (PRY48, pPGI1::pREV1) transformed with GAL2$_{6SA/N376Y/M435I}$, and PsXyl1. FWV169 is a 2μ plasmid expressing *ZWF1, SOL3* and *GND1*. The transformants were pre-grown in selective SC medium with 2 % glucose as a permissive carbon source. Fermentation done in SC selective media with 3 % glucose and 2 % xylose. **(A)** Glucose and xylose consumption at different time points. The consumption of glucose (solid lines, plotted on left Y axis) and xylose (symbols only, plotted on right Y axis) **(B)** Titer of xylitol (plotted as bars), measured at different time points for each of the construct tested. **(C)** Calculation of xylitol (g/L) per OD$_{600nm}$ values in different time point for different strains tested. Mean values and standard deviation of triplicate measurements are shown. The error bars may be smaller than the symbols.

The results showed that reducing the expression of *PGI1* did not increase xylitol production and in fact, the yield decreased as the activity of Pgi1 slowed down with the weakest promoter *pREV1* giving the lowest titer of xylitol (Figure 4.25 B). The growth of the strain PRY51 with the weakest promoter *pREV1* was stunted and glucose consumption was slower, but it did not result in any overall improvement in xylitol yield. Nevertheless, when observed closely at early hours of fermentation, PRY51 gives a highest value of xylitol per OD$_{600nm}$ until ~20 hours (Figure 4.25 C). The xylitol per OD$_{600nm}$ value until ~20 hours seems to be highest for the weakest promoter *pREV1* and lowest for strongest promoter *pCOX9* used with a difference of 30 %. The data is presented in Figure 4.25 C. Since this time window corresponds to the glucose availability phase, this observation suggests that the promotor replacement indeed led to the desired redirection of the glucose-6-P flux. However, at the same time, it compromised the growth of the strain and had an overall negative impact on xylitol titers in the course of the diauxic shift.
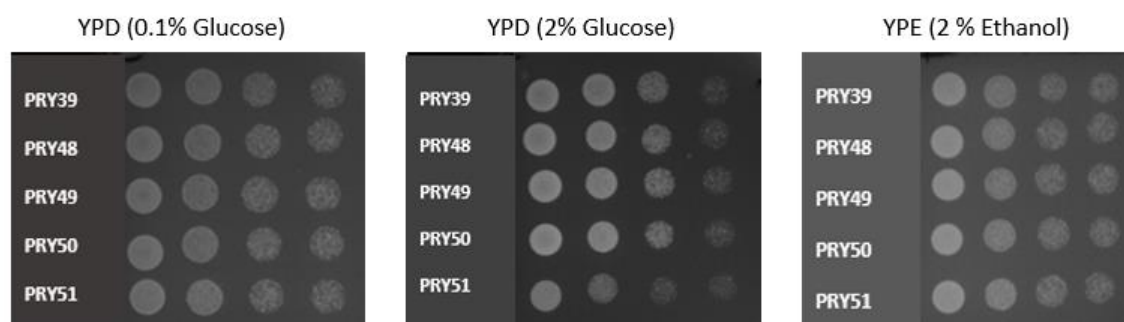
Figure 4.26: Growth conferred by strains indicated on varying sugars. Strains PRY39 (CEN.PK2-1c, Δgre3), PRY48 (PRY39, *pZWF1::pHXT7*), PRY49(PRY48, *pPGI1::pCOX9*), PRY50(PRY48, *pPGI1::pRNR2*), PRY51 (PRY48, *pPGI1::pREV1*) pre- grown in YP media with 1 % glucose as a carbon source and spotted on to selective YP solid medium containing indicated carbon sources. Cells were grown at 30 °C for 28 hours.

Additionally, drop tests were performed on five strains (PRY39, PRY48, PRY49, PRY50, and PRY51) in three different growth media: 0.1 % glucose, 2 % glucose, and 2 % Ethanol. The results from the drop test (Figure 4.26) revealed a slower growth phenotype for strain

PRY51, which was characterized by the weakest promoter (*pREV1*) used for the regulation of the *PGI1* gene, when grown in 2 % glucose. However, this effect was not observed when cells were grown in a lower amount of glucose (0.1 %) or an ethanol-rich medium (2 % ethanol). These results confirm the downregulated effect of Pgi1 on cell growth during a high glycolytic flux, as seen under high glucose concentration (2 %). This effect was not observed when the activity of Pgi1 was regulated by two other mediocre promoters, *pCOX9* or *pRNR2*. In conclusion, the weakest promoter, *pREV1*, resulted in the slowest glycolytic flux during a high glucose condition giving highest xylitol per OD_{600nm} value only until 20 hours of fermentation time. After 20 hours, the total yield of xylitol per OD_{600nm} values could not be improved by downregulating *PGI1* (Figure 4.25 B, C).

4.2.7 Investigation of multiple approaches for increasing NADPH supplementation in the cytosol

In order to improve the level of NADPH in the cytosol for the purpose of increasing xylitol production, different genetic modifications were performed on different targets. The first approach involved the introduction of $NADP^+$ dependent glyceraldehyde-3-P dehydrogenase *GPD1* from *Kluveromyces lactis* into the CEN.PK2-1D wild type strain or its $\Delta tdh3$ derivative (deletion of the major glyceraldehyde-3-P dehydrogenase isoform). Another approach involved the modification of various gene candidates to increase the yield of xylitol. These genetic manipulations included the genomic overexpression of *POS5*, deletion of *ALD6*, and deletion of *PHO13*. *POS5* is mitochondrial NADH kinase that phosphorylates NADH, thus producing NADPH. *ALD6* is cytosolic aldehyde dehydrogenase required for conversion of acetaldehyde to acetate via generation of NADPH. *PHO13* a conserved phosphatase and its deletion is described to have positive impact in xylose metabolism (Kim et al. 2015). The results of these modifications were then compared with regards to the amount of xylitol produced in a wild type (PRY39) or Zwf1 overexpressed (PRY48) background strain for assessing their efficacy in improving xylitol production.

4.2.7.1 Heterologous expression of *GPD1* from *Kluveromyces lactis*

Manipulation of glycolytic pathway was done for the step where the enzymatic conversion of glyceraldehyde-3-P to 1, 3 - bisphosphoglycerate occurs. Here, the comparison of NAD^+ dependent wild type GPDH from *S. cerevisiae* was done with additional $NADP^+$ dependent Gpd1 from *Kluveromyces lactis*. This effect was tested through a 2μ plasmid-based expression of *Kluveromyces lactis* Gpd1 in a wild type or *TDH3* disrupted strain. The fermentation results with glucose and xylose seen in Figure 4.27 A, B reveals a retarded

glycolysis flux by *TDH3* deletion as observed from the slower growth and glucose consumption by *TDH3* deleted strain. Similarly, the ethanol production and consumption both went higher with the wildtype background strain. The overall fermentation result shows a negative effect of *TDH3* deletion for the titer of xylitol. In a same way, overexpression of *K. lactis* Gpd1 also decreased the titer of xylitol in both wildtype and Δ*tdh3* background strains.
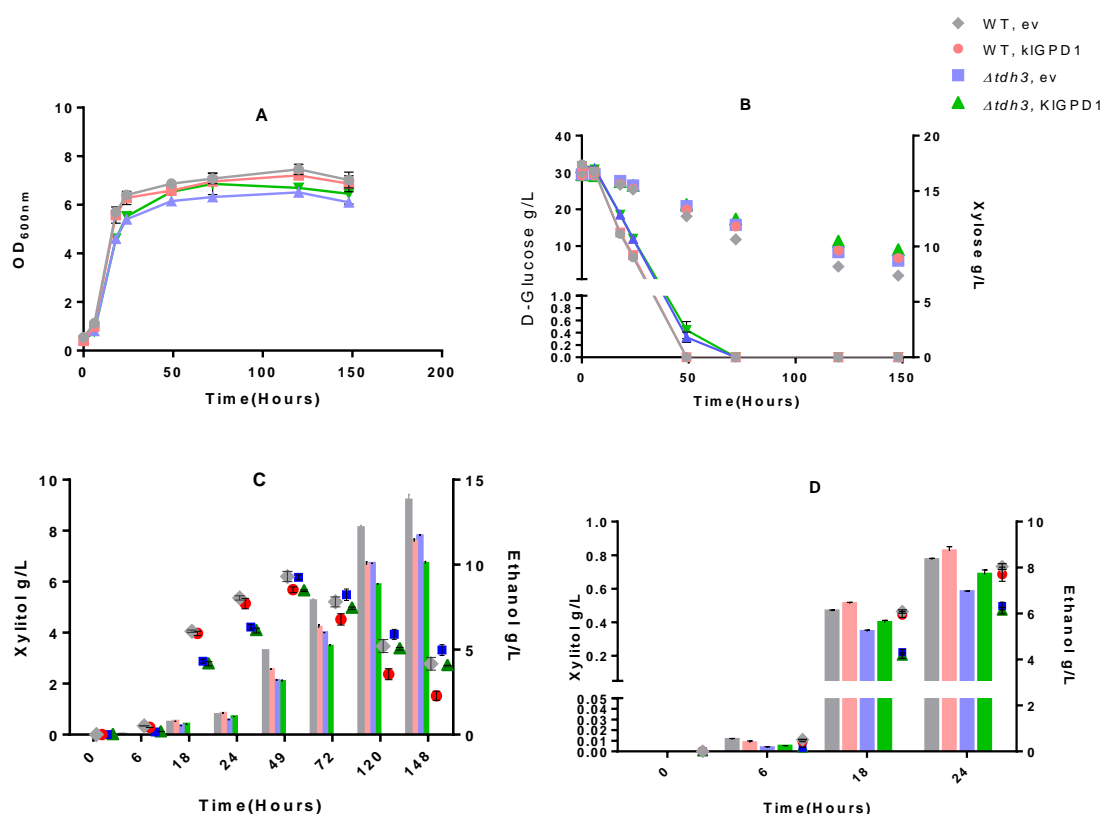
Figure 4.27: Effect of *Kluveromyces lactis GPD1* in CEN.PK2-1D. Strains CEN.PK2-1D wildtype or CEN.PK2-1D Δ*tdh3* was transformed with -GPD1 or empty vector-, and PsXyl1. WT represents wild type strain. Δ*tdh3* represents strain has a deletion of *TDH3*. KlGPD1 represents plasmid expressing GPD1, whereas ev represents empty vector control. All genes were expressed via 2μ plasmid. The transformants were pre-grown in selective SC medium with 1 % glucose as a permissive carbon source. Fermentation done in SC selective media with 3 % glucose and 2 % xylose. **(A)** Growth of the different indicated strains **(B)** Glucose and xylose consumption at different time points. The consumption of glucose (solid lines, plotted on left Y axis) and xylose (symbols only, plotted on right Y axis). **(C)** Titer of xylitol (plotted as bars, left axis), and amount of ethanol (plotted as symbols, right axis) measured at different time points until 148 hours of fermentation. **(D)** Titer of xylitol (plotted as bars, left axis), and amount of ethanol (plotted as symbols, right axis) measured at different time points until 24 hours of fermentation. Mean values and standard deviation of triplicate measurements are shown. The error bars may be smaller than the symbols.

Interestingly, a magnified view at early hours of fermentation (Figure 4.27 D) points out the positive role of Gpd1 expression in both wild type and *TDH3* deleted strains until 24 hours of growth. At later time points, which correspond to the ethanol consumption phase, this

effect is reversed (compare panels C and D); this is readily explained by Gpd1 operating in the gluconeogenesis direction, i.e. consuming NADPH. Even though the titer of xylitol was increased by the *GPD1* overexpression in early phases, the *TDH3* deletion did not make a further positive impact for the titer of xylitol at any time point. Thus, the effect of the *GPD1* expression seems not to be limited by the availability of glyceraldehyde-3-P.

4.2.7.2 Targeting loci *POS5, PHO13* and *ALD6* for increasing the pool of NADPH

To elevate the intracellular NADPH content and improve xylitol production, various genetic modifications were individually carried out on different genetic targets. One such target was the gene *POS5*, a NADH kinase responsible for NADPH production in mitochondria. Another was the deletion of the gene *PHO13*, which has been reported to improve xylose uptake and metabolism. Additionally, the deletion of the acetaldehyde producing NADP$^+$ dependent *ALD6*, which is also known as a second major source of cytosolic NADPH after ZWF1, was investigated. These genetic modifications were tested in two different strain backgrounds, the parental PRY39 and the *ZWF1* overexpressing PRY48 to asses both their individual and potential additive effects.

4.2.7.2.1 Cytosolic expression of *POS5*

The present study investigates the potential role of *POS5* overexpression. Since Pos5 is a mitochondrial protein, the N-terminal targeting sequence (amino acids 1-17) was deleted (Yukawa et al. 2021) for a cytosolic localization. The truncated coding sequence was placed under the control of the rather weak *pRNR2,* since a stronger expression had rather detrimental effects in a previous study (Harth. S, unpublished result). Despite initial expectations, the results showed that the overexpression of *POS5* did not lead to an increase in xylitol titer in either strain. On the contrary, both strains exhibited a decrease in xylitol yield with *POS5* overexpression. Specifically, xylitol titers were found to be 3.5 g/L for PRY53 (PRY39, *pRNR2-POS5*) and 5 g/L for PRY39, whereas PRY48 produced 11 g/L at 148 hours (Figure 4.28 A). Hence, the integration of *POS5* in PRY39 resulted in a decrease in xylitol yield by approximately 30 %. Similar observations were made in strain background PRY48, where the integration of *POS5* produced 7 g/L, compared to 11 g/L produced by PRY48, indicating a decrease in xylitol yield by approximately 40 % at 148 hours (Figure 4.28 B).

Despite no overall improvement in yield conferred by *POS5* overexpression, an interesting observation was made when examining the yield of xylitol during the early hours of fermentation. A magnified view of yield until 24 hours shows increased productivity by PRY53 (PRY39, *pRNR2-POS5*) strain with almost 8 % higher yield than PRY39 strain

when values were compared at 24 hour of fermentation time (Figure 4.28 C). This suggests an early hour of fermentation time to be favorable period for the higher yield of xylitol in strain when overexpressed with *POS5* gene. Until 24 hours of time point, the yield produced by *POS5* overexpression in PRY39 strain is even higher than PRY39 overexpressed with *ZWF1* with a difference of 3 %. This observation is not reproduced in the context of PRY48 strain as seen that PRY54 (PRY48, *pRNR2-POS5*) strain produces lower yield of xylitol than PRY48 even for early hours of fermentation until (24 hours) as seen in Figure 4.28 B.

4.2.7.2.2 Deletion of *PHO13*

To investigate the potential role of the *PHO13* gene in xylitol production, *PHO13* was deleted via a KanMX cassette in strains PRY39 and PRY48, resulting in strains PRY46 (PRY39, Δ*pho13*) and PRY47 (PRY48, Δ*pho13*), respectively. The fermentation results showed that the deletion of *PHO13* did not significantly impact xylitol production or other metabolite measurements in either strain. In PRY39, xylitol production was measured at 148 hrs 4 g/L for PRY39, Δ*pho13*, which is a 20% decrease compared to the production of 5 g/L in the original PRY39 strain (Figure 4.28 A). Similarly, when this modification was made in the PRY48 strain background, a reduction in xylitol production was observed, with PRY48 producing 11 g/L and PRY48, Δ*pho13* producing 7.5 g/L at 148 hours, indicating a decline of about 30 % in xylitol yield (Figure 4.28 B). These results show that the deletion of *PHO13* is rather detrimental for xylitol production by PRY39 and PRY48.

4.2.7.2.3 Deletion of *ALD6*

The deletion of the *ALD6* gene, encoding an $NADP^+$-dependent acetaldehyde dehydrogenase, had varying effects on xylitol titer in the two yeast strains tested. In strain PRY39, the deletion of *ALD6* resulted in a 60 % increase in xylitol yield at 148 hours, with 8 g/L produced by the *ALD6*-deleted strain compared to 5 g/L produced by the original strain (Figure 4.28 A). This higher xylitol yield in strain PRY39 could be attributed to the upregulation of Zwf1 reaction or decreased acetate formation. However, in strain PRY48, the deletion of *ALD6* did not have a similar effect, and instead led to a 40 % decline in xylitol titer at 148 hours, with only 6.5 g/L produced by the *ALD6*-deleted strain compared to 11 g/L produced by the original strain (Figure 4.28 B).

These results suggest that the role of *ALD6* deletion on xylitol production may depend on the strain background employed. The lack of effect in strain PRY48 could be due to the overexpression of Zwf1 masking the effect of *ALD6* deletion, or limited $NADP^+$ availability in the cell. Enzymatic activity tests were performed in the next chapter to investigate if the

deletion may have led to an upregulation of *ZWF1* to (over)compensate the loss of NADPH
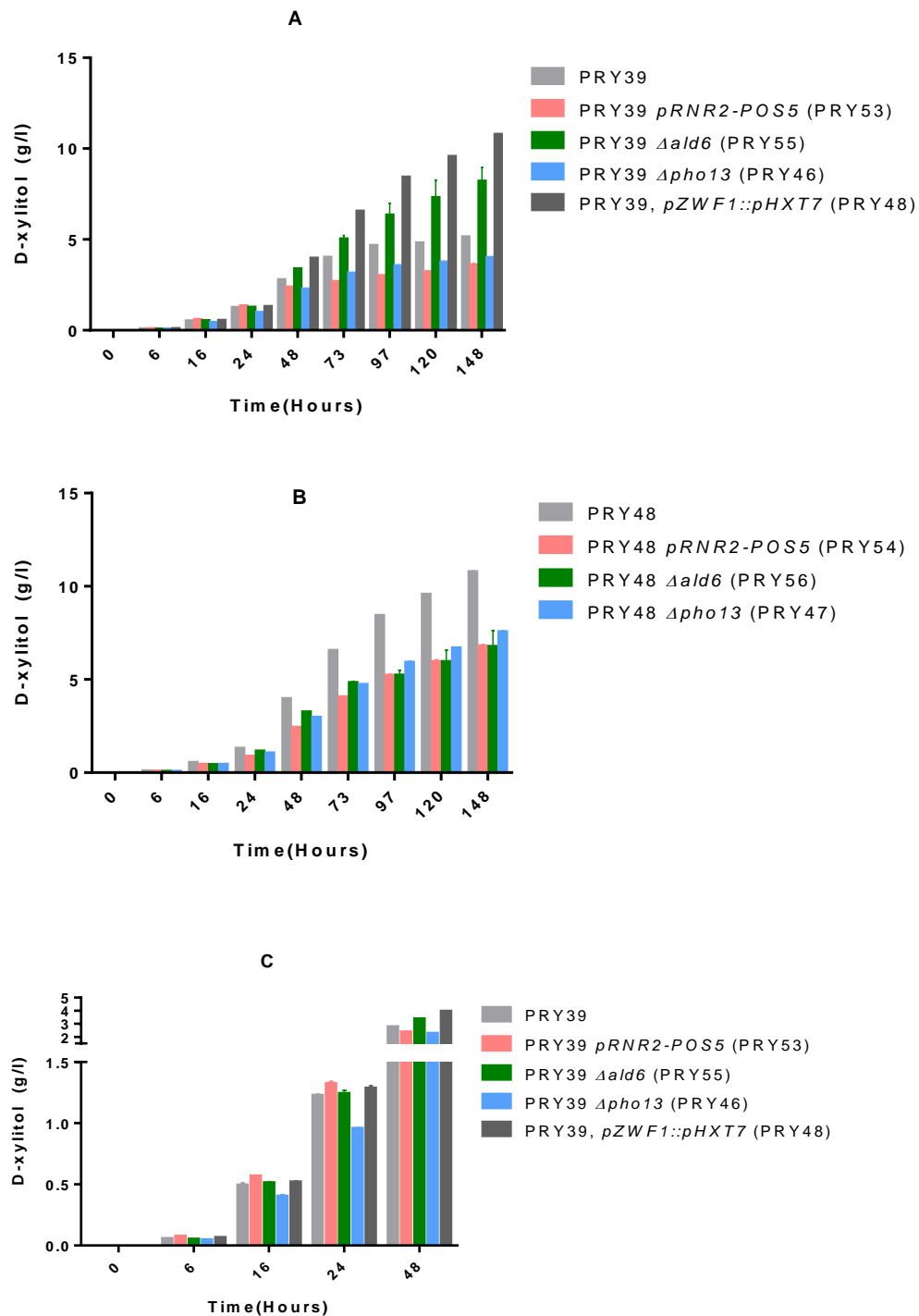
Figure 4.28: Different engineered strains tested for the production of xylitol. All strains were transformed with GAL2*6SA/N376Y/M435I* and PsXyl1. The transformants were pre-grown in selective SC medium with 2% glucose as a permissive carbon source. Fermentation done in SC selective media with 3% glucose and 2% xylose. **(A)** Comparison of strains PRY39 (CEN.PK2-1c, *Δgre3*), PRY39 *pRNR2-POS5* (PRY53), PRY39 *Δald6* (PRY55), PRY39 *Δpho13* (PRY46), PRY39 *pZWF1::pHXT7* (PRY48) for xylitol production at different time points. **(B)** Comparison of strains PRY48 (PRY39, *pZWF1::pHXT7*), PRY48 *pRNR2-POS5* (PRY54), PRY48 *Δald6* (PRY56), PRY48 *Δpho13* (PRY47), for xylitol production at different time points. **(C)** A magnified view of xylitol titer produced

by different PRY39 derived strains (from graph A) only until 48 hours of fermentation time. Mean values and standard deviation of triplicate measurements are shown. The error bars may be smaller than the symbols.

due to the lack of Ald6. Overall, these findings highlight the importance of understanding the specific genetic and metabolic context of each strain in order to optimize xylitol production through genetic engineering.

4.2.7.2.4 Enzymatic activity test of Zwf1

An enzymatic activity test was performed to determine the influence of the deletion of *ALD6* on the Zwf1 activity for the production of xylitol. Zwf1 enzymatic tests were performed in strains PRY39, PRY48 and PRY39 $\Delta ald6$ using G-6-P as a substrate and NADP$^+$ as a cofactor.
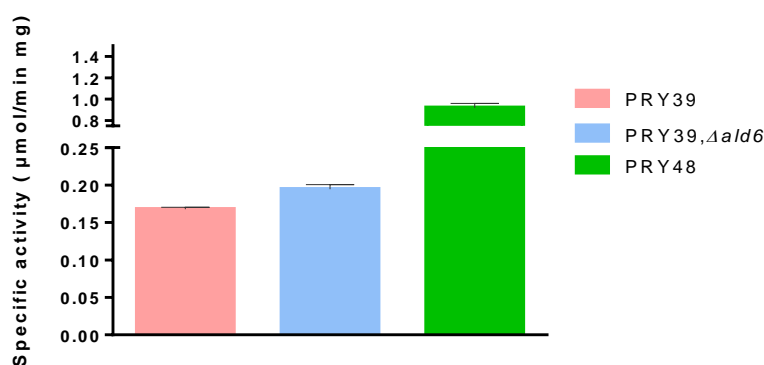
Figure 4.29: Glucose-6-P dehydrogenase activities in the strain PRY39, PRY39 $\Delta ald6$ (PRY55) and PRY48 (PRY39, *pZWF1::pHXT7*). The activities of the glucose-6-P dehydrogenase/Zwf1 was measured in protein extracts from the indicated strains. Strains PRY39, PRY39 $\Delta ald6$ and PRY48 were transformed with GAL2$_{6SA/N376Y/M435I}$ and PsXyl1 via 2µ plasmid. Cells were pre-grown in SC selective media with 2 % glucose as a permissive carbon source, and sample taken after 24 hours of fermentation. The activities are calculated as units per milligram of total protein. Values and error bars represent mean and standard deviation of three biological replicates for each genotype

Activity of Zwf1 is expectedly strongly increased in PRY48 where Zwf1 protein is overproduced through promoter exchange. Specific activity of PRY39 and PRY48 was found to be 0.17 and 0.90 µmol/min mg respectively. The results of the test, in Figure 4.29, furthermore shows that the deletion of *ALD6* slightly elevated the activity of Zwf1 in the PRY39 strain, which may at least partly explain the higher titer of xylitol observed for PRY39, $\Delta ald6$ (Figure 4.28 A). The specific activity of PRY39 $\Delta ald6$ was calculated to be 0.20 µmol/min mg. Hence, a 20 % rise in the activity of Zwf1 was observed by the deletion of *ALD6* in PRY39, which was still ~75 % lower than PRY48 strain (Figure 4.29). This is also in accordance to the titer of xylitol where strain PRY39 $\Delta ald6$ produced 60 % higher xylitol compared to strain PRY39 when calculated at the end time point (148 hours) as

seen in chapter 4.2.7.2.3, Figure 4.28 A. This indicates that the overexpression of *ZWF1* was a crucial factor in the increased production of xylitol, and that the deletion of *ALD6* may have facilitated the increased production by enabling the upregulation of *ZWF1* controlled by the native promoter. However, this increase was much lower than the sole effect of promoter replacement at *ZWF1*. The results of this enzymatic activity test further confirm the significance of Zwf1 overexpression and *ALD6* deletion in the production of xylitol.

4.2.7.3 Effect of *XKS1* deletion on xylitol production in strain PRY48

Although *S. cerevisiae* cannot grow on xylose as a sole carbon source, it does contain multiple genes encoding proteins with xylitol dehydrogenase activity, e.g. *XYL2*, *SOR1* and *SOR2*. Thus, xylitol could be partly converted to xylulose, which, after phosphorylation by the single xylulokinase Xks1, could enter the non-oxidative pentose phosphate pathway, which would decrease the product titers. To prevent this, it was chosen to delete rather the *XKS1* gene than the multiple xylitol dehydrogenase genes.
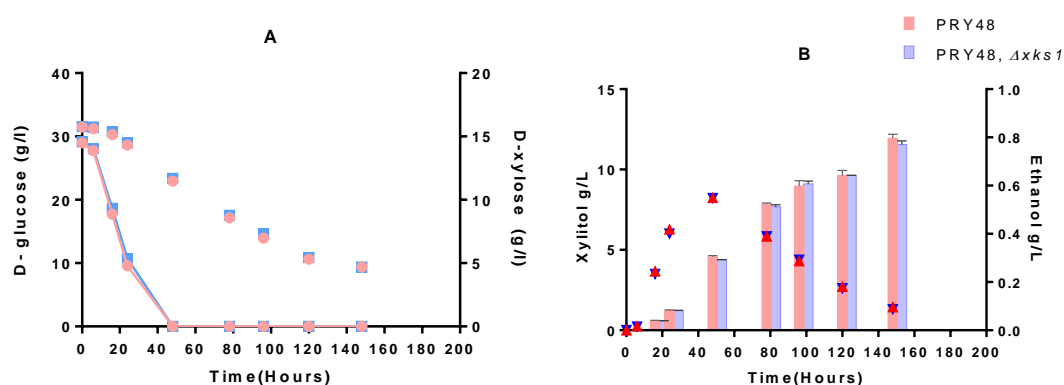
Figure 4.30: Strains PRY48 and PRY48 *Δxks1* (PRY52) transformed with GAL2$_{6SA/N376Y/M435I}$, and PsXyl1. The transformants were pre-grown in selective SC medium with 2 % glucose as a permissive carbon source. Fermentation done in SC selective media with 3 % glucose and 2 % xylose. **(A)** Glucose and xylose consumption at different time points. The consumption of glucose (solid lines, plotted on left Y axis) and xylose (symbols only, plotted on right Y axis) **(B)** Titer of xylitol (plotted as bars, left Y axis) and amount of ethanol (symbols only, right Y axis) measured at different time points for each of the construct tested. Mean values and standard deviation of triplicate measurements are shown. The error bars may be smaller than the symbols.

The effect of *XKS1* deletion on xylitol production was compared in strain PRY48. To check for any possible flux of xylitol down the pathway, CRISPR/Cas9-mediated deletion of the xylulokinase gene (*XKS1*) was carried out in PRY48 to generate strain PRY52. Both strains were fermented with glucose and xylose, and HPLC measurements were taken at different time points. Results (Figure 4.30 B) showed no effect from the deletion of *XKS1* on xylitol production, which remained at about 12 g/L at 148 hours for both strains PRY48

and PRY52. This is consistent with the observation, that the xylitol yield (mol per mol consumed xylose) approaches 100 % and that the xylitol dehydrogenases are only weakly expressed in the presence of glucose. Nevertheless, the deletion of *XKS1* may be beneficial under conditions that favor the upregulation of xylitol dehydrogenase genes (e.g. in the absence of glucose).

4.2.7.4 Impact of carbon source on xylitol production

Choice of sugar source during fermentation has a significant impact on cellular metabolism and signaling systems, leading to activation of different organelles and regulation of various genes. The previous chapters have analyzed xylitol production using glucose as the primary carbon source for yeast growth. To further explore the response of different sugars on xylitol titer, two additional tests were conducted using galactose and ethanol as main carbon sources. The first test involves fermenting 3 % galactose and 2 % xylose in the PRY48 strain. The second test utilizes 2 % ethanol and 2 % xylose in both the PRY39 and PRY48 strains. These experiments aim to shed light on the influence of different sugar sources on xylitol production and the role they play in modulating cellular processes.

4.2.7.4.1 Xylitol yield using galactose as a carbon source

Zwf1 overexpressing cells PRY48 when grown in 3 % galactose and 2 % xylose shows a significant drop in xylitol titer compared to fermentations with glucose. Comparison of glucose and galactose as a carbon source in Figure 4.31 A shows different growth behavior.
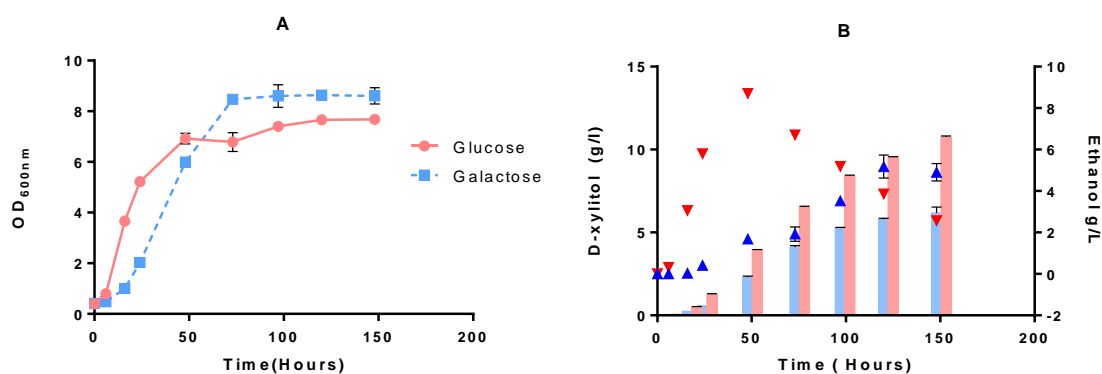
Figure 4.31: Xylitol production with growth in galactose or glucose. Strains PRY48 transformed with GAL2$_{6SA/N376Y/M435I}$, and PsXyl1. The transformants were pre-grown in selective SC medium with 2 % glucose as a permissive carbon source. Fermentation done in SC selective media with 2 % xylose and, 3 % galactose or glucose as a carbon source **(A)** Growth of the strains in different time points **(B)** Titer of xylitol (plotted as bars, left Y axis) and amount of ethanol (symbols only, right Y axis) measured at different time points for each of the construct tested. Mean values and standard deviation of triplicate measurements are shown. The error bars may be smaller than the symbols.

With galactose, cells grow more slowly but reach a higher final cell density. Furthermore, ethanol production is affected by growth in galactose. During the growth on galactose, maximum amount of ethanol observed was 5 g/L at 120 hours, whereas for glucose grown cells the ethanol titer was 9 g/L at 48 hours. Both the pattern of growth and ethanol formation are consistent with the more respirative metabolism of galactose in comparison to glucose. Titer of xylitol was almost 6 g/L at 148 hours for galactose grown cells which is almost half the production level attained by glucose usage (Figure 4.31 B).

4.2.7.4.2 Xylitol yield using ethanol as a carbon source

Since a strong production of xylitol was observed in previous chapters during the ethanol consumption phase, it was next tested how ethanol as a sole source of carbon would affect the production pattern. The yield of xylitol was determined for the PRY39 and PRY48 strains. The fermentation result seen in Figure 4.32 C surprisingly shows a different behavior of xylitol production for the two strains. When the strain PRY39 and PRY48 were compared, a higher amount of xylitol was obtained by the PRY39 strain, which is in contrast to glucose-based fermentation results described in previous chapters.

Here, the xylitol titer was 8.7 g/L and 7.7 g/L for PRY39 and PRY48 respectively at 148 hours, a difference of about 13 %. The higher amount for xylitol was observed for PRY39 for any selected time points of fermentation. Similarly, the ethanol consumption was also higher for PRY39 strain in comparison to PRY48. Absorbance values taken at 600nm shows the growth of the strain PRY39 slightly higher than PRY48, but the difference was not significant over the fermentation period (Figure 4.32 A). The overall result suggests a completely opposite observation obtained with the Zwf1 overexpression on the xylitol productivity when the glucose was interchanged with ethanol. This might have been due to the opposite direction of the flux which occurs during the ethanol growth.
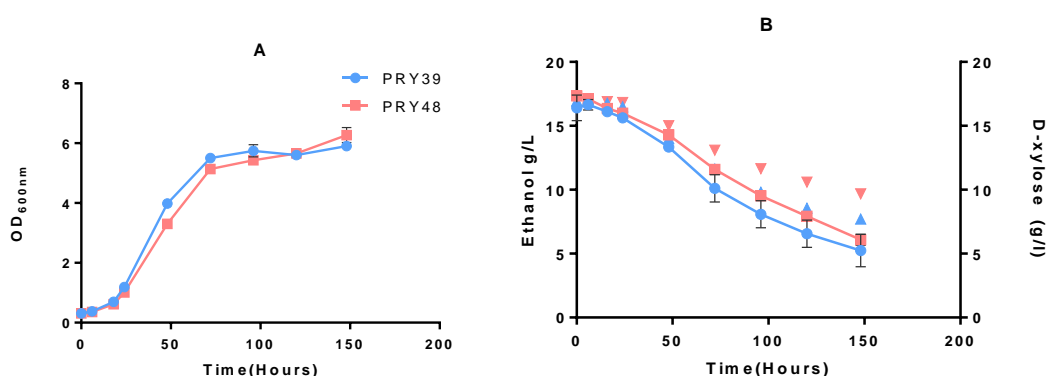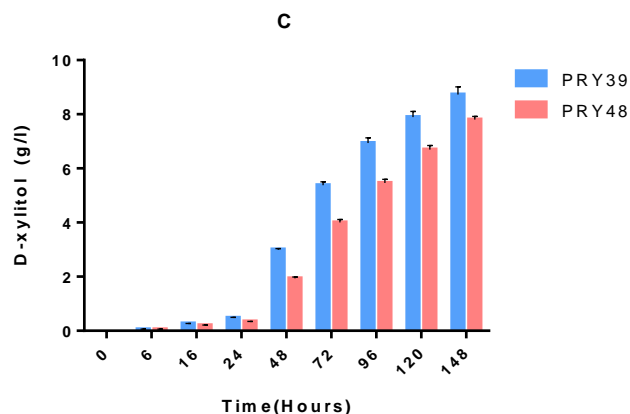
Figure 4.32: Xylitol production with growth ethanol as a carbon source. Strains PRY39 and PRY48 (PRY39, *pZWF1::pHXT7*) transformed with GAL2$_{6SA/N376Y/M435I}$, and PsXyl1. The transformants were pre-grown in selective SC medium with 2 % glucose as a permissive carbon source. Fermentation done in SC selective media with 2 % ethanol and 2 % xylose **(A)** Growth of the strains in different time points **(B)** Ethanol and xylose consumption at different time points. The consumption of ethanol (solid lines, plotted on left Y axis) and xylose (symbols only, plotted on right Y axis) **(C)** Titer of xylitol measured at different time points for each of the construct tested. Mean values and standard deviation of triplicate measurements are shown. The error bars may be smaller than the symbols.

In this study on xylitol transport and production in *S. cerevisiae* (Chapter 4.2), the Gal2 mutant variant Gal2$_{6SA/N376Y/M435I}$ was found to be the best xylitol importer among ten different hexose transporters tested, but did not improve xylitol export. Among different xylose reductases tested for their ability to produce xylitol, the xylose reductase from *Pichia stipitis* was the most efficient. In terms of increasing cytosolic NADPH levels to improve xylitol production, overexpression of the *ZWF1* gene was found to be the most effective strategy, resulting in higher xylitol titers.

5 Discussion

The present thesis work endeavors to harness the potential of yeast as a microbial platform for sustainable way to produce biochemicals. To this end, the focus of present thesis was on the utilization of pentose sugar - xylose, a substantial component of lignocellulosic biomass, for various applications. The first portion of this research efforts centered on the establishment of the Weimberg pathway for the assimilation of xylose sugar as a carbon source for the growth of *Saccharomyces cerevisiae*. The subsequent part of the thesis was mainly dedicated to enhancing the production of xylitol through multiple optimization strategies.

5.1 Weimberg pathway for α-ketoglutarate (AKG) production

The primary focus of the first part of the present doctoral thesis is to expand the sugar catabolism possibilities of yeast, with a specific focus on xylose. While glucose is a rapidly utilized sugar that is prevalent in a wide range of organisms, xylose is a pentose that is difficult to consume for some microbes, including *S. cerevisiae*. Growth of the strain with xylose as a carbon source is taken as a direct measure of activity of Weimberg pathway in *S. cerevisiae* strain comprising complete set of the required heterologous genes. In the pathway, xylose is converted via several intermediates to a final product α-ketoglutarate (AKG), which is an intermediate metabolite of TCA (Tricarboxylic acid) cycle and presence of this compound is expected for the growth of the strain.

Borgström and the colleagues reported a successful implementation of the Weimberg pathway in *S. cerevisiae* (Borgström et al. 2019). Specifically, they integrated genes *xylB*, *xylD*, *ksaD*, and *xylX* into the genome of *S. cerevisiae* strain with *FRA2* deletion, resulting in the expression of a functional pathway. The authors found that a single copy of each gene was sufficient to achieve pathway activity, as demonstrated by the detection of all pathway metabolites via mass spectrometry analysis. They found the additional expression of downstream genes, including *xylD*, *ksaD*, and *xylX*, further benefited xylose conversion to AKG through the pathway. These fermentation experiments were primarily conducted in a glucose-xylose mixture, which supported the activity of the pathway. In the same work, to further optimize the Weimberg pathway in *S. cerevisiae*, additional evolutionary engineering efforts were undertaken. The resulting evolved strain TMB4590 demonstrated the ability to grow solely on xylose as a carbon source. This indicates the possibility of Weimberg pathway to utilize xylose as a sole carbon source in *S. cerevisiae* and strongly suggests the implementation of techniques like evolutionary engineering could be beneficial to furthermore improvise the activity of the pathway. Interestingly,

authors found out the evolved strain TMB4590 contained higher expression of the downstream genes- *xylD*, *ksaD*, and *xylX*, and comparatively lower expression of *xylB*. The authors hypothesized that this phenomenon may be due to the toxicity of xylonate, a product of XylB activity. The evolved xylose growing TMB4590 strain possibly appeared to favor the production of minimal xylonate levels to avoid its toxic effects and thus showed enhanced pathway activity with this gene dosage optimization (Borgström et al. 2019). In present work, initially various expression strategies were employed, including genome integration of *xylB* and multicopy plasmid expression of downstream genes *xylD*, *xylX*, *ksaD* or, the multicopy plasmid-based expression of entire pathway genes *xylB*, *xylD*, *ksaD*, *xylX*. To modulate the activity of XylB, expression of this gene was carried out either via genome integration or with multicopy plasmid based expression. However, none of these strategies resulted in strains that could grow on xylose as a sole carbon source until 200 hours (Figure 4.1). This could be attributed to several limitations like- insufficient gene expression, suboptimal production of AKG, cofactor availability, the transport of AKG into the mitochondria, or suboptimal gene expression, hence proposes a need to provide sufficient amount of time for gene expression or introduction of mutation which might be beneficial for improvising the carbon flux through the pathway. To address this issue, evolutionary engineering strategies were pursued, where the strains were modified in various ways prior to evolution. One strategy involved the use of yeast mutator strains which were created by deleting genes such as *RAD27* or *MSH2* to enhance mutagenesis (for details chapter 5.1.1). Another strategy involved expressing pathway genes in two different compartments, cytosol and mitochondria, resulting in two copies of each pathway genes in the genome (for details see chapter 5.1.2). Strains after evolution was found to be able to grow in xylose however, it remained unclear if there is involvement of Weimberg pathway or oxidoreductive route played prominent role or there existed interconnected network of both oxidoreductive and Weimberg pathway. In addition to evolutionary engineering attempts to resolve the performance of the pathway activity, additionally, a screening platform constructed with a glutamate auxotrophic strain revealed that xylose supplementation was unable to complement the auxotrophic behavior of the strain containing complete Weimberg pathway (for details see chapter 5.1.4).

This study aims to explore the degradation of xylose through the heterologously expressed Weimberg pathway using four different genes (Borgström et al. 2019). However, the process is not straightforward, as the Weimberg pathway and its efficient expression are limited by several known and unknown factors. The first enzyme in the pathway, XylB from *Caulobacter crescentus*, catalyzes the conversion of xylose to xylonate, which is known to be toxic for yeast (Borgström et al. 2019; Wasserstrom et al. 2018). The second enzyme,

XylD from *Caulobacter crescentus*, requires [4Fe-4S] for its activity. Experimental evidence from Andberg and their teams shows the XylD from *Caulobacter crescentus* requires iron sulfur cluster for their activity. Authors, with phylogenetic and mutational analysis, suggests the three conserved cysteine residues C60, C128 and C201 in XylD are needed for the coordination of the Fe/S cluster (Andberg et al. 2016). There are several reports where expression of iron sulfur proteins from prokaryotes faces difficulties when expressed in *S. cerevisiae*. Partow and their teams found the difficulty of expressing MEP (2-C-methyl-D-erythritol 4-phosphate) pathway enzymes in yeast where genes like IspG and IspH were involved and known to require iron sulfur cluster for the activity (Partow et al. 2012). Similarly, Benisch and Boles faced difficulty in expressing iron sulfur cluster requiring bacterial enzyme 6-phosphogluconate dehydratase (PGDH) in *S. cerevisiae* (Benisch and Boles 2014). These dehydratases pose a major bottleneck, probably due to inefficient assembly of the cofactor on a heterologous protein in the cytosol of yeast. Despite previous reports of difficulties in expressing prokaryotic iron sulfur-requiring genes in *S. cerevisiae*, there have been some promising insights suggesting that deletion of the *FRA2* gene could improve the activity of *xylD* gene that encodes an iron sulfur-requiring enzyme to catalyze the conversion of xylonate to 2-keto-3-deoxyxylonate (2K3DX). *FRA2* is a negative iron regulon, and its deletion is shown to favor a cytosolic pool of iron sulfur clusters. There are some studies that reports elevated activity of XylD in a *FRA2* deleted strain of *S. cerevisiae* (Salusjärvi et al. 2017; Borgström et al. 2019). Similarly, Yukawa and the teams showed successful expression of *xylD* in a *FRA2* deleted strain, resulting the conversion of xylose to 1,2,4 -butanetriol (Yukawa et al. 2021). Based on these observations, the present study aims to express the heterologous Weimberg pathway for growth on xylose as the sole carbon source in a strain with a deleted *FRA2* gene. Despite the existing previous reports of successful activity of the iron sulfur cluster requiring prokaryotic XylD enzyme in a *FRA2* deleted *S. cerevisiae* strain, there still remains the need for optimization of activity of XylD to achieve optimal performance. As an alternative to *xylD*, in this thesis, another dehydratase *orf41* from *Arthrobacter nicotinovorans*, belonging to the enolase family of proteins was tested which might instead require Mg^{+2} for their activity as observed with most of the protein belonging to enolase family. Strain were constructed where pathway genes like *xylB*, *ksaD* and *xylX* together with *orf41* from *Arthrobacter nicotinovorans* was included for this study (Mihasan et al. 2013). In this study, the activity of Orf41 as a dehydratase to activate the Weimberg pathway could not be confirmed as seen in Figure 4.1 where strains either with *xylD* or *orf41* as a dehydratase, both failed to grow in xylose as a carbon source. This dehydratase (Orf41) has not been yet extensively studied in *S. cerevisiae*. There might be limitation in the activity of Orf41 from *Arthrobacter nicotinovorans* in *S. cerevisiae*, however if pathway

genes other than *orf41* is a limiting step still remains unclear.

Beside the first two genes *xylB* and *xylD* (or *orf41*) derived from *Caulobacter crescentus* and *Arthrobacter nicotinovorans* used in present study, two more genes are required for the conversion of 2-Keto 3-deoxy xylonate to AKG. For this *xylX* from *Caulobacter crescentus* and *ksaD* from *Corynebacterium glutamicum* was employed. *ksaD* gene from *Corynebacterium glutamicum* is employed for the present study due to its reported higher activity compared to similar gene *xylA* from *Caulobacter crescentus*, both of them are known for conversion AKG semialdehyde to AKG (Borgström et al. 2019). Apart from the possible toxicity issues of xylonate and inefficient activity of dehydratases from the upper branch of the pathway, there might be limitation in lower branch of Weimberg pathway as well. The lower branch of the Weimberg pathway, consisting of genes *ksaD* and *xylX* from *C. glutamicum* and *C. crescentus*, respectively, has not been widely studied in *S. cerevisiae*. Finally, the production of AKG, the goal of the pathway, is uncertain due to the potential limitations of the molecular route towards mitochondria and AKG driven gluconeogenesis.

5.1.1 Optimizing Weimberg pathway via yeast mutators

In this study, a nonspecific genome mutagenesis approach was employed to resolve before mentioned limitations under evolutionary pressure to utilize xylose as a sole carbon source via the Weimberg pathway. A method of mutagenesis was implemented through yeast mutators, with the aim of triggering the genetic components that confer growth on xylose as a sole carbon source. The use of yeast mutator strains Δ*rad27* or Δ*msh2* for the Weimberg pathway was motivated by the literature that has exploited the possibility of mutators to increase the mutation rate in the genome of *S. cerevisiae* (Loeillet et al. 2020). The mutations perpetuated by the strain were non-specific, but a well-defined selection process was used to favor desired superior candidates that grew better in xylose. A similar experiment was performed in *E. coli*, where mutH and mutT mutator strains gave rise to strains capable of growing in glucose via an engineered non -oxidative glycolysis pathway, where a mutation in the non-oxidative branch of PPP (Pentose phosphate pathway) being found to be responsible (Lin et al. 2018). Evolutionary engineering experiments in *E. coli* have shown the benefits of employing mutator strains, with fast adaptation to stressful environments and selective pressure applied to increase the frequency of the mutator phenotype from 0.001 % to 100 % within a short time interval (Sniegowski et al. 1997; Tenaillon et al. 1999; Maddamsetti and Grant 2020; Mao et al. 1997). In bacteria and haploid yeasts, the importance of these systems is described as error-induced extinction occurring within a few cell divisions if both DNA polymerase proofreading and mismatch

repair systems are lacking, due to mutation rates exceeding the error threshold of one inactivating mutation per essential gene per cell division (Fijalkowska and Schaaper 1996; Herr et al. 2011; Herr et al. 2014; Williams et al. 2013; Morrison et al. 1993).

The yeast mutator approach was employed in this study to enhance evolutionary engineering through serial transfer in shake flask in selective media. With each sequential transfer to fresh culture in a similarly carbon-stressed environment, constant accumulation of selection pressure was observed, leading to the selection of mutant cells with higher specific growth rate. The artificial selection pressure applied resulted in the expected domination of a superior strain from the mixed population in the flask. A limiting amount of nutrient, including galactose, was considered to trigger mutation and modification, as galactose has the potential to activate mitochondria, which is a compartment involved in the AKG metabolism.

The growth of the strains in xylose as seen in Figure 4.4 B suggests that it is possible for yeast to thrive in the absence of favorable sugar conditions for a period of around 77 days. The presence of non-metabolizable xylose, could have contributed to carbon circulation albeit slowly. The mutator strains grew up to an optical density (OD_{600nm}) of 3 in xylose as the sole carbon source, as seen in Figure 4.4 (A, B). To determine the pathway responsible for xylose growth, attempts were made to delete genes *XKS1* and *xylX*, which correspond to the oxidoreductive route and the Weimberg pathway, respectively. The only successful deletion was observed in strain PRY28 with the deletion of *XKS1*. However, this deletion also resulted in the loss of the acquired property as seen in Figure 4.5. All other evolved strains failed to produce viable colonies after CRISPR/Cas9 for *XKS1* deletion. Similarly, deletion of Weimberg pathway genes failed with use of different targets for all the mutator strains tested. The reason for this might be due to the presence of defective molecular tools particularly to repair the CRISPR/Cas9 targeted site via homologous recombination, changes in homologous regions, or a detrimental event in the yeast genome.

The role of Rad27 in yeast replication and genome stability has been widely studied and the findings suggest its significance in maintaining the accuracy of the DNA replication and repair process. According to a study by Loeillet et al. 2020, Rad27 is responsible for a broad mutational spectrum with a significant increase in base substitution and small InDels. Direct deletion of *RAD27* in yeast was found to result in slower growth even in glucose-containing media (Parenteau and Wellinger 1999). This phenotype was also observed in the present work (result not shown). The absence of *RAD27* has also been linked to a higher mutation rate as seen in studies that measured resistance towards canavanine (Xie et al. 2001) and a higher chromosomal rearrangement (Chen and

Kolodner 1999). The role of Rad27 in homologous recombination events has also been established, where its absence leads to a requirement for other cellular factors to repair Okazaki fragments (Lorraine S. Symington* 1998). The role of Rad27 in cell division has also been investigated, with studies showing an increased rate of mitotic crossing over in *RAD27* mutants (Tishkoff et al. 1997), and increased recombination events for *RAD27*/erc11 (Cross 1995). Studies on mutator strains in *E. coli* have shown a higher mutation rate and varied fitness for mutator strains (Gibson et al. 1970; Cox and Gibson 1974). Hence, the DNA replication accuracy is crucial for maintaining the quality of cells and reducing the mutation rate, and any defect in this system is expected to increase the mutation rate.

MSH2 is another mutator candidate gene used in the present thesis and it is a component of the mismatch repair system in yeast. In this study, confirmation of *MSH2* deletion leading to *TRP1* revertant mutants was done in the CEN.PK2-1C strain where a point mutation confers tryptophan auxotrophy. Growth test was compared in two different media SCD or SCD-Trp. Higher number of colonies were obtained for *Δmsh2* strain compared to wild type (Figure 4.2 C, D), where sequencing result of the mutator strains, those which were able to grow in SC media without tryptophan supplementation, clearly shows a reversion of stop codon TAA to TGG or TAT in PRY25 and PRY28 respectively (Figure 4.3). There are literature based evidences where deletion of *MSH2* was shown to increase the resistance to canavanine by causing several mutations in *CAN1* through incorporation of unmatched nucleotides and deletion events (Marsischky et al. 1996). A similar study in the fungus *Aspergillus fumigatus* showed that the deletion of mshA (the homolog of *MSH2*) confers an adaptive advantage against the antibiotic azole and a positive impact on virulence (dos Reis et al. 2019). A study has determined the mutagenic role of *MSH2* deletion by measuring the number of mutants, finding a 40-fold increase in strains with the deletion of *MSH2* (Boyce and Idnurm 2019). Another study by Lang et al. 2013, calculated the mutational efficiency through whole-genome sequencing and revealed a 200-fold increase in the mutational signature with the deletion of *MSH2*. Similarly, Serero et al. 2014 reports accumulation of unique and diverse mutational spectrum attributed to mutator genes in yeast. The link between Msh2 deficiency and high numbers of mutants is not only limited to random and inconsequential genomic signatures but also has a significant impact on clinical disciplines. A higher frequency of *Candida glabrata* with antibiotic resistance was directly correlated to the deletion of the MMR gene *MSH2* (Healey et al. 2016). Several studies have shown that mice with a defect in MMR and polymerase proofreading activity displayed an elevated mutational rate and a higher occurrence of cancer (Baker et al. 1995; Wind et al. 1995; Edelmann et al. 1997; Reitmair et al. 1996).

There is abundant literature on *RAD27* and *MSH2* deletion in the emergence of strains with desired characteristics, which is also observed in this work based on the ability of the mutators to grow in xylose as a sole carbon source (Figure 4.4). However, due to time limitations, the mutator role for the activation of the Weimberg pathway was not further investigated. The strains were obtained but the reverse engineering became difficult to perform and advanced techniques may be required to validate the phenotypes obtained. It is possible that the mutator strain generated a hypermutated population which could have exacerbated some unfavourable effects in the strain and reduced its fitness. The reverse genomic engineering could also have been made difficult by the sensitivity of the evolved strain to antifungals used during the selection on the CRISPR/Cas9 technique. The deletion of the gene could have become cumbersome due to the defect in the DNA repair ability of the evolved strain. Therefore, a repair of *RAD27* and *MSH2* might be a prerequisite for performing genome editing in the evolved strains. A thorough in-depth study of the characteristics of the mutator evolved strain obtained from the current study could provide new insights into xylose-based evolution and its relevance at a cellular level.

In conclusion, studying the impact of yeast mutators on large populations could be a strategy to reveal the specific "hotspots" in the genome where they can have the greatest influence. Further investigation of the evolved mutator strains obtained in this work could provide insight into the origin of xylose-related mutations and their relationship with the genome. Techniques such as whole genome sequencing, bioinformatics, and reverse engineering may be necessary to fully understand the molecular factors contributing to growth on xylose.

5.1.2   Sub-cellular engineering of the Weimberg pathway

In this study, various metabolic engineering strategies were employed to enhance the flux of xylose through the Weimberg pathway. One of the potential key aspects of the Weimberg pathway could be the involvement of mitochondria in providing sufficient iron sulfur clusters for the XylD enzyme and the integration of AKG into the TCA cycle, which majorly highlights the importance of mitochondrial engineering in establishing the functionality of the Weimberg pathway.

This versatility of eukaryotic cells, including yeast, is due to their complex design that contains different compartments with unique structures and functions. The mitochondria, the powerhouses of cells, have a unique environment compared to the cytosol, which includes a higher pH, lower oxygen levels, and a rich pool of reducing equivalents. Bacterial origin enzymes that require the loading of iron sulfur clusters for expression,

prefer this environment and mitochondria is the generating site for these clusters (Mühlenhoff and Lill 2000). As a result of these differences, many different pathways experience difficulties in cytosolic expression in yeast, such as the production of branched chain amino acids and the synthesis of isoprenoid compounds (Mühlenhoff and Lill 2000; Kirby et al. 2016; Avalos et al. 2013; Benisch and Boles 2014).

The activity of XylD, the key enzyme in the Weimberg pathway, has been shown to be a limiting factor in the conversion of xylonate to 2- keto 3- deoxy xylonate in *S. cerevisiae* due to the requirement of 4Fe-4S clusters. This cofactor is inadequately supplied in the cytoplasm of *S. cerevisiae*, leading to a bottleneck in the pathway. In a study by Salusjärvi and colleagues, the activity of XylD was increased 14 times by mitochondrial targeting, but this still did not result in an increase in the intermediates or end products of the Dahms pathway 2K3DXA (2-keto-3-deoxyxylonic acid) or 3DPA (3-deoxypentonic acid) (Salusjärvi et al. 2017). The reason for this might be the poor transport of metabolites to and from the mitochondria, potentially due to the toxicity of xylonic acid during transport to the mitochondria. To my best knowledge, the expression of the remaining genes in the Weimberg pathway (*xylB*, *xylX*, and *ksaD*) has not been investigated in the yeast mitochondria yet. In addition, despite a potential advantage of mitochondrial site with iron-sulfur clusters and end product AKG uptake, a comprehensive comparison between dual cellular compartments in context of Weimberg pathway has not been reported yet.

The confinement of different metabolic pathways into the mitochondria through compartmental engineering has been demonstrated to be a promising approach for increasing the production of various metabolites. For example, a study by Avalos and the team showed that the expression of the Ehrlich pathway in mitochondria led to a 260 % increase in isobutanol production, whereas the improvement was limited to only 10 % with only cytosolic expression (Avalos et al. 2013). Noteworthy, the isobutanol pathway also involves an iron-sulfur cluster dependent enzyme, the dihydroxyacid dehydratase, which is natively localized in mitochondria. From a work done by Salusjärvi and coworkers, where 14 times elevated activity of XylD could be observed by compartmentalizing the Weimberg pathway into the mitochondria, and the possible reason may be due to its exposure to the mitochondrial iron-sulfur cluster biogenesis machinery. The confinement of all other enzymes involved in the Weimberg pathway into the mitochondria was not tested before and therefore it was realized a necessary experiment as an attempt to establish the overall pathway functionality. It should be noted that the mitochondria have two different membranes - the outer and the inner - and they have limited permeability for solutes dependent on molecular masses and type of molecule. Therefore, to make the

intermediates of the Weimberg pathway abundant in both the cytoplasm and the mitochondria, a dual expression strategy was employed. This has already been demonstrated with the production of isoprenoids, where a dual compartmentation of the pathway led to a 2.1 and 1.6-fold increase in the titer of isoprenoids compared to strains with only mitochondrial or cytoplasmic pathways, respectively (Lv et al. 2016). Present study aims to simultaneously express the pathway genes in both the cytoplasm and mitochondria of *S. cerevisiae*. Strain AHY02 was created for this purpose, which expresses pathway genes *xylB*, *xylD*, *ksaD*, and *xylX* in both compartments. Despite the advantage of mitochondrial expression for cofactor availability, the expression of the pathway genes in the mitochondria alone was not sufficient to induce growth in xylose as a carbon source (Adriana Happel, Bachelors Thesis 2021). The inability of the modified strains to grow in xylose might be due to the lack of functionality of one or more heterologous genes expressed. Similarly, the permeability of mitochondria for AKG might be a limiting step. In addition, it needs to be determined if AKG is produced from the pathway is in sufficient amount to induce the growth of engineered strains in xylose as a sole carbon source.

The results of the evolution of strains AHY02 and CEN.PK2-1C showed that they were able to grow on xylose sugar from day 178 (Figure 4.7). To study the pathway responsible for this phenomenon, an attempt was made to disrupt the Weimberg pathway in strain AHY02 and the oxidoreductive pathway in both AHY02 and CEN.PK2-1C. The deletion of the Weimberg pathway was attempted using the CRISPR/Cas9 approach targeting either *xylX* or *ksaD*; and G418 integration to the genomic locus of AHY02 where mitochondrial copies of Weimberg pathway multicassette was located (originally *URA3* locus), but all attempts failed and no colonies were observed. This could be due to the strain trying to maintain the locus due to the stress pressure that occurred during evolution or the emergence of some vital regulatory elements in this genomic area. Further study of the genome or regulatory factors existing in the evolved strain AHY02 is needed to gain a clear explanation.

Next, testing the role of oxidoreductive pathway for the observed xylose growth in evolved strains AHY02 and CEN.PK2-1C was done. The oxidoreductive pathway, which exists naturally in *S. cerevisiae*, was disrupted by deleting the *XKS1* gene, which went successful for both evolved strains- AHY02 and CEN.PK2-1C. Interestingly, there was a severe effect with the deletion of *XKS1*, and the strains were unable to grow in xylose. This demonstrates the indispensable role of Xks1, which converts xylulose to xylulose 5-P, in the evolved strains for growth on xylose. Xylulose-5-P is converted to ribulose-5-P, the

precursor of ribose-5-P. The pentose phosphates are converted to glycolytic intermediates fructose-6-P and glyceraldehyde-3-P through the non-oxidative pentose phosphate pathway. As observed in Figure 4.8 (A and C), the inability of the Δ*xks1* strains to grow in xylose suggest the possible role of xylose metabolic wiring to glycolysis via the oxidoreductive route and pentose phosphate pathway. Still, the direct or indirect influence of the Weimberg pathway for xylose growth in strain AHY02 cannot be completely ruled out.

Evolutionary engineering is a complex process where random mutations and the selection pressure can lead to new properties of proteins. One assumption could be the emergence of a xylose isomerase pathway, because the strain AHY02 does not contain a major xylose reductase *GRE3*, and the xylose growth seems to be linked with Xks1. In Figure 4.8 B, the observation is made that the evolved strain AHY02 is not able to utilize xylitol, it can be assumed that there might be emergence of protein that can convert xylose to xylulose directly. Xylose isomerase is commonly found in prokaryotes and its heterologous expression in yeast enabled the xylose to xylulose conversion. Besides, some fungi like *Piromyces* (Silva et al. 2021) and *Orpinomyces* species (Madhavan et al. 2009) have been shown possess xylose isomerases able to convert xylose to xylulose in *S. cerevisiae*. The stress exerted by xylose during evolution in strain AHY02 might have triggered some latent enzymes to function as a xylose isomerase in yeast. AHY02 growing on xylose but not xylitol as a carbon source might also suggest the transporter as a bottleneck. As observed by Jordan et al. 2016 and the result from the present thesis (chapter 4.2.1), there are certain transporters like Hxt11, Hxt15, and Gal2, which enable xylitol uptake. The evolved clone might have modified the transporter for a superior xylose but poorer xylitol transporter. Nevertheless, the hypothesis needs to be validated with sequencing of the genome. It cannot be completely excluded that the heterologous Weimberg pathway genes *xylB*, *xylD*, *ksaD*, *xylX* could have some accessory role in parallel to the native oxidoreductive route. The fact that the deletion of the Weimberg pathway genes was not possible in the evolved strains may support this view. However, it cannot be ruled out at present that the deletion was unsuccessful due to some genome alterations during the evolution process, which are not related to the functionality of the Weimberg pathway.

The evolved strains AHY02 and CEN.PK2-1C exhibit different patterns of growth in response to xylitol as a carbon source. While the AHY02 strain showed a poor growth in xylitol as the sole carbon source, as shown in Figure 4.8 B, the CEN.PK2-1C strain was able to utilize xylitol to a higher rate (Figure 4.8 D), although growth on xylose was approximately two times higher (Figure 4.8 C). This difference in growth behavior could be

due to the evolved strain's ability to maintain a balanced expression of the oxidoreductive pathway and the pentose phosphate pathway, which are both involved in the utilization of xylose. It has to be noted that the *GRE3* gene, a major xylose reductase leading to the production of xylitol, was deleted in AHY02 strain prior to evolution. This might have led to the emergence of another reductase for xylitol production during evolutionary process, and the upregulated activity of both steps (xylose reductase and xylitol dehydrogenase). If the emergence of another NADPH dependent reductase have occurred, it can be assumed that during evolution, cellular machinery is adapted for overproduction of NADPH to optimize the conversion of xylose to xylitol. When xylitol is used as a carbon source (Figure 4.8 B), absence of activity of the emerged xylose reductase might led to over accumulation of NADPH, which is not beneficial for cell vitality. Similar explanation was stated by Harth and the coworkers where NADPH overexpressing reductase YlsDR from *Yarrowia lipolytica* shows severe growth defect in a yeast provided that NADPH recirculation could not occur (Harth et al. 2020). The case seems different for CEN.PK2-1C strain, as seen from the Figure 4.8 D. Although slowly, growth does occur with xylitol as a carbon source. Evolved strain CEN.PK2-1C capable of utilizing both xylose and xylitol suggests the activation of the oxidoreductive route and PPP. It was reported by different groups that the overexpression of *XKS1*, and of the PPP genes *TAL1, TKL1, RPE1, RKI1* is beneficial for growth on xylose (Farwick et al. 2014; Kuyper et al. 2005; Demeke et al. 2013; Karhumaa et al. 2007). Particularly, the overexpression of *XKS1* and *TAL1* is regarded as crucial (Linck et al. 2014; Becker and Boles 2003) .Thus, it can be straightforwardly assumed that some similar changes in expression level in evolved strains AHY02 and CEN.PK2-1C might have occured. Still, due to evolutionary engineering being a random process, an entirely different modification event could have also occurred which needs more detailed investigation. To get a better understanding of the biochemical changes that have occurred during the evolution process and its effect on the utilization of xylose and xylitol, proteomics and metabolomics could be furthermore conducted with the evolved clones. This might be helpful to identify any differences in the metabolic pathways involved and the enzymes responsible for the utilization of the different carbon sources. Furthermore, the study of the genetic basis of the evolved strains could provide insight into the potential mechanisms behind the differences in the utilization of xylose and xylitol that could be helpful to engineer yeast strains with improved performance in utilizing these carbon sources.

5.1.3   Xylose-evolved strains with characteristic cell cluster formation

The xylose evolved strains displayed some phenotypical changes, in terms of their colony texture and appearance in liquid media. Although there was no change in the shape, size,

or color of the colonies, a distinct difference was observed in the texture of the colonies with the evolved strains appearing as a non-smooth type. In liquid culture, the evolved strains showed a tendency to precipitate, with cells in the flask appearing as particle-like clusters, in contrast to the wild-type yeast that was homogeneously distributed. Similar findings were described by Oud et al. 2013 as fast sedimenting clusters after a series of evolution experiments. The authors suggested that this phenomenon may be due to the evolution of cells towards multicellularity. They found genome sequencing results revealing genome duplication events and mutations in *ACE2* to be responsible for the fast sedimenting clusters of cells. *ACE2* is a zinc finger transcriptional factor that activates genes in the G1 phase of the cell cycle, particularly *CTS1*, a gene involved in septum destruction after cytokinesis (Voth et al. 2005; Saputo et al. 2012; Doolin et al. 2001). The study by Oud et al. 2013 showed that different evolved isolates had either deletion or nucleotide exchange in *ACE2*, specifically at position 1,112, in the same region of *ACE2*. The multicellularity of yeast has also been described by other authors to facilitate the growth of cells on sucrose when the carbon is scarce, probably by improving the cooperation between individual cells (Koschwanez et al. 2011). Present experiment revealed that all the xylose growing evolved strains - PRY24, PRY25, PRY27, PRY28, AHY02 and CEN.PK2-1C -displayed fast sedimenting clusters, which closely resemble the observation made by Oud et al. 2013. Although the precise time point at which the precipitate emerged was not clearly determined, it was noted that the precipitating cells were observed prior to the day on which a distinct growth on xylose was detected. This suggests that the phenomenon of fast sedimentation may have assisted these strains for coping with the stress of sugar limitation, which subsequently prompted modifications that allowed them to grow on xylose. Therefore, investigating the genetic basis and the relevance of clumping for growth of the evolved strain could be an interesting target for future studies.

Recent literature, such as the review by Opalek and Wloch-Salamon 2020, have highlighted the significance of heterogeneous group formation in enabling *S. cerevisiae* to carry out tasks that are beyond the scope of individual cells. The ability to form such cooperative groups has been shown to enhance the yeast's adaptation to specific life conditions, including nutrient stress. This strategy enables *S. cerevisiae* to better cope with challenging environments, ultimately resulting in increased survival and growth. As such, the exploration of the mechanisms underlying the formation and function of these cooperative groups might be of great interest in understanding the biology of *S. cerevisiae*, and has potential implications in various fields such as biotechnology and medicine.

5.1.4 Abolishing the endogenous AKG production to screen for a functional Weimberg pathway

To investigate the activation of the Weimberg pathway in yeast, different strain engineering strategies were tested. The methods employed included the generation of a mutator strain (chapter 4.1.1) and the dual compartmentation of genes in the cytosol and mitochondria (chapter 4.1.2). Both strategies were based upon xylose for energy and carbon source, and none of these strategies led to a clear success in activating the Weimberg pathway in the strain. Thereafter, a more specific and direct strategy was implemented where xylose can be used as a source of glutamate (or AKG) via Weimberg pathway, and glucose can be used as a carbon and energy source for the growth of the strain. In this way, a minimal amount of xylose to AKG conversion might be sufficient to confirm the acitivity of the pathway. In this screening system, the ability of the strain to endogenously produce AKG was abolished. As a consequence, the strain is auxotrophic for glutamate, which is produced from AKG by different glutamate dehydrogenases. This phenotype was achieved by deleting several genes involved in converting isocitrate to AKG, namely *IDH2*, *IDP1*, *IDP2*, and *IDP3*. The resulting strain was unable to grow in a defined medium without the supplementation of 20 mg/L glutamate. When the strain was tested with sterile filtered 2.5 g/L AKG, no growth was observed even with increasing the concentration of AKG up to 20 g/L (Figure 4.10- C, D). However, a poor growth was observed when the pH of the defined medium containing 20 g/L glucose and 2.5 g/L AKG was lowered to 5 (Figure 4.11). This suggests that the uptake of AKG may have occurred via passive diffusion in its protonated form. The published work from Zhang et al. 2020 showed that growth on AKG as a sole carbon source is pH-dependent and occurs in the range from pH 2.5 to 5.0, but not at pH 6.0. This is consistent with the observations shown in Figure 4.11- A, B and the lack of growth after AKG supplementation is likely due to poor transport of AKG. Noteworthy, Zhang and colleagues also observed that AKG is not consumed even at pH 4.0, as long as glucose is present as a carbon source. Nevertheless, the results shown in this thesis suggest that the constructed strain could be used for screening of the intracellular production of AKG. This proposes the need for further optimization of experimental design. The pH condition and the concentration of glucose/AKG used may need to be carefully altered in the experimental set up to fully understand the limitations of growth on AKG.

When the concentrations of xylose were varied (10 g/L and 40 g/L; Figure 4.10- A, B), this did not lead to a rise in OD_{600nm}. To test if the activation of the pathway requires a longer time due to the complexity of the reaction, and if the glucose is particularly inhibiting the

transport of xylose during the growth, the test was done with SC media supplementing with maltose and xylose for a longer time i.e until 28 days. Despite providing ample time (28 days) for the expression of the Weimberg pathway for AKG productivity, strains were still unable to utilize xylose for this purpose, as shown in Figure 4.12. The inability of xylose to complement the auxotrophic behavior of the strain suggests that either the Weimberg pathway is not functional or gene expression is limited due to unknown cellular or genetic factors. Another possibility is that the deletion of *IDH2* and *IDP1*, which disrupts the TCA cycle in mitochondria, may have led to the strain becoming a petite strain with defective mitochondria, making expression of the Weimberg pathway difficult. This explanation is by the observations made by McCammon and McAlister-Henn 2003, where authors showed a high frequency of petite mutants in yeast strains with deleted *IDH2* and *IDP2*. The generation of petite clones would compromise mitochondrial activity, which in present case is unfavorable because the cytosolic production of AKG is dependent on mitochondrial involvement in iron sulfur cluster biogenesis, specifically for the activity of the xylonate dehydratase (XylD) that converts xylonate to 3-keto-2-deoxy-xylonate.

A study conducted by Borgström et al. 2019 demonstrated the functional expression of the Weimberg pathway in *S. cerevisiae* using mass spectrometry during co-fermentation of glucose and xylose. However, the approach employed in present work differs in that the testing the Weimberg pathway was performed in a screening platform using a glutamate auxotrophic strain and xylose as the sole source of this amino acid. The experimental results, as presented in Figure 4.12, indicate that the glutamate auxotrophic strain is incapable of utilizing xylose via the Weimberg pathway. Additionally, the presence of glycolytic substrate glucose or maltose did not activate the Weimberg pathway for xylose conversion, ruling out the possibility that the lack of growth was due to a carbon limitation. A similar strategy but in a different microbial background, a recent study conducted by Lu et al. 2021 showed success in the production of AKG from xylose through the Weimberg pathway in an *E. coli* strain, leading to an increase in the yield of itaconic acid. One possible reason for this discrepancy could be the simpler gene expression machinery in the prokaryotic host used in Lu et al. 2021, compared to the complex cellular structure of the eukaryotic *S. cerevisiae*. Additionally, difficulties in accessing iron sulfur clusters in the cytosol may have limited the expression of the bacterial xylonate dehydratase, which is an essential factor in the Weimberg pathway. *E. coli* is known to have an adequate pool of iron sulfur clusters in the cytosol (Lu et al. 2021). Furthermore, differences in the selection of candidate genes from different organisms may also have played a role in the activity and efficiency of the resulting protein. In the study by Lu et al. 2021, all genes for the Weimberg pathway were taken from *Burkholderia xenovorans*, in contrast to the present

work, where genes from *Caulobacter crescentus* and *Corynebacterium glutamicum* were used (Borgström et al. 2019). This difference in gene origin might have, to some extent, also contributed to the contrasting results.

The attempts carried out to obtain successful clones through the yeast mutator approach and mitochondrial - cytosolic expression approach were unsuccessful. Furthermore, the third approach of glutamate auxotrophy was also unable to yield a functional Weimberg pathway until day 28. Based on these results, it can be assumed that, under the current experimental conditions, either one or all of the genes *xylD/orf41*, *ksaD*, and *xylX* are not being expressed with sufficient quantities or activities to produce the necessary amount of AKG from xylose. This furthermore suggests a deeper understanding of the Weimberg pathway and its gene expression is necessary for successful AKG production in *S. cerevisiae*. In future studies, the mutator phenotype may be introduced into the strain with abolished AKG production as a more direct screening system.

5.2   Metabolic engineering for the production of xylitol

The second part of this thesis delves into the high production of xylitol using xylose as a substrate. To achieve this, the first step involved was the screening of the best transporter of xylose, as well as investigating xylitol import and export capabilities of different sugar transporters from *S. cerevisiae*. This was followed by an identification of the best xylose reductase for the reaction. In addition, the availability of NADPH in the cytosol is crucial for the yield of xylitol. To address this, several different approaches were investigated to increase the NADPH level in the cytosol.

5.2.1   Xylitol uptake in *S. cerevisiae*

Since the export, but also the re-uptake of the produced xylitol are factors that can strongly influence the productivity of the engineered strains, a number of known sugar transporters from *S. cerevisiae* was analyzed for their ability to mediate xylitol uptake. Knowing that all tested transporters are facilitators, it is reasonable to assume that they can function in both directions, depending on the orientation of the concentration gradient. The selected transporters were Hxt1, Hxt2, Hxt3, Hxt4, Hxt5, Hxt7, Hxt10, Hxt11, Hxt14, and Hxt15, as well as the galactose permease Gal2 and its mutant variants - $Gal2_{6SA}$, $Gal2_{N376Y/M435I}$, and $Gal2_{6SA/N376Y/M435I}$. The capacity for xylitol import was assessed in a screening strain AFY10, which lacks all endogenous hexose transporter genes (hxt^0) and contains one overexpression cassette for comprising *XKS1, RKI1, RPE1, TAL1 and TKL1* genes under the control of constitutive promoters (Farwick et al. 2014). It can grow on xylitol, if a xylitol

transporter and a xylitol dehydrogenase (*XYL2*) are overexpressed (Jordan et al. 2016).

The main transporters of xylose are Hxt1, Hxt2, Hxt4, Hxt7, Hxt11, and Gal2 (Nijland et al. 2016; Saloheimo et al. 2007; Shin et al. 2015; Farwick et al. 2014). However, when these known xylose transporters were individually tested with xylitol as the substrate, only Hxt11 and Gal2 were able to import xylitol, as demonstrated by the growth of AFY10 (Figure 4.13). This limited transport may be due to structural differences between xylitol and xylose, which can result in changes in affinity and transport dynamics. When compared to other transporters, such as Hxt8, Hxt9, Hxt10, Hxt13, Hxt14, and Hxt15, Hxt15 was found to be the best xylitol importer, as shown in this work and by Jordan et al. 2016. This highlights the difficulty in predicting xylitol transporters based solely on their known sugar preferences or sequence homologies.

Interestingly, Hxt11 and Hxt15, although not most closely related proteins within the Hxt family, were found to be superior xylitol transporters. Hxt11 is 98 % identical in protein sequence to Hxt9, and the expression is not regulated by the external carbon environment. On the other hand, Hxt15 is 99 % identical in sequence to Hxt16, which does not transport xylitol (Jordan et al. 2016). A ligand docking model proposed by Jordan et al. 2016 revealed that sole polymorphisms between Hxt15 and Hxt16, positions 276 and 520, are distant from the sugar binding pocket and therefore may affect the function of the transporter via long-distance effects.

The findings of this study revealed that Hxt11 and Hxt15 show a different behavior in the presence of glucose and xylose. When glucose was used, Hxt11 was found to be more strongly inhibited compared to Hxt15. In contrast, when xylose was used instead of glucose, a much higher inhibition effect was observed for Hxt15 (Figure 4.15). This observation was particularly significant because the xylose uninhibited behavior of Hxt11 was found to be comparable to the best Gal2 variants (Gal2$_{N376Y/M435I}$) or even better than the wild type Gal2. It is worth mentioning that Hxt11 has been previously identified as a hidden xylose transporter (Shin et al. 2015). The authors noted that Hxt11 possessed special characteristics, such as its insensitivity to degradation at high levels of glucose, which could be attributed to its N-terminal tail. In fact, when this N-terminus was transferred to Hxt2, it conferred greater stability to the latter (Shin et al. 2017).

On the other hand, Gal2 wildtype was already reported to be superior to different hexose transporters for xylose uptake (Farwick et al. 2014). Gal2 has also been shown to facilitate xylitol uptake (Tani et al. 2016). Further studies have then shown that several mutations in Gal2 could improve pentose uptake efficiency and also led to the discovery of mutations

that alleviate the inhibition effect of other sugars present in the hydrolysates, mainly glucose (Farwick et al. 2014). To further expand on these findings, a series of mutation-based experiments were conducted on the Gal2 protein. In the present work, a mutant Gal2 variant, where six serine residues in the N-terminal tail were changed to alanine residues, was tested for its ability to transport xylitol. This mutation was chosen based on the work of Tamayo Rojas et al. 2021, who found that changing serine to alanine results in a more stable membrane protein by preventing the endocytosis and degradation of the transporter. The results of a 2 % xylitol drop test did not yield clear conclusions about the properties of the mutated Gal2 protein (Gal2$_{6SA}$) compared to the wild type. However, the drop test data with 1 % xylitol showed that the Gal2$_{6SA}$ protein was a better candidate for xylitol transport compared to the wild type (Figure 4.14). The results indicate that the Gal2$_{6SA}$ mutant is not only a superior xylose transporter as previously reported, but is also a better importer for xylitol when compared to wildtype Gal2. This similarity in transport characteristics of Gal2$_{6SA}$ mutants for both xylose and xylitol could be due to membrane stabilization events as explained by Tamayo Rojas et al. 2021. The breakdown of the Gal2 permease due to ubiquitination and subsequent transport into the vacuole, is also connected to the media environment that the cell is exposed to. Specifically, glucose has been shown to play a role in impairing the stability of Gal2 and inducing its ubiquitination (DeJuan and Lagunas 1986). Findings from this work shows that xylitol import is also similarly inhibited by the presence of glucose for Gal2 wildtype and Gal2$_{6SA}$ (Figure 4.15). The reason for glucose inhibition of xylitol transport is explained by the poor affinity of Gal2 wild-type towards xylitol as was similarly observed with xylose (Tamayo Rojas et al. 2021) and by competitive inhibition by glucose in the media (Farwick et al. 2014). Similarly, xylitol import is also inhibited by presence of xylose in the media but, to a lesser extent than with glucose (Figure 4.15). This phenomenon of glucose-inhibited polyol transport has also been observed in *S. cerevisiae*, where Maxwell and colleagues found that the uptake of mannitol was inhibited by the presence of glucose (Maxwell and Spoerl 1970). Additionally, the uptake of another polyol, ribitol, was shown to be inhibited by glucose in a study done in *Candida* species (Miersch 1977). Some studies on plant models shows the inhibitory effect of the sugar on its -ol form as observed in this thesis. Noiraud et al. 2001 showed that mannose confers the inhibition on the mannitol transport. Such inhibitory effect of one sugar on the transport of another is commonly encountered in the field of transporters, such as glucose transporter being inhibited by fructose, and vice versa (D'Amore et al. 1989). It is also reported the xylose transporter is inhibited by presence of glucose (Farwick et al. 2014). Altogether this study gives insight into the fact that the Gal2$_{6SA}$, which improved xylose transport, can similarly act as a better xylitol importer, but the presence of xylose or glucose molecules can still exhibit inhibition of xylitol import.

One of the major challenges in yeast sugar transport is the competitive inhibition of transport by other sugars, such as glucose or xylose. To address this issue, the N376Y/M435I double mutant of Gal2 was selected, as it was shown to have a higher xylose uptake even in the presence of glucose (Rojas et al. 2021). It should be noted that the asparagine to tyrosine conversion at position 376 alone was previously shown to confer glucose-insensitivity of xylose transport (Farwick et al. 2014), while the methionine to isoleucine shift at position 435 was discovered through error-prone PCR and was found to increase xylose transport capacity (Rojas et al. 2021). The results from the present study indicate that the N376Y/M435I mutation was able to fully counteract the inhibition effect of glucose or xylose on xylitol transport (Figure 4.15). Additionally, this mutant was found to be far superior for alone xylitol import, compared to Gal2 WT or Gal2$_{6SA}$ mutant as seen in the 1 % xylitol growth test (Figure 4.14). The combination of N376Y and M435I mutations also conferred glucose-uninhibited transport of arabinose and was shown to result in a highly increased capacity of arabinose transport in the presence of glucose (Rojas et al. 2021). From this work, the N376Y/M435I mutation of *GAL2* was found to be a successful solution for glucose/xylose uninhibited xylitol import in yeast as demonstrated by growth tests using varying amounts of xylitol (Figure 4.14 and Figure 4.15).

To further enhance the xylitol import capabilities, the N376Y/M435I variant of *GAL2* was tested in conjunction with the membrane stabilized form, *GAL2$_{6SA}$*. This combination resulted in eight different substitution mutations in *GAL2*, referred to as *GAL2$_{6SA/N376Y/M435I}$* (Rojas et al. 2021). The results showed similar xylitol import characteristics as the N376Y/M435I variant when tested in a 2 % xylitol drop test (Figure 4.13). However, a more in-depth investigation of varying xylitol concentrations was also performed, which allowed for a clearer differentiation between the Gal2$_{6SA/N376Y/M435I}$ mutants. The best xylitol importer was identified as the Gal2$_{6SA/N376Y/M435I}$ form, demonstrated by its ability to support growth even at a nominal amount of 0.5 % xylitol (Figure 4.14). Concentration of xylitol when used 1 %, was also able to segregate a marginal difference in xylitol import characteristics of Gal2 WT and Gal2$_{6SA}$. The removal of ubiquitination signals improved the import of xylitol at a 1 % concentration, which was not distinguishable at a 2 % concentration where saturation of the transporter may have occurred. This highlights the importance of substrate concentration in determining the characteristics of individual transporters. In conclusion, among all the transporters tested, Gal2$_{6SA/N376Y/M435I}$ was found to be the most efficient xylitol importer. The role of ubiquitination in affecting xylitol import was also observed, with the *GAL2$_{6SA}$* form demonstrating improved performance compared to the *GAL2* wild type, although still not surpassing the Gal2$_{N376Y/M435I}$ variant or Gal2$_{6SA/N376Y/M435I}$ form. This observation is in agreement to xylose transporting characteristics observed in

Rojas et al. 2021, where eight substitution mutation served to best glucose uninhibited transport of xylose.

The imposition of mutational effects on hexose transporters has been widely studied in the literature and has been proven to be a promising approach for enhancing membrane transport kinetics. Farwick et al. 2014 identified several mutant candidates on Gal2 that improve xylose or arabinose transport. In Verhoeven et al. 2018, a three different amino acid conversions in position 376 of Gal2 showed glucose-insensitive arabinose transport, highlighting the importance of this position for discrimination between pentoses and hexoses. A study by Nijland et al. 2014 showed that the chimeric transporter Hxt36, formed by the fusion of the N-terminus of Hxt3 and the C-terminus of Hxt6, and comprising a mutation N367I, was able to completely abolish glucose transport and improve xylose uptake.

In conclusion, this study shows, by directly comparing known xylitol transporters, that Gal2 is the best transporter for xylitol import, outperforming other hexose transporters such as Hxt11 and Hxt15. The study also revealed for the first time the possibility to improve xylitol import through mutations in the Gal2 protein. The combined mutation in six serine-alanine and N376Y/M435I significantly improved the xylitol transport capacity of Gal2.

5.2.2 Xylitol export by *S. cerevisiae*

The previous experiments in this study in chapter 4.2.1 aimed to investigate the characteristics of xylitol import, and led to a subsequent investigation into xylitol export. Production of xylitol in EBY.VW4000 strain grown with xylose and glucose as a substrate (Figure 4.16 B) revealed that all the different mutations proved beneficial for the rise in titer of xylitol with the highest producer being Gal2$_{6SA/N376Y/M435I}$. However, since this variant shows both a higher capacity for xylose uptake (Rojas et al. 2021) and an improved transport of xylitol (in the import direction), it was not clarified if higher titer of xylitol was due to a more efficient xylose import or an improved xylitol export (or both). To understand whether the best xylitol importer, Gal2$_{6SA/N376Y/M435I}$, could also function as a best exporter, an assay system was designed that uncouples xylose uptake and xylitol export. Xylose in the form of xylobiose was transported into cells and then cleaved to produce xylitol. The success of this strategy was demonstrated by comparing the results of strains with and without the xylobiose transporter CDT2. The strain without CDT2 was unable to import xylobiose and produce xylitol, while the presence of CDT2 resulted in increasing xylitol production over time, with a final titer of approximately 1 g/L after 79 hours (Figure 4.18). Comparison of Gal2 variants with empty vector control revealed that the highest xylitol

production was observed in the empty vector control, with a titer of 1.14 g/L (Figure 4.19). Gal2 wild type and Gal2$_{6SA/N376Y/M435I}$ produced 0.79 g/L and 0.67 g/L of xylitol, respectively. This suggests that Gal2$_{6SA/N376Y/M435I}$, which was identified as the best xylitol importer in previous experiments, is not the best exporter. In fact, the modification reduced xylitol export capacity by approximately 15 %. Interestingly, the finding that the highest xylitol production was observed in the empty vector control, with increment of approximately 44 % compared to the Gal2 WT, shows that an efficient xylitol exporter exists in yeast (Figure 4.19). Even though the native 'hypothetical' xylitol exporter exists in both *GAL2* WT and *GAL2*$_{6SA/N376Y/M435I}$, the 2μ based overexpression might have led to overcrowding of the plasma membrane and thus a higher effect is observed only with empty vector control. One of the possible candidates could be Fps1. Previous studies have proposed that the facilitative glycerol transporter, Fps1, may play a role in xylitol efflux due to the structural similarity of both polyols (Su et al. 2013). It was described that the primary function of Fps1 is associated with glycerol transport, and it has been shown to primarily act as a xylitol exporter rather than an importer. This is also in accordance with this thesis findings where xylitol import was not seen with empty vector control in the drop test result (Figure 4.13) and there was requirement of additional transporter in order to let the strain grow in xylitol as a carbon source (Chapter 4.2.1). It is likely that Fps1 mediated the efflux of xylitol in the empty vector control in this work, although further investigation is needed to confirm this hypothesis.

Probably the overexpression of any other transporter tends to compete for the available space in the membrane and thereby reduces the available area for the native xylitol exporter of yeast. When Gal2 is stabilized by preventing its ubiquitination in Gal2$_{6SA/N376Y/M435I}$, this leads to even higher oversaturation of the membrane. This might be the possible reason for the lower xylitol export with Gal2$_{6SA/N376Y/M435I}$ when compared to the wild type. Similarly, the uptake of glucose is more compromised by Gal2$_{6SA/N376Y/M435I}$ than by Gal2 WT overexpression which is clearly observed during glucose xylose cofermentation in present thesis (chapter 4.2.2, Figure 4.16 A, 4.17 A), the similar observation is also reported by Rojas et al. 2021. Again, when efflux of xylose is measured for each of the strain, Gal2 wildtype is found to be the best xylose exporter. Empty vector control produces least among all, and the mutant Gal2$_{6SA/N376Y/M435I}$ produces less than the wild type. This furthermore shows that mutations that were helpful to import xylitol (chapter 4.2.1) or xylose (Rojas et al. 2021) have a contrary effect on the efflux of xylose. It is tempting to speculate that the higher net uptake rate of xylose by the Gal2$_{6SA/N376Y/M435I}$ mutant is, at least in part, due to a reduced efflux of the sugar. Thus, the mutation(s) may affect the transporter function in an asymmetrical manner, for instance by favoring the

outward facing conformation. The study can be further extended to examine the phenomenon of xylitol export but in the presence of inhibitory molecules. Transporter Gal2 with mutation 6SA/N376Y/M435I is described specifically for glucose uninhibited xylose (Rojas et al. 2021) or xylitol import (Chapter 4.2.1). Thus, future work can be focused in the examination of xylitol export in presence of glucose.

The collective findings of this study have shed light on the role of the xylose transporter Gal2 and its mutant Gal2$_{6SA/N376Y/M435I}$ in xylitol production. Results have indicated that the superior xylitol production observed in the Gal2$_{6SA/N376Y/M435I}$ mutant, as shown in Figure 4.16 B, is primarily attributed to its enhanced ability to import xylose, rather than its efficiency in exporting xylitol. Therefore, despite the fact that the Gal2$_{6SA/N376Y/M435I}$ mutant was found to be a poor xylitol exporter, its remarkable ability to import xylose makes it beneficial for xylitol production. Thus, it can be concluded that the robust xylose import capacity of the mutant strain Gal2$_{6SA/N376Y/M435I}$ has contributed significantly to its ability to produce high titers of xylitol.

An ideal strain for xylitol production would have high xylitol excretion and low uptake by cells described by Su et al. 2013, potentially directing carbon towards the desired product and optimizing substrate-based product formation that might otherwise be inhibited by xylitol produced inside. The limited understanding of xylitol efflux has hindered the optimization of xylose consumption in the bacterium *Corynebacterium glutamicum*, with attempts such as cofactor manipulation proving ineffective (Sasaki et al. 2010). Understanding the efflux of xylitol could lead to significant improvements in microbial production of xylitol at a large scale, increasing xylitol titers, controlling its secretion, and promoting high substrate-product conversion, thereby providing high levels of purity. This insight could be valuable for the development of xylitol-based drugs and their efficacy in eukaryotic models. The precise export and import mechanism of xylitol in eukaryotic systems could have notable implications for xylitol transportation, drug discovery, and development in other eukaryotic systems due to its numerous clinical and nutritional applications.

5.2.3   Cofactor as a main limiting factor for the yield of xylitol

The availability of cofactors, such as NAD(P)H, can be a limiting factor in the production of many products, including xylitol. These cofactors are essential for the proper functioning of metabolic pathways, and a shortage of them can negatively impact the efficiency of the process. In order to optimize the production of xylitol and other products, it is crucial to ensure a sufficient supply of these cofactors, which can be achieved through various

means such as strain engineering in a manner that elevates the cellular NADPH pool. In this work, different attempts were undertaken to ensure higher pool of NADPH in the cytoplasm of yeast. The strategies targeted (i) the overexpression the oxidative PPP (Pentose phosphate pathway) genes, (ii) deletion of the acetaldehyde dehydrogenase *ALD6*, (iii) replacement of the endogenous GAPDH genes by the heterologous *GDP1* gene and (iv) the deletion of the *PHO13* gene as a possibility to pleiotropically upregulate the oxidative PPP genes. Among all, the overexpression of the initial enzyme of the oxidative pentose phosphate pathway (Zwf1) proved to be the best strategy for improving the yield of xylitol.

5.2.3.1 Overexpression of *ZWF1* by promoter exchange

The results of the fermentation experiments show that the PRY48 strain produces significantly more xylitol than the PRY39 strain, with almost double the amount being produced (Figure 4.22). This highlights the key role played by the oxidative pentose phosphate pathway (PPP) gene *ZWF1* in enhancing xylitol production. The PRY48 strain was optimized for xylitol yield through the addition of a glucose-unrestricted xylose transporter Gal2$_{6SA/N376Y/M435I}$ and the expression of a codon-optimized Xyl1 from *Pichia stipitis*, as well as overexpression of Zwf1. It has to be noted that PRY48 strain used throughout the study overexpresses a Zwf1 variant with a deletion of the glutamate residue at position 59 due to its 50 % higher enzymatic activity compared to the CEN.PK2-1C wildtype sequence (Figure 4.23).

The oxidative PPP intersects with the glycolytic pathway at the glucose-6-phosphate intermediate and the activity of Zwf1, the first enzyme of the oxidative PPP, converts glucose-6-phosphate to 6-phospho-gluconolactone, leading to NADPH synthesis. There have been numerous studies that have shown that the titer of NADPH-dependent products increases in cells that express higher levels of glucose-6-phosphate dehydrogenase protein (Zwf1). For instance, overexpression of Zwf1 has been found to boost the production of terpenoids such as strictosidine (Brown et al. 2015), carotenoids (Zhao et al. 2015), squalene (Paramasivan and Mutturi 2017) in *S. cerevisiae* ,as well as an improved lysine production in *Corynebacterium glutamicum* reported by Becker et al. 2007. Similarly, elevated activity of Zwf1 serves beneficial for high yield of octanoic acid (Wernig et al. 2021), xylitol in *S. cerevisiae* (Kwon et al. 2006). In the study by Kwon et al. 2006, a 25 % increase in xylitol titer was reported when *ZWF1* was expressed via a plasmid in *S. cerevisiae* strain BJ3505. In this study, a 100 % increase in xylitol titer was obtained when Zwf1 was overexpressed genomically through promoter exchange with *pHXT7* in the CEN.PK2-1C strain. The enzymatic activity test further supports this as shown in Figure

4.23, where specific activity was found to be 0.16 and 0.91 µmol/min mg for PRY39 and PRY48, respectively, when cells were grown in SC media with 2 % glucose. The results in Figure 4.22 indicate that the productivity at any given time point is higher for the PRY48 strain. Notably, the increase of the titer is highly accelerated during the ethanol phase of growth, which is even more pronounced for the PRY48 strain compared to the PRY39 strain. After 48 hours, when the cells have depleted all the available glucose, the yield for the PRY48 strain increases dramatically. The ethanol production is almost identical for both strains until 48 hours, but after that, the ethanol consumed by the PRY48 strain is much faster than that of the PRY39 strain. This could be due to a more favorable condition for gluconeogenesis, as glycolysis turns backwards and the higher expression of Zwf1 results in a better consumption of the substrate glucose-6-phosphate (G-6-P) at the junction. The relationship between ethanol consumption and xylitol production during the gluconeogenesis phase may suggest that the diversion of G-6-P to the oxidative PPP requires an increased rate of gluconeogenesis to ensure sufficient flux toward UDP-glucose.
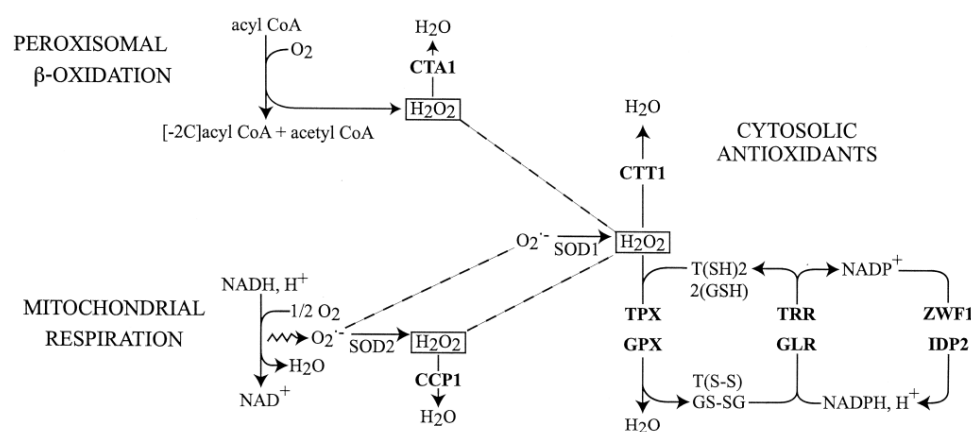
Figure 5.1: The sources and detoxification of H_2O_2 in yeast cells. In peroxisomes, fatty acids are converted to acyl CoA via β-oxidation during which generation of H_2O_2 occurs. In mitochondria, oxidative pathways convert acetyl CoA to Co_2 and reducing equivalents for electron transport. By product of electron transport are superoxide anions which gets converted by mitochondrial or cytosolic superoxide dismutase (SOD2 and SOD1) forming H_2O_2. H_2O_2 is intracellularly degraded by peroxisomal catalase (CTA1) and to mitochondrial cytochrome c peroxidase (CCP1). Cytosolic catalase (CTT1) and thiol dependent peroxidases [thioredoxin peroxidase (TPX) and glutathione peroxidase (GPX)] assists the process. Cofactors for the peroxidases are reduced by thioredoxin or glutathione reductases (TRR or GLR), using NADPH as a source of reducing equivalents. The cytosolic source of NADPH can be *ZWF1* or *IDP2*. The figure was taken from Minard and Mcalister-Henn 2001

On the other hand, the higher rate of ethanol consumption by the PRY48 strain (Figure 4.22 B), may suggests a potential role of *ZWF1* overexpression in the regulation of the mitochondrial activity. Respiration, which uses O_2 as an electron acceptor, is a solely

mitochondrial process that also results in surplus amount of reactive oxygen species. These reactive species are harmful to cell growth and energy production. Similarly, when cells are glucose-starved, they use ethanol, acetate, and fatty acids as energy sources (Minard and Mcalister-Henn 2001). During oxidative processes, higher levels of H_2O_2 are produced in cells, and NADPH produced by Zwf1 is believed to be the main cytoplasmic antioxidant (Inoue et al. 1999; Park et al. 2000) (as described in Figure 5.1). Hence, in this context, the higher activity of Zwf1 in the PRY48 strain may have assisted the cell in coping with toxic molecules, resulting in faster ethanol consumption and, in addition, an even higher rate of gluconeogenesis. This ultimately could have resulted in further activation at the oxidative PPP junction, leading to a higher NADPH pool and elevated xylitol titer.

5.2.4   Influence of the carbon source on the xylitol titer

Result from chapter 4.2.6.1 clearly shows that the amount of produced xylitol is doubled in Zwf1 overexpression strain PRY48, and the titer strikingly went higher during the gluconeogenesis phase, where ethanol is a main carbon source. Thus, it was plausible to assume that in ethanol-xylose mixture, PRY48 would behave similarly. Hence, a fermentation was performed using ethanol instead of glucose. However, the fermentation result shows the opposite trend as seen in Figure 4.32. When PRY48 and PRY39 were compared in ethanol-xylose mixture, the xylitol titer is unexpectedly higher for PRY39 strain at any time point (Figure 4.32 C). Highest difference in xylitol productivity was observed at 48 hour time point, where PRY39 produces an about 60 % higher yield than PRY48. It is not completely understood why the cell behaves differently during the diauxic shift and ethanol-grown conditions. One possible explanation is the accumulation of storage carbohydrates during glycolysis. Prior to start of main fermentation in ethanol-xylose mixture, the cells were precultured in glucose. During growth on glucose, G-6-P intersects with two other synthesis processes as G-6-P is a substrate for both the oxidative PPP and a starting molecule for trehalose and glycogen synthesis. The accumulation of trehalose could have went specifically higher for PRY39 strain during preculture because the overexpression of Zwf1 (PRY48) drives G-6-P molecule more towards oxidative PPP and less G-6-P is available for trehalose synthesis. Presence of preexisting trehalose in PRY39 might have made more G-6-P available during the ethanol-xylose growth condition, leading to increased NADPH synthesis in PRY39 when grown in ethanol. This theory requires further confirmation through quantification of trehalose during different growth conditions and a transcriptomics study to understand the regulation of glycolytic and TCA cycle genes during various carbon source conditions and their potential interactions.

Galactose was chosen as an alternative sugar variant to evaluate its suitability for xylitol

production in the *ZWF1* overexpressing strain PRY48. The results show a negative effect on both ethanol and xylitol productivity (Figure 4.31B). The decreased ethanol yield observed in the co-fermentation with galactose is due to rather respiratory mode of metabolism induced by galactose, which is a well-known phenomenon (Polakis and Bartley 1965; Polakis et al. 1965). In that scenario, activation of mitochondrial respiration from galactose might have caused metabolic burden, leading to a decreased xylitol titer. In conclusion, the results from the co-fermentation of galactose and xylose suggest that the activation of mitochondrial respiration from galactose is detrimental to ethanol and xylitol productivity in a Zwf1 overexpressing strain background. These findings could have implications for the selection of sugar variants for industrial bioprocesses, particularly those utilizing Zwf1 overexpressed strains. Further studies are needed to better understand the underlying mechanisms and optimize co-fermentation strategies for alternative sugar variants.

5.2.5   Effect of the remaining oxidative PPP genes *SOL3* and *GND1*

After observing the strong effect of Zwf1 on xylitol production, study was expanded to investigate other genes in the oxidative PPP. Zwf1 converts G-6-P and NADP$^+$ to 6PGL (6- phosphogluconolactone) and NADPH, which is then converted to D-gluconate-6-P by Sol3. Its further conversion to Ribulose-5-P by Gnd1 yields another molecule of NADPH. Based upon the hypothesis that the overexpression of *ZWF1* might increase the substrate available for the Gnd1-catalyzed reaction, an experiment was conducted where all three oxidative PPP genes were overexpressed. To this end, a multicopy expression plasmid FWV93 that contains *ZWF1*, *SOL3* and *GND1* under the control of different strong promoters (Wernig et al. 2021) was introduced into the production strain PRY48. The results (Figure 4.24 B) showed that the FWV93 transformed strain did not have an increased xylitol titer, with yields almost the same as the empty vector used. The observation is consistent with the finding from Wernig et al. 2021 where overexpression of FWV93 did not further improve the octanoic acid titer. Thus, it can be concluded that the expression of the endogenous copies of *GND1* and *SOL3* (and/or their paralogs *GND2* and *SOL4*) is not limiting. It could also be assumed that a limitation of NADP$^+$ might have occurred in PRY48 and further NADP$^+$ requiring reactions are therefore not helpful. Additionally, the large amount of 6PGL produced by Zwf1 might cause negative feedback inhibition of the non-oxidative PPP loop. Overall, this experiment suggest that genomically overexpressed *ZWF1* is the best way to increase xylitol yield in glucose-xylose mixtures, and that additional expression of *ZWF1*, *SOL3*, and *GND1* is not beneficial.

5.2.6   Downregulation of *PGI1*

Besides the amount of the Zwf1 protein, the availability of its substrate G-6-P is a second determinant of the flux towards the oxidative PPP. To accumulate more G-6-P, it was attempted to decrease its diversion to the competing reaction through manipulation of the *PGI1* gene expression. For this, the native *PGI1* promoter was replaced by weaker ones. Strains PRY49 (*pCOx9-PGI1*), PRY50 (*pRNR2-PGI1*) and PRY51 (*pREV1-PGI1*) were generated where the strength of the promoters is *pPGI1 > pCOX9 > pRNR2 > pREV1* (Lee et al. 2015; Keren et al. 2013). To investigate the influence of the promoter replacement on growth, and thereby indirectly on the glycolytic flux, drop tests were performed on different media. Figure 4.26 shows a pronounced effect of *pREV1-PGI1* (PRY51) on higher glucose concentration (2 %) whereas no apparent difference was seen for 0.2 % glucose and on ethanol (2 %). This is expectable, as during higher glucose condition, the Pgi1 limitation is more pronounced than in low glucose or under the gluconeogenic regime. The fermentation experiments (Figure 4.25) showed more subtle differences in the retardation of glucose consumption, which is in agreement with the strength of each of the three promoters (although the differences may not be clearly seen in the Figure 4.25 A due to the scaling of the graph, the underlying measured glucose concentrations unequivocally show the trend at all time points of the glucose phase). This confirms that promoter replacements had the intended effect.

Regarding the production of xylitol, when the full fermentation time is observed, the results show that all of the weaker promoters used did not lead to an increase of the final xylitol titer and that the wild type *pPGI1* was superior (Figure 4.25 B).

It is possible that a downregulated glycolysis could exert a feedback inhibition which could ultimately retard the synthesis of G-6-P, e.g. by regulating the hexokinase activity or glucose transporter expression. Also, it might be possible that a retarded glycolysis exerts a negative influence on cellular metabolism including Zwf1 activity. Contradicting this hypothesis, the xylitol per OD_{600nm} value inversely correlates with the promoter strength and is highest for the weakest promoter used (*pREV1*) during the first few hours, i.e. during the glucose consumption phase (Figure 4.25 C), which is in accordance with the expectation. Thus, a higher glucose level is the best scenario for observing the difference occurring in G-6-P accumulation due to the *PGI1* downregulation. The promoter replacement strategy may therefore be beneficial under conditions with constant glucose supply, such as fed-batch fermentations. The downregulation of *PGI1* (in combination with *ZWF1* overexpression and other strategies) was previously shown to improve the production of fatty acids (Yu et al. 2018), especially during the glucose consumption phase

(Wernig et al. 2021), supporting the results of this work. It has to be noted, however, that the decreased fitness of the strains is an undesired trait from a biotechnological prospective. The applicability of the strategy is therefore limited by the intended fermentation regime.

5.2.7 Integration of an NADP⁺-dependent G3PDH

Glyceraldehyde-3-Phosphate dehydrogenase Gdp1 from *Kluyveromyces lactis* is the first discovered fungal NADP⁺ dependent G3PDH (Verho et al. 2002). The strategy to implement *GDP1* from *K. lactis* (KlGDP1) for higher yield of xylitol is motivated by the observation that NADP⁺ dependent Gdp1 expression had shown success for boosting the turnover of NADP⁺ to NADPH in the cytosol, as shown in the work of Verho and the coworkers (Verho et al. 2003). The authors observed a stimulated xylose fermentation via the oxidoreductive pathway in *S. cerevisiae* when GDP1 was overexpressed and this was attributed to an improved supply of NADPH for the reduction of xylose. Chen and the coworkers found that expression of NADP⁺ dependent G-3PDH (gapN) from *Streptococcus* mutants increased the NADPH dependent 3HP (3-Hydroxypropionic acid) formation by 30 % (Chen et al. 2014b). In another study, replacement of NAD⁺ dependent G3PDH by gapN from *S. mutans* showed rise in ethanol and decline in glycerol productivity (Bro et al. 2006). Similarly, the expression of gapN from *Bacillus cereus* significantly increased ethanol yield and decreased glycerol production in anaerobic growth of *S. cerevisiae*, which is another example for metabolic engineering using an NADP⁺ dependent glycolytic gene in *S. cerevisiae* (Zhang et al. 2011). A switch in cofactor specificity of glutamate dehydrogenase towards NADP⁺ was able to rise ethanol yield by 8 % in *S. cerevisiae* as shown by Nissen et al. 2000. This exemplifies that the NADPH pool engineering is not restricted to G3PDH.

In the present work, *GDP1* expression was carried out in two different strains – CEN.PK2-1D wildtype or CEN.PK2-1D Δ*tdh3*. In the latter, the major isoform of the endogenous (NAD⁺ dependent) G3PDH was deleted (Linck et al. 2014) to increase the availability of the substrate and thereby increase its turnover by Gpd1. Reduced glycolytic flux is confirmed by a decreased glucose consumption for the Δ*tdh3* strain (Figure 4.27 B). Deletion of *TDH3* does not completely abolish glycolysis because Tdh1 and Tdh2 are still active, thus this strain is able to grow in glucose even without Kl*GDP1*. During early hour of fermentation until ~21 hours, Kl*GDP1* expression leads to a higher yield of xylitol, which is seen for both WT and *TDH3* deleted background (Figure 4.27 D). Only in the presence of glucose Gdp1 is operating in the NADPH generating direction and thereby a higher xylitol yield is obtained. From this, it can be said that NADPH limitation during early

glycolysis seems to be evidently overcome by expressing KlGdp1. In accordance with the expectation, this is not the case in later stages of fermentation (i.e. during the gluconeogenic regime), where the trend is rather opposite (Figure 4.27 C). This is explained by NADPH consumption by KlGdp1 during gluconeogenesis. An interesting observation is that the strain expressing KlGdp1 consumes ethanol faster than the empty vector control as seen at 148 hour in Figure 4.27 C. A high rate of ethanol consumption does not correlate with a high xylitol production, which is in contrast to the observation made with *ZWF1* experiment (Figure 4.22 B), where the faster ethanol consumer is generally a better xylitol producer. This disparity is not fully understood but it can be explained by the NADPH consumption by KlGdp1, whereas Zwf1 is unlikely to consume NADPH even during gluconeogenesis. Altogether, the study elaborates a successful approach to increase NADPH in the cell, via heterologous protein expression of G3PDH having affinity towards $NADP^+$, in particular in the phase when glucose is abundant. To ameliorate this, other gene targets can be chosen where the reaction is irreversible throughout the metabolism so that NADPH is not utilized by the reaction at any time course. Beside this, the expression of the KlGdp1 in *S. cerevisiae* could be further strengthened through codon optimization of the gene for *S. cerevisiae*.

5.2.8   Deletion of *ALD6*

Acetic acid is a known growth inhibitory compound for yeast. Ald6 is the major cytosolic acetaldehyde dehydrogenase isoenzyme involved in acetate production and the deletion of *ALD6* is known to significantly reduce its accumulation (Lee et al. 2012; Eglinton et al. 2002; Karhumaa et al. 2009; Sonderegger et al. 2004; Wahlbom et al. 2007). Some studies have reported that the deletion of *ALD6* in a xylose-metabolizing strain led to an increase in xylose consumption rates via the oxidoreductive pathway (Kim et al. 2013). The authors interpreted this as a consequence of reduced acetate accumulation. Interestingly, the deletion of *ALD6* was also found to have a beneficial effect on the reduction of D-galacturonic acid to L-galactonate by an NADPH-dependent reductase (Harth 2022) . This finding appears counterintuitive, since Ald6 is, besides Zwf1, the second major source of cytosolic NADPH (Grabowska and Chelstowska 2003). To test if this effect is generic, the influence of the *ALD6* deletion on the NADPH-dependent reduction of xylose was tested in this study. As shown in Figure 4.28 A, a 60 % higher level of xylitol for the PRY55 (PRY39 *Δald6*) strain was observed compared to PRY39 at 148 hr. The reduction of acetate production and its toxicity seems an unlikely explanation for this observation, although it may play a role in lignocellulosic hydrolysates (Kim et al. 2013), which already contain high amount of acetic acid due to the pretreatment process. Strikingly, a higher

accumulated xylitol titer after the deletion of *ALD6* was observed even in a xylose-metabolizing strain, in which xylitol is only an intermediate of the oxidoreductive pathway (Kim et al. 2013). This suggests that the increase in xylitol supply possibly outweighed the consumption of xylitol through the downstream metabolism. Thus, the deletion of *ALD6* may have increased the activity of xylose reductase, possibly through an increased NADPH pool, which is the main factor for improving the xylitol yield. One possible explanation could be an overcompensatory upregulation of *ZWF1* to counteract the loss of Ald6 as a second NADPH source. To test this hypothesis, a Zwf1 enzyme activity test was performed with glucose-grown cells. As shown in Figure 4.29, Zwf1 activity in the *Δald6* strain is 33 % higher than in the parental strain, which is consistent with previous results observed in a very different strain background, engineered for L-galactonate production (Harth 2022). This suggests that the higher yield of xylitol in PRY39 *Δald6* is at least partly due to an enhanced *ZWF1* overexpression. In the case of strain PRY48 (with overexpressed *ZWF1*), the deletion of *ALD6* did not make any positive difference (Figure 4.28 B), which is likely due to an already high level of *ZWF1* expression driven by a constitutive promoter that is not responsive to perturbations of the cellular NADPH pool. The sensitivity of the *ZWF1* expression to the deletion of *ALD6* in the PRY39 background can be explained based on the transcription factor dependency of their promoters as Stb5 is a common transcription factor regulating both *pZWF1* and *pALD6* (Ouyang et al. 2018).

5.2.9   Deletion of *PHO13*

Deletion of *PHO13,* when performed in a PRY39 (native *ZWF1*) and PRY48 (*ZWF1* overexpressed), did not confer a positive effect on the xylitol titer (Figure 4.28, A and B). This strategy was based on the already reported evidence, where authors found that Δ*pho13* leads in *S. cerevisiae* not only to a higher xylose consumption via the oxidoreductive pathway (Xu et al. 2016; Kim et al. 2015) but also to the upregulation of PPP genes mediated by the transcription factor Stb5 (Kim et al. 2015). Due to the observation that availability of NADPH is limiting the xylitol titer in this study, it was plausible to assume that the upregulation of the PPP could be beneficial for xylitol production. The absence of an effect could be explained by the fact that the deletion of *PHO13* increases the transcript levels of *GND1*, *SOL3* and *TAL1*, but not that of *ZWF1* (Kim et al. 2015). The overexpression of *ZWF1* was shown in this study to be the crucial genetic target for improving the production of xylitol (chapter 4.2.6.1) and the overexpression of *GND1* and *SOL3* did not further improve the yields (chapter 4.2.6.2). The latter observation is consistent with the absence of an effect even in the PRY48 strain background, where Zwf1 activity is not limiting. Besides its effect on the PPP gene

expression, the deletion of *PHO13* was shown to be beneficial for xylose fermentation through the oxidoreductive pathway by minimizing the hydrolysis of xylulose-5-phosphate by the Pho13 phosphatase activity (Kim et al. 2015; Xu et al. 2016). On the other hand, the finding from Shen et al. 2012 showed that *PHO13* deletion effect is more pronounced in XR/XDH rather than XI expressing strains, although both pathways result in xylulose-5-phosphate. This suggests that the *PHO13* deletion does not act solely at the phosphatase activity level. Noteworthy, the other studies investigating the *PHO13* deletion were performed in strain backgrounds other than CEN.PK used in this study, which may also account for different patterns of regulation.

5.2.10 Expression of a cytosolic Pos5

As an additional strategy to increase the NADPH concentration in the cytoplasm, a *POS5* version encoding a truncated NADH kinase (without the mitochondrial targeting sequence) was expressed under the control of the mediocre promoter *pRNR2.* A weak promoter was chosen because a strong overexpression of *POS5* was reported to cause a strong growth phenotype (Kim et al. 2018; Hou et al. 2009). Pos5 can phosphorylate both NADH and NAD, but its preference for NADH is around 50-fold compared to oxidized cofactor (Outten and Culotta 2003). The deletion of the mitochondrial targeting sequence was based on previous work (Strand et al. 2003). Glucose-xylose fermentation results (Figure 4.28 A, B) show that its expression in the cytoplasm is not able to increase the overall yield of xylitol. Nevertheless, a slight increase of xylitol titers was observed in the PRY39 strain background during the glucose phase (up to 24 hr), which is reminiscent of the results obtained after downregulation of *PGI1* or expression of *KlGDP1* (Figure 4.28 C). This is expectable since cytosolic NADH is abundantly produced during glycolysis, but not during the respiratory phase of metabolism. In the PRY48 background, the production of xylitol is decreased even at early stages of the fermentation, suggesting that the negative consequences of the *POS5* expression, such as the growth retardation, outweigh the positive ones. The growth and ethanol consumption of recombinant strains PRY39, *pRNR2- POS5* and PRY48, *pRNR2-POS5* is lower than with the parent strains PRY39 and PRY48 (data not shown), consistent with previous studies. This is likely due to the perturbations of the cofactor balance and/or to an increased ATP consumption. In contrast to present thesis results, a study from Zhao and their team shows *POS5* to be even more effective than *ZWF1* to increase the NADPH-dependent carotenoid synthesis (Zhao et al. 2015). However, in their study, the *POS5* expression not only resulted in higher NADH-kinase activities, but also in increased transcript levels of genes involved in carotenoid biosynthesis. It is therefore impossible to attribute the increased carotenoid titers solely to

the increased level of NADPH. In another study, the expression of cytosolic Pos5 was intended to improve the consumption of xylose via the oxidoreductive pathway (which involves xylitol as an intermediate). Whereas the channeling of xylose to ethanol was improved under aerobic conditions, xylitol accumulated under anaerobic conditions, probably due to accumulation of NADH that served as a substrate for Pos5 (Hou et al. 2009). As a further example of the cytosolic Pos5 expression strategy, Yukawa et al. 2021 introduced it into a strain engineered for 1,2,4-butanetriol (BT) production from xylose. This led to a notable increase of the product (about 20 %). Interestingly, the concentration of xylitol, an unwanted side-product not involved in the BT pathway, was not increased. All these examples show that the effects of a cytosolic Pos5 expression are complex and context-dependent.

Conclusion

To conclude, the present PhD thesis aims at the conversion of xylose into two different products – α-ketoglutarate (via the Weimberg pathway) or xylitol. In the first part of this thesis, for establishing the Weimberg pathway, when heterologous codon optimized genes from different source organisms like *Caulobacter crescentus*, *Corynebacterium glutamicum*, and *Arthrobacter nicotinovorans* were expressed in *S. cerevisiae*, the resulting strains were not able to grow with xylose as a sole carbon source. Strain modification approaches like yeast mutator strains and cytosolic-mitochondrial expression of the pathway, followed with evolutionary engineering, as well, did not led to clear success. In order to make a more direct approach, a screening strategy was employed where xylose was used as a source of glutamate. This way, comparatively less amounts of α-ketoglutarate are required via the Weimberg pathway as glucose can serve as a sole carbon source for the growth, and xylose oxidation via the Weimberg pathway just provides AKG for the growth of glutamate auxotrophic strain. Despite this, the strain was still unable to grow using xylose as a glutamate/AKG source. This implies that successfully expressing the Weimberg pathway in *S. cerevisiae* may require addressing additional limiting factors for optimal activities.

In the second part of this thesis, xylose should be converted to produce xylitol - a sweetener compound. This study in-depth investigated different aspect of xylitol production such as xylitol transport, screening of the best xylose reductase, and genetic modifications to increase the cellular pool of NADPH. NADPH is the cofactor required for the activity of xylose reductase that converts xylose to xylitol. When the abilities of different hexose transporters and their variants for the transport of xylitol across the membrane were examined, the finding from present study reveals a mutant variant of Gal2 -

$Gal2_{6SA/N376Y/M435I}$ - to be the best xylitol importer but not the best exporter. Furthermore, to optimize the production of xylitol, different reductase variants were tested from different source organisms, among which xylose reductase from *Pichia stipitis* produced the highest yield. Furthermore, different NADPH supplementation strategies were tested to reach higher yields of xylitol where *ZWF1* overexpression and *ALD6* deletion were found to be the best strategy, among others, to result in a higher titer of xylitol.

6 Deutsche Zusammenfassung

Xylose, ein mengenmäßig großer Zuckeranteil von lignocellulosehaltiger Biomasse, ist ein Molekül mit einem Fünf-Kohlenstoff-Skelett. Seit Jahrzehnten wird die Verwendung dieses Zuckers, insbesondere als Substrat für die Produktion von Biokraftstoffen wie Ethanol durch mikrobielle Wirtsorganismen wie *Saccharomyces cerevisiae*, intensiv beforscht. In dieser Hefe wird Xylose natürlicherweise nicht als Kohlenstoffquelle verwendet, aber ihre Verstoffwechselung konnte durch *Metabolic Engineering* - entweder über den oxidoreduktiven Weg oder mit Hilfe einer Isomerase - erreicht werden. Beide Wege enthalten Xylulose als gemeinsames Zwischenprodukt, das vor dem Eintritt in den endogenen Stoffwechsel über den nicht-oxidativen Pentosephosphatweg (noxPPP) phosphoryliert werden muss.

Außerdem existiert in einigen Bakterien ein nicht-phosphorylierender oxidativer Weg für den Xyloseabbau, bekannt als Weimberg-Stoffwechselweg, bei dem ein Molekül Xylose durch eine Reihe von Enzymen - Xylose-Dehydrogenase (XylB), Xylonat-Dehydratase (XylD), 3-Keto-2-deoxy-Xylonat-Dehydratase (XylX) und α-Ketoglutarat-Semialdehyd-Dehydrogenase (KsaD) - in α-Ketoglutarat (AKG) umgewandelt wird. Neben mehreren nützlichen Eigenschaften als Produkt, könnte AKG durch seine Verstoffwechselung im Citratzyklus für das Wachstum der Zellen genutzt werden.

Ein Ziel der vorliegenden Studie ist es, einen funktionellen Weimberg-Stoffwechselweg in *S. cerevisiae* zu etablieren. Frühere Studien haben gezeigt, dass dies keine triviale Aufgabe ist, unter anderem aufgrund der Toxizität von Xylonat (dem ersten Zwischenprodukt) und der Beteiligung eines Eisen-Schwefel-Cluster abhängigen Enzyms, der D-Xylonat-Dehydratase. Die Assemblierung von Eisen-Schwefel-Clustern an heterologen Proteinen in Hefezellen hat sich in früheren Arbeiten häufig als schwierig erwiesen.

Um den Weimberg-Stoffwechselweg in Hefe zu etablieren, wurden die Gene *xylB*, *xylD* und *xylX* von *Caulobacter cresentus* und *ksaD* von *Corynebacterium glutamicum* gewählt. In einer Variante wurde die Dehydratase *xylD* durch *orf41* von *Arthrobacter nicotinovorans* ersetzt; es wird angenommen, dass Orf41 unabhängig von Eisen-Schwefel-Clustern ist. Das Wachstum von Hefezellen auf Xylose als einziger Kohlenstoffquelle wurde als Indikator für einen funktionellen Weimberg-Stoffwechselweg erwartet. Die heterologe Expression der codonoptimierten Gene reichte jedoch nicht aus, um dieses Ziel zu erreichen. Aufgrund der Komplexität der Interaktionen des heterologen Stoffwechselweges mit den endogenen zellulären Prozessen wurde angenommen, dass

potenzielle Limitationen durch gerichtete Evolution (*Evolutionary Engineering*) überwunden werden könnten, unter Verwendung von Xylose als einziger Kohlenstoffquelle. Über zahlreiche Generationen hinweg wurde ein Stamm mit genomisch integrierten Genen des Weimberg-Weges einem steigenden Selektionsdruck ausgesetzt. Als eine Variante des *Evolutionary Engineering*-Ansatzes wurden Mutatorstämme erzeugt. Dafür wurden Gene deletiert, die an Nukleotid-Exzisionreparatur- (*RAD27*) und *Mismatch Repair*-Mechanismen (*MSH2*) beteiligt sind. Einige der resultierenden Stämme - PRY24, PRY25, PRY27 und PRY28 - konnten nach gerichteter Evolution auf Xylose als einziger Kohlenstoffquelle wachsen. Als Kontrolle wurde auch der Stamm PRY19 ohne Mutatorphänotyp einbezogen. Bemerkenswerterweise konnten nur die Mutatorstämme Xylose als alleinige Kohlenstoffquelle nutzen, was die Plausibilität des Ansatzes zeigt.

Neben der Mutatorstamm-Strategie wurde im Rahmen dieser Studie ein weiterer Ansatz verfolgt, bei dem der Weimberg-Stoffwechselweg gleichzeitig im Zytoplasma und in den Mitochondrien exprimiert wurde. Die zugrundeliegende Überlegung war, dass die Biogenese von Eisen-Schwefel-Clustern auf XylD im Organell effizienter stattfinden könnte und dass AKG im endogenen Stoffwechsel ein Zwischenprodukt des Citratzyklus ist. In dem Stamm AHY02 wurden alle Enzyme des Weimberg-Weges mit mitochondrialen Zielsteuerungssequenzen versehen und zusätzlich zytoplasmatisch exprimiert. Die Lokalisation der mitochondrialen Varianten wurde durch Fluoreszenzmikroskopie bestätigt. Zusammen mit AHY02 wurde auch der CEN.PK2-1C Wildtypstamm als Kontrolle für die Evolution einbezogen. Nachdem eine Selektion auf Xylose-haltigen Medien stattgefunden hat, konnten beide Stämme - AHY02 und CEN.PK2-1C - im Laufe der gerichteten Evolution wachsen. Die Deletion des Xylulokinase (*XKS1*)-Gens war für beide evolvierte Stämme in Xylose-haltigen Medien letal. Dies legt die Möglichkeit nahe, dass die Evolution der endogenen Gene des oxidoreduktiven Weges und des noxPPP für das Wachstum der selektierten Zellen verantwortlich ist. Für den evolvierten Stamm AHY02 könnte es auch möglich sein, dass der Weimberg-Stoffwechselweg zusätzlich zur oxidoreduktiven Route zum Wachstum beigetragen hat. Um die zugrundeliegenden molekularen Mechanismen aufzuklären, wären in Zukunft Genomsequenzierungs- und *Reverse Engineering*-Ansätze erforderlich.

Zusätzlich zum *Screening* nach Wachstum auf Xylose als einziger Kohlenstoffquelle, wurde ein weniger stringentes Testsystem entwickelt, um einen geringen metabolischen Fluss von Xylose in Richtung AKG nachzuweisen. Dazu wurden alle Gene, die für die Umwandlung von Isocitrat in AKG notwendig sind, deletiert, wodurch ein Glutamat-auxotropher Stamm generiert wurde. In diesem System können die Zellen auf anderen

Kohlenstoffquellen wachsen, während Xylose nur als AKG-Quelle für die Synthese von Glutamat bereitgestellt wird. Die Stämme PRY59 und PRY60 mit dem vollständigen Weimberg-Stoffwechselweg, einschließlich der Xylonat-Dehydratasen XylD oder Orf41, wurden durch Deletion von *IDH2*, *IDP1*, *IDP2* und *IDP3* Glutamat-auxotroph gemacht. Erwartungsgemäß konnten sie nur mit Glutamat-Supplementierung wachsen. Wenn jedoch PRY59 und PRY60 auf Glukose- oder Maltose-haltigen Medien mit 10 g/L oder 40 g/L Xylose angeimpft wurden, konnte kein Wachstum beobachtet werden. Dies deutet darauf hin, dass Xylose nicht in ausreichender Menge in AKG umgewandelt wurde, um als Glutamatquelle verwendet werden zu können. Die Etablierung des Weimberg-Weges in *S. cerevisiae* ist somit eine anspruchsvolle Aufgabe, möglicherweise aufgrund mehrerer bekannter und unbekannter Einschränkungen.

Der zweite Teil dieser Arbeit zielt darauf ab, Xylose in den kommerziell wertvollen Stoff Xylitol umzuwandeln. Xylitol ist ein Süßungsmittel, das vor allem in Süßigkeiten, Getränken und Zahnpflegeprodukten Verwendung findet. Da für seine Verstoffwechselung kein Insulin erforderlich ist, ist Xylitol auch für Diabetiker geeignet. Die Produktion von Xylitol erfolgt derzeit über chemische Verfahren, die verschiedene Nachteile, wie einen hohen Druck- und Temperaturbedarf, aufweisen.

Um eine umweltfreundlichere Alternative zu schaffen wurde daher *S. cerevisiae* als ein mikrobieller Wirt für die Xylitol-Produktion eingesetzt. Die Umwandlung von Xylose in Xylitol erfolgt in *S. cerevisiae* natürlicherweise durch die Wirkung der Xylose-Reduktase (XR). Der erste Schritt für die Xylitol-Produktion ist die Aufnahme von Xylose über Transporter, gefolgt von der XR-katalysierten Umwandlung zu Xylitol im Cytoplasma. Die Biotransformation endet mit dem Export von Xylitol durch einen Transporter. In der vorliegenden Arbeit wurden verschiedene Hefe-eigene Hexose-Transporter für die Aufnahme von Xylose sowie für die Aufnahme und den Efflux von Xylitol getestet. Die Transporter-Variante $Gal2_{6SA/N376Y/M435I}$, die aus früheren Studien als überlegen für den Xylose-Transport bekannt ist, zeigte auch die besten Eigenschaften für die Aufnahme von Xylitol. Da die Gal2-Permease als Facilitator fungiert, wurde angenommen, dass sie auch den Efflux von Xylitol vermitteln könnte. Um die Aufnahme von Xylose und den Efflux von Xylitol zu entkoppeln, wurde ein Testsystem entwickelt, in dem das Disaccharid Xylobiose von dem spezialisierten CDT-2-Transporter aus *Neurospora crassa* aufgenommen wird. Xylobiose wird anschließend intrazellulär durch β-Xylosidasen (ebenfalls aus *N. crassa*) in Xylosyl-Monosaccharide gespalten und durch die XR zu Xylitol reduziert. Mit diesem Testsystem konnte gezeigt werden, dass der Efflux von Xylitol durch einen anderen Transporter ermöglicht wird, während $Gal2_{6SA/N376Y/M435I}$ sogar einen negativen Einfluss auf

diesen Prozess hatte. Dies zeigt die Komplexität der Import-Export-Dynamik in Hefe und deutet darauf hin, dass ein bidirektionaler Xylose-Transporter mit Xylitol als Substrat wahrscheinlich unidirektional fungiert.

Die XR-katalysierte Umwandlung von Xylose in Xylitol erfordert Redox-Cofaktoren. Die meisten in der Natur vorkommenden XR, einschließlich derer aus *S. cerevisiae*, sind NADPH-abhängig. Um einen geeigneten XR-Kandidaten zu finden, wurden verschiedene Reduktasegene - *GRE3* aus *S. cerevisiae*, *XYL1* aus *Pichia stipitis*, *XYL1* aus *Candida parapsilosis* und *xyrB* aus *Aspergillus niger* – in Hefe eingebracht und in ihrer Fähigkeit, die Xylitolproduktion zu steigern, verglichen. Die höchste Ausbeute an Xylitol wurde mit *XYL1* aus *P. stipitis* erzielt. Mit Ausnahme der Xyl1 aus *C. parapsilosis* (NADH-abhängig), die die Xylitol-Produktion im Vergleich zur Leervektorkontrolle nicht verbesserte, sind alle anderen Xylose-Reduktasen NADPH-abhängig. Die cytoplasmatische NADPH-Versorgungsroute in *S. cerevisiae* ist limitiert und hauptsächlich auf den oxidativen Pentosephosphatweg (oxPPP) zurückzuführen. In dieser Arbeit wurden Modifikationen an verschiedenen Kontrollpunkten des Stoffwechsels durchgeführt, um die cytoplasmatische NADPH-Konzentration zu erhöhen, was nicht nur für die Produktion von Xylitol, sondern auch für andere NADPH-abhängige Reaktionen nützlich sein könnte.

Um den Eintritt von Glucose-6-Phosphat in den oxPPP zu erhöhen, wurde das Phosphoglucose-Isomerase-Gen (*PGI1*) durch einen Promotor-Austausch herunterreguliert. Die Einführung schwächerer Promotoren verbesserte die Ausbeute an Xylitol pro verbrauchter Glukose, verringerte jedoch gleichzeitig die volumetrische Xylitol-Produktion aufgrund negativer Auswirkungen auf die zelluläre Fitness. Als eine komplementäre Strategie verbesserte die Überexpression des endogenen Glucose-6-Phosphat-Dehydrogenase-Gens *ZWF1* die Produktion von Xylitol unter allen Bedingungen deutlich. Die zusätzliche Überexpression von Plasmid-kodiertem *ZWF1* zusammen mit Genen, die für die 6-Phosphogluconolactonase (*SOL3*) und 6-Phosphogluconat-Dehydrogenase (*GND1*) kodieren, führte nicht zu weiteren Verbesserungen, was darauf hindeutet, dass die Aktivität der nachgeschalteten Enzyme des oxPPP die Produktion von Xylitol nicht begrenzt. Als eine eher pleiotrope Strategie zur Modulation der Aktivität des PPP - und damit der Bereitstellung von NADPH (wie in früheren Arbeiten berichtet) - wurde die Deletion des *PHO13*-Gens getestet. Diese Modifikation zeigte jedoch im Kontext dieser Studie keine positiven Auswirkungen.

Die Einführung eines heterologen NADP$^+$-abhängigen Glyceraldehyd-3-Phosphat-Dehydrogenase-Gens (*GPD1* von *Kluyveromyces lactis*) war eine weitere angewandte Strategie zur Manipulation des zentralen Kohlenstoff-Stoffwechsels. Dies führte zu

höheren Xylitol-Ausbeuten pro verbrauchter Glukose. In Bezug auf die volumetrische Produktion von Xylitol war dieser Ansatz im Vergleich zur Überexpression von *ZWF1* jedoch deutlich unterlegen. Wenn zusätzlich zur Expression von *GPD1* das endogene Glyceraldehyd-3-Phosphat-Dehydrogenase-Gen *TDH3* ausgeschaltet wurde, um die Verfügbarkeit des Substrats für Gpd1 zu steigern, führte das zu einem negativen Wachstumsphänotyp und damit zu insgesamt niedrigeren Produktausbeuten.

In vorherigen Arbeiten wurde berichtet, dass die Deletion des Acetaldehyd-Dehydrogenase-Gens *ALD6* für den Xylose-Katabolismus über den oxidoreduktiven Weg und für die NADPH-abhängige Reduktion von D-Galacturonsäure vorteilhaft ist, obwohl das Ald6-Enzym NADPH produziert. Diese Beobachtungen werden durch diese Arbeit unterstützt, da ein höherer Xylitol-Titer in einem *Δald6*-Stamm beobachtet wurde. Die vorgelegten Daten legen nahe, dass dies zumindest teilweise durch einen Kompensationsmechanismus erklärt werden kann, da die Zwf1-Aktivität im *Δald6*-Hintergrund erhöht wurde.

Schließlich wurde eine Strategie getestet, um den NADPH-Pool durch NADH-Phosphorylierung zu erhöhen. Dazu wurde die normalerweise mitochondriale NADH-Kinase Pos5 ohne mitochondriales Targeting-Signal zusätzlich zur nativen Variante exprimiert. Dies führte zu einer leicht erhöhten Xylitol-Ausbeute pro verbrauchter Glukose, jedoch nur während der fermentativen Phase des diauxischen Wachstums, in der die NADH-Versorgung hoch ist. Dies ist konsistent mit der höheren Präferenz von Pos5 für NADH im Vergleich zu NAD$^+$.

Zusammenfassend erwiesen sich die Überexpression des Glucose-6-Phosphat-Dehydrogenase-Gens *ZWF1*, gefolgt von der Deletion des Acetaldehyddehydrogenase-Gens *ALD6*, als vielversprechendste Strategien zur volumetrischen Verbesserung der Xylitol-Produktion in *S. cerevisiae*. Die Kombination beider Strategien zeigte keine additive Wirkung. Zudem zeigten die Herunterregulierung der Phosphoglucose-Isomerase, die Einführung einer NADP$^+$-abhängigen Glyceraldehyd-3-Phosphat-Dehydrogenase und die cytoplasmatische Expression einer NADH-Kinase ein Potenzial zur Verbesserung der NADPH-Bereitstellung. Dies erscheint insbesondere unter Bedingungen mit einer konstanten Glukosezufuhr, wie z. B. in *Fed-Batch* oder *Simultaneous Saccharification and Fermentation* (SSF) Regimen, vielversprechend. Diese Beobachtungen sind sehr wahrscheinlich auch für die Optimierung weiterer NADPH-abhängiger Produktionswege relevant.

7 Publication bibliography

Alexander, Jessica L.; Barrasa, M. Inmaculada; Orr-Weaver, Terry L. (2015): Replication fork progression during re-replication requires the DNA damage checkpoint and double-strand break repair. In *Current biology : CB* 25 (12), pp. 1654–1660. DOI: 10.1016/j.cub.2015.04.058.

Alkim, Ceren; Cam, Yvan; Trichez, Debora; Auriol, Clément; Spina, Lucie; Vax, Amélie et al. (2015): Optimization of ethylene glycol production from (D)-xylose via a synthetic pathway implemented in Escherichia coli. In *Microbial cell factories* 14, p. 127. DOI: 10.1186/s12934-015-0312-7.

Andberg, Martina; Aro-Kärkkäinen, Niina; Carlson, Paul; Oja, Merja; Bozonnet, Sophie; Toivari, Mervi et al. (2016): Characterization and mutagenesis of two novel iron-sulphur cluster pentonate dehydratases. In *Applied microbiology and biotechnology* 100 (17), pp. 7549–7563. DOI: 10.1007/s00253-016-7530-8.

Anderlund; M; al, et (2001): Expression of Bifunctional Enzymes with Xylose Reductase and Xylitol Dehydrogenase Activity in Saccharomyces cerevisiae Alters Product Formation during Xylose Fermentation.

Arias, Emily E.; Walter, Johannes C. (2007): Strength in numbers: preventing rereplication via multiple mechanisms in eukaryotic cells. In *Genes & development* 21 (5), pp. 497–518. DOI: 10.1101/gad.1508907.

Avalos, José L.; Fink, Gerald R.; Stephanopoulos, Gregory (2013): Compartmentalization of metabolic pathways in yeast mitochondria improves the production of branched-chain alcohols. In *Nature biotechnology* 31 (4), pp. 335–341. DOI: 10.1038/nbt.2509.

Baker, Sean M.; Bronner, C. Eric; Zhang, Lin; Plug, Annemieke W.; Robatzek, Merrilee; Warren, Gwynedd et al. (1995): Male mice defective in the DNA mismatch repair gene PMS2 exhibit abnormal chromosome synapsis in meiosis. In *Cell* 82 (2), pp. 309–319.

Balk, Janneke; Aguilar Netz, Daili J.; Tepper, Katharina; Pierik, Antonio J.; Lill, Roland (2005): The essential WD40 protein Cia1 is involved in a late step of cytosolic and nuclear iron-sulfur protein assembly. In *Molecular and cellular biology* 25 (24), pp. 10833–10841. DOI: 10.1128/MCB.25.24.10833-10841.2005.

Balk, Janneke; Pierik, Antonio J.; Netz, Daili J. Aguilar; Mühlenhoff, Ulrich; Lill, Roland (2004): The hydrogenase-like Nar1p is essential for maturation of cytosolic and nuclear iron-sulphur proteins. In *The EMBO journal* 23 (10), pp. 2105–2115. DOI: 10.1038/sj.emboj.7600216.

Bandyopadhyay, Sibali; Gama, Filipe; Molina-Navarro, Maria Micaela; Gualberto, José Manuel; Claxton, Ronald; Naik, Sunil G. et al. (2008): Chloroplast monothiol glutaredoxins as scaffold proteins for the assembly and delivery of 2Fe-2S clusters. In *The EMBO journal* 27 (7), pp. 1122–1133. DOI: 10.1038/emboj.2008.50.

Barathikannan, Kaliyan; Agastian, Paul (2016): Xylitol: Production, Optimization and Industrial Application. In *Int.J.Curr.Microbiol.App.Sci* 5 (9), pp. 324–339. DOI: 10.20546/ijcmas.2016.509.036.

Bar-On, Yinon M.; Phillips, Rob; Milo, Ron (2018): The biomass distribution on Earth. In *Proceedings of the National Academy of Sciences of the United States of America* 115 (25), pp. 6506–6511. DOI: 10.1073/pnas.1711842115.

Bayliak, Maria; Burdyliuk, Nadia; Lushchak, Volodymyr (2017): Growth on Alpha-Ketoglutarate Increases Oxidative Stress Resistance in the Yeast Saccharomyces cerevisiae. In *International journal of microbiology* 2017, p. 5792192. DOI: 10.1155/2017/5792192.

Becker, Jessica; Boles, Eckhard (2003): A modified Saccharomyces cerevisiae strain that consumes L-Arabinose and produces ethanol. In *Applied and environmental microbiology* 69 (7), pp. 4144–4150. DOI: 10.1128/AEM.69.7.4144-4150.2003.

Becker, Judith; Klopprogge, Corinna; Herold, Andrea; Zelder, Oskar; Bolten, Christoph J.; Wittmann, Christoph (2007): Metabolic flux engineering of L-lysine production in Corynebacterium glutamicum--over expression and modification of G6P dehydrogenase. In *Journal of biotechnology* 132 (2), pp. 99–109. DOI: 10.1016/j.jbiotec.2007.05.026.

Bedford, J. J.; Bagnasco, S. M.; Kador, P. F.; Harris, H. W.; Burg, M. B. (1987): Characterization and purification of a mammalian osmoregulatory protein, aldose reductase, induced in renal medullary cells by high extracellular NaCl. In *Journal of Biological Chemistry* 262 (29), pp. 14255–14259. DOI: 10.1016/S0021-9258(18)47931-8.

Beinert, Helmut; Holm, Richard H.; Munck, Eckard (1997): Iron-sulfur clusters: nature's modular, multipurpose structures. In *Science (New York, N.Y.)* 277 (5326), pp. 653–659.

Benisch, Feline; Boles, Eckhard (2014): The bacterial Entner-Doudoroff pathway does not replace glycolysis in Saccharomyces cerevisiae due to the lack of activity of iron-sulfur cluster enzyme 6-phosphogluconate dehydratase. In *Journal of biotechnology* 171, pp. 45–55. DOI: 10.1016/j.jbiotec.2013.11.025.

Bernofsky, Carl; Utter, Merton F. (1968): Interconversions of mitochondrial pyridine nucleotides. In *Science* 159 (3821), pp. 1362–1363.

Bieganowski, Pawel; Seidle, Heather F.; Wojcik, Marzena; Brenner, Charles (2006): Synthetic lethal and biochemical analyses of NAD and NADH kinases in Saccharomyces cerevisiae establish separation of cellular functions. In *The Journal of biological chemistry* 281 (32), pp. 22439–22445. DOI: 10.1074/jbc.M513919200.

Blow, J. Julian; Dutta, Anindya (2005): Preventing re-replication of chromosomal DNA. In *Nature reviews. Molecular cell biology* 6 (6), pp. 476–486. DOI: 10.1038/nrm1663.

Boiteux, Serge; Jinks-Robertson, Sue (2013): DNA repair mechanisms and the bypass of DNA damage in Saccharomyces cerevisiae. In *Genetics* 193 (4), pp. 1025–1064. DOI: 10.1534/genetics.112.145219.

Bojunga, N.; Entian, K-D (1999): Cat8p, the activator of gluconeogenic genes in Saccharomyces cerevisiae, regulates carbon source-dependent expression of NADP-dependent cytosolic isocitrate dehydrogenase (Idp2p) and lactate permease (Jen1p). In *Molecular and General Genetics MGG* 262 (4-5), pp. 869–875.

Boles, Eckhard; Hollenberg, Cornelis P. (1997): The molecular genetics of hexose transport in yeasts. In *FEMS microbiology reviews* 21 (1), pp. 85–111.

Borgström, Celina; Wasserstrom, Lisa; Almqvist, Henrik; Broberg, Kristina; Klein, Bianca; Noack, Stephan et al. (2019): Identification of modifications procuring growth on xylose in recombinant Saccharomyces cerevisiae strains carrying the Weimberg pathway. In *Metabolic engineering* 55, pp. 1–11. DOI: 10.1016/j.ymben.2019.05.010.

Boyce, Kylie J.; Idnurm, Alexander (2019): Lighting Up Mutation: a New Unbiased System for the Measurement of Microbial Mutation Rates.

Braithwaite, Elena; Wu, Xiaohua; Wang, Zhigang (1998): Repair of DNA lesions induced by polycyclic aromatic hydrocarbons in human cell-free extracts: involvement of two excision repair mechanisms in vitro. In *Carcinogenesis* 19 (7), pp. 1239–1246.

Bro, Christoffer; Regenberg, Birgitte; Förster, Jochen; Nielsen, Jens (2006): In silico aided metabolic engineering of Saccharomyces cerevisiae for improved bioethanol production. In *Metabolic engineering* 8 (2), pp. 102–111. DOI: 10.1016/j.ymben.2005.09.007.

Brown, Stephanie; Clastre, Marc; Courdavault, Vincent; O'Connor, Sarah E. (2015): De novo production of the plant-derived alkaloid strictosidine in yeast. In *Proceedings of the National Academy of Sciences* 112 (11), pp. 3205–3210.

Bruinenberg, Peter M. (1986): The NADP (H) redox couple in yeast metabolism. In *Antonie Van Leeuwenhoek* 52, pp. 411–429.

Burdyliuk, Nadia; Bayliak, Maria (2017): Effects of Long-Term Cultivation on Medium with Alpha-Ketoglutarate Supplementation on Metabolic Processes of Saccharomyces cerevisiae. In *Journal of aging research* 2017, p. 8754879. DOI: 10.1155/2017/8754879.

Bych, Katrine; Kerscher, Stefan; Netz, Daili J. A.; Pierik, Antonio J.; Zwicker, Klaus; Huynen, Martijn A. et al. (2008): The iron-sulphur protein Ind1 is required for effective complex I assembly. In *The EMBO journal* 27 (12), pp. 1736–1746. DOI: 10.1038/emboj.2008.98.

Cam, Yvan; Alkim, Ceren; Trichez, Debora; Trebosc, Vincent; Vax, Amélie; Bartolo, François et al.

(2016): Engineering of a Synthetic Metabolic Pathway for the Assimilation of (d)-Xylose into Value-Added Chemicals. In *ACS synthetic biology* 5 (7), pp. 607–618. DOI: 10.1021/acssynbio.5b00103.

Cameron, Jessie M.; Janer, Alexandre; Levandovskiy, Valeriy; Mackay, Nevena; Rouault, Tracey A.; Tong, Wing-Hang et al. (2011): Mutations in iron-sulfur cluster scaffold genes NFU1 and BOLA3 cause a fatal deficiency of multiple respiratory chain and 2-oxoacid dehydrogenase enzymes. In *American journal of human genetics* 89 (4), pp. 486–495. DOI: 10.1016/j.ajhg.2011.08.011.

Chen, Clark; Kolodner, Richard D. (1999): Gross chromosomal rearrangements in Saccharomyces cerevisiae replication and recombination defective mutants. In *Nature genetics* 23 (1), pp. 81–85.

Chen, Hongzhang (2014a): Biotechnology of Lignocellulose. Theory and Practice. 1st ed. Dordrecht: Springer Netherlands. Available online at https://ebookcentral.proquest.com/lib/kxp/detail.action?docID=1731532.

Chen, Xi; Jiang, Zi-Hua; Chen, Sanfeng; Qin, Wensheng (2010): Microbial and bioconversion production of D-xylitol and its detection and application. In *International Journal of Biological Sciences* 6 (7), p. 834.

Chen, Yun; Bao, Jichen; Kim, Il-Kwon; Siewers, Verena; Nielsen, Jens (2014b): Coupled incremental precursor and co-factor supply improves 3-hydroxypropionic acid production in Saccharomyces cerevisiae. In *Metabolic engineering* 22, pp. 104–109. DOI: 10.1016/j.ymben.2014.01.005.

Cherry, J. Michael; Hong, Eurie L.; Amundsen, Craig; Balakrishnan, Rama; Binkley, Gail; Chan, Esther T. et al. (2012): Saccharomyces Genome Database: the genomics resource of budding yeast. In *Nucleic acids research* 40 (Database issue), D700-5. DOI: 10.1093/nar/gkr1029.

Chomvong, Kulika; Bauer, Stefan; Benjamin, Daniel I.; Li, Xin; Nomura, Daniel K.; Cate, Jamie H. D. (2016): Bypassing the Pentose Phosphate Pathway: Towards Modular Utilization of Xylose. In *PloS one* 11 (6), e0158111. DOI: 10.1371/journal.pone.0158111.

Cox, Edward C.; Gibson, Thomas C. (1974): Selection for high mutation rates in chemostats. In *Genetics* 77 (2), pp. 169–184.

Cross, F. R. (1995): Mutations in RAD27 define a potential link between G1 cyclins and DNA replication.

Cupp, J. R.; McAlister-Henn, L. (1991): NAD(+)-dependent isocitrate dehydrogenase. Cloning, nucleotide sequence, and disruption of the IDH2 gene from Saccharomyces cerevisiae. In *Journal of Biological Chemistry* 266 (33), pp. 22199–22205. DOI: 10.1016/S0021-9258(18)54554-3.

Cupp, J. R.; McAlister-Henn, L. (1992): Cloning and characterization of the gene encoding the IDH1 subunit of NAD(+)-dependent isocitrate dehydrogenase from Saccharomyces cerevisiae. In *Journal of Biological Chemistry* 267 (23), pp. 16417–16423. DOI: 10.1016/S0021-9258(18)42019-4.

Cupp, Jill R.; McAlister-Henn, Lee (1993): Kinetic analysis of NAD+isocitrate dehydrogenase with altered isocitrate binding sites: contribution of IDH1 and IDH2 subunits to regulation and catalysis. In *Biochemistry* 32 (36), pp. 9323–9328.

Dahms, A. Stephen (1974): 3-Deoxy-D-pentulosonic acid aldolase and its role in a new pathway of D-xylose degradation. In *Biochemical and biophysical research communications* 60 (4), pp. 1433–1439.

Dahn, Kristine M.; Davis, Brian P.; Pittman, Paul E.; Kenealy, William R.; Jeffries, Thomas W. (1996): Increased xylose reductase activity in the xylose-fermenting yeast Pichia stipitis by overexpression of XYL1. In *Applied biochemistry and biotechnology* 57, pp. 267–276.

D'Amore, Tony; Russell, Inge; Stewart, Graham G. (1989): Sugar utilization by yeast during fermentation. In *Journal of industrial microbiology and biotechnology* 4 (4), pp. 315–323.

DeJuan, C.; Lagunas, R. (1986): Inactivation of the galactose transport system in Saccharomyces cerevisiae. In *FEBS letters* 207 (2), pp. 258–261. DOI: 10.1016/0014-5793(86)81500-9.

Demeke, Mekonnen M.; Dietz, Heiko; Li, Yingying; Foulquié-Moreno, María R.; Mutturi, Sarma; Deprez, Sylvie et al. (2013): Development of a D-xylose fermenting and inhibitor tolerant industrial Saccharomyces cerevisiae strain with high performance in lignocellulose hydrolysates using metabolic and evolutionary engineering. In *Biotechnology for biofuels* 6 (1), pp. 1–24.

Diderich, J. A.; Schepper, M.; van Hoek, P.; Luttik, M. A.; van Dijken, J. P.; Pronk, J. T. et al. (1999): Glucose uptake kinetics and transcription of HXT genes in chemostat cultures of Saccharomyces cerevisiae. In *The Journal of biological chemistry* 274 (22), pp. 15350–15359. DOI: 10.1074/jbc.274.22.15350.

Diderich, J. A.; Schuurmans, J. M.; van Gaalen, M. C.; Kruckeberg, A. L.; van Dam, K. (2001): Functional analysis of the hexose transporter homologue HXT5 in Saccharomyces cerevisiae. In *Yeast (Chichester, England)* 18 (16), pp. 1515–1524. DOI: 10.1002/yea.779.

Doolin, M. T.; Johnson, A. L.; Johnston, L. H.; Butler, G. (2001): Overlapping and distinct roles of the duplicated yeast transcription factors Ace2p and Swi5p. In *Molecular microbiology* 40 (2), pp. 422–432. DOI: 10.1046/j.1365-2958.2001.02388.x.

dos Reis, Thaila Fernanda; Lilian Pereira Silva; Patrícia Alves de Castro; Rafaela Andrade do Carmo; Marjorie Mendes Marini; José Franco da Silveira et al. (2019): The Aspergillus fumigatus Mismatch Repair MSH2 Homolog Is Important for Virulence and Azole Resistance.

Dutkiewicz, Rafal; Marszalek, Jaroslaw; Schilke, Brenda; Craig, Elizabeth A.; Lill, Roland; Mühlenhoff, Ulrich (2006): The Hsp70 chaperone Ssq1p is dispensable for iron-sulfur cluster formation on the scaffold protein Isu1p. In *The Journal of biological chemistry* 281 (12), pp. 7801–7808. DOI: 10.1074/jbc.M513301200.

Dwight, Selina S.; Balakrishnan, Rama; Christie, Karen R.; Costanzo, Maria C.; Dolinski, Kara; Engel, Stacia R. et al. (2004): Saccharomyces genome database: underlying principles and organisation. In *Briefings in bioinformatics* 5 (1), pp. 9–22.

Edelmann, Winfried; Yang, Kan; Umar, Asad; Heyer, Joerg; Lau, Kirkland; Fan, Kunhua et al. (1997): Mutation in the mismatch repair gene Msh6 causes cancer susceptibility. In *Cell* 91 (4), pp. 467–477.

Eglinton, Jeffrey M.; Heinrich, Anthony J.; Pollnitz, Alan P.; Langridge, Peter; Henschke, Paul A.; Barros Lopes, Miguel de (2002): Decreasing acetic acid accumulation by a glycerol overproducing strain of Saccharomyces cerevisiae by deleting the ALD6 aldehyde dehydrogenase gene. In *Yeast (Chichester, England)* 19 (4), pp. 295–301. DOI: 10.1002/yea.834.

Ellis, Elizabeth M. (2002): Microbial aldo-keto reductases. In *FEMS microbiology letters* 216 (2), pp. 123–131.

Farwick, Alexander; Bruder, Stefan; Schadeweg, Virginia; Oreb, Mislav; Boles, Eckhard (2014): Engineering of yeast hexose transporters to transport D-xylose without inhibition by D-glucose. In *Proceedings of the National Academy of Sciences of the United States of America* 111 (14), pp. 5159–5164. DOI: 10.1073/pnas.1323464111.

Fijalkowska, Iwona J.; Schaaper, Roel M. (1996): Mutants in the Exo I motif of Escherichia coli dnaQ: defective proofreading and inviability due to error catastrophe. In *Proceedings of the National Academy of Sciences* 93 (7), pp. 2856–2861.

Gancedo, Carlos; Flores, Carmen-Lisset; Gancedo, Juana M. (2016): The Expanding Landscape of Moonlighting Proteins in Yeasts. In *Microbiology and molecular biology reviews : MMBR* 80 (3), pp. 765–777. DOI: 10.1128/MMBR.00012-16.

Gari, Kerstin; León Ortiz, Ana María; Borel, Valérie; Flynn, Helen; Skehel, J. Mark; Boulton, Simon J. (2012): MMS19 links cytoplasmic iron-sulfur cluster assembly to DNA metabolism. In *Science (New York, N.Y.)* 337 (6091), pp. 243–245.

Gasmi Benahmed, Asma; Gasmi, Amin; Arshad, Maria; Shanaida, Mariia; Lysiuk, Roman; Peana, Massimiliano et al. (2020): Health benefits of xylitol. In *Applied microbiology and biotechnology* 104 (17), pp. 7225–7237. DOI: 10.1007/s00253-020-10708-7.

Generoso, Wesley Cardoso; Gottardi, Manuela; Oreb, Mislav; Boles, Eckhard (2016): Simplified

CRISPR-Cas genome editing for Saccharomyces cerevisiae. In *Journal of microbiological methods* 127, pp. 203–205. DOI: 10.1016/j.mimet.2016.06.020.

Gibson, Daniel G.; Young, Lei; Chuang, Ray-Yuan; Venter, J. Craig; Hutchison, Clyde A.; Smith, Hamilton O. (2009): Enzymatic assembly of DNA molecules up to several hundred kilobases. In *Nature methods* 6 (5), pp. 343–345. DOI: 10.1038/nmeth.1318.

Gibson, Thomas C.; Scheppe, Mary L.; Cox, Edward C. (1970): Fitness of an Escherichia coli mutator gene. In *Science* 169 (3946), pp. 686–688.

Gírio, F. M.; Fonseca, C.; Carvalheiro, F.; Duarte, L. C.; Marques, S.; Bogel-Łukasik, R. (2010): Hemicelluloses for fuel ethanol: A review. In *Bioresource technology* 101 (13), pp. 4775–4800. DOI: 10.1016/j.biortech.2010.01.088.

Goffeau, André; Barrell, Bart G.; Bussey, Howard; Davis, Ronald W.; Dujon, Bernard; Feldmann, Heinz et al. (1996): Life with 6000 genes. In *Science (New York, N.Y.)* 274 (5287), pp. 546–567.

Grabowska, Dorota; Chelstowska, Anna (2003): The ALD6 gene product is indispensable for providing NADPH in yeast cells lacking glucose-6-phosphate dehydrogenase activity. In *The Journal of biological chemistry* 278 (16), pp. 13984–13988. DOI: 10.1074/jbc.M210076200.

Green, Brian M.; Finn, Kenneth J.; Li, Joachim J. (2010): Loss of DNA replication control is a potent inducer of gene amplification. In *Science (New York, N.Y.)* 329 (5994), pp. 943–946.

Green, Brian M.; Li, Joachim J. (2005): Loss of rereplication control in Saccharomyces cerevisiae results in extensive DNA damage. In *Molecular biology of the cell* 16 (1), pp. 421–432. DOI: 10.1091/mbc.e04-09-0833.

Grimshaw, Charles E. (1992): Aldose reductase: model for a new paradigm of enzymic perfection in detoxification catalysts. In *Biochemistry* 31 (42), pp. 10139–10145.

Grote, Andreas; Hiller, Karsten; Scheer, Maurice; Münch, Richard; Nörtemann, Bernd; Hempel, Dietmar C.; Jahn, Dieter (2005): JCat: a novel tool to adapt codon usage of a target gene to its potential expression host. In *Nucleic acids research* 33 (Web Server issue), W526-31. DOI: 10.1093/nar/gki376.

Guerriero, Gea; Hausman, Jean-Francois; Strauss, Joseph; Ertan, Haluk; Siddiqui, Khawar Sohail (2016): Lignocellulosic bioma ss : Biosynthesis, degradation, and industrial utilization. In *Eng. Life Sci.* 16 (1), pp. 1–16. DOI: 10.1002/elsc.201400196.

Güldener, Ulrich; Heck, Susanne; Fiedler, Thomas; Beinhauer, Jens and H. Hegemann, Johannes (1996): A new efficient gene disruption cassette for repeated use in budding yeast.

Ha, Suk-Jin; Galazka, Jonathan M.; Kim, Soo Rin; Choi, Jin-Ho; Yang, Xiaomin; Seo, Jin-Ho et al. (2011): Engineered Saccharomyces cerevisiae capable of simultaneous cellobiose and xylose fermentation. In *Proceedings of the National Academy of Sciences of the United States of America* 108 (2), pp. 504–509. DOI: 10.1073/pnas.1010456108.

Habraken, Yvette; Sung, Patrick; Prakash, Louise; Prakash, Satya (1993): Yeast excision repair gene RAD2 encodes a single-stranded DNA endonuclease. In *Nature* 366 (6453), pp. 365–368.

Harrington, John J.; Lieber, Michael R. (1994): Functional domains within FEN-1 and RAD2 define a family of structure-specific endonucleases: implications for nucleotide excision repair. In *Genes & development* 8 (11), pp. 1344–1355.

Harth, Simon (2022): Metabolic engineering of saccharomyces cerevisiae towards the biotransformation of D-galacturonic acid to L-galactonate: Dissertation, Frankfurt am Main, Johann Wolfgang Goethe-Universität, 2022.

Harth, Simon; Wagner, Jacqueline; Sens, Tamina; Choe, Jun-Yong; Benz, J. Philipp; Weuster-Botz, Dirk; Oreb, Mislav (2020): Engineering cofactor supply and NADH-dependent D-galacturonic acid reductases for redox-balanced production of L-galactonate in Saccharomyces cerevisiae. In *Scientific reports* 10 (1), p. 19021. DOI: 10.1038/s41598-020-75926-5.

Haselbeck, R. J.; McAlister-Henn, L. (1991): Isolation, nucleotide sequence, and disruption of the Saccharomyces cerevisiae gene encoding mitochondrial NADP(H)-specific isocitrate

dehydrogenase. In *Journal of Biological Chemistry* 266 (4), pp. 2339–2345. DOI: 10.1016/S0021-9258(18)52249-3.

Haurie, V.; Perrot, M.; Mini, T.; Jenö, P.; Sagliocco, F.; Boucherie, H. (2001): The transcriptional activator Cat8p provides a major contribution to the reprogramming of carbon metabolism during the diauxic shift in Saccharomyces cerevisiae. In *The Journal of biological chemistry* 276 (1), pp. 76–85. DOI: 10.1074/jbc.M008752200.

Hausmann, Anja; Aguilar Netz, Daili J.; Balk, Janneke; Pierik, Antonio J.; Mühlenhoff, Ulrich; Lill, Roland (2005): The eukaryotic P loop NTPase Nbp35: an essential component of the cytosolic and nuclear iron–sulfur protein assembly machinery. In *Proceedings of the National Academy of Sciences* 102 (9), pp. 3266–3271.

Healey, Kelley R.; Zhao, Yanan; Perez, Winder B.; Lockhart, Shawn R.; Sobel, Jack D.; Farmakiotis, Dimitrios et al. (2016): Prevalent mutator genotype identified in fungal pathogen Candida glabrata promotes multi-drug resistance. In *Nature communications* 7, p. 11128. DOI: 10.1038/ncomms11128.

Henke, B.; Girzalsky, W.; Berteaux-Lecellier, V.; Erdmann, R. (1998): IDP3 encodes a peroxisomal NADP-dependent isocitrate dehydrogenase required for the beta-oxidation of unsaturated fatty acids. In *The Journal of biological chemistry* 273 (6), pp. 3702–3711. DOI: 10.1074/jbc.273.6.3702.

Herr, Alan J.; Kennedy, Scott R.; Knowels, Gary M.; Schultz, Eric M.; Preston, Bradley D. (2014): DNA replication error-induced extinction of diploid yeast. In *Genetics* 196 (3), pp. 677–691. DOI: 10.1534/genetics.113.160960.

Herr, Alan J.; Ogawa, Masanori; Lawrence, Nicole A.; Williams, Lindsey N.; Eggington, Julie M.; Singh, Mallika et al. (2011): Mutator suppression and escape from replication error-induced extinction in yeast. In *PLoS genetics* 7 (10), e1002282. DOI: 10.1371/journal.pgen.1002282.

Ho, N. W.Y.; Lin, F. P.; Huang, S.; Andrews, P. C.; Tsao, G. T. (1990): Purification, characterization, and amino terminal sequence of xylose reductase from Candida shehatae. In *Enzyme and microbial technology* 12 (1), pp. 33–39.

Horak, J.; Wolf, D. H. (1997): Catabolite inactivation of the galactose transporter in the yeast Saccharomyces cerevisiae: ubiquitination, endocytosis, and degradation in the vacuole.

Hou, Jin; Vemuri, Goutham N.; Bao, Xiaoming; Olsson, Lisbeth (2009): Impact of overexpressing NADH kinase on glucose and xylose metabolism in recombinant xylose-utilizing Saccharomyces cerevisiae. In *Applied microbiology and biotechnology* 82 (5), pp. 909–919. DOI: 10.1007/s00253-009-1900-4.

Inoue, Y.; Matsuda, T.; Sugiyama, K.; Izawa, S.; Kimura, A. (1999): Genetic analysis of glutathione peroxidase in oxidative stress response of Saccharomyces cerevisiae. In *The Journal of biological chemistry* 274 (38), pp. 27002–27009. DOI: 10.1074/jbc.274.38.27002.

Islam, Md Shahidul; Indrajit, Mitesh (2012): Effects of xylitol on blood glucose, glucose tolerance, serum insulin and lipid profile in a type 2 diabetes model of rats. In *Annals of Nutrition and Metabolism* 61 (1), pp. 57–64.

Jeffries (1985): Emerging technology for fermenting D-xylose.

Jeong, Eun Ye; Kim, In Seon; Lee, Hung (2002): Identification of lysine-78 as an essential residue in the Saccharomyces cerevisiae xylose reductase. In *FEMS microbiology letters* 209 (2), pp. 223–228.

Johnsen, Ulrike; Dambeck, Michael; Zaiss, Henning; Fuhrer, Tobias; Soppa, Jörg; Sauer, Uwe; Schönheit, Peter (2009): D-xylose degradation pathway in the halophilic archaeon Haloferax volcanii. In *The Journal of biological chemistry* 284 (40), pp. 27290–27303. DOI: 10.1074/jbc.M109.003814.

Johnson, Robert E.; Kovvali, Gopala K.; Prakash, Louise; Prakash, Satya (1995): Requirement of the yeast RTH1 5′ to 3′ exonuclease for the stability of simple repetitive DNA. In *Science* 269 (5221), pp. 238–240.

Jordan, Paulina; Choe, Jun-Yong; Boles, Eckhard; Oreb, Mislav (2016): Hxt13, Hxt15, Hxt16 and Hxt17 from Saccharomyces cerevisiae represent a novel type of polyol transporters. In

Scientific reports 6, p. 23502. DOI: 10.1038/srep23502.

Karhumaa, Kaisa; Påhlman, Anna-Karin; Hahn-Hägerdal, Bärbel; Levander, Fredrik; Gorwa-Grauslund, Marie-F (2009): Proteome analysis of the xylose-fermenting mutant yeast strain TMB 3400. In *Yeast (Chichester, England)* 26 (7), pp. 371–382. DOI: 10.1002/yea.1673.

Karhumaa, Kaisa; Sanchez, Rosa Garcia; Hahn-Hägerdal, Bärbel; Gorwa-Grauslund, Marie-F (2007): Comparison of the xylose reductase-xylitol dehydrogenase and the xylose isomerase pathways for xylose fermentation by recombinant Saccharomyces cerevisiae. In *Microbial cell factories* 6, pp. 1–10.

Kawai, Shigeyuki; Suzuki, Sachiko; Mori, Shigetarou; Murata, Kousaku (2001): Molecular cloning and identification of UTR1 of a yeast Saccharomyces cerevisiae as a gene encoding an NAD kinase. In *FEMS microbiology letters* 200 (2), pp. 181–184.

Keren, Leeat; Zackay, Ora; Lotan-Pompan, Maya; Barenholz, Uri; Dekel, Erez; Sasson, Vered et al. (2013): Promoters maintain their relative activity levels under different growth conditions. In *Molecular systems biology* 9, p. 701. DOI: 10.1038/msb.2013.59.

Kim, Jae-Eung; Jang, In-Seung; Sung, Bong Hyun; Kim, Sun Chang; Lee, Ju Young (2018): Rerouting of NADPH synthetic pathways for increased protopanaxadiol production in Saccharomyces cerevisiae. In *Scientific reports* 8 (1), p. 15820. DOI: 10.1038/s41598-018-34210-3.

Kim, Soo Rin; Skerker, Jeffrey M.; Kang, Wei; Lesmana, Anastashia; Wei, Na; Arkin, Adam P.; Jin, Yong-Su (2013): Rational and evolutionary engineering approaches uncover a small set of genetic changes efficient for rapid xylose fermentation in Saccharomyces cerevisiae. In *PloS one* 8 (2), e57048. DOI: 10.1371/journal.pone.0057048.

Kim, Soo Rin; Xu, Haiqing; Lesmana, Anastashia; Kuzmanovic, Uros; Au, Matthew; Florencia, Clarissa et al. (2015): Deletion of PHO13, encoding haloacid dehalogenase type IIA phosphatase, results in upregulation of the pentose phosphate pathway in Saccharomyces cerevisiae. In *Applied and environmental microbiology* 81 (5), pp. 1601–1609. DOI: 10.1128/AEM.03474-14.

Kirby, James; Dietzel, Kevin L.; Wichmann, Gale; Chan, Rossana; Antipov, Eugene; Moss, Nathan et al. (2016): Engineering a functional 1-deoxy-D-xylulose 5-phosphate (DXP) pathway in Saccharomyces cerevisiae. In *Metabolic engineering* 38, pp. 494–503. DOI: 10.1016/j.ymben.2016.10.017.

Kjeldsen, Thomas (2000): Yeast secretory expression of insulin precursors. In *Applied microbiology and biotechnology* 54, pp. 277–286.

Kokoska, Robert J.; Stefanovic, Lela; Tran, Hiep T.; Resnick, Michael A.; Gordenin, Dmitry A.; Petes, Thomas D. (1998): Destabilization of yeast micro-and minisatellite DNA sequences by mutations affecting a nuclease involved in Okazaki fragment processing (rad27) and DNA polymerase δ (pol3-t). In *Molecular and cellular biology* 18 (5), pp. 2779–2788.

Koschwanez, John H.; Foster, Kevin R.; Murray, Andrew W. (2011): Sucrose utilization in budding yeast as a model for the origin of undifferentiated multicellularity. In *PLoS biology* 9 (8), e1001122. DOI: 10.1371/journal.pbio.1001122.

Kötter, Peter; Ciriacy, Michael (1993): Xylose fermentation by Saccharomyces cerevisiae. In *Applied microbiology and biotechnology* 38, pp. 776–783.

Kotyk, A. (1967): Properties of the sugar carrier in baker's yeast: II. Specificity of transport. In *Folia microbiologica* 12, pp. 121–131.

Kruckeberg, Arthur L. (1996): The hexose transporter family of Saccharomyces cerevisiae. In *Archives of microbiology* 166, pp. 283–292.

Kumánovics, Attila; Chen, Opal S.; Li, Liangtao; Bagley, Dustin; Adkins, Erika M.; Lin, Huilan et al. (2008): Identification of FRA1 and FRA2 as genes involved in regulating the yeast iron regulon in response to decreased mitochondrial iron-sulfur cluster synthesis. In *The Journal of biological chemistry* 283 (16), pp. 10276–10286. DOI: 10.1074/jbc.M801160200.

Kuyper, Marko; Hartog, Miranda M. P.; Toirkens, Maurice J.; Almering, Marinka J. H.; Winkler, Aaron A.; van Dijken, Johannes P.; Pronk, Jack T. (2005): Metabolic engineering of a xylose-

isomerase-expressing Saccharomyces cerevisiae strain for rapid anaerobic xylose fermentation. In *FEMS yeast research* 5 (4-5), pp. 399–409. DOI: 10.1016/j.femsyr.2004.09.010.

Kwon, Do-Hyun; Kim, Myoung-Dong; Lee, Tae-Hee; Oh, Yong-Joo; Ryu, Yeon-Woo; Seo, Jin-Ho (2006): Elevation of glucose 6-phosphate dehydrogenase activity increases xylitol production in recombinant Saccharomyces cerevisiae. In *Journal of Molecular Catalysis B: Enzymatic* 43 (1-4), pp. 86–89. DOI: 10.1016/j.molcatb.2006.06.014.

Lang, Gregory I.; Parsons, Lance; Gammie, Alison E. (2013): Mutation rates, spectra, and genome-wide distribution of spontaneous mutations in mismatch repair deficient yeast. In *G3: Genes, Genomes, Genetics* 3 (9), pp. 1453–1465.

Lange, Heike; Kaut, Anita; Kispal, Gyula; Lill, Roland (2000): A mitochondrial ferredoxin is essential for biogenesis of cellular iron-sulfur proteins. In *Proceedings of the National Academy of Sciences* 97 (3), pp. 1050–1055.

Langeveld, J. W. A.; Dixon, J.; Jaworski, J. F. (2010): Development Perspectives Of The Biobased Economy: A Review. In *Crop Sci.* 50, S-142-S-151. DOI: 10.2135/cropsci2009.09.0529.

Larochelle, Marc; Drouin, Simon; Robert, François; Turcotte, Bernard (2006): Oxidative stress-activated zinc cluster protein Stb5 has dual activator/repressor functions required for pentose phosphate pathway regulation and NADPH production. In *Molecular and cellular biology* 26 (17), pp. 6690–6701. DOI: 10.1128/MCB.02450-05.

Lawlis, V. B.; Dennis, M. S.; Chen, E. Y.; Smith, D. H.; Henner, DJ239604 (1984): Cloning and sequencing of the xylose isomerase and xylulose kinase genes of Escherichia coli. In *Applied and environmental microbiology* 47 (1), pp. 15–21.

Lee, Hung (1998): Review: The structure and function of yeast xylose (aldose) reductases. In *Yeast* 14 (11), pp. 977–984. DOI: 10.1002/(SICI)1097-0061(199808)14:11<977::AID-YEA302>3.0.CO;2-J.

Lee, Jaekwon; Godon, Christian; Lagniel, Gilles; Spector, Daniel; Garin, Jérome; Labarre, Jean; Toledano, Michel B. (1999): Yap1 and Skn7 control two specialized oxidative stress response regulons in yeast. In *Journal of Biological Chemistry* 274 (23), pp. 16040–16046.

Lee, Jung-Kul; Koo, Bong-Seong; Kim, Sang-Yong (2003): Cloning and characterization of the xyl1 gene, encoding an NADH-preferring xylose reductase from Candida parapsilosis, and its functional expression in Candida tropicalis. In *Applied and environmental microbiology* 69 (10), pp. 6179–6188. DOI: 10.1128/AEM.69.10.6179-6188.2003.

Lee, Michael E.; DeLoache, William C.; Cervantes, Bernardo; Dueber, John E. (2015): A Highly Characterized Yeast Toolkit for Modular, Multipart Assembly. In *ACS synthetic biology* 4 (9), pp. 975–986. DOI: 10.1021/sb500366v.

Lee, Sung-Haeng; Kodaki, Tsutomu; Park, Yong-Cheol; Seo, Jin-Ho (2012): Effects of NADH-preferring xylose reductase expression on ethanol production from xylose in xylose-metabolizing recombinant Saccharomyces cerevisiae. In *Journal of biotechnology* 158 (4), pp. 184–191. DOI: 10.1016/j.jbiotec.2011.06.005.

Lee, Susan D.; Surtees, Jennifer A.; Alani, Eric (2007): Saccharomyces cerevisiae MSH2–MSH3 and MSH2–MSH6 complexes display distinct requirements for DNA binding domain I in mismatch recognition. In *Journal of molecular biology* 366 (1), pp. 53–66.

Li, Xiaowei; Chen, Yun; Nielsen, Jens (2019): Harnessing xylose pathways for biofuels production. In *Current opinion in biotechnology* 57, pp. 56–65. DOI: 10.1016/j.copbio.2019.01.006.

Li, Xin; Yu, Vivian Yaci; Lin, Yuping; Chomvong, Kulika; Estrela, Raíssa; Park, Annsea et al. (2015): Expanding xylose metabolism in yeast for plant cell wall conversion to biofuels. In *Elife* 4, e05896.

Lill, Roland (2009): Function and biogenesis of iron-sulphur proteins. In *Nature* 460 (7257), pp. 831–838. DOI: 10.1038/nature08301.

Lill, Roland; Dutkiewicz, Rafal; Freibert, Sven A.; Heidenreich, Torsten; Mascarenhas, Judita; Netz, Daili J. et al. (2015): The role of mitochondria and the CIA machinery in the maturation of cytosolic and nuclear iron-sulfur proteins. In *European journal of cell biology* 94 (7-9), pp. 280–

291. DOI: 10.1016/j.ejcb.2015.05.002.

Lill, Roland; Hoffmann, Bastian; Molik, Sabine; Pierik, Antonio J.; Rietzschel, Nicole; Stehling, Oliver et al. (2012): The role of mitochondria in cellular iron-sulfur protein biogenesis and iron metabolism. In *Biochimica et biophysica acta* 1823 (9), pp. 1491–1508. DOI: 10.1016/j.bbamcr.2012.05.009.

Lill, Roland; Mühlenhoff, Ulrich (2008): Maturation of iron-sulfur proteins in eukaryotes: mechanisms, connected processes, and diseases. In *Annual review of biochemistry* 77, pp. 669–700. DOI: 10.1146/annurev.biochem.76.052705.162653.

Lin, Paul P.; Jaeger, Alec J.; Wu, Tung-Yun; Xu, Sharon C.; Lee, Abraxa S.; Gao, Fanke et al. (2018): Construction and evolution of an Escherichia coli strain relying on nonoxidative glycolysis for sugar catabolism. In *Proc Natl Acad Sci USA* 115 (14), pp. 3538–3546. DOI: 10.1073/pnas.1802191115.

Linck, Annabell; Vu, Xuan-Khang; Essl, Christine; Hiesl, Charlotte; Boles, Eckhard; Oreb, Mislav (2014): On the role of GAPDH isoenzymes during pentose fermentation in engineered Saccharomyces cerevisiae. In *FEMS yeast research* 14 (3), pp. 389–398. DOI: 10.1111/1567-1364.12137.

Liu, Huaiwei; Lu, Ting (2015): Autonomous production of 1,4-butanediol via a de novo biosynthesis pathway in engineered Escherichia coli. In *Metabolic engineering* 29, pp. 135–141. DOI: 10.1016/j.ymben.2015.03.009.

Loeillet, Sophie; Herzog, Mareike; Puddu, Fabio; Legoix, Patricia; Baulande, Sylvain; Jackson, Stephen P.; Nicolas, Alain G. (2020): Trajectory and uniqueness of mutational signatures in yeast mutators. In *Proceedings of the National Academy of Sciences of the United States of America*, pp. 24947–24956. DOI: 10.1073/pnas.2011332117.

Loftus, Thomas M.; Hall, Linda V.; Anderson, Sondra L.; McAlister-Henn, Lee (1994): Isolation, characterization, and disruption of the yeast gene encoding cytosolic NADP-specific isocitrate dehydrogenase. In *Biochemistry* 33 (32), pp. 9661–9667.

Lokman, B. Christien; van Santen, Pieter; Verdoes, Jan C.; Krüse, Jaap; Leer, Rob J.; Posno, Mark; Pouwels, Peter H. (1991): Organization and characterization of three genes involved in D-xylose catabolism in Lactobacillus pentosus. In *Molecular and General Genetics MGG* 230, pp. 161–169.

Lõoke, Marko; Kristjuhan, Kersti; Kristjuhan, Arnold (2011): Extraction of genomic DNA from yeasts for PCR-based applications. In *BioTechniques* 50 (5), pp. 325–328. DOI: 10.2144/000113672.

Lorraine S. Symington* (1998): Homologous recombination is required for the viability of rad27 mutants.

Lu, Ken W.; Wang, Chris T.; Chang, Hengray; Wang, Ryan S.; Shen, Claire R. (2021): Overcoming glutamate auxotrophy in Escherichia coli itaconate overproducer by the Weimberg pathway. In *Metabolic engineering communications* 13, e00190. DOI: 10.1016/j.mec.2021.e00190.

Lv, Xiaomei; Wang, Fan; Zhou, Pingping; Ye, Lidan; Xie, Wenping; Xu, Haoming; Yu, Hongwei (2016): Dual regulation of cytoplasmic and mitochondrial acetyl-CoA utilization for improved isoprene production in Saccharomyces cerevisiae. In *Nature communications* 7, p. 12851. DOI: 10.1038/ncomms12851.

Lynch, Michael; Sung, Way; Morris, Krystalynne; Coffey, Nicole; Landry, Christian R.; Dopman, Erik B. et al. (2008): A genome-wide view of the spectrum of spontaneous mutations in yeast. In *Proceedings of the National Academy of Sciences* 105 (27), pp. 9272–9277.

Lynd, L. R.; Wyman, C. E.; Gerngross, T. U. (1999): Biocommodity Engineering. In *Biotechnology progress* 15 (5), pp. 777–793. DOI: 10.1021/bp990109e.

Maddamsetti, Rohan; Grant, Nkrumah A. (2020): Divergent evolution of mutation rates and biases in the long-term evolution experiment with Escherichia coli. In *Genome biology and evolution* 12 (9), pp. 1591–1603.

Madhavan, Anjali; Tamalampudi, Sriappareddy; Ushida, Kazunari; Kanai, Daisuke; Katahira, Satoshi; Srivastava, Aradhana et al. (2009): Xylose isomerase from polycentric fungus Orpinomyces: gene sequencing, cloning, and expression in Saccharomyces cerevisiae for

bioconversion of xylose to ethanol. In *Applied microbiology and biotechnology* 82 (6), pp. 1067–1078. DOI: 10.1007/s00253-008-1794-6.

Mao, Emily F.; Lane, Laura; Lee, Jean; Miller, Jeffrey H. (1997): Proliferation of mutators in a cell population. In *Journal of bacteriology* 179 (2), pp. 417–422.

Marsischky, Gerald T.; Filosi, Nicole; Kane, Michael F.; Kolodner, Richard (1996): Redundancy of Saccharomyces cerevisiae MSH3 and MSH6 in MSH2-dependent mismatch repair. In *Genes & development* 10 (4), pp. 407–420.

Mathew, Anil K.; Abraham, Amith; Mallapureddy, Kiran Kumar; Sukumaran, Rajeev K. (2018): Lignocellulosic Biorefinery Wastes, or Resources? In : Waste Biorefinery: Elsevier, pp. 267–297.

Maxwell, W. A.; Spoerl, Edward (1970): Mannitol Uptake by Saccharomyces cerevisiae.

McAlister, L.; Holland, M. J. (1985): Differential expression of the three yeast glyceraldehyde-3-phosphate dehydrogenase genes. In *Journal of Biological Chemistry* 260 (28), pp. 15019–15027. DOI: 10.1016/S0021-9258(18)95696-6.

McCammon, Mark T.; McAlister-Henn, Lee (2003): Multiple cellular consequences of isocitrate dehydrogenase isozyme dysfunction. In *Archives of biochemistry and biophysics* 419 (2), pp. 222–233. DOI: 10.1016/j.abb.2003.08.022.

Meinander, N. Q.; Hahn-Hägerdal, B. (1997): Influence of cosubstrate concentration on xylose conversion by recombinant, XYL1-expressing Saccharomyces cerevisiae: a comparison of different sugars and ethanol as cosubstrates.

Merrill, Bradley J.; Holm, Connie (1998): The RAD52 recombinational repair pathway is essential in pol30 (PCNA) mutants that accumulate small single-stranded DNA fragments during DNA synthesis. In *Genetics* 148 (2), pp. 611–624.

Miersch, J. (1977): Transport of ribitol and D-glucose in the yeast <Emphasis Type="Italic">Candida guillermondii </Emphasis>. In *Folia microbiologica* 22, pp. 363–372.

Mihasan, Marius; Stefan, Marius; Hritcu, Lucian; Artenie, Vlad; Brandsch, Roderich (2013): Evidence of a plasmid-encoded oxidative xylose-catabolic pathway in Arthrobacter nicotinovorans pAO1. In *Research in microbiology* 164 (1), pp. 22–30. DOI: 10.1016/j.resmic.2012.10.003.

Minard, K. I.; Jennings, G. T.; Loftus, T. M.; Xuan, D.; McAlister-Henn, L. (1998): Sources of NADPH and expression of mammalian NADP+-specific isocitrate dehydrogenases in Saccharomyces cerevisiae. In *The Journal of biological chemistry* 273 (47), pp. 31486–31493. DOI: 10.1074/jbc.273.47.31486.

Minard, Karyl I.; Mcalister-Henn, L. E.E. (2001): ANTIOXIDANT FUNCTION OF CYTOSOLIC SOURCES OF NADPH IN YEAST.

Minard, Karyl I.; McAlister-Henn, Lee (2001): Antioxidant function of cytosolic sources of NADPH in yeast. In *Free Radical Biology and Medicine* 31 (6), pp. 832–843.

Minard, Karyl I.; McAlister-Henn, Lee (2005): Sources of NADPH in yeast vary with carbon source. In *The Journal of biological chemistry* 280 (48), pp. 39890–39896. DOI: 10.1074/jbc.M509461200.

Monir, Minhaj Uddin; Hasan, Md. Yeasir; Ahmed, Mohammad Tofayal; Aziz, Azrina Abd; Hossain, Md. Alam; Woobaidullah, A. S. M. et al. (2021): Optimization of fuel properties in two different peat reserve areas using surface response methodology and square regression analysis. In *Biomass Conv. Bioref.* DOI: 10.1007/s13399-021-01656-x.

Morrison, A.; Johnson, A. L.; Johnston, L. H.; Sugino, A. (1993): Pathway correcting DNA replication errors in Saccharomyces cerevisiae. In *The EMBO journal* 12 (4), pp. 1467–1473. DOI: 10.1002/j.1460-2075.1993.tb05790.x.

Mühlenhoff, Ulrich; Gerber, Jana; Richhardt, Nadine; Lill, Roland (2003): Components involved in assembly and dislocation of iron-sulfur clusters on the scaffold protein Isu1p. In *The EMBO journal* 22 (18), pp. 4815–4825. DOI: 10.1093/emboj/cdg446.

Mühlenhoff, Ulrich; Lill, Roland (2000): Biogenesis of iron–sulfur proteins in eukaryotes: a novel

task of mitochondria that is inherited from bacteria. In *Biochimica et Biophysica Acta (BBA)-Bioenergetics* 1459 (2-3), pp. 370–382.

Mühlenhoff, Ulrich; Molik, Sabine; Godoy, José R.; Uzarska, Marta A.; Richter, Nadine; Seubert, Andreas et al. (2010): Cytosolic monothiol glutaredoxins function in intracellular iron sensing and trafficking via their bound iron-sulfur cluster. In *Cell metabolism* 12 (4), pp. 373–385. DOI: 10.1016/j.cmet.2010.08.001.

Mumberg, Dominik; Muller, Rolf; and Funk Martin (1994): Regulatable promoters of Saccharomyces cerevisiae: I comparison of transcriptional activity and their use for el heterologous expression p.

Navarro-Aviño, Juan P.; Prasad, Rajendra; Miralles, Vicente J.; Benito, Rosa M.; Serrano, Ramon (1999): A proposal for nomenclature of aldehyde dehydrogenases inSaccharomyces cerevisiae and characterization of the stress-inducibleALD2 andALD3 genes. In *Yeast* 15 (10A), pp. 829–842. DOI: 10.1002/(SICI)1097-0061(199907)15:10A<829::AID-YEA423>3.0.CO;2-9.

Navarro-Sastre, Aleix; Tort, Frederic; Stehling, Oliver; Uzarska, Marta A.; Arranz, José Antonio; Del Toro, Mireia et al. (2011): A fatal mitochondrial disease is associated with defective NFU1 function in the maturation of a subset of mitochondrial Fe-S proteins. In *American journal of human genetics* 89 (5), pp. 656–667. DOI: 10.1016/j.ajhg.2011.10.005.

Netz, Daili J. A.; Mascarenhas, Judita; Stehling, Oliver; Pierik, Antonio J.; Lill, Roland (2014): Maturation of cytosolic and nuclear iron-sulfur proteins. In *Trends in cell biology* 24 (5), pp. 303–312. DOI: 10.1016/j.tcb.2013.11.005.

Netz, Daili J. A.; Pierik, Antonio J.; Stümpfig, Martin; Mühlenhoff, Ulrich; Lill, Roland (2007): The Cfd1-Nbp35 complex acts as a scaffold for iron-sulfur protein assembly in the yeast cytosol. In *Nature chemical biology* 3 (5), pp. 278–286. DOI: 10.1038/nchembio872.

Netz, Daili J. A.; Stith, Carrie M.; Stümpfig, Martin; Köpf, Gabriele; Vogel, Daniel; Genau, Heide M. et al. (2011): Eukaryotic DNA polymerases require an iron-sulfur cluster for the formation of active complexes. In *Nature chemical biology* 8 (1), pp. 125–132. DOI: 10.1038/nchembio.721.

Netz, Daili J. A.; Stümpfig, Martin; Doré, Carole; Mühlenhoff, Ulrich; Pierik, Antonio J.; Lill, Roland (2010): Tah18 transfers electrons to Dre2 in cytosolic iron-sulfur protein biogenesis. In *Nature chemical biology* 6 (10), pp. 758–765. DOI: 10.1038/nchembio.432.

Neuhauser; W; Haltrich; D; Kulbe; D, K. et al. (1997): NAD (P) H-dependent aldose reductase from the xylose-assimilating yeast Candida tenuis: Isolation, characterization and biochemical properties of the enzyme. In *Biochemical Journal* (326(3)), pp. 683–692.

Nijland, Jeroen G.; Shin, Hyun Yong; Jong, René M. de; Waal, Paul P. de; Klaassen, Paul; Driessen, Arnold J. M. (2014): Engineering of an endogenous hexose transporter into a specific D-xylose transporter facilitates glucose-xylose co-consumption in Saccharomyces cerevisiae. In *Biotechnology for biofuels* 7 (1), pp. 1–11.

Nijland, Jeroen G.; Vos, Erwin; Shin, Hyun Yong; Waal, Paul P. de; Klaassen, Paul; Driessen, Arnold J. M. (2016): Improving pentose fermentation by preventing ubiquitination of hexose transporters in Saccharomyces cerevisiae. In *Biotechnology for biofuels* 9, p. 158. DOI: 10.1186/s13068-016-0573-3.

Nishant, K. T.; Wei, Wu; Mancera, Eugenio; Argueso, Juan Lucas; Schlattl, Andreas; Delhomme, Nicolas et al. (2010): The baker's yeast diploid genome is remarkably stable in vegetative growth and meiosis. In *PLoS genetics* 6 (9), e1001109. DOI: 10.1371/journal.pgen.1001109.

Nishizawa, K.; Shimoda, E.; Kasahara, M. (1995): Substrate recognition domain of the Gal2 galactose transporter in yeast Saccharomyces cerevisiae as revealed by chimeric galactose-glucose transporters. In *The Journal of biological chemistry* 270 (6), pp. 2423–2426. DOI: 10.1074/jbc.270.6.2423.

Nissen, Torben L.; Kielland-Brandt, Morten C.; Nielsen, Jens; Villadsen, John (2000): Optimization of ethanol production in Saccharomyces cerevisiae by metabolic engineering of the ammonium assimilation. In *Metabolic engineering* 2 (1), pp. 69–77.

Noiraud, Nathalie; Maurousset, Laurence; Lemoine, Rémi (2001): Identification of a mannitol transporter, AgMaT1, in celery phloem. In *The plant cell* 13 (3), pp. 695–705.

Opalek, Monika; Wloch-Salamon, Dominika (2020): Aspects of Multicellularity in Saccharomyces cerevisiae Yeast: A Review of Evolutionary and Physiological Mechanisms. In *Genes* 11 (6). DOI: 10.3390/genes11060690.

Oud, Bart; Guadalupe-Medina, Victor; Nijkamp, Jurgen F.; Ridder, Dick de; Pronk, Jack T.; van Maris, Antonius J. A.; Daran, Jean-Marc (2013): Genome duplication and mutations in ACE2 cause multicellular, fast-sedimenting phenotypes in evolved Saccharomyces cerevisiae. In *Proc Natl Acad Sci USA* 110 (45), E4223-E4231.

Outten, Caryn E.; Culotta, Valeria C. (2003): A novel NADH kinase is the mitochondrial source of NADPH in Saccharomyces cerevisiae. In *The EMBO journal* 22 (9), pp. 2015–2024. DOI: 10.1093/emboj/cdg211.

Ouyang, Liming; Holland, Petter; Lu, Hongzhong; Bergenholm, David; Nielsen, Jens (2018): Integrated analysis of the yeast NADPH-regulator Stb5 reveals distinct differences in NADPH requirements and regulation in different states of yeast metabolism. In *FEMS yeast research* 18 (8). DOI: 10.1093/femsyr/foy091.

Özcan, Sabire; Johnston, Mark (1999): Function and regulation of yeast hexose transporters. In *Microbiology and molecular biology reviews* 63 (3), pp. 554–569.

Pao, Stephanie S.; Paulsen, Ian T.; Saier Jr, Milton H. (1998): Major facilitator superfamily. In *Microbiology and molecular biology reviews* 62 (1), pp. 1–34.

Papapetridis, Ioannis; Verhoeven, Maarten D.; Wiersma, Sanne J.; Goudriaan, Maaike; van Maris, Antonius J. A.; Pronk, Jack T. (2018): Laboratory evolution for forced glucose-xylose co-consumption enables identification of mutations that improve mixed-sugar fermentation by xylose-fermenting Saccharomyces cerevisiae. In *FEMS yeast research* 18 (6). DOI: 10.1093/femsyr/foy056.

Paramasivan, Kalaivani; Mutturi, Sarma (2017): Regeneration of NADPH Coupled with HMG-CoA Reductase Activity Increases Squalene Synthesis in Saccharomyces cerevisiae. In *Journal of agricultural and food chemistry* 65 (37), pp. 8162–8170. DOI: 10.1021/acs.jafc.7b02945.

Parenteau, Julie; Wellinger, Raymund J. (1999): Accumulation of Single-Stranded DNA and Destabilization of Telomeric Repeats in Yeast Mutant Strains Carrying a Deletion of RAD27.

Park, Sung Goo; Cha, Mee-Kyung; Jeong, Woojin; Kim, Il-Han (2000): Distinct physiological functions of thiol peroxidase isoenzymes in Saccharomyces cerevisiae. In *The Journal of biological chemistry* 275 (8), pp. 5723–5732.

Partow, Siavash; Siewers, Verena; Daviet, Laurent; Schalk, Michel; Nielsen, Jens (2012): Reconstruction and evaluation of the synthetic bacterial MEP pathway in Saccharomyces cerevisiae. In *PloS one* 7 (12), e52498. DOI: 10.1371/journal.pone.0052498.

Paul, Viktoria Désirée; Lill, Roland (2015): Biogenesis of cytosolic and nuclear iron-sulfur proteins and their role in genome stability. In *Biochimica et biophysica acta* 1853 (6), pp. 1528–1539. DOI: 10.1016/j.bbamcr.2014.12.018.

Pereira, Brian; Li, Zheng-Jun; Mey, Marjan de; Lim, Chin Giaw; Zhang, Haoran; Hoeltgen, Claude; Stephanopoulos, Gregory (2016): Efficient utilization of pentoses for bioproduction of the renewable two-carbon compounds ethylene glycol and glycolate. In *Metabolic engineering* 34, pp. 80–87. DOI: 10.1016/j.ymben.2015.12.004.

Polakis, E. S.; Bartley, W. (1965): Changes in the enzyme activities of Saccharomyces cerevisiae during aerobic growth on different carbon sources. In *Biochemical Journal* 97 (1), pp. 284–297.

Polakis, E. S.; Bartley, W.; Meek, G. A. (1965): Changes in the activities of respiratory enzymes during the aerobic growth of yeast on different carbon sources. In *Biochemical Journal* 97 (1), pp. 298–302.

Porro, Danilo; Brambilla, Luca; Ranzi, Bianca Maria; Martegani, Enzo; Alberghina, Lilia (1995): Development of metabolically engineered Saccharomyces cerevisiae cells for the production of lactic acid. In *Biotechnology progress* 11 (3), pp. 294–298.

Prolla, T. A.; Pang, Q.; Alani, E.; Kolodner, R. D.; Liskay, R. M. (1994): MLH1, PMS1, and MSH2 interactions during the initiation of DNA mismatch repair in yeast. In *Science (New York, N.Y.)* 265 (5175), pp. 1091–1093. DOI: 10.1126/science.8066446.

Raab, Andreas M.; Gebhardt, Gabi; Bolotina, Natalia; Weuster-Botz, Dirk; Lang, Christine (2010): Metabolic engineering of Saccharomyces cerevisiae for the biotechnological production of succinic acid. In *Metabolic engineering* 12 (6), pp. 518–525. DOI: 10.1016/j.ymben.2010.08.005.

Reagan, Michael S.; Pittenger, Christopher; Siede, Wolfram; Friedberg, Errol C. (1995): Characterization of a mutant strain of Saccharomyces cerevisiae with a deletion of the RAD27 gene, a structural homolog of the RAD2 nucleotide excision repair gene. In *Journal of bacteriology* 177 (2), pp. 364–371.

Reifenberger, E.; Boles, E.; Ciriacy, M. (1997): Kinetic characterization of individual hexose transporters of Saccharomyces cerevisiae and their relation to the triggering mechanisms of glucose repression. In *European journal of biochemistry* 245 (2), pp. 324–333. DOI: 10.1111/j.1432-1033.1997.00324.x.

Reifenberger, E.; Freidel, K.; Ciriacy, M. (1995): Identification of novel HXT genes in Saccharomyces cerevisiae reveals the impact of individual hexose transporters on glycolytic flux. In *Molecular microbiology* 16 (1), pp. 157–167. DOI: 10.1111/j.1365-2958.1995.tb02400.x.

Reitmair, Armin H.; Cai, Jian-Chun; Bjerknes, Matthew; Redston, Mark; Cheng, Hazel; Pind, Molly T. L. et al. (1996): MSH2 deficiency contributes to accelerated APC-mediated intestinal tumorigenesis. In *Cancer research* 56 (13), pp. 2922–2926.

Rezaei, Mohammad N.; Aslankoohi, Elham; Verstrepen, Kevin J.; Courtin, Christophe M. (2015): Contribution of the tricarboxylic acid (TCA) cycle and the glyoxylate shunt in Saccharomyces cerevisiae to succinic acid production during dough fermentation. In *International journal of food microbiology* 204, pp. 24–32. DOI: 10.1016/j.ijfoodmicro.2015.03.004.

Reznicek, O.; Facey, S. J.; Waal, P. P. de; Teunissen, A. W. R. H.; Bont, J. A. M. de; Nijland, J. G. et al. (2015): Improved xylose uptake in Saccharomyces cerevisiae due to directed evolution of galactose permease Gal2 for sugar co-consumption. In *Journal of applied microbiology* 119 (1), pp. 99–111. DOI: 10.1111/jam.12825.

Richard, G-F; Dujon, B.; Haber, J. E. (1999): Double-strand break repair can lead to high frequencies of deletions within short CAG/CTG trinucleotide repeats. In *Molecular and General Genetics MGG* 261, pp. 871–882.

Ringel, Alison E.; Ryznar, Rebecca; Picariello, Hannah; Huang, Kuan-lin; Lazarus, Asmitha G.; Holmes, Scott G. (2013): Yeast Tdh3 (glyceraldehyde 3-phosphate dehydrogenase) is a Sir2-interacting factor that regulates transcriptional silencing and rDNA recombination. In *PLoS genetics* 9 (10), e1003871. DOI: 10.1371/journal.pgen.1003871.

Rizzi, Manfred; Erlemann, Petra; Bui-Thanh, Ngoc-Anh; Dellweg, Hanswerner (1988): Xylose fermentation by yeasts: 4. Purification and kinetic studies of xylose reductase from Pichia stipitis. In *Applied microbiology and biotechnology* 29, pp. 148–154.

Ro, Dae-Kyun; Paradise, Eric M.; Ouellet, Mario; Fisher, Karl J.; Newman, Karyn L.; Ndungu, John M. et al. (2006): Production of the antimalarial drug precursor artemisinic acid in engineered yeast. In *Nature* 440 (7086), pp. 940–943.

Rojas, Sebastian A. Tamayo; Schadeweg, Virginia; Kirchner, Ferdinand; Boles, Eckhard; Oreb, Mislav (2021): Identification of a glucose-insensitive variant of Gal2 from Saccharomyces cerevisiae exhibiting a high pentose transport capacity. In *Scientific reports* 11 (1), p. 24404. DOI: 10.1038/s41598-021-03822-7.

Roret, Thomas; Tsan, Pascale; Couturier, Jérémy; Zhang, Bo; Johnson, Michael K.; Rouhier, Nicolas; Didierjean, Claude (2014): Structural and spectroscopic insights into BolA-glutaredoxin complexes. In *The Journal of biological chemistry* 289 (35), pp. 24588–24598. DOI: 10.1074/jbc.M114.572701.

Rouhier, Nicolas; Unno, Hideaki; Bandyopadhyay, Sibali; Masip, Lluis; Kim, Sung-Kun; Hirasawa, Masakazu et al. (2007): Functional, structural, and spectroscopic characterization of a

glutathione-ligated [2Fe–2S] cluster in poplar glutaredoxin C1. In *Proceedings of the National Academy of Sciences* 104 (18), pp. 7379–7384.

Roy, Amit; Solodovnikova, Natalia; Nicholson, Tracy; Antholine, William; Walden, William E. (2003): A novel eukaryotic factor for cytosolic Fe-S cluster assembly. In *The EMBO journal* 22 (18), pp. 4826–4835. DOI: 10.1093/emboj/cdg455.

Rygus, T.; Scheler, A.; Allmansberger, R.; Hillen, W. (1991): Molecular cloning, structure, promoters and regulatory elements for transcription of the Bacillus megaterium encoded regulon for xylose utilization. In *Archives of microbiology* 155, pp. 535–542.

Saloheimo, Anu; Rauta, Jenita; Stasyk, Oleh V.; Sibirny, Andrei A.; Penttilä, Merja; Ruohonen, Laura (2007): Xylose transport studies with xylose-utilizing Saccharomyces cerevisiae strains expressing heterologous and homologous permeases. In *Applied microbiology and biotechnology* 74 (5), pp. 1041–1052. DOI: 10.1007/s00253-006-0747-1.

Salusjärvi, Laura; Toivari, Mervi; Vehkomäki, Maija-Leena; Koivistoinen, Outi; Mojzita, Dominik; Niemelä, Klaus et al. (2017): Production of ethylene glycol or glycolic acid from D-xylose in Saccharomyces cerevisiae. In *Applied microbiology and biotechnology* 101 (22), pp. 8151–8163. DOI: 10.1007/s00253-017-8547-3.

Saputo, Sarah; Chabrier-Rosello, Yeissa; Luca, Francis C.; Kumar, Anuj; Krysan, Damian J. (2012): The RAM network in pathogenic fungi. In *Eukaryotic cell* 11 (6), pp. 708–717. DOI: 10.1128/EC.00044-12.

Sasaki, Miho; Jojima, Toru; Inui, Masayuki; Yukawa, Hideaki (2010): Xylitol production by recombinant Corynebacterium glutamicum under oxygen deprivation. In *Applied microbiology and biotechnology* 86 (4), pp. 1057–1066. DOI: 10.1007/s00253-009-2372-2.

Scheinin, A.; Mäkinen, K. K.; Tammisalo, E.; Rekola, M. (1975): Turku sugar studies XVIII. Incidence of dental caries in relation to 1-year consumption of xylitol chewing gum. In *Acta odontologica Scandinavica* 33 (5), pp. 269–278. DOI: 10.3109/00016357509004632.

Sedlak, Miroslav; Ho, Nancy W. Y. (2004): Characterization of the effectiveness of hexose transporters for transporting xylose during glucose and xylose co-fermentation by a recombinant Saccharomyces yeast. In *Yeast (Chichester, England)* 21 (8), pp. 671–684. DOI: 10.1002/yea.1060.

Serero, Alexandre; Jubin, Claire; Loeillet, Sophie; Legoix-Né, Patricia; Nicolas, Alain G. (2014): Mutational landscape of yeast mutator strains. In *Proc Natl Acad Sci USA* 111 (5), pp. 1897–1902. DOI: 10.1073/pnas.1314423111.

Sharma, Anil K.; Pallesen, Leif J.; Spang, Robert J.; Walden, William E. (2010): Cytosolic iron-sulfur cluster assembly (CIA) system: factors, mechanism, and relevance to cellular iron regulation. In *The Journal of biological chemistry* 285 (35), pp. 26745–26751. DOI: 10.1074/jbc.R110.122218.

Sheftel, Alex D.; Stehling, Oliver; Pierik, Antonio J.; Elsässer, Hans-Peter; Mühlenhoff, Ulrich; Webert, Holger et al. (2010): Humans possess two mitochondrial ferredoxins, Fdx1 and Fdx2, with distinct roles in steroidogenesis, heme, and Fe/S cluster biosynthesis. In *Proceedings of the National Academy of Sciences of the United States of America* 107 (26), pp. 11775–11780. DOI: 10.1073/pnas.1004250107.

Shen, Yu; Chen, Xiao; Peng, Bingyin; Chen, Liyuan; Hou, Jin; Bao, Xiaoming (2012): An efficient xylose-fermenting recombinant Saccharomyces cerevisiae strain obtained through adaptive evolution and its global transcription profile. In *Applied microbiology and biotechnology* 96 (4), pp. 1079–1091. DOI: 10.1007/s00253-012-4418-0.

Shi, Feng; Kawai, Shigeyuki; Mori, Shigetarou; Kono, Emi; Murata, Kousaku (2005): Identification of ATP-NADH kinase isozymes and their contribution to supply of NADP(H) in Saccharomyces cerevisiae. In *The FEBS journal* 272 (13), pp. 3337–3349. DOI: 10.1111/j.1742-4658.2005.04749.x.

Shi, Feng; Li, Zhijun; Sun, Mingdi; Li, Yongfu (2011): Role of mitochondrial NADH kinase and NADPH supply in the respiratory chain activity of Saccharomyces cerevisiae. In *Acta biochimica et biophysica Sinica* 43 (12), pp. 989–995. DOI: 10.1093/abbs/gmr092.

Shi, Yanbo; Ghosh, Manik; Kovtunovych, Gennadiy; Crooks, Daniel R.; Rouault, Tracey A. (2012): Both human ferredoxins 1 and 2 and ferredoxin reductase are important for iron-sulfur cluster biogenesis. In *Biochimica et biophysica acta* 1823 (2), pp. 484–492. DOI: 10.1016/j.bbamcr.2011.11.002.

Shin, Hyun Yong; Nijland, Jeroen G.; Waal, Paul P. de; Driessen, Arnold J. M. (2017): The amino-terminal tail of Hxt11 confers membrane stability to the Hxt2 sugar transporter and improves xylose fermentation in the presence of acetic acid. In *Biotechnology and bioengineering* 114 (9), pp. 1937–1945. DOI: 10.1002/bit.26322.

Shin, Hyun Yong; Nijland, Jeroen G.; Waal, Paul P. de; Jong, René M. de; Klaassen, Paul; Driessen, Arnold J. M. (2015): An engineered cryptic Hxt11 sugar transporter facilitates glucose-xylose co-consumption in Saccharomyces cerevisiae. In *Biotechnology for biofuels* 8, p. 176. DOI: 10.1186/s13068-015-0360-6.

Siddiqui, Khalid; On, Kin Fan; Diffley, John F. X. (2013): Regulating DNA replication in eukarya. In *Cold Spring Harbor perspectives in biology* 5 (9). DOI: 10.1101/cshperspect.a012930.

Silva, Paulo César; Ceja-Navarro, Javier A.; Azevedo, Flávio; Karaoz, Ulas; Brodie, Eoin L.; Johansson, Björn (2021): A novel D-xylose isomerase from the gut of the wood feeding beetle Odontotaenius disjunctus efficiently expressed in Saccharomyces cerevisiae. In *Scientific reports* 11 (1), p. 4766. DOI: 10.1038/s41598-021-83937-z.

Sniegowski, Paul D.; Gerrish, Philip J.; Lenski, Richard E. (1997): Evolution of high mutation rates in experimental populations of E. coli. In *Nature* 387 (6634), pp. 703–705.

Sommers, C. H.; Miller, E. J.; Dujon, B.; Prakash, S.; Prakash, L. (1995): Conditional lethality of null mutations in RTH1 that encodes the yeast counterpart of a mammalian 5'- to 3'-exonuclease required for lagging strand DNA synthesis in reconstituted systems. In *The Journal of biological chemistry* 270 (9), pp. 4193–4196. DOI: 10.1074/jbc.270.9.4193.

Sonderegger, Marco; Schümperli, Michael; Sauer, Uwe (2004): Metabolic engineering of a phosphoketolase pathway for pentose catabolism in Saccharomyces cerevisiae. In *Applied and environmental microbiology* 70 (5), pp. 2892–2897. DOI: 10.1128/AEM.70.5.2892-2897.2004.

Stehling, Oliver; Lill, Roland (2013): The role of mitochondria in cellular iron-sulfur protein biogenesis: mechanisms, connected processes, and diseases. In *Cold Spring Harbor perspectives in biology* 5 (8), a011312. DOI: 10.1101/cshperspect.a011312.

Stehling, Oliver; Vashisht, Ajay A.; Mascarenhas, Judita; Jonsson, Zophonias O.; Sharma, Tanu; Netz, Daili J. A. et al. (2012): MMS19 assembles iron-sulfur proteins required for DNA metabolism and genomic integrity. In *Science (New York, N.Y.)* 337 (6091), pp. 195–199. DOI: 10.1126/science.1219723.

Stephens, Craig; Christen, Beat; Fuchs, Thomas; Sundaram, Vidyodhaya; Watanabe, Kelly; Jenal, Urs (2007): Genetic analysis of a novel pathway for D-xylose metabolism in Caulobacter crescentus. In *Journal of bacteriology* 189 (5), pp. 2181–2185. DOI: 10.1128/JB.01438-06.

Strand, Micheline K.; Stuart, Gregory R.; Longley, Matthew J.; Graziewicz, Maria A.; Dominick, Olivia C.; Copeland, William C. (2003): POS5 gene of Saccharomyces cerevisiae encodes a mitochondrial NADH kinase required for stability of mitochondrial DNA. In *Eukaryotic cell* 2 (4), pp. 809–820. DOI: 10.1128/EC.2.4.809-820.2003.

Su, Buli; Wu, Mianbin; Lin, Jianping; Yang, Lirong (2013): Metabolic engineering strategies for improving xylitol production from hemicellulosic sugars. In *Biotechnology letters* 35 (11), pp. 1781–1789. DOI: 10.1007/s10529-013-1279-2.

Tamayo Rojas, Sebastian A.; Schmidl, Sina; Boles, Eckhard; Oreb, Mislav (2021): Glucose-induced internalization of the S. cerevisiae galactose permease Gal2 is dependent on phosphorylation and ubiquitination of its aminoterminal cytoplasmic tail. In *FEMS yeast research* 21 (3). DOI: 10.1093/femsyr/foab019.

Tani, Tatsunori; Taguchi, Hisataka; Fujimori, Kazuhiro E.; Sahara, Takehiko; Ohgiya, Satoru; Kamagata, Yoichi; Akamatsu, Takashi (2016): Isolation and characterization of xylitol-assimilating mutants of recombinant Saccharomyces cerevisiae. In *Journal of bioscience and bioengineering* 122 (4), pp. 446–455. DOI: 10.1016/j.jbiosc.2016.03.008.

Tenaillon, Olivier; Toupance, Bruno; Le Nagard, Hervé; Taddei, François; Godelle, Bernard (1999): Mutators, population size, adaptive landscape and the adaptation of asexual populations of bacteria. In *Genetics* 152 (2), pp. 485–493.

Terebieniec, Agata; Chroumpi, Tania; Dilokpimol, Adiphol; Aguilar-Pontes, Maria Victoria; Mäkelä, Miia R.; Vries, Ronald P. de (2021): Characterization of d-xylose reductase, XyrB, from Aspergillus niger. In *Biotechnology reports (Amsterdam, Netherlands)* 30, e00610. DOI: 10.1016/j.btre.2021.e00610.

Tishkoff, Daniel X.; Filosi, Nicole; Gaida, Gretchen M.; Kolodner, Richard D. (1997): A novel mutation avoidance mechanism dependent on S. cerevisiae RAD27 is distinct from DNA mismatch repair. In *Cell* 88 (2), pp. 253–263.

Toivari, Mervi H.; Salusjärvi, Laura; Ruohonen, Laura; Penttilä, Merja (2004): Endogenous xylose pathway in Saccharomyces cerevisiae. In *Applied and environmental microbiology* 70 (6), pp. 3681–3686. DOI: 10.1128/AEM.70.6.3681-3686.2004.

Tosti, Elena; Katakowski, Joseph A.; Schaetzlein, Sonja; Kim, Hyun-Soo; Ryan, Colm J.; Shales, Michael et al. (2014): Evolutionarily conserved genetic interactions with budding and fission yeast MutS identify orthologous relationships in mismatch repair-deficient cancer cells. In *Genome Medicine* 6, pp. 1–14.

Träff, K. L.; Jönsson, L. J.; Hahn-Hägerdal, B. (2002): Putative xylose and arabinose reductases in Saccharomyces cerevisiae. In *Yeast (Chichester, England)* 19 (14), pp. 1233–1241. DOI: 10.1002/yea.913.

Träff, K. L.; Otero Cordero, R. R.; van Zyl, W. H.; Hahn-Hägerdal, B. (2001): Deletion of the GRE3 aldose reductase gene and its influence on xylose metabolism in recombinant strains of Saccharomyces cerevisiae expressing the xylA and XKS1 genes. In *Applied and environmental microbiology* 67 (12), pp. 5668–5674. DOI: 10.1128/AEM.67.12.5668-5674.2001.

Turchi, J. J.; Bambara, R. A. (1993): Completion of mammalian lagging strand DNA replication using purified proteins. In *Journal of Biological Chemistry* 268 (20), pp. 15136–15141. DOI: 10.1016/S0021-9258(18)82447-4.

Uzarska, Marta A.; Dutkiewicz, Rafal; Freibert, Sven-Andreas; Lill, Roland; Mühlenhoff, Ulrich (2013): The mitochondrial Hsp70 chaperone Ssq1 facilitates Fe/S cluster transfer from Isu1 to Grx5 by complex formation. In *Molecular biology of the cell* 24 (12), pp. 1830–1841.

Vallen, Elizabeth A.; Cross, Frederick R. (1995): Mutations in RAD27 define a potential link between G1 cyclins and DNA replication. In *Molecular and cellular biology* 15 (8), pp. 4291–4302.

van Houten, Bennett (1990): Nucleotide excision repair in Escherichia coli. In *Microbiological reviews* 54 (1), pp. 18–51.

van Nguyen, Q.; Co, Carl; Li, Joachim J. (2001): Cyclin-dependent kinases prevent DNA re-replication through multiple mechanisms. In *Nature* 411 (6841), pp. 1068–1073.

van Roermund, C. W.; Elgersma, Y.; Singh, N.; Wanders, R. J.; Tabak, H. F. (1995): The membrane of peroxisomes in Saccharomyces cerevisiae is impermeable to NAD(H) and acetyl-CoA under in vivo conditions. In *The EMBO journal* 14 (14), pp. 3480–3486. DOI: 10.1002/j.1460-2075.1995.tb07354.x.

van Roermund, C. W.; Hettema, E. H.; Kal, A. J.; van den Berg, M.; Tabak, H. F.; Wanders, R. J. (1998): Peroxisomal beta-oxidation of polyunsaturated fatty acids in Saccharomyces cerevisiae: isocitrate dehydrogenase provides NADPH for reduction of double bonds at even positions. In *The EMBO journal* 17 (3), pp. 677–687. DOI: 10.1093/emboj/17.3.677.

Verduyn, C.; van Kleef, R.; Frank, J.; Schreuder, H.; van Dijken, J. P.; Scheffers, W. A. (1985): Properties of the NAD (P) H-dependent xylose reductase from the xylose-fermenting yeast Pichia stipitis. In *Biochemical Journal* 226 (3), pp. 669–677.

Verho, Ritva; Londesborough, John; Penttilä, Merja; Richard, Peter (2003): Engineering redox cofactor regeneration for improved pentose fermentation in Saccharomyces cerevisiae. In *Applied and environmental microbiology* 69 (10), pp. 5892–5897. DOI: 10.1128/AEM.69.10.5892-5897.2003.

Verho, Ritva; Richard, Peter; Jonson, Per Harald; Sundqvist, Lena; Londesborough, John; Penttilä, Merja (2002): Identification of the first fungal NADP-GAPDH from Kluyveromyces lactis. In *Biochemistry* 41 (46), pp. 13833–13838. DOI: 10.1021/bi0265325.

Verhoeven, Maarten D.; Bracher, Jasmine M.; Nijland, Jeroen G.; Bouwknegt, Jonna; Daran, Jean-Marc G.; Driessen, Arnold J. M. et al. (2018): Laboratory evolution of a glucose-phosphorylation-deficient, arabinose-fermenting S. cerevisiae strain reveals mutations in GAL2 that enable glucose-insensitive l-arabinose uptake. In *FEMS yeast research* 18 (6). DOI: 10.1093/femsyr/foy062.

Voth, Warren P.; Olsen, Aileen E.; Sbia, Mohammed; Freedman, Karen H.; Stillman, David J. (2005): ACE2, CBK1, and BUD4 in budding and cell separation. In *Eukaryotic cell* 4 (6), pp. 1018–1028. DOI: 10.1128/EC.4.6.1018-1028.2005.

Waga, S.; Bauer, G.; Stillman, B. (1994): Reconstitution of complete SV40 DNA replication with purified replication factors. In *Journal of Biological Chemistry* 269 (14), pp. 10923–10934. DOI: 10.1016/S0021-9258(17)34146-7.

Waga, Shou; Stillman, Bruce (1994): Anatomy of a DNA replication fork revealed by reconstitution of SV40 DNA replication in vitro. In *Nature* 369 (6477), pp. 207–212.

Wahlbom, Fredrik; Sonderegger, Marco; Sauer, Uwe Erich (2007): Metabolic engineering for improved xylose utilisation of Saccharomyces cerevisiae: Google Patents.

Walfridsson, M.; Anderlund, M.; Bao, X.; Hahn-Hägerdal, B. (1997): Expression of different levels of enzymes from the Pichia stipitis XYL1 and XYL2 genes in Saccharomyces cerevisiae and its effects on product formation during xylose utilisation. In *Applied microbiology and biotechnology* 48, pp. 218–224.

Walker, L. P.; Wilson, D. B. (1991): Enzymatic hydrolysis of cellulose: an overview. In *Bioresource technology* 36 (1), pp. 3–14.

Wang, Fangqian; Ouyang, Denghao; Zhou, Ziyuan; Page, Samuel J.; Liu, Dehua; Zhao, Xuebing (2021): Lignocellulosic biomass as sustainable feedstock and materials for power generation and energy storage. In *Journal of Energy Chemistry* 57, pp. 247–280.

Wang, Zhigang; Wu, Xiaohua; Friedberg, Errol C. (1993): Nucleotide-excision repair of DNA in cell-free extracts of the yeast Saccharomyces cerevisiae. In *Proceedings of the National Academy of Sciences* 90 (11), pp. 4907–4911.

Wasserstrom, Lisa; Portugal-Nunes, Diogo; Almqvist, Henrik; Sandström, Anders G.; Lidén, Gunnar; Gorwa-Grauslund, Marie F. (2018): Exploring D-xylose oxidation in Saccharomyces cerevisiae through the Weimberg pathway. In *AMB Express* 8 (1), p. 33. DOI: 10.1186/s13568-018-0564-9.

Webert, Holger; Freibert, Sven-Andreas; Gallo, Angelo; Heidenreich, Torsten; Linne, Uwe; Amlacher, Stefan et al. (2014): Functional reconstitution of mitochondrial Fe/S cluster synthesis on Isu1 reveals the involvement of ferredoxin. In *Nature communications* 5, p. 5013. DOI: 10.1038/ncomms6013.

Weerapana, Eranthie; Wang, Chu; Simon, Gabriel M.; Richter, Florian; Khare, Sagar; Dillon, Myles B. D. et al. (2010): Quantitative reactivity profiling predicts functional cysteines in proteomes. In *Nature* 468 (7325), pp. 790–795. DOI: 10.1038/nature09472.

Weimberg, Ralph (1961): Pentose oxidation by Pseudomonas fragi. In *Journal of Biological Chemistry* 236 (3), pp. 629–635.

Wernig, Florian; Baumann, Leonie; Boles, Eckhard; Oreb, Mislav (2021): Production of octanoic acid in Saccharomyces cerevisiae: Investigation of new precursor supply engineering strategies and intrinsic limitations. In *Biotechnology and bioengineering* 118 (8), pp. 3046–3057. DOI: 10.1002/bit.27814.

White, Peter J.; Borts, Rhona H.; Hirst, Mark C. (1999): Stability of the human fragile X (CGG) n triplet repeat array in Saccharomyces cerevisiae deficient in aspects of DNA metabolism. In *Molecular and cellular biology* 19 (8), pp. 5675–5684.

White, W. Hunter; Skatrud, Paul L.; Xue, Zhixiong; Toyn, Jeremy H. (2003): Specialization of function among aldehyde dehydrogenases: the ALD2 and ALD3 genes are required for β-

alanine biosynthesis in Saccharomyces cerevisiae. In *Genetics* 163 (1), pp. 69–77.

Wieczorke, R.; Krampe, S.; Weierstall, T.; Freidel, K.; Hollenberg, C. P.; Boles, E. (1999): Concurrent knock-out of at least 20 transporter genes is required to block uptake of hexoses in Saccharomyces cerevisiae. In *FEBS letters* 464 (3), pp. 123–128. DOI: 10.1016/s0014-5793(99)01698-1.

Wiedemann, Nils; Urzica, Eugen; Guiard, Bernard; Müller, Hanne; Lohaus, Christiane; Meyer, Helmut E. et al. (2006): Essential role of Isd11 in mitochondrial iron-sulfur cluster synthesis on Isu scaffold proteins. In *The EMBO journal* 25 (1), pp. 184–195. DOI: 10.1038/sj.emboj.7600906.

Williams, Lindsey N.; Herr, Alan J.; Preston, Bradley D. (2013): Emergence of DNA polymerase ε antimutators that escape error-induced extinction in yeast. In *Genetics* 193 (3), pp. 751–770. DOI: 10.1534/genetics.112.146910.

Wind, Niels de; Dekker, Marleen; Berns, Anton; Radman, Miroslav; te Riele, Hein (1995): Inactivation of the mouse Msh2 gene results in mismatch repair deficiency, methylation tolerance, hyperrecombination, and predisposition to cancer. In *Cell* 82 (2), pp. 321–330.

Wood, R. D. (1997): Nucleotide excision repair in mammalian cells. In *The Journal of biological chemistry* 272 (38), pp. 23465–23468. DOI: 10.1074/jbc.272.38.23465.

Xie, Y.; Liu, Y.; Argueso, J. L.; Henricksen, L. A.; Kao, H. I.; Bambara, R. A.; Alani, E. (2001): Identification of rad27 mutations that confer differential defects in mutation avoidance, repeat tract instability, and flap cleavage. In *Molecular and cellular biology* 21 (15), pp. 4889–4899. DOI: 10.1128/MCB.21.15.4889-4899.2001.

Xu, Haiqing; Kim, Sooah; Sorek, Hagit; Lee, Youngsuk; Jeong, Deokyeol; Kim, Jungyeon et al. (2016): PHO13 deletion-induced transcriptional activation prevents sedoheptulose accumulation during xylose metabolism in engineered Saccharomyces cerevisiae. In *Metabolic engineering* 34, pp. 88–96. DOI: 10.1016/j.ymben.2015.12.007.

Yokoyama, Shin-Ichiro; Suzuki, Tohru; Kawai, Keiichi; Horitsu, Hiroyuki; Takamizawa, Kazuhiro (1995): Purification, characterization and structure analysis of NADPH-dependent D-xylose reductases from Candida tropicalis. In *Journal of fermentation and bioengineering* 79 (3), pp. 217–223.

Yu, Tao; Zhou, Yongjin J.; Huang, Mingtao; Liu, Quanli; Pereira, Rui; David, Florian; Nielsen, Jens (2018): Reprogramming Yeast Metabolism from Alcoholic Fermentation to Lipogenesis. In *Cell* 174 (6), 1549-1558.e14. DOI: 10.1016/j.cell.2018.07.013.

Yukawa, Takahiro; Bamba, Takahiro; Guirimand, Gregory; Matsuda, Mami; Hasunuma, Tomohisa; Kondo, Akihiko (2021): Optimization of 1,2,4-butanetriol production from xylose in Saccharomyces cerevisiae by metabolic engineering of NADH/NADPH balance. In *Biotechnology and bioengineering* 118 (1), pp. 175–185. DOI: 10.1002/bit.27560.

Zha, Jian; Shen, Minghua; Hu, Menglong; Song, Hao; Yuan, Yingjin (2014): Enhanced expression of genes involved in initial xylose metabolism and the oxidative pentose phosphate pathway in the improved xylose-utilizing Saccharomyces cerevisiae through evolutionary engineering. In *Journal of industrial microbiology & biotechnology* 41 (1), pp. 27–39. DOI: 10.1007/s10295-013-1350-y.

Zhang, Jinrui; van den Herik, Bas Mees; Wahl, Sebastian Aljoscha (2020): Alpha-ketoglutarate utilization in Saccharomyces cerevisiae: transport, compartmentation and catabolism. In *Scientific reports* 10 (1), p. 12838. DOI: 10.1038/s41598-020-69178-6.

Zhang, Liang; Tang, Yan; Guo, Zhong-peng; Ding, Zhong-yang; Shi, Gui-yang (2011): Improving the ethanol yield by reducing glycerol formation using cofactor regulation in Saccharomyces cerevisiae. In *Biotechnology letters* 33 (7), pp. 1375–1380. DOI: 10.1007/s10529-011-0588-6.

Zhang, Yan; Lyver, Elise R.; Nakamaru-Ogiso, Eiko; Yoon, Heeyong; Amutha, Boominathan; Lee, Dong-Woo et al. (2008): Dre2, a conserved eukaryotic Fe/S cluster protein, functions in cytosolic Fe/S protein biogenesis. In *Molecular and cellular biology* 28 (18), pp. 5569–5582. DOI: 10.1128/MCB.00642-08.

Zhang, Yugang; Lin, Zhewang; Wang, Miao; Lin, Hening (2018): Selective Usage of Isozymes for Stress Response. In *ACS chemical biology* 13 (11), pp. 3059–3064. DOI: 10.1021/acschembio.8b00767.

Zhao, X.; Shi, F.; Zhan, W. (2015): Overexpression of ZWF1 and POS5 improves carotenoid biosynthesis in recombinant Saccharomyces cerevisiae. In *Letters in applied microbiology* 61 (4), pp. 354–360. DOI: 10.1111/lam.12463.

Zhu, Fan Xiu; Biswas, Esther E.; Biswas, Subhasis B. (1997): Purification and characterization of the DNA polymerase α associated exonuclease: the RTH1 gene product. In *Biochemistry* 36 (20), pp. 5947–5954.

8 Register of Abbreviations

%	percent
Δ	(gene) deletion
°C	degrees Celsius
µL	micro liter
µM	micro molar
µm	micro meter
2µ	Two micron origin of replication
2K3DX	2-keto 3- deoxy xylonate
A	(DNA) adenine
ADP	adenosine diphosphate
AKG	α-ketoglutarate
AKG semialdehyde	α-ketoglutarate semialdehyde
ALD6	acetaldehyde dehydrogenase
AmpR	β-lactamase gene
ATP	adenosine triphosphate
bp	base pair
C	(DNA) cytosine
cal/g	Calories per gram
CamR	chloramphenicol acetyltransferase gene
ClonNAT	nourseothricin N-acetyltransferase gene
CO_2	carbon dioxide
CoA	coenzyme A
D	Dextrose
ddH_2O	double distilled water
DH	dehydrogenase
DHAP	dihydroxyacetone phosphate
DNA	desoxyribonucleic acid
EG	Ethylene glycol
et al.	et alii, Latin
ev	Empty vector
F6P	fructose-6-phosphate
FBP	fructose-1-6-bisphosphate
Fe/S cluster	Iron sulfur cluster
fw	forward primer
G	Galactose
G	(DNA) guanine
g	(weight) gram
g/L	Gram per liter
G3P	glyceraldehyde-3-phosphate
G3PDH	Glyceraldehyde 3 Phosphate dehydrogenase
G418	geneticin
G-6-P	Glucose -6- Phosphate dehydrogenase
GalA	D-galacturonic acid
GalOA	L-galactonate

GFP	Green Fluorescence protein
GPD1	glyceraldehyde-3-phosphate dehydrogenase gene
GPD1	Glyceraldehyde 3 -P dehydrogenase
GRAS	generally regarded as safe
His	Histidine
HPLC	High performance liquid chromatography
hr (s)	Hour (s)
hxt^0	Hexose null
hygR	hygromycin B phosphotransferase gene
K	(amino acid) lysine
KanMX	aminoglycoside phosphotransferase gene
KanR	neomycin phosphotransferase II gene
kb	kilo base
KsaD	α-ketoglutarate semialdehyde dehydrogenase
L	liter
L-Ara	L-arabinose
leu	Leucine
M	maltose
M	molar
M	(amino acid) methionine
mg	milli gram
min	minute
mM	milli molar
mol	mole
MTS	Mitochondrial targeting sequence
mU	milli units (enzyme activity)
NAD^+	nicotinamide adenine dinucleotide, oxidized
NADH	nicotinamide adenine dinucleotide, reduced
$NADP^+$	nicotinamide adenine dinucleotide phosphate, oxidized
NADPH	nicotinamide adenine dinucleotide phosphate, reduced
ng	nano gram
NHEJ	non-homologous end joining
nm	nano meters
nox -PPP	Non oxidative Pentose phosphate pathway
OD_{600nm}	optical density measured at wavelength 600nm
ORF	open reading frame
oxPPP	oxidative pentose phosphate pathway
PCR	Polymerase chain reaction
PGI1	phosphoglucose isomerase gene
pH	potential of hydrogen
PPP	pentose phosphate pathway
R	(amino acid) arginine
RNA	ribonucleic acid
rpm	rounds per minute

rRNA	ribosomal RNA
rv	(primer) Reverse primer
SC	synthetic complete
Sc drop out	Sc selective media without some amino acids
sec	second
T	thymine
TCA-cycle	tricarboxylic acid cycle, citric acid cycle
Trp	Tryptophan
U	unit (enzyme activity)
U	(DNA) uracil
ura	uracil
vmax	maximal enzyme velocity
w/v	weight per volume
WT	wild type
x g	centrifugal force
XDH	Xylitol dehydrogenase
XKS1	xylulokinase
XR	Xylose reductase
XylB	xylose dehydrogenase
XylD	xylonate dehydratase
Xylose	D-xylose
XylX	3-keto-2-deoxy-xylonate dehydratase
YPD	Yeast peptone dextrose (culture media)